

Centre Eau Terre Environnement

**DU MILIEU NATUREL AUX MÉSOCOSMES : UTILISATION DU BIOFILM
COMME BIOINDICATEUR DE LA CONTAMINATION MÉTALLIQUE DES
COURS D'EAU EN RÉGION MINIÈRE**

Par

Vincent Laderriere

Thèse présentée pour l'obtention du grade de
Philosophiae Doctor (Ph.D.)
en sciences de l'Eau

Jury d'évaluation

Présidente du jury et
examinatrice interne

Isabelle Lavoie
INRS – Eau Terre Environnement

Examinateur externe

Ahmed Tlili
EAWAG

Examinatrice externe

Giulia Cheloni
CNRS

Directeur de recherche

Claude Fortin
INRS – Eau Terre Environnement

Codirectrice de recherche

Séverine Le Faucher
UPPA

Codirectrice de recherche

Soizic Morin
INRAE

REMERCIEMENTS

Une thèse, sans surprise, c'est long. Autrement dit, j'ai connu nombre de belles personnes avec qui j'ai passé de beaux moments durant mon passage à l'INRS. Alors si en lisant ces lignes, un lecteur non cité vient à s'estimer avoir été lésé, je l'invite chaleureusement à me contacter afin que cette faute me soit pardonnée.

En toute logique, je commencerai par la fin avec ce qui s'annonce être "le grand air de la diva" de ce périple académique. Je tiens à remercier en tout premier lieu Ahmed Tlili, Giulia Cheloni ainsi qu'Isabelle Lavoie pour avoir accepté d'évaluer mes travaux de thèse. Évidemment, la professeure Lavoie se voit attribuer une mention spéciale pour m'avoir supervisé lors de mes stages et avec qui j'aurai gratté tout un tas de supports afin de récupérer le fameux Graal visqueux et verdâtre. Je remercie également très chaleureusement Séverine Le Faucheur ainsi que Soizic Morin, mes deux mamans de thèse. Merci pour vos encouragements, votre bonne humeur et votre patience pour votre étudiant expatrié de l'autre côté de l'océan. Je me sens chanceux de vous avoir eu comme co-directrices. Pour finir le bal des chefs, je remercie évidemment mon directeur de stage/maitrise/thèse (pour ne citer que ça), Claude Fortin (dit "le Maître de la spéciation"). "Chef merci chef" de m'avoir offert toutes ces opportunités et de les avoir accompagnés de patience et de bienveillance. Tu m'auras laissé la porte grande ouverte, et ce en tout temps. J'ai beaucoup grandi durant ces années dans ton équipe et si j'ai la chance de continuer en recherche, soit assuré qu'il y aura un peu de "Claude" dans ce qui en découlera. J'espère juste oublier qu'il existe plusieurs caractères d'apostrophes...

Que serait un directeur de recherche sans une équipe de recherche. Grand merci à tous mes collègues de l'équipe Fortin dont beaucoup sont devenus mes amis. Je pense en premier lieu à "Carolisme", ma sœur de thèse. Je te trouve bien trop intéressante pour être mon amie, et ce temps commun à l'INRS aura donné lieu à tout un tas d'aventures personnelles et professionnelles. J'espère que nous en parlerons encore dans 20 ans, sur une terrasse ou ailleurs, avec un verre d'alcool et des sourires. Océane, dans le meilleur comme dans le pire, sache que j'ai aimé t'avoir sur le bureau d'en face. Tu parles beaucoup, mais nos discussions de bureau vont rester un souvenir ardent ! D'une manière ou d'une autre, j'espère que cela continuera ! Merci aussi à Kim pour son amitié, sa bonne humeur et d'avoir su (et de savoir encore d'ailleurs) l'emplacement de toute chose au labo. Je pense aussi à Laura, une ancienne Fortin devenue Lavoie. Merci pour ta bienveillance, ta bonne humeur, tes envolées lyriques, les "rides" à Oka et même de m'embêter tous les jours en me criant bonjour. Mais sache que je ne te

pardonnerai jamais cette histoire de "hoody". Je tiens à remercier Maxime, pour le travail accompli lors de son stage. Je n'oublie pas non plus les anciens comme les derniers arrivés. Merci à Sébastien, Sandra, Fengjie, Zhongzhi, Camille, Lou, Faouzia, Émeric, Imad, Mariem, Rahma, Julien et Louise. Merci aussi à Julie, Betty, Bertille, Hamidou, Léa sans oublier Marion, mes collègues de l'IRSTEA de Cestas. Merci de m'avoir accepté dans votre tribu pour les rendez-vous raclette et les mardi soir au bar (et toutes les autres choses aussi). Si j'ai appréhendé quitter le Québec pour revenir en France 6 mois, j'y ai finalement vécu des moments que je n'oublierai pas. En écrivant ces lignes, il me tarde de tous vous revoir. Aussi, comment oublier l'indescriptible Jean-Paul. Merci de m'avoir accepté comme colocataire pendant mes 6 mois à Bordeaux. Merci pour tes conseils et ta précieuse aide en statistique, mais surtout, merci d'avoir croisé mon chemin. Tu fais partie des êtres humains qui m'inspirent ! Je remercie tous les techniciens de laboratoire de l'INRS tout comme de l'IRSTEA de Cestas pour leur aide dans la réalisation de mes expériences. Une mention spéciale à Mélissa Eon pour son plein support lors des enfers que je lui ai fait vivre chaque mardi de manip à l'IRSTEA.

Les expatriés savent que loin de chez soi, on finit par se créer une "petite famille". Lors de ces années au Québec, j'ai pu compter sur des personnalités extravagantes qui m'ont fait me sentir chez moi, ici au Québec. J'aimerai tout particulièrement remercier Sophie, Elisabeth, Marc-Alexandre, Thomas, Nishodi, Fx, Ben, Giulio, Élisa, Flora, Vilmentes, Hélène, Anthony, Marco, Maeva... et tous ceux pour qui je manque de place (et y en a !). J'ai aussi eu la chance de me constituer ma "petite famille québécoise". Merci donc à Marianne, Marc, Justine, Sacha, Paul-Michel, Mathieu et bien sûr, Geneviève. Ancienne membre du labo Fortin, cette dernière a été une collègue, mais aussi une amie. J'espère que nos aventures "*outdoor*" (ou n'importe quoi d'autre) continueront même si tu portes définitivement trop de Arc'teryx. Je n'oublie évidemment pas Romain, mon acolyte français dans cette gang québécoise. On en aura bu des IPA, et on ne va pas s'arrêter sur le chemin d'un si beau palmarès ! Je pense aussi à Catherine, ma colocataire pendant 3 longues années avec qui j'ai aimé côtoyer la même maison. Merci pour les notes enivrantes de chants et de pop/jazz qui auront flotté en ces lieux.

Enfin, une pensée pour ma famille. Merci à mes parents de m'avoir permis de faire des études selon un tracé hasardeux et de m'avoir toujours encouragé à m'écouter. Merci à mes deux frères qui, bien que je sois loin depuis un bout, ont toujours été là pour moi. Mention spéciale aussi à ma belle-sœur Fanny !

Je terminerai ces lignes en remerciant Marie. Merci d'avoir choisi le Canada plutôt que la Guadeloupe pour ta maitrise. Je sais ton amour pour l'océan, mais j'aurai raté quelque chose.

RÉSUMÉ

Bien que les métaux soient naturellement présents dans les écosystèmes d'eau douce, les activités anthropiques telles que les opérations minières peuvent entraîner une augmentation de leurs concentrations et des conséquences environnementales sur le long terme. Rejetés dans les milieux aquatiques, les contaminants métalliques sont susceptibles d'avoir des répercussions sur les communautés microbiennes comme le biofilm périphytique, qui joue un rôle clé dans la production primaire des écosystèmes des cours d'eau. Le biofilm est un modèle intéressant, car il est ubiquiste, sédentaire, à la base de la chaîne trophique et se compose d'un consortium de microorganismes de différents règnes vivant dans une matrice d'exopolysaccharides.

Ces travaux de thèse portent sur les liens existants entre la bioaccumulation des métaux, la composition physico-chimique de l'eau, les variables environnementales (température et photopériode) et la structure de la communauté du biofilm (*c.à.d* autotrophe et hétérotrophe). Sur le terrain, la teneur en métaux du biofilm s'est montrée fortement corrélée à la concentration ambiante en ions métalliques libres (Cu, Ni et Cd), et ce, malgré des différences dans les caractéristiques physico-chimiques de l'eau, le climat ou le type d'écosystème. Néanmoins, un effet protecteur apparent du pH a été mis en évidence et les effets de compétition entre les métaux dissous pour les sites de fixation à la surface des organismes du biofilm étaient en accord avec les principes du modèle du ligand biotique. En parallèle, une première série d'expériences en laboratoire visait à vérifier l'influence de facteurs environnementaux (température et photopériode) sur l'accumulation du Ni par un biofilm cultivé en laboratoire. Les résultats indiquent qu'une température plus élevée favorise la bioaccumulation et augmente la sensibilité des biofilms exposés à différentes concentrations en Ni. Une deuxième série d'expériences a permis d'examiner les relations existantes entre toxicité, bioaccumulation et acquisition de tolérance de deux biofilms naturels récoltés durant deux saisons distinctes (été et hiver). Les communautés estivales divergeaient structurellement des communautés d'hiver, et présentaient un contenu bioaccumulé en Ni significativement supérieur pour une même concentration d'exposition. Dans un contexte où les biofilms d'eau douce peuvent être utilisés comme indicateurs d'exposition aux métaux, ces résultats impliquent que des variations saisonnières dans la bioaccumulation des métaux sont susceptibles de se produire. De plus, ces variations ont été montrées comme principalement conditionnées par la structure et les fonctions initiales de la communauté du biofilm.

Ces travaux démontrent le potentiel universel des biofilms périphytiques d'eau douce comme outil de biosurveillance et d'évaluation du risque écotoxicologique des contaminants métalliques.

Mots-clés : Biofilm périphytique; métaux; spéciation; biosuivi; bioaccumulation; BLM; PICT; facteurs environnementaux; température; photopériode

ABSTRACT

While metals occur naturally in freshwater ecosystems, anthropogenic activities such as mining operations represent a long-standing concern of discharge. When released into aquatic environments, metal contaminants are likely to impact microbial communities such as periphytic biofilms, which play a key role in the primary production in stream ecosystems. The biofilm is an interesting model because it is ubiquitous, sedentary, at the base of the trophic chain and represents a consortium of microorganisms from different kingdoms living in an exopolysaccharide matrix. This work presented in this thesis focuses on the links between metal bioaccumulation, water physico-chemical characteristics, environmental variables (temperature and photoperiod) and biofilm community structure (*i.e.* autotrophic and heterotrophic).

In the field, biofilm metal contents were highly correlated to the ambient free metal ion concentrations despite different physico-chemical characteristics of the ambient water, climate or ecosystem types. Nevertheless, the apparent protective effect of pH was demonstrated and the observed competition effects among dissolved cations for surface binding sites of biofilm organisms were in agreement with the principles of the biotic ligand model. In parallel, a first series of laboratory experiments were carried out to verify the influence of environmental factors (temperature and photoperiod) on Ni accumulation by a biofilm grown in the laboratory. These experiments showed that increasing temperature enhanced the accumulation capacity and sensitivity of biofilms exposed to different Ni concentrations. A second series of experiments examined the relationships between toxicity, bioaccumulation and tolerance acquisition of two natural biofilms collected in two distinct seasons (summer and winter). The two communities were structurally divergent and showed higher bioaccumulated Ni content in summer biofilms compared to winter ones, for a given exposure concentration. In a context where freshwater biofilms can be used as indicators of metal exposure, these laboratory results imply that seasonal variations in metal bioaccumulation response are likely to occur and that this response is primarily conditioned by the initial structure and functions of the biofilm community.

Nevertheless, this project demonstrates the universal potential of periphytic freshwater biofilms as a tool for biomonitoring and ecological risk assessment of metallic contaminants.

Keywords: Periphytic biofilm; metals; speciation; biomonitoring; bioaccumulation; BLM; PICT; environmental factors; temperature; photoperiod

TABLE DES MATIÈRES

REMERCIEMENTS	III
RÉSUMÉ	V
ABSTRACT	VII
TABLE DES MATIÈRES	IX
LISTE DES FIGURES.....	XIII
LISTE DES TABLEAUX	XVII
LISTE DES ABRÉVIATIONS.....	XIX
1 INTRODUCTION.....	1
1.1 MISE EN CONTEXTE	1
1.2 REVUE DE LITTÉRATURE GÉNÉRALE	3
1.2.1 <i>Le biofilm, un modèle biologique pour appréhender les changements dans le fonctionnement des écosystèmes aquatiques</i>	3
1.2.1.1 Le biofilm : définition et structure	3
1.2.1.2 Fonctions dans les écosystèmes d'eau douce.....	6
1.2.1.3 Le biofilm comme bioindicateur dans un contexte de contamination anthropique	7
1.2.2 <i>Les métaux, devenir dans l'environnement et effets sur le biofilm</i>	10
1.2.2.1 Contexte d'aujourd'hui : entre exploitations minières, enjeux économiques et législation	10
1.2.2.2 Cycle naturel des métaux et perturbations anthropiques.....	11
1.2.2.3 Concept de spéciation, de ligands et de biodisponibilité.....	13
1.2.2.4 Métaux d'étude	16
1.2.2.5 Interaction des métaux avec le vivant et modèle du ligand biotique	18
1.2.2.6 Mécanismes de toxicité des métaux	22
1.2.3 <i>Biosuivi à grande échelle : variables à prendre en compte pour comprendre la réponse des biofilms face aux métaux</i>	25
1.2.3.1 Influence de variables biotiques : le concept du « PICT »	25
1.2.3.2 Influence de variables abiotiques : du facteur environnemental au facteur de stress environnemental	27
1.3 STRUCTURE DE LA THÈSE	30
2 BIBLIOGRAPHIE INTRODUCTION.....	33
3 EXPLORING THE ROLE OF WATER CHEMISTRY ON METAL ACCUMULATION IN BIOFILMS FROM STREAMS IN MINING AREAS	51
3.1 GRAPHICAL ABSTRACT	53
3.2 ABSTRACT.....	53
3.3 INTRODUCTION	55
3.4 MATERIALS & METHODS	57

3.4.1	<i>Study area</i>	57
3.4.1.1	<i>Northern Nunavik region</i>	59
3.4.1.2	<i>Southern Ontario region</i>	59
3.4.2	<i>Surface water collection and analyses</i>	60
3.4.3	<i>Biofilm collection and metal content</i>	61
3.4.4	<i>Analyses</i>	62
3.4.5	<i>Metal speciation</i>	62
3.4.6	<i>Metal accumulation model</i>	63
3.4.7	<i>Data treatment</i>	64
3.5	RESULTS & DISCUSSIONS.....	64
3.5.1	<i>General water chemistry</i>	64
3.5.2	<i>Dissolved metal concentrations</i>	65
3.5.3	<i>Biofilm metal contents as a function of total dissolved and free ion concentrations</i>	67
3.5.4	<i>Relationships between metal accumulation and free metal ion concentration on a regional scale</i>	70
3.5.5	<i>Relationships between metal accumulation and free metal ion concentration on a global scale</i>	73
3.5.6	<i>Competing effects</i>	75
3.6	CONCLUSIONS.....	82
3.7	ACKNOWLEDGEMENTS	84
4	BIBLIOGRAPHIE 1^{ER} ARTICLE	85
5	SEASONAL FACTORS AFFECT THE SENSITIVITY OF BIOFILMS TO NICKEL AND ITS ACCUMULATION.....	91
5.1	ABSTRACT.....	93
5.2	INTRODUCTION	95
5.3	MATERIALS & METHODS	97
5.3.1	<i>Biofilm culture</i>	97
5.3.2	<i>Biofilm exposure experiments</i>	97
5.3.3	<i>Biofilm sampling and analysis</i>	99
5.3.4	<i>Exposure medium analysis and Ni speciation</i>	101
5.3.5	<i>Data and statistical analyses</i>	101
5.4	RESULTS.....	102
5.4.1	<i>Effects of temperature and light conditions on control biofilms</i>	102
5.4.2	<i>Effects of temperature and light conditions on Ni-exposed biofilms</i>	105
5.4.3	<i>Influence of the photoperiod and temperature on Ni bioaccumulation</i>	106
5.4.4	<i>Influence of temperature and light on Ni toxicity</i>	109
5.4.5	<i>Interaction between environmental factors and biofilm parameters</i>	111

5.5	DISCUSSION.....	112
5.5.1	<i>Ni effect on biofilm.....</i>	112
5.5.2	<i>Influence of temperature and light variations on metabolism</i>	114
5.5.3	<i>Interactions between environmental factors and nickel toxicity and accumulation</i>	116
5.6	CONCLUSIONS.....	118
5.7	ACKNOWLEDGMENTS.....	119
6	BIBLIOGRAPHIE 2^E ARTICLE	121
7	ROLE OF SEASONALITY IN THE RESPONSE AND TOLERANCE OF PERIPHYTIC BIOFILM TO NICKEL.....	127
7.1	ABSTRACT.....	129
7.2	INTRODUCTION	131
7.3	MATERIALS & METHODS	133
7.3.1	<i>Experimental set-up</i>	133
7.3.2	<i>Water analyses and Ni speciation.....</i>	135
7.3.3	<i>Biofilm characterization and tolerance assessment.....</i>	136
7.3.3.1	Short-term bioassays and tolerance assessment	136
7.3.3.2	Bioaccumulation	136
7.3.3.3	Chlorophyll-a extraction	137
7.3.3.4	Protein content.....	137
7.3.3.5	Polysaccharide content.....	138
7.3.3.6	Extracellular enzymatic activities	138
7.3.4	<i>Statistical analyses.....</i>	138
7.4	RESULTS.....	139
7.4.1	<i>Physico-chemical data</i>	139
7.4.2	<i>Structural and functional characteristics of biofilms</i>	141
7.4.3	<i>Nickel bioaccumulation by biofilms</i>	144
7.4.4	<i>Short-term bioassays and tolerance assessment.....</i>	146
7.5	DISCUSSION.....	149
7.5.1	<i>Community descriptors under Ni exposure.....</i>	149
7.5.2	<i>Bioaccumulation in relation to the studied descriptors.....</i>	151
7.5.3	<i>Community tolerance acquisition under Ni exposure</i>	152
7.6	CONCLUSION.....	154
7.7	ACKNOWLEDGMENTS.....	155
8	BIBLIOGRAPHIE 3^E ARTICLE	157
9	DISCUSSION GÉNÉRALE ET CONCLUSION	165
9.1	APPROCHE DE TERRAIN	165
9.2	APPROCHE EN MICROCOMSES	170

9.2.1	<i>Effet de la température et de la photopériode sur la bioaccumulation du Ni par le biofilm</i>	171
9.2.2	<i>Mise en lien de la bioaccumulation avec la structure, la sensibilité et la tolérance d'un biofilm exposé au Ni</i>	174
9.3	CONCORDANCE DES DONNEES DE LABORATOIRE AU MILIEU NATUREL	176
9.4	CONCLUSION	178
10	BIBLIOGRAPHIE DISCUSSION	181
11	ANNEXE I	183
12	ANNEXE II	184
13	ANNEXE III	190

LISTE DES FIGURES

FIGURE 1-1 : SCHEMA ILLUSTRATIF DU BIOFILM PRESENT SUR DES SUBSTRATS IMMERGES EN MILIEU NATUREL. LA ZONE QUI NOUS INTERESSE MAJORITAIREMENT ICI EST LA ZONE BENTHIQUE ET DONC LA FACE DES ROCHES ORIENTEE VERS LA SURFACE POUVANT PROFITER D'UN ACCES A LA LUMIERE. TIRE DE BATTIN <i>ET AL.</i> (2016).	4
FIGURE 1-2 : SCHEMA DECRIVANT LES PRINCIPALES PROPRIETES DE LA MATRICE CONSTITUTIVE DU BIOFILM. LA MATRICE EST COMPOSEE D'EPS QUI SERVENT DE BASE ARCHITECTURALE. DES PHENOMENES DE SORPTION, DE RETENTION, DE COOPERATION ET DE COMPETITION S'Y DEROUENT. C'EST DONC UN MICROHABITAT A PART ENTIERE A LA FOIS COMPLEXE ET RICHE EN BIODIVERSITE. TIRE DE FLEMMING <i>ET AL.</i> (2016).	6
FIGURE 1-3 : REPRESENTATION GRAPHIQUE DE L'ORDRE ET DE LA MAGNITUDE DES CONCENTRATIONS NATURELLES DES ELEMENTS TRACES SOUS FORME DISSOUTE DANS LES MILIEUX LOTIQUES (VALEURS MOYENNES MONDIALES). TIREE DE GAILLARDET <i>ET AL.</i> (2004).	12
FIGURE 1-4 : CLASSIFICATION DES INTERACTIONS MAJEURES ENTRE LES PRINCIPAUX COMPOSES ET LES METAUX TRACES PRESENTS DANS LES ECOSYSTEMES AQUATIQUES. TIRÉE DE WEHRLI & BEHRA (2015). ME = MÉTAL. EDTA = ACIDE ÉTHYLÉNEDIAMINETRACETIQUE. NTA = ACIDE NITRILOTRIACÉTIQUE.	14
FIGURE 1-5 : MODE D'INTERACTION D'UN ION METALLIQUE A LA SURFACE BIOLOGIQUE SELON LE MODELE DU LIGAND BIOTIQUE. M^{2+} = ION METALLIQUE LIBRE; ML = METAL COMPLEXE; L^{2-} = LIGAND (ACIDES AMINES, CITRATE, $S_2O_3^{2-}$, CO_3^{2-} , Cl^- , ETC.); X-M = METAL COMPLEXE A LA SURFACE CELLULAIRE. ADAPTEE DE LAVOIE <i>ET AL.</i> (2016).....	20
FIGURE 1-6 : SCHEMA ILLUSTRANT LA MOBILITE DES METAUX DANS LA CELLULE QUI PEUT ENTRAINER LA PRODUCTION DE FORMES REACTIVES DE L'OXYGENE. L'INTERNALISATION DE METAUX PEUT MODIFIER LA PERMEABILITE MEMBRANAIRE ET, UNE FOIS DANS LE MILIEU INTRACELLULAIRE, INDUIRE UN STRESS OXYDATIF. D'AUTRES MECANISMES PEUVENT ETRE AFFECTES COMME LE SYSTEME PHOTOSYNTHETIQUE DE LA CELLULE, L'ACTIVITE MITOCHONDRIALE, L'EXPRESSION GENETIQUE, ET EVENTUELLEMENT ABOUTIR A LA MORT CELLULAIRE. IL EXISTE EGALEMENT DES SYSTEMES DE DEFENSE COMME LA PRODUCTION D'EPS, LA COMPLEXATION DES METAUX PAR DES LIGANDS INTRACELLULAIRES OU ENCORE L'EXPULSION DE CEUX-CI HORS DE LA CELLULE. ADAPTE DE PINTO <i>ET AL.</i> (2003) ET MORIN <i>ET AL.</i> (2012).	23
FIGURE 1-7 : PRINCIPE DU CONCEPT DU « PICT » (<i>POLLUTION INDUCED COMMUNITY TOLERANCE</i>). LA COMMUNAUTÉ « DOWNSTREAM » REPRÉSENTE UNE COMMUNAUTÉ PRÉALABLEMENT EXPOSÉE À UN CONTAMINANT, DEVENUE PLUS TOLÉRANTE, TANDIS QUE LA COMMUNAUTÉ « UPSTREAM » CORRESPOND À UNE COMMUNAUTÉ DE RÉFÉRENCE NON PRÉALABLEMENT EXPOSÉE. CETTE DERNIÈRE SE CARACTÉRISE PAR UNE COURBE DOSE-RÉPONSE AVEC UNE EC_{50} PLUS FAIBLE PAR RAPPORT AU POURCENTAGE D'ACTIVITÉ DU BIOMARQUEUR D'EFFET CONSIDÉRÉ. TIRÉE DE TLILI <i>ET AL.</i> (2020).....	26
FIGURE 3-1 : SAMPLING SITES IN NUNAVIK (QC) AND IN THE SUDBURY AREA (ON) IN CANADA. THE SHADED ZONES (LIGHT GRAY) REPRESENT IN BOTH CASES THE MINING OR URBAN AREAS. WWTP = WASTEWATER TREATMENT PLANT; JC = JUNCTION CREEK; MBC = MALEY BRANCH CREEK; VR = VEUVE RIVER; FBC = FROOD BRANCH CREEK; CC = CONISTON CREEK; NC = NOLIN CREEK; CCC = COPPER CLIFF CREEK.	58
FIGURE 3-2 : BOX PLOTS OF MAJOR PHYSICOCHEMICAL PARAMETERS FOR THE SURFACE WATERS SAMPLED IN JULY AND AUGUST FOR NUNAVIK (BLUE), AND IN SEPTEMBER FOR SUDBURY (RED). EXCEPT FOR TEMPERATURE AND DOC, DATA ARE PRESENTED ON A LOG SCALE. A T-TEST WAS PERFORMED ON MEANS FOR COMPARISON WITH SIGNIFICANCE THRESHOLDS OF: $P \leq 0.0001$ ****; $P \leq 0.001$ ***; $P \leq 0.01$ **; $P \leq 0.05$ *; $P > 0.05$ NS.....	65

FIGURE 3-3 : REGRESSIONS OF BIOFILM METAL CONTENTS (Cu, Ni AND Cd) AS A FUNCTION OF FREE METAL SPECIES (Cu ²⁺ , Ni ²⁺ , Cd ²⁺) FOR SITES WHERE pH > 6. NUNAVIK DATA ARE REPRESENTED AS BLUE CIRCLES AND SUDBURY DATA AS RED TRIANGLES.	71
FIGURE 3-4 : LINEAR REGRESSION ANALYSES OF BIOFILM METAL CONTENTS (Cu, Ni AND Cd) AS A FUNCTION OF FREE METAL SPECIES (Cu ²⁺ , Ni ²⁺ , Cd ²⁺) FOR ALL SAMPLES FROM NUNAVIK (CIRCLES) AND SUDBURY (TRIANGLES) IN 2016. THE COLOR GRADIENT REPRESENTS THE OBSERVED pH VALUES FOR EACH SITE. UPPER FIGURES REPRESENT DATA FOR BIOFILMS COLLECTED AT ALL SITES AND LOWER FIGURES CORRESPOND TO BIOFILMS COLLECTED AT SITES WITH A pH HIGHER THAN 6.	74
FIGURE 3-5 : RATIO OF BIOFILM METAL CONTENTS TO FREE METAL ION CONCENTRATIONS FOR Cu, Ni AND Cd AS A FUNCTION OF FREE PROTON, CALCIUM, AND MAGNESIUM CONCENTRATIONS. SYMBOLS ARE IDENTICAL TO THOSE USED IN FIGURES 3-3 AND 3-4. KENDALL'S COEFFICIENTS (T) ARE PRESENTED FOR EACH REGION (BLUE FOR NUNAVIK AND RED FOR SUDBURY).	76
FIGURE 3-6 : THE UPPER PANEL PRESENTS THREE EXAMPLES OF CORRELATIONS, WITH A LOWER THE KENDALL COEFFICIENT INDICATING A GREATER EFFECT OF COMPETITION UPON BIOFILM METAL CONTENT (CIRCLES FOR NUNAVIK DATA AND TRIANGLES FOR SUDBURY DATA). THE MIDDLE AND LOWER PANEL PRESENTS, FOR EACH REGION, THE RATIO OF BIOFILM METAL CONTENT TO FREE METAL ION CONCENTRATION FOR Cu, Ni AND Cd AS A FUNCTION OF THE FREE SPECIES. THE VALUES REPRESENT THE KENDALL'S CORRELATION COEFFICIENT.....	79
FIGURE 5-1 : GRAPHICAL REPRESENTATION OF THE EXPERIMENTAL DESIGN. THE RECTANGLES REPRESENT THE MICROCOSMS AND EACH SQUARE, A BIOFILM TILE. CALCULATED FREE NICKEL ION CONCENTRATIONS [Ni ²⁺] ARE PRESENTED.	98
FIGURE 5-2 : DOSE RESPONSES OF THE BIOMASS, THE CONCENTRATION OF CHLOROPHYLL-A AND THE AUTOTROPHIC INDEX (N = 3) AS A FUNCTION OF THE FREE Ni CONCENTRATION FOR EACH CONDITION OF TEMPERATURE AND PHOTOPERIOD (T14P16 = 14°C IN 16/8; T14P12 = 14°C IN 12/12; AND T20P16 = 20°C IN 16/8). THE CURVES PLOTTED CORRESPOND TO SECOND DEGREE POLYNOMIAL REGRESSIONS. A VERSION OF THIS FIGURE PRESENTING ALL THE SAMPLING TIMES IS PROVIDED IN THE APPENDIX II (SEE FIGURE 12-3).....	106
FIGURE 5-3 : INTERNALIZED Ni CONCENTRATIONS BY BIOFILMS (N = 3 FOR DIFFERENT THE DIFFERENT CONDITIONS (14°C AND 16/8 LIGHT/DARK CYCLE IN BLUE; 14°C AND 12/12 LIGHT/DARK CYCLE IN YELLOW; 20°C 16/8 LIGHT/DARK CYCLE IN RED) AS A FUNCTION OF THE CALCULATED FREE Ni CONCENTRATIONS. EACH PANEL REPRESENTS AN EXPOSURE TIME. THE REGRESSIONS CORRESPOND TO MICHAELIS-MENTEN MODELS. THE Ni ACCUMULATION OF CONTROL SAMPLES WERE RANGING FROM 0.03 TO 0.6 µM OF Ni ²⁺ WHATEVER THE SAMPLING TIMES (NON EXPOSED CHANNELS).	107
FIGURE 5-4 : PHOTOSYNTHESIS EFFICIENCY AS FUNCTION OF Ni EXPOSURE FOR THREE ENVIRONMENTAL CONDITIONS TESTED. SCATTERPLOTS PRESENT TIME-RESPONSE CURVES BASED ON THE DECREASE IN Φ_{PSII} AFTER Ni ADDITION (MEAN ± SD; N = 3) FOR EACH EXPOSURE DURATION. MEASUREMENTS OF ALL T_0 SAMPLES (BEFORE ADDITION OF Ni IN THE MEDIA) WERE USED AS A REFERENCE TO MODEL RELATIVE DOSE-RESPONSE CURVES. THE DOTTED LINE SHOWS THE MEDIAN VALUE OF THE CONTROL SAMPLES. VALUES OF CONTROL SAMPLES (NON EXPOSED CHANNELS) WERE RANGING FROM 0.39 TO 0.50 WHATEVER THE SAMPLING TIMES. A SUMMARY OF THE EFFECTIVE CONCENTRATIONS CALCULATED FROM EACH TIME CURVE IS PROVIDED IN THE TABLE FOR EACH CONDITION (ESTIMATE ± STANDARD ERROR). THE LETTERS INDICATES SIGNIFICANT DIFFERENCES BETWEEN CONDITIONS WITHIN A SAME SAMPLING TIME (P < 0.05).110	110
FIGURE 5-5 : LINEAR DISCRIMINANT ANALYSIS (LDA) OF THE DIFFERENT CONDITIONS AFTER THE 7 DAYS OF EXPOSURE (LEFT PANEL) BASED ON THE DIFFERENT STUDIED BIOMARKERS (RIGHT PANEL) FOR ALL Ni TREATMENTS. ALL THE PARAMETERS WERE NORMALIZED BY THEIR START VALUES (I.E. BY THEIR RESPECTIVE T_0) IN ORDER TO DISCRIMINATE THE INFLUENCE OF ENVIRONMENTAL FACTORS ON RESPONSE TO Ni.	112
FIGURE 7-1: GRAPHICAL REPRESENTATION OF THE EXPERIMENTAL DESIGN. EACH SQUARE REPRESENTS A GLASS TILE COLONIZED BY BIOFILMS.	134

FIGURE 7-2 : BOXPLOTS OF PROTEINS (A), POLYSACCHARIDES (B), B-GLUCOSIDASE (C) AND B-GLUCOSAMINIDASE (D) MEASURED IN BIOFILMS AS A FUNCTION OF THE AVERAGE FREE Ni²⁺ EXPOSURE CONCENTRATION (μ M) FOR THE TWO PHOTOPERIODS TESTED (I.E. 16/8 AND 8/16 OF LIGHT/DARK CYCLE) AND FOR THE FIRST AND LAST SAMPLING TIMES (DAYS 7 (IN WHITE) AND 28 (IN RED); N = 3). THE LETTERS CORRESPOND TO THE SIGNIFICANT DIFFERENCES DEFINED BY A POST HOC TUKEY TEST (P < 0.05) WITHIN A GIVEN PHOTOPERIOD. ALL SAMPLING TIMES ARE PRESENTED IN APPENDIX III (SEE FIGURE 13-3). 143

FIGURE 7-3: BOXPLOTS OF Ni ACCUMULATION BY BIOFILMS (μ MOL/G DW) AS A FUNCTION OF THE AVERAGE FREE Ni²⁺ CONCENTRATIONS OF EXPOSURE (μ M) FOR THE TWO PHOTOPERIODS TESTED (I.E. 16/8 AND 8/16 OF LIGHT/DARK CYCLE) AND FOR ALL SAMPLING TIMES POOLED TOGETHER (DAYS 7, 14, 21 AND 28; N = 12). THE LETTERS CORRESPOND TO THE SIGNIFICATIVE GROUPS DEFINED BY A POST HOC TUKEY TEST (P < 0.05). SEE THE FIGURE 13-2 PRESENTED IN APPENDIX III FOR A PRESENTATION AS A FUNCTION OF THE DIFFERENT SAMPLING TIMES (DAY 7, 14, 21 AND 28). 145

FIGURE 7-4 : DOSE-RESPONSE CURVES OF THE PSII YIELDS IN RELATIVE UNITS (Φ_{PSII} ; MEAN \pm SD; N = 3) AS A FUNCTION OF THE TOTAL Ni CONCENTRATIONS (μ M) USED FOR THE SHORT-TERM TOXICITY TEST AFTER 6 HOURS OF EXPOSURE. THE FIGURE PRESENTS THE DATA AFTER 7 AND 14 DAYS OF CHRONIC EXPOSURE. A VERSION WITH THE FOUR SAMPLING DATES IS PRESENTED IN APPENDIX III (SEE FIGURE 13-4). THE COLORS AND SHAPES REFER TO THE PHOTOPERIOD TESTED. THE TITLES REFER TO THE LONG-TERM EXPOSURE CONDITIONS: C0 = CONTROL (I.E. NO Ni); C1 = [Ni²⁺] = 0.06 μ M; C2 = [Ni²⁺] = 0.6 μ M; C3 = [Ni²⁺] = 6 μ M..... 147

FIGURE 9-1 : QUANTITES DE METAUX BIOACCUMULES PAR LE BIOFILM (Cu, Ni ET Cd) EN FONCTION DES CONCENTRATIONS EN IONS METALLIQUES LIBRES (Cu²⁺, Ni²⁺, Cd²⁺). LE GRADIENT DE COULEUR REPRESENTE LES VALEURS DE pH RELEVEES POUR CHAQUE SITE D'ECHANTILLONNAGE. LA FORME DES POINTS FAIT REFERENCE A L'ETUDE DONT SONT ORIGINAIRES LES DONNEES. LES DROITES REPRESENTENT LES REGRESSIONS TRACEES AVEC L'ENSEMBLE DES DONNEES PRESENTANT UN pH SUPERIEUR OU EGAL A 6..... 166

FIGURE 9-2 : REGRESSIONS DES TENEURS EN METAUX BIOACCUMULES PAR LE BIOFILM (Cu, Ni ET Cd) EN FONCTION DES CONCENTRATIONS EN IONS METALLIQUES (Cu²⁺, Ni²⁺, Cd²⁺) POUR LES SITES A pH > 6. LES COULEURS ET LES FORMES REPRESENTENT LES POINTS ET LES REGRESSIONS ISSUES DES DIFFERENTES REGIONS REPRESENTEES : ABITIBI (ROND VERT ; LEGUAY ET AL. 2016), ESTRIE (CARRE MARRON ; LEGUAY ET AL. 2016), MAURICIE (LOSANGE JAUNE ; LAVOIE ET AL. 2012; LEGUAY ET AL. 2016), NUNAVIK (TRIANGLE BLEU ; LADERRIERE ET AL. 2020; LADERRIERE ET AL. 2021) ET SUDBURY (TRIANGLE INVERSE ROUGE ; LADERRIERE ET AL. 2021). 168

FIGURE 9-3 : ANALYSE EN COMPOSANTES PRINCIPALES (ACP) EFFECTUEE SUR L'ENSEMBLE DES DESCRIPTEURS UTILISES POUR ANALYSER LA REPONSE DU BIOFILM APRES 7 JOURS D'EXPOSITION A DIFFERENTES CONCENTRATIONS EN Ni SOUS TROIS CONDITIONS ENVIRONNEMENTALES DE PHOTOPERIODE ET DE TEMPERATURE. L'ACP DE GAUCHE DISCRIMINE SELON LA CONDITION ENVIRONNEMENTALE TANDIS QUE L'ACP DE DROITE DISCRIMINE SELON LA CONCENTRATION D'EXPOSITION EN IONS Ni²⁺. LES SYMBOLES DE TAILLES SUPERIEURES SPECIFIQUES A CHAQUE CONDITION (FIGURE DE GAUCHE) OU CONCENTRATIONS D'EXPOSITION EN NICKEL LIBRE (FIGURE DE DROITE) FONT REFERENCE AU BARYCENTRE DES DONNEES. 172

FIGURE 9-4 : TENEURS DE Ni ACCUMULE DANS LE BIOFILM (N = 3) EN FONCTION DU TEMPS (EN JOURS) SELON DIFFERENTS TRAITEMENTS EN Ni, Ca ET Mg. LES COULEURS FONT REFERENCE AU TEMPS D'ECHANTILLONNAGE DU BIOFILM. LA TEMPERATURE ETAIT MAINTENUE A 14°C SOUS UNE ILLUMINATION D'ENVIRON 80 μ MOL-PHOTONS/CM²/S ET UN CYCLE DIURNE/NOCTURNE DE 16/8 (H/H). 173

FIGURE 9-5 : ANALYSES LINEAIRES DISCRIMINANTES (LDA) EFFECTUEES POUR CHAQUE DESCRIPTEUR ETUDIE AVEC LA PHOTOPERIODE COMME VARIABLE DISCRIMINANTE (16/8 A GAUCHE ET 8/16 A DROITE) ET TOUS LES TRAITEMENTS EN Ni CONFONDUS. 175

FIGURE 9-6 : TENEURS EN Ni BIOACCUMULES PAR LE BIOFILM EN FONCTION DE LA CONCENTRATION EN IONS Ni²⁺. LES DROITES CORRESPONDENT AUX REGRESSIONS MODELISEES (AVEC INTERVALLES DE CONFIANCE A 95%) VIA LES DONNEES DE TERRAIN DES DEUX REGIONS ETUDIEES (NUNAVIK EN

BLEU ET DE SUDBURY EN ROUGE). LES COULEURS ET LES FORMES DES POINTS DIFFERENTIENT LES CONDITIONS (AINSIX QUE LES ARTICLES REFERENTS) UTILISEES DANS LES EXPOSITIONS EN MICROCOsmES. À NOTER QUE LES DONNEES REPRESENTEES SUR LA PRESENTE FIGURE SONT SEULEMENT CELLES POUR LESQUELLES UN EQUILIBRE ENTRE CONCENTRATIONS DANS L'EAU ET DANS LE BIOFILM ETAIT ATTEINT (C.A.D APRES 7 JOURS D'EXPOSITION DANS LE CAS DES DEUX CHAPITRES).....	177
FIGURE 12-1: MAJOR CHEMICAL FORMS OF Ni IN THE FRAUIL MEDIUM (EXPRESSED IN PERCENTAGE) AS A FUNCTION THE TOTAL CONCENTRATION IN THE MEDIUM. ONLY PREDOMINANT CHEMICAL FORMS (ABOVE 1%) ARE REPRESENTED.....	186
FIGURE 12-2 : TIME COURSE OF CONTROL SAMPLES WITH THE BIOMASS, THE CONCENTRATION OF CHLOROPHYLL-A, THE AUTOTROPHIC INDEX AND THE PHOTOSYNTHETIC YIELD (N = 3) AS A FUNCTION OF TIME FOR EACH CONDITION OF TEMPERATURE AND PHOTOPERIOD (T14P16 = 14°C IN 16/8 IN BLUE; T14P12 = 14°C IN 12/12 IN YELLOW; AND T20P16 = 20°C IN 16/8 IN RED). THE CURVES PLOTTED CORRESPOND TO SECOND DEGREE POLYNOMIAL REGRESSIONS.....	188
FIGURE 12-3 : DOSE RESPONSES OF THE BIOMASS, THE CONCENTRATION OF CHLOROPHYLL-A AND THE AUTOTROPHIC INDEX (N = 3) AS A FUNCTION OF THE FREE Ni CONCENTRATION FOR EACH ENVIRONMENTAL CONDITION OF TEMPERATURE AND PHOTOPERIOD (14°C WITH 16/8 IN BLUE; 14°C WITH 12/12 IN YELLOW; AND 20°C WITH 16/8 IN RED) AND THE DIFFERENT SAMPLING TIMES. THE CURVES PLOTTED CORRESPOND TO SECOND DEGREE POLYNOMIAL REGRESSIONS.....	189
FIGURE 13-1 : BOXPLOTS OF THE ACCUMULATED CONCENTRATIONS INSIDE BIOFILMS AS A FUNCTION OF THE AVERAGE FREE Ni CONCENTRATIONS OF EXPOSURE (μ M) FOR THE TWO PHOTOPERIODS TESTED (I.E. 16/8 AND 8/16 OF LIGHT/DARK CYCLE) AND FOR THE DIFFERENT SAMPLING TIMES (N = 3). THE COLORS ARE REPRESENTING THE SAMPLING TIMES. THE LETTERS CORRESPOND TO THE SIGNIFICATIVE GROUPS DEFINED BY A POST HOC TUKEY TEST (P < 0.05).	191
FIGURE 13-2 : BOXPLOTS OF PROTEINS (A), POLYSACCHARIDES (B), β -GLUCOSIDASE (C) AND β -GLUCOSAMINIDASE (D) MEASURED IN BIOFILMS AS A FUNCTION OF THE AVERAGE FREE Ni CONCENTRATION OF EXPOSURE (μ M) FOR THE TWO PHOTOPERIODS TESTED (I.E. 16/8 AND 8/16 OF LIGHT/DARK CYCLE) AND FOR THE DIFFERENT SAMPLING TIMES (N = 3). THE COLORS ARE REPRESENTING THE SAMPLING TIMES. THE LETTERS CORRESPOND TO THE SIGNIFICATIVE GROUPS DEFINED BY A POST HOC TUKEY TEST (P < 0.05) WITHIN A SAME PHOTOPERIOD.	192
FIGURE 13-3 : DOSE RESPONSE CURVES OF THE PSII YIELDS IN RELATIVE UNITS (Φ_{PSII} ; MEAN \pm SD; N = 3) AS A FUNCTION OF THE TOTAL Ni CONCENTRATIONS (μ M) USED FOR THE SHORT-TERM TOXICITY TEST AFTER 6 HOURS OF EXPOSURE. THE FIGURE PRESENTS THE DATA FOR THE DIFFERENT SAMPLING TIMES OF EACH EXPOSURE UNITS. THE COLORS AND SHAPES REFER TO THE PHOTOPERIOD TESTED.	193

LISTE DES TABLEAUX

TABLEAU 1-1 : CONCENTRATIONS TYPIQUES EN Cd, Cu ET Ni DANS DES RIVIERES DETERMINEES APRES FILTRATION (0.2 µM) ET ACIDIFICATION (GAILLARDET <i>ET AL.</i> , 2004, CITES PAR TERCIER-WAEBER <i>ET AL.</i> , 2012). ¹ GAMME DE CONCENTRATIONS TOTALES DISSOLUES MESUREES (ET MOYENNE MONDIALE). ADAPTE DE TERCIER-WAEBER <i>ET AL.</i> (2012).....	16
TABLE 3-1 : COEFFICIENTS OF DETERMINATION (R^2 VALUES) FROM LINEAR REGRESSION ANALYSES OF ACCUMULATED METALS ($[M]_{Bio}$) AS A FUNCTION OF DISSOLVED OR FREE METAL CONCENTRATION. SIGNIFICANCE THRESHOLD VALUES ARE: $P \leq 0.0001$ "****"; $P \leq 0.001$ "***"; $P \leq 0.01$ **"; $P \leq 0.05$ **"; $P > 0.05$ "NS". ALL DATA REFERS TO DATA FROM NUNAVIK AND SUDBURY TOGETHER.....	68
TABLE 5-1 : MEANS ± STANDARD DEVIATIONS (N = 6) OF DRY BIOMASS, CHLOROPHYLL-A CONCENTRATIONS, INTERNALIZED Ni CONCENTRATIONS, PHOTOSYNTHETIC YIELD AND AUTOTROPHIC INDEX IN CONTROL BIOFILM. IN THE CASE OF CONDITION T1P1 AT TIME 7, CHL-A CONCENTRATIONS WERE ESTIMATED BY REGRESSION USING VALUES OBTAINED BY PHYTO-PAM AND NOT BY SPECTROPHOTOMETRY. SEE MATERIALS AND METHODS FOR MORE DETAILS. **" INDICATES SIGNIFICANT DIFFERENCES BETWEEN TIMES WITHIN CONDITIONS ($P < 0.05$). A FIGURE PRESENTING THE DATA AS REGRESSIONS IS ALSO PROVIDED IN THE APPENDIX II (SEE FIGURE 12-2).	103
TABLE 5-2 : RESULTS OF THE THREE-WAY ANOVA WITH TIME AS A REPEATED MEASURE APPLIED ON ACCUMULATED Ni BY BIOFILMS BETWEEN CONDITIONS T1P1 AND T1P2. THESE TWO EXPERIMENTS DIFFER BY THE PHOTOPERIOD USED: 16/8 AGAINST 12/12. DFN: DEGREES OF FREEDOM IN THE NUMERATOR. DFD: DEGREES OF FREEDOM IN THE DENOMINATOR. F: F-STATISTIC VALUE. P: P-VALUE OF THE F-STATISTIC. GES: GENERALIZED EFFECT SIZE (AMOUNT OF VARIABILITY DUE TO THE WITHIN-SUBJECTS FACTOR).	108
TABLE 5-3 : RESULTS OF THE THREE-WAY ANOVA WITH TIME AS A REPEATED MEASURE APPLIED ON ACCUMULATED Ni CONCENTRATIONS BY BIOFILMS BETWEEN CONDITIONS T1P1 AND T2P1. THESE TWO EXPERIMENTS DIFFER BY THE PHOTOPERIOD USED: A LIGHT/DARK CYCLE OF 16/8 AGAINST 12/12. DFN: DEGREES OF FREEDOM IN THE NUMERATOR. DFD: DEGREES OF FREEDOM IN THE DENOMINATOR. F: F-STATISTIC VALUE. P: P-VALUE OF THE F-STATISTIC. GES: GENERALIZED EFFECT SIZE (AMOUNT OF VARIABILITY DUE TO THE WITHIN-SUBJECTS FACTOR).	109
TABLE 7-1 : PHYSICO-CHEMICAL CHARACTERISTICS OF EXPOSURE MEDIA OF THE FOUR CHANNEL SYSTEMS. THE VALUES ARE PRESENTED AS MEANS ± STANDARD DEVIATIONS (N = 24). B/DL = BELOW DETECTION (0.007 µM). N/A = NOT AVAILABLE. THE LETTERS A AND B RESPECTIVELY REFER TO THE RESULTS OF TUKEY TESTS PERFORMED BETWEEN (A) THE DIFFERENT CONDITIONS IN COMPARISON TO THE CONTROL (C0) WITHIN A GIVEN PHOTOPERIOD, AND (B) THE TWO PHOTOPERIODS TESTED WITHIN A GIVEN CONDITION. THE COLUMN HEADS REFER TO THE LONG-TERM EXPOSURE CONDITIONS: C0 = CONTROL (I.E. NO Ni); C1 = [Ni ²⁺] = 0.06 µM; C2 = [Ni ²⁺] = 0.6 µM; C3 = [Ni ²⁺] = 6 µM.	140
TABLE 7-2 : MAIN DESCRIPTORS (MEAN ± STANDARD DEVIATION) OF BIOFILMS UNDER CONTROL AND Ni-EXPOSURE CONDITIONS AT 0, 0.06, 0.6 AND 6 mM OF Ni ²⁺ (NAMED RESPECTIVELY C0, C1, C2 AND C3). THE LETTERS ^A AND ^B REFER TO THE RESULTS OF TUKEY TESTS PERFORMED BETWEEN (A) THE DIFFERENT CONDITIONS IN COMPARISON TO THE CONTROL (C0) WITHIN A GIVEN SAMPLING TIME AND PHOTOPERIOD, AND (B) THE TWO PHOTOPERIODS TESTED WITHIN A GIVEN CONDITION AND TIME, RESPECTIVELY.....	142
TABLE 7-3 : TABLE SHOWING MEAN PSII YIELD VALUES (N = 3) AND CALCULATED EC _{20s} FROM DOSE-RESPONSE CURVES FOR EACH TREATMENT, SAMPLING TIME AND PHOTOPERIOD. THE EC VALUES ARE EXPRESSED AS µM OF TOTAL DISSOLVED Ni. HOWEVER, Ni WAS CALCULATED TO BE PRESENT AT 94.4% UNDER ITS FREE FORM (Ni ²⁺) IN THE DAUTA MEDIUM. THE LETTERS A AND B RESPECTIVELY REFER TO THE RESULTS OF TUKEY TESTS PERFORMED BETWEEN (A) THE DIFFERENT CONDITIONS IN COMPARISON TO THE CONTROL (C0) WITHIN THE SAME SAMPLING TIME AND PHOTOPERIOD, AND (B) THE TWO PHOTOPERIODS TESTED WITHIN THE SAME CONDITION AND EXPOSURE TIME. N/S =	

NON-SIGNIFICANT CALCULATED EFFECTIVE CONCENTRATIONS. N/A = NOT AVAILABLE DUE TO THE ABSENCE OF ANY ACUTE EFFECTS IN THE SHORT-TERM TOXICITY TESTS.	149
TABLE 11-1 : VALUES AND STANDARD DEVIATIONS (N = 3) OF THE PHYSICOCHEMICAL PARAMETERS OF THE SURFACE WATER SAMPLED IN JULY AND AUGUST 2016 FOR NUNAVIK DATA AND IN SEPTEMBER 2016 IN THE CASE OF SUDBURY DATA.	183
TABLE 11-2 : MEAN (\pm STANDARD DEVIATION, N = 3) OF THE FREE ION CALCULATED CONCENTRATIONS SAMPLED IN JULY AND AUGUST 2016 FOR NUNAVIK DATA AND IN SEPTEMBER 2016 IN THE CASE OF SUDBURY DATA.....	183
TABLE 11-3 : MEAN (\pm STANDARD DEVIATION, N = 3) OF THE METAL CONCENTRATIONS IN BIOFILMS SAMPLED IN JULY AND AUGUST 2016 FOR NUNAVIK DATA AND IN SEPTEMBER 2016 IN THE CASE OF SUDBURY DATA.	183
TABLE 12-1 : RECIPES FOR THE FRAUIL MEDIUM USED FOR THE CULTURE OF BIOFILM AND THE EXPERIMENTS OF NI EXPOSURE (MOREL ET AL. 1975).	184
TABLE 12-2 : VALUES AND STANDARD DEVIATIONS (N = 5) OF THE PHYSICOCHEMICAL PARAMETERS OF THE CAP-ROUGE RIVER AT THE TIME OF BIOFILM SAMPLING.	185
TABLE 12-3 : TIME COURSE OF TOTAL AND FREE NI CONCENTRATIONS DURING EXPOSURE FOR THE THREE ENVIRONMENTAL CONDITIONS TESTED. B/DL = BELOW DETECTION LIMIT. N/A = NON AVAILABLE. LIMIT OF DETECTION = 0.01 μ M.....	187
TABLE 13-1 : PHYSICO-CHEMICAL CHARACTERISTICS OF EXPOSURE MEDIA OF THE FOUR CHANNEL SYSTEMS. THE VALUES ARE PRESENTED AS MEANS \pm STANDARD DEVIATIONS (N = 24). B/DL = BELOW DETECTION (0.007 μ M). N/A = NOT AVAILABLE. THE LETTERS A AND B RESPECTIVELY REFER TO THE RESULTS OF TUKEY TESTS PERFORMED BETWEEN (A) THE DIFFERENT CONDITIONS IN COMPARISON TO THE CONTROL (C0) WITHIN A GIVEN PHOTOPERIOD, AND (B) THE TWO PHOTOPERIODS TESTED WITHIN A GIVEN CONDITION.....	190
TABLE 13-2 : RECIPES FOR THE DAUTA MEDIUM USED FOR THE SHORT-TERM TOXICITY TEST (DAUTA, 1982)... 194	
TABLEAU 13-3 : PHYSICO-CHEMICAL CHARACTERISTICS OF EXPOSURE MEDIA OF THE FOUR CHANNEL SYSTEMS FOR ALL SAMPLING TIMES AND FOR THE EXPERIMENT USING A PHOTOPERIOD OF 16/8. THE VALUES ARE PRESENTED AS MEANS \pm STANDARD DEVIATIONS (N = 3). B/DL = BELOW DETECTION (CA = 0.04 μ M; MG = 0.12 μ M, Ni = 0.007 μ M).....	195
TABLEAU 13-4 : PHYSICO-CHEMICAL CHARACTERISTICS OF EXPOSURE MEDIA OF THE FOUR CHANNEL SYSTEMS FOR ALL SAMPLING TIMES AND FOR THE EXPERIMENT USING A PHOTOPERIOD OF 8/16. THE VALUES ARE PRESENTED AS MEANS \pm STANDARD DEVIATIONS (N = 3). B/DL = BELOW DETECTION (CA = 0.04 μ M; MG = 0.12 μ M, Ni = 0.007 μ M).....	196

LISTE DES ABRÉVIATIONS

ADN	Acide désoxyribonucléique
ADP	Adénosine diphosphate
AEAs	Activités enzymatiques anti-oxydantes
AI	Autotrophic index
AMD/DMA	Acid mine drainage (Drainage minier acide)
ANCOVA	Analyse de covariance
ANOVA	Analyse de variance
APX	Ascorbate peroxydase
ATP	Adénosine triphosphate
Au	Or
BLM	Biotic Ligand Model
BSA	Bovine Serum Albumin
Ca	Calcium
CAT	Catalase
Cat	Cations
CCME	Conseil canadien des ministres de l'environnement
Cd	Cadmium
CEX	Concentrations effective à X%
Chl-a	Chlorophyll-a
CLSM	Confocal laser scanning microscopy
Co	Cobalt
CTR	Copper transporters
Cu	Cuivre
DCE	DCE
DFd	Degrés de liberté au dénumérateur
DFn	Degrés de liberté au numérateur
DOC/COD	Dissolved organic carbon (Carbone organique dissous)
DOM/MOD	Dissolved organic matter (Matière organique dissoute)
DW	Dry Weight
EC/CE	Effective concentration (Concentration effective)
EDTA	Ethylenediaminetetraacetic acid
EPS	Extracellular polymeric substances (Exopolysaccharides)
F	F-statistic value
FA/AF	Fulvic acid (Acide fulvique)
Fe	Fer
FIAM	Free ion activity model
ges	Effet de taille généralisé
Gism	β -Glucosaminidase
GPX	Glutathion peroxydase
HA/AH	Humic acid (Acide humique)
HDPE	High density polyethylene

Hg	Mercure
IAEA	International atomic energy agency (Agence internationale de l'énergie atomique)
ICP-AES	Inductively Coupled Plasma – Atomic Emission Spectrometry (Spectrométrie d'émission atomique à plasma à couplage inductif)
ICP-MS	Inductively Coupled Plasma – Mass Spectrometry (Spectrométrie de masse à plasma à couplage inductif)
IDEC	Indice diatomées de l'est du Canada
J	Flux d'internalisation
K	Potassium
K (K_{ML} , K_{M-R} , K_{ML-R} , etc.)	Constante d'équilibre réactionnelle
K_{int}	Constante d'internalisation
L	Ligand
lap	Leucine-aminopeptidase
LCEE	Loi canadienne sur l'évaluation environnementale
LD	Limit of detection (Limite de détection)
LDA/ALD	Linear discriminant analysis (Analyse linéaire discriminante)
LDPE	Low density polyethylene
LQ	Limit of quantification (Limite de quantification)
LQE	Loi sur la qualité de l'environnement
M ou Me	Métal
Mg	Magnésium
MIL	Modèle de l'ion libre
ML	Métal complexé avec un Ligand
Mn	Manganèse
Mo	Molybdène
MO/OM	Organic matter (Matière organique)
M_T	Métal total
MUF	7-hydroxy-4-methylcoumarin
M^{z+}	Ion métallique libre
$[M]_{Bio}$	Concentration métallique intracellulaire
Na	Sodium
Ni	Nickel
NIST	National Institute of Standards and Technology's
NTA	Nitrilotriacetic acid
p	p-value
P	Phosphore
PAR	Photosynthetically active radiation
Pb	Plomb
PC	Polycarbonate
PCA/ACP	Principal component analysis (Analyse en composante principale)
PES	Polyéthersulfone
Phyto-PAM	Pulse Amplitude Modulated fluorimeter
PICT	Pollution induced community tolerance
PP	Polypropylene

PSI	Photosystem I
PSII	Photosystem II
qPCR	Réaction de polymérisation quantitative en chaîne en temps réel
R	Radical
R ²	Coefficient de détermination (Pearson)
ROS	Reactive oxygen species
Se	Selenium
Si	Silice
SOD	Superoxyde dismutase
STXM	Scanning transmission X-ray microscopy
T	Température
TOC/COT	Total organic carbon (Carbone organique total)
UV	Ultraviolet radiation
V	Vanadium
WHAM7	Windermere Humic Acid Model VII
X	Répétiteur membranaire
XIF	X-ray fluorescence imaging
XM	Métal complexé avec une membrane biologique
z	Charge du métal
Zn	Zinc
α	Valeur seuil du test statistique
βGlu	β-Glucosidase
τ	Coefficient de détermination (Kendall)
Φ _{PSII}	Rendement quantique optimale du PSII

1 INTRODUCTION

1.1 Mise en contexte

Le Québec, et plus généralement le Canada, vit actuellement une période d'exploration et d'exploitation minière sans précédent à l'exemple de l'initiative gouvernementale « Plan Nord ». L'essor de ces activités, bien que bénéfiques sur le plan économique, peut néanmoins conduire à des pressions importantes pour les écosystèmes naturels. À ce titre, les écosystèmes aquatiques sont particulièrement sujets à la contamination par les activités anthropiques. Afin d'être en mesure d'appréhender l'exposition des organismes aquatiques aux contaminants et les effets qui en découlent, il apparaît essentiel d'avoir une bonne connaissance de base des écosystèmes à risque. Ceci est d'autant plus vrai dans le contexte de changements globaux que l'on connaît actuellement.

À l'heure actuelle, une des approches utilisées dans l'investigation de l'impact des activités anthropiques sur les milieux aquatiques est l'analyse physico-chimique des eaux de surface et les réglementations en vigueur sont d'ailleurs souvent basées sur des mesures s'y rapportant. Bien qu'utiles, elles ne permettent d'obtenir qu'une information partielle liée aux effets des changements environnementaux sur les communautés biologiques, car celles-ci ne donnent qu'une vision instantanée de l'écosystème pour un site de prélèvement donné. L'effet de dilution par les précipitations, le gradient amont/aval ou encore la fréquence et la durée des rejets sont autant de variables sur lesquelles une analyse de l'eau ne fournit qu'une vision partielle. De plus, ce type d'approche ne permet pas d'avoir accès à de l'information sur la biodisponibilité des contaminants et donc sur leur réelle toxicité. En effet, considérant un contaminant métallique, sa toxicité est relative à sa spéciation chimique. La spéciation chimique correspond à la forme chimique et/ou physique sous laquelle le métal est présent dans le milieu aquatique. Cette spéciation dépend autant des paramètres physico-chimiques de l'eau (pH, alcalinité, etc.) que des concentrations d'autres composés également présents dans le milieu (matière organique, nutriments, autres métaux, etc.). Finalement, il convient aussi de noter que les analyses physico-chimiques des eaux ne peuvent être utilisées que dans un cadre prédictif d'impacts, ne pouvant remplacer une mesure biologique directe. Les organismes aquatiques étant en constante interaction physique, chimique et biologique avec leur écosystème, ils sont capables de nous apporter des informations pertinentes sur les fluctuations environnementales subies par le milieu naturel.

Si de nombreux organismes peuvent prétendre à cette fonction, tous ne peuvent pas être utilisés pour l'évaluation de la qualité de leur environnement. En effet, un bon bioindicateur doit présenter plusieurs caractéristiques : il doit être scientifiquement bien connu (biologiquement et écologiquement), être lié à des fonctions clés de l'écosystème, se montrer sensible aux modifications du milieu et être facile à mesurer/interpréter. Tous ces points sont autant de conditions qui restreignent le choix du modèle biologique que l'on va considérer. Ceci est également à remettre en perspective avec un contexte anthropique : si l'on considère la présence de contaminants dans le milieu, des individus vont invariablement disparaître et libérer des niches écologiques laissant place à de nouvelles espèces qui ne seront pas ou moins affectées par la contamination en question. Ce point souligne l'importance d'avoir une bonne connaissance du modèle biologique utilisé afin d'être capable de mesurer les modifications de l'écosystème de son état d'origine. Aujourd'hui, plusieurs approches de biosuivi ont été développées au fil des années à l'exemple de l'indice biologique global normalisé (IBGN) ou de l'indice des diatomées de l'est du Canada (IDEC).

Dans ce contexte, les microorganismes regroupent beaucoup de caractéristiques intéressantes. En effet, ils sont à la base de la chaîne trophique et répondent rapidement aux changements de leur environnement. Ils sont également ubiquistes et d'une grande diversité d'espèces. Le biofilm d'eau douce correspond à un consortium complexe d'organismes microscopiques de divers règnes du vivant qui se développent à la surface de substrats immersés. Ces dernières années, un effort de recherche conséquent a été effectué afin de comprendre les effets des contaminations métalliques sur le biofilm en laboratoire ou en milieux naturels. Cet effort a permis de montrer que le biofilm pouvait être un bioindicateur robuste dans le suivi des contaminations métalliques comme organiques, et un excellent proxy de la biodisponibilité des contaminants. Ce constat ouvre la possibilité au développement d'une approche multimétrique ou d'un modèle prédictif qui intégrerait la réponse des organismes vivants aux méthodes actuelles d'évaluation de la qualité des eaux et qui permettrait ainsi de mieux quantifier les effets des activités anthropiques. Cette perspective d'outil de biosuivi représenterait une avancée majeure pour tous les acteurs du suivi de la qualité des écosystèmes allant des organismes de bassins versants, aux gouvernements en passant par les compagnies industrielles.

1.2 Revue de littérature générale

1.2.1 Le biofilm, un modèle biologique pour appréhender les changements dans le fonctionnement des écosystèmes aquatiques

1.2.1.1 Le biofilm : définition et structure

L'appellation *biofilm* regroupe différents types de communautés de microorganismes. Qu'ils tapissent les cathéters ou implants dans le domaine médical, qu'ils se développent le long des coques immergées des bateaux ou qu'ils forment la plaque dentaire, tous sont autant d'exemples de biofilms (Battin *et al.* 2016). Toutefois, le biofilm qui nous intéresse ici correspond aux communautés de microorganismes qui colonisent la surface des substrats immergés (notamment à l'interface eau-sédiment) des milieux lotiques et lentiques à l'échelle mondiale : le *biofilm périphytique*. En limnologie, le terme *périphyton* désigne les communautés microbiennes associées aux surfaces solides immergées (Wetzel, 1983). Ce terme fait toutefois exception d'organismes tels que les champignons, les bactéries ou les protozoaires. Le terme *biofilm* se veut donc moins discriminant en incluant l'ensemble des organismes qui composent ce mélange complexe et hétérogène, regroupant ainsi plusieurs règnes du vivant. Selon le type de substrat, d'autres termes peuvent être utilisés afin de définir plus précisément le *périphyton*, comme par exemple *l'épiphyton* (associé à des macrophytes et algues), *épilithon* (associé à des roches minérales), *épipélon* (surface des sédiments) ou encore *épipsammon* (associé au sable ; Wetzel, (1983)). Dans ce document, bien que le modèle biologique considéré correspondant spécifiquement à un *biofilm épilithique*, les termes *biofilm*, *périphyton* ou *épilithon* ne seront donc pas distingués et l'appellation *biofilm* sera préférée.

La structure du biofilm est grandement influencée par une multitude de processus qu'ils soient biotiques ou abiotiques. En effet, les conditions environnementales autant physiques (température, lumière, type de support, régime hydrodynamique) que chimiques (pH, dureté de l'eau, concentration en nutriments, présence de contaminants) influencent sa conformation comme sa composition (Battin *et al.* 2016). Par exemple, selon le type de régime hydrologique (turbulent ou laminaire) d'un cours d'eau, le biofilm présente une structure plus compacte ou à l'inverse, plus étendue et lâche. Les phénomènes de compétition de par la forte diversité microbienne du biofilm, ou la prédation par des organismes variés à l'exemple d'insectes, mollusques (particulièrement les gastéropodes), crustacés ou poissons sont des exemples de paramètres biotiques ayant aussi une forte influence sur la composition (Guasch *et al.*, 2016; Mebane *et al.*, 2020; Neury-Ormanni *et al.*, 2020).

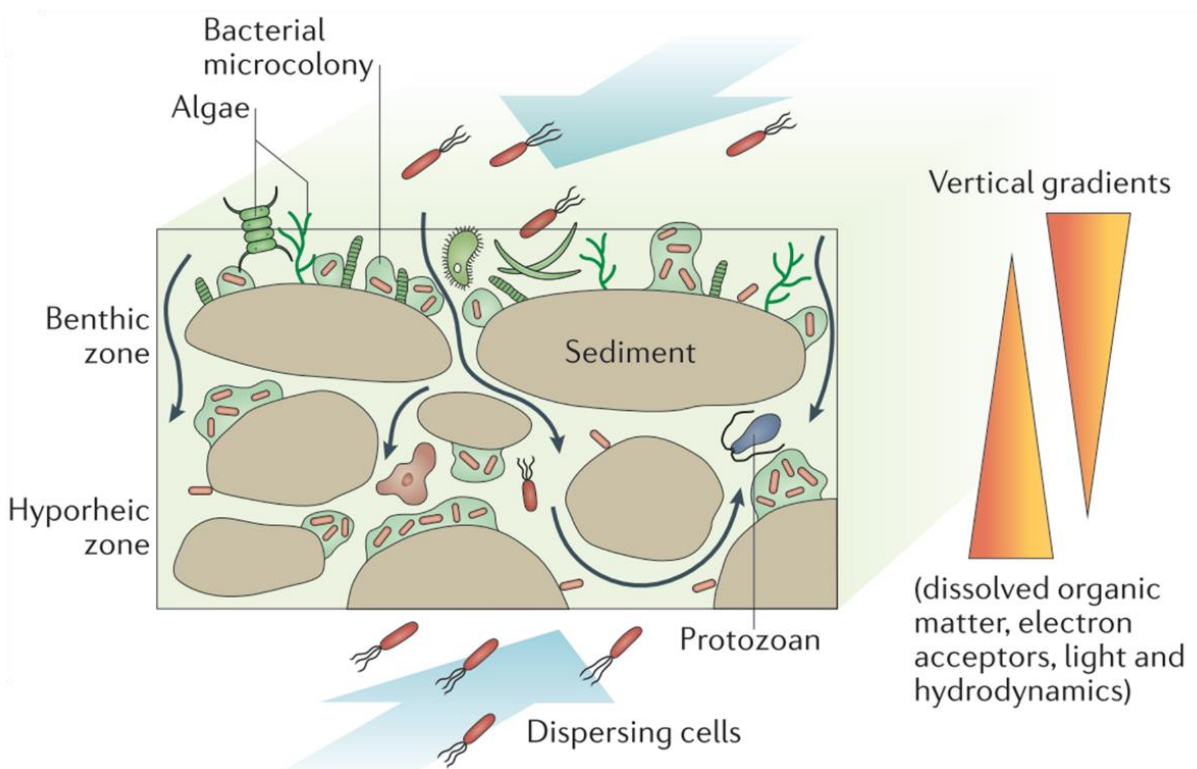


Figure 1-1 : Schéma illustratif du biofilm présent sur des substrats immergés en milieu naturel. La zone qui nous intéresse majoritairement ici est la zone benthique et donc la face des roches orientée vers la surface pouvant profiter d'un accès à la lumière. Tiré de Battin et al. (2016).

Comme défini par Characklis & Wilderer (1990), le biofilm peut-être décrit comme « une communauté microbienne adhérente à une surface et incluse dans une matrice de polymères extracellulaires » (Figure 1-1). En effet, l'ensemble de ces organismes est présent dans une matrice extracellulaire poreuse principalement composée de substances polymériques extracellulaires (*extracellular polymeric substances* ; EPS). Ce terme regroupe différents composés à l'exemple de polysaccharides, de protéines, de lipides, d'enzymes ou encore d'acides nucléiques (Aguilera et al. 2008; Flemming et al. 2016). D'autres substances comme des carbohydrates, des substances humiques et inorganiques peuvent également s'y retrouver (Pistocchi et al., 2000; D'Abzac et al., 2013; Bonnneau et al., 2020). L'ensemble de ces composés est issu des organismes eux-mêmes vivant au sein de cette matrice (Flemming et al., 2007; Flemming & Wingender, 2010) et permet une grande variété de réactions chimiques. Ces EPS sont constituées de groupements fonctionnels très variés, à l'exemple des groupements carboxyliques (Aguilera et al. 2008). Cette matrice joue premièrement un rôle de rétention pour divers produits métaboliques à l'exemple d'enzymes extracellulaires, d'ADN ou de débris

organiques qui peuvent être réutilisés par les organismes en son sein. Ainsi, cette matrice peut être comparée à un système externe de digestion et de recyclage qui joue un rôle important dans le cycle énergétique et des nutriments (Flemming & Wingender 2010). Elle permet aussi au biofilm d'être cohésif et d'offrir un environnement intermédiaire de protection contre des phénomènes comme l'érosion, la dessiccation, la prédation, les radiations ultraviolettes, etc. (Vu *et al.*, 2009; Flemming & Wingender, 2010). Elle assure de plus l'immobilisation, la proximité et les interactions entre cellules et ce, qu'elles soient de la même espèce ou non (Romaní, 2010). De plus, les EPS sont également capables de complexer certains métaux à l'exemple du Cu, du Cd, ou du Pb (Flemming & Wingender, 2010; D'Abzac *et al.*, 2013; Hobbs *et al.*, 2019). En effet, des études ont démontré que certaines espèces d'algues, ou du biofilm, exposées à différentes concentrations en métaux augmentaient leurs productions d'EPS ou de polymères (Jang *et al.* 2001; Aguilera *et al.* 2008; Loustau *et al.* 2019). Cette augmentation est souvent interprétée comme une stratégie de défense afin de maintenir ces métaux hors de la cellule (Pistocchi *et al.*, 2000). Toutefois, bien que ces composés complexent les métaux, les concentrations en métal dissous entre la colonne d'eau et les sites de complexation de la matrice devraient être à l'équilibre et ainsi ne peuvent pas réduire l'exposition aux métaux ; le rôle des EPS est donc à nuancer. Néanmoins, des études cinétiques ont permis de démontrer que les EPS pouvaient jouer un rôle dans la vitesse de diffusion des contaminants (métalliques ou organiques) au travers de la matrice (Buffel *et al.*, 2009; Dranguet *et al.*, 2017; Chaumet *et al.*, 2019). Cette matrice a donc un effet de rétention des organismes vivant en son sein et permet d'apporter une intégration temporelle d'une exposition aux métaux dans un contexte de contamination (Arini *et al.*, 2013; Bonet *et al.*, 2013; Hobbs *et al.*, 2019). Ce point représente un avantage conséquent par rapport aux dosages des métaux dans les eaux de surface qui permettent seulement d'avoir une information instantanée. En d'autres termes, cette matrice, ainsi que les organismes qui y vivent, peuvent être considérés comme un microhabitat à part entière où une grande diversité d'organismes interagissent par des phénomènes de coopération comme de compétition au même titre que dans un écosystème (Nadell *et al.*, 2016; Figure 1-2). Le biofilm est donc un ensemble très riche en matière de biodiversité et est le siège d'importantes activités métaboliques et enzymatiques qui sont en lien avec les processus écosystémiques et les cycles biogéochimiques des environnements naturels (Battin *et al.*, 2016).

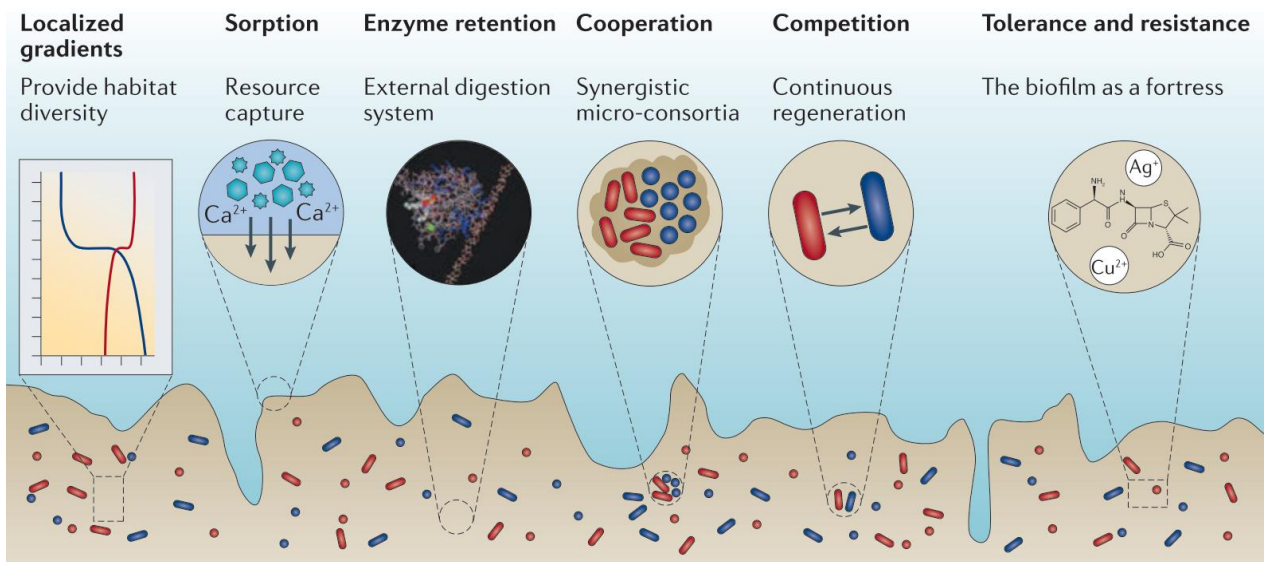


Figure 1-2 : Schéma décrivant les principales propriétés de la matrice constitutive du biofilm. La matrice est composée d'EPS qui servent de base architecturale. Des phénomènes de sorption, de rétention, de coopération et de compétition s'y déroulent. C'est donc un microhabitat à part entière à la fois complexe et riche en biodiversité. Tiré de Flemming *et al.* (2016).

1.2.1.2 Fonctions dans les écosystèmes d'eau douce

Les biofilms périphytiques correspondent à des communautés qui, en plus d'être à la base de la chaîne trophique, contribuent de manière substantielle aux flux d'énergie, aux cycles des nutriments ou aux flux biogéochimiques globaux (Battin *et al.*, 2003; Tercier-Waeber *et al.*, 2009; Battin *et al.*, 2016). À ce titre, le biofilm peut être subdivisé en deux compartiments principaux qui n'ont pas forcément les mêmes rôles d'un point de vue écosystémique : le phototrophe et l'hétérotrophe. Le compartiment phototrophe regroupe les organismes autotrophes photosynthétiques telles les microalgues et les cyanobactéries. Ces organismes, qui effectuent la photosynthèse, sont impliqués dans la fixation/réduction du dioxyde de carbone (CO₂), la production de dioxygène (O₂) ainsi que de matière organique (MO) (Roeselers *et al.*, 2008). La matière organique joue un rôle clé dans les écosystèmes d'eau douce, car elle alimente à terme des organismes de niveau supérieur dans la chaîne trophique eux-mêmes alimentant encore les maillons suivants. À ce titre, les organismes du compartiment hétérotrophe jouent un rôle majeur dans la transformation de la MO (Romaní, 2010). C'est notamment le cas par exemple des bactéries et des champignons. Ceux-ci sont impliqués dans la dégradation de la MO et dans le cycle des nutriments à l'exemple de l'azote ou du phosphore (Findlay *et al.*, 2003). La MO est composée de molécules hétérogènes de haut poids moléculaire qui doivent au préalable être

hydrolysées afin d'être transformées en molécules de plus faibles poids et donc accessibles pour les communautés bactériennes et fongiques. Ce processus est réalisé par les enzymes extracellulaires (Vu *et al.*, 2009). La β -glucosidase (β -Glu), la leucine-aminopeptidase (Lap), la β -glucosaminidase (Glsm) sont des exemples d'enzymes bactériennes retrouvées dans les milieux aquatiques. Elles interviennent principalement dans les cycles du carbone et de l'azote nécessaires au métabolisme bactérien et sont donc responsables de la dégradation de polymères. Cependant elles peuvent également être impliquées dans d'autres fonctions telles que la lyse des parois cellulaires microbiennes pour la croissance microbienne ou le broutage des protozoaires. Par exemple, la β -glucosidase est impliquée dans l'étape finale de la décomposition de la cellulose et des polysaccharides tandis que la β -glucosaminidase intervient dans la décomposition des peptidoglycans et de la chitine (Romaní *et al.*, 2008). Néanmoins, cette minéralisation permet de rendre les nutriments de nouveau disponibles pour les organismes phototrophes qui ensuite produisent de la matière organique pour les organismes hétérotrophes dans un cycle symbiotique qui contribue aux cycles biogéochimiques (Romaní, 2010; Battin *et al.*, 2016).

Le biofilm joue donc un rôle important en tant qu'acteur des productions primaire et secondaire, mais aussi en étant l'un des premiers maillons de la chaîne trophique (Zou *et al.*, 2016). En effet, les biofilms sont consommés par divers consommateurs, comprenant des organismes de la microméiofaune (e.g. rotifères; Weitere *et al.*, 2018; Neury-Ormanni *et al.*, 2020) ou de la méso/macro faune (p. ex. poissons; Álvarez & Peckarsky, 2005; Schneck *et al.*, 2013). De par ses fonctions clés au sein des écosystèmes d'eau douce, il est en mesure de jouer un rôle dans le devenir des contaminants en milieu naturel (Hobbs *et al.*, 2019; Bonnneau *et al.*, 2020).

1.2.1.3 Le biofilm comme bioindicateur dans un contexte de contamination anthropique

Aujourd'hui, l'approche bioindicatrice est souvent utilisée pour investiguer la question de l'effet d'un contaminant en intégrant la composante biologique des écosystèmes et ce, jusque dans la législation (exemple de la Directive européenne Cadre sur l'Eau 2000/60/CE). Beaucoup d'espèces peuvent regrouper des caractéristiques intéressantes comme bioindicateur : microorganismes, flore ou faune, le choix est vaste. Pour citer quelques exemples, on peut trouver dans la littérature des études portant sur des oiseaux (Defo *et al.*, 2014), des poissons

(Giguère *et al.*, 2005; Campbell & Hare, 2009; Martyniuk *et al.*, 2020), des invertébrés (Crémazy *et al.*, 2019; Mebane *et al.*, 2020; Neury-Ormanni *et al.*, 2020), des algues vertes unicellulaires (Le Faucher *et al.*, 2011; Kochoni & Fortin, 2019; Liu *et al.* 2020), des diatomées (Morin *et al.*, 2017; Pandey *et al.*, 2017; Lavoie *et al.*, 2018) ou encore le biofilm (Lavoie *et al.*, 2012; Leguay *et al.*, 2016; Laderriere *et al.*, 2020; Pandey, 2020). Namba *et al.* (2020) ont fait une méta-analyse des études publiées de 1991 à 2015 s'intéressant aux contaminations métalliques en milieux lotiques. Les auteurs ont montré que les macro-invertébrés benthiques ont été le plus souvent choisis tout au long de cette période (59-76% selon les tranches de 5 ans considérés par les auteurs), suivis par le biofilm périphytique (jusqu'à 30 %) et les poissons (jusqu'à 20 %), et le nombre d'études étudiant au moins 2 groupes biologiques en même temps était très limité (10%). Néanmoins, les études portant sur le biofilm sont en augmentation ces dernières années. Le biofilm est un modèle biologique pertinent, car il possède plusieurs propriétés intéressantes, il est : (1) ubiquiste ; (2) sédentaire ; (3) influencé par les processus environnementaux chimiques comme physiques (luminosité, température, hydrodynamique) ; (4) caractérisé par un cycle de vie court (il réagit donc rapidement aux changements) ; et (5) à la base de la chaîne trophique (Guasch *et al.*, 2016a). Compte tenu de toutes ces caractéristiques, les biofilms ont le potentiel d'être un outil efficace pour intégrer les variations spatiales et temporelles des sources de contaminants ainsi que les effets écologiques possibles sur les niveaux trophiques supérieurs (Hobbs *et al.*, 2019).

À plus petite échelle d'organisation biologique, le biomarqueur est une mesure biochimique ou moléculaire dans des cellules ou tissus indiquant un effet du contaminant. Les biomarqueurs peuvent ainsi autant correspondre à des processus métaboliques, à des structures (exemple des anomalies physiologiques) ou encore à des fonctions mesurables du système biologique (Lagadic *et al.*, 1997). Le biofilm étant un ensemble de communautés, de nombreuses méthodes peuvent être utilisées pour détecter l'effet des substances toxiques sur celui-ci. Le choix d'un biomarqueur ou d'un autre peut dépendre de l'effet attendu du contaminant considéré et donc la fonction à considérer. Là encore, le choix est vaste. Durant les dernières années, les biomarqueurs ciblant la composante phototrophe (et notamment algale) ont été très largement utilisés (Corcoll *et al.* 2012). La fluorescence de la chlorophylle-a (Corcoll *et al.*, 2011; Oukarroum *et al.*, 2012), l'activité photosynthétique (Kim Tiam *et al.*, 2015; Cheloni & Slaveykova, 2018), la synthèse de phytochélatines (Faucher *et al.*, 2005; Lavoie *et al.*, 2012), l'expression de certains gènes (Lavoie *et al.*, 2016; Dranguet *et al.*, 2017; Tiam *et al.*, 2018), les profils en acides gras (Fadhlaoui *et al.*, 2020; Pandey, 2020) et les déformations tératologiques de diatomées (Morin *et al.*, 2012; Lavoie *et al.*, 2014; Pandey *et al.*, 2017) en sont des exemples non-exhaustifs. Concernant le

compartiment hétérotrophe, des études ont également utilisé la respiration microbienne (Tlili et al., 2010) ou encore l'activité d'enzymes extracellulaires (β -glucosidase, β -glucosaminidase, leucine-aminopeptidase, etc) donnant une information plus mécanistique (Fechner et al., 2011; Faburé et al., 2015; Pesce et al., 2018). Ciblant non spécifiquement l'un ou l'autre compartiment, les enzymes antioxydantes ont aussi largement été utilisées dans la littérature (Bonnineau et al., 2013; Bonet et al., 2013). Du côté de la matrice, les protéines totales comme les polysaccharides peuvent nous renseigner sur la structure de celle-ci (Pistocchi et al., 2000; Romaní et al., 2008; Chaumet et al., 2019). La microméiofaune joue également un rôle crucial notamment par effet de consommation, consommation qui peut être modulée selon les effets de certains contaminants (Guasch et al., 2016c; Neury-Ormanni et al., 2020). Cette faune est définie par l'ensemble des consommateurs primaires des biofilms périphytiques, regroupant des protozoaires et des organismes pluricellulaires compris entre 2 μm et 2 mm (Weitere et al., 2018). En plus de participer à la richesse spécifique des biofilms, ces organismes participent également au transfert des contaminants le long de la chaîne trophique en tant que consommateurs primaires (Ancion et al., 2013; Scheibener et al., 2017; Mebane et al., 2020).

L'approche *multimarqueurs* ciblant différents compartiments est intéressante pour démêler les effets des contaminants sur les biofilms. En revanche, certains biomarqueurs permettent de mesurer les effets des contaminants sur le biofilm de manière plus générale afin d'appréhender au mieux le risque que peuvent encourir les écosystèmes aquatiques (Sabater et al., 2007). On pourra ainsi citer la composition taxonomique (Lavoie et al., 2012; Tlili et al., 2020) ou la qualité nutritionnelle (Guo et al., 2016; Fadhlaoui et al., 2020). La bioaccumulation peut également être utilisé comme biomarqueur d'exposition (Hobbs et al., 2019; Fernandes et al., 2020; Bonnineau et al., 2020). Celle-ci a en effet été démontrée comme étant liée à la structure, à la composition des communautés algales et bactériennes ainsi qu'à leurs fonctions (Duong et al., 2008; Bonet et al., 2013; Lebrun et al., 2015). Néanmoins, des divergences existent dans la littérature suggérant par exemple que l'accumulation est indépendante de la composition de la communauté (Stewart et al., 2015). Toutefois, la composition taxonomique reflète également les effets des contaminants à l'échelle de la communauté. Une exposition peut en effet entraîner le passage d'une communauté sensible à une une progressivement tolérante. Cependant, les approches basées sur la composition taxonomique ne reflètent généralement pas de manière adéquate les relations de cause à effet, et une analyse de toxicité des effets à court terme est souvent nécessaire à l'exemple de l'approche PICT (*Pollution Induced Community Tolerance* ; Tlili et al., 2016; voir section 1.2.3.1). Les techniques récentes de biologie moléculaire (à l'exemple du séquençage d'ADN), de la protéomique ou de la métabolomique sont prometteuses pour mesurer

la tolérance de ces communautés aux contaminants (Bricheux *et al.*, 2013; Friesen *et al.*, 2017; Gonçalves *et al.*, 2018).

Par leur complexité et leurs rôles écosystémiques, les biofilms sont susceptibles d'avoir de multiples interactions avec tous types de contaminants et influencer leur devenir dans l'environnement (Edwards & Kjellerup, 2013). En effet, que ce soit pour leurs capacités de sorption, d'accumulation ou de séquestration, les biofilms peuvent donc être considérés comme des systèmes d'alerte précoce pour la détection des effets de contaminants sur les milieux naturels (Bonnineau *et al.*, 2020).

1.2.2 Les métaux, devenir dans l'environnement et effets sur le biofilm

1.2.2.1 Contexte d'aujourd'hui : entre exploitations minières, enjeux économiques et législation

Depuis l'ère industrielle, les activités minières représentent un pôle économique en constante croissance. En effet, la demande en métaux est en augmentation depuis plus d'un siècle. Rien qu'au Canada, ce sont plus de 60 minéraux différents qui sont exploités dans plus de 200 mines en cours d'exploitation. À titre d'illustration, le Canada est le plus grand producteur mondial de potasse et fait partie des producteurs mondiaux les plus importants de métaux comme l'aluminium (Al), le cobalt (Co), le nickel (Ni) et l'or (Au). Cependant, les actifs miniers canadiens ne s'arrêtent pas aux frontières nationales. Les compagnies canadiennes exploitent en effet dans plus d'une centaine de pays étrangers pour des valeurs d'actifs miniers de l'ordre de 250 G\$ CAD. Ce secteur économique représente ainsi 3,3% du PIB total du pays et emploie près d'un demi-million de personnes (Ressources naturelles Canada, 2016). De plus, le Canada est loin d'être le seul pays à avoir d'importants actifs dans le domaine de l'exploitation minière (Graedel & Cao, 2010). Pourtant, suite à ce contexte économique positif peuvent découler des problèmes environnementaux notamment dus aux rejets urbains et industriels dans les eaux naturelles. La question de la qualité de l'eau et de l'accès à l'eau potable peut engendrer des conflits sociétaux allant de l'échelle locale à mondiale (Shoreman-Ouimet & Kopnina, 2015; Murguía *et al.*, 2016). En effet, on estime aujourd'hui qu'environ 80 % des eaux utilisées par l'Homme sont rejetées dans l'environnement sans aucun traitement. Des études ont en effet montré qu'environ 65 % des rivières dans lesquelles sont déversés des rejets d'origine anthropique sont dans un état passable à médiocre (Nations-Unies, 2018). Ceci est à remettre dans un contexte de croissance

démographique avec une demande mondiale en eau potable augmentant d'environ 1% par an (Vörösmarty *et al.*, 2010). Il apparaît donc crucial d'améliorer les pratiques existantes, mais aussi de développer de nouveaux outils de détection et de suivi des contaminations anthropiques. Il existe cependant de nombreuses réglementations et législations qui permettent d'encadrer les activités productrices de rejets. Les critères de la bonne qualité des écosystèmes aquatiques en matière de concentrations métalliques varient d'un pays à l'autre. Au Canada, les recommandations du Conseil canadien des ministres de l'Environnement (CCME) sont souvent citées comme référence (Conseil canadien des ministres de l'Environnement, 2018) et la plupart des nouveaux projets miniers sont assujettis à la *Loi canadienne sur l'évaluation environnementale* (LCEE 2012; Justice, 2012). Au Québec, l'industrie minière doit respecter les critères établis dans la *Loi sur la qualité de l'environnement (LQE)* (article 22 de la LQE ainsi que la *Directive 019*; Québec, 2017) ainsi que dans la *Loi sur les mines* (Québec, 1988). Pour autre exemple, dans le cas de la France et plus généralement de l'Union européenne (UE), ce sont souvent les normes de qualité environnementale (NQE) de la directive-cadre sur l'eau (DCE) qui font office de critères pour la protection de la vie aquatique (exemple de la *Directive 2013/39/UE*; Parlement européen et Conseil de l'Union européenne, 2013). La mise en place de l'*European Union's Registration, Evaluation, Autorisation and Restrictions of Chemicals (REACH)* participe aussi à la protection de l'environnement puisqu'elle correspond à la principale réglementation sur les produits chimiques de l'UE.

1.2.2.2 Cycle naturel des métaux et perturbations anthropiques

Les métaux sont naturellement présents dans la croûte terrestre. Ils se retrouvent dans les écosystèmes aquatiques sous différentes formes chimiques, souvent à l'état de trace, et leurs concentrations varient selon la géologie de la région (Figure 1-3). En effet, c'est en grande partie les produits de l'érosion des sols par l'eau qui vont déterminer la composition physico-chimique des eaux naturelles. Outre l'érosion de la roche, d'autres phénomènes sont impliqués dans le passage des métaux vers les eaux naturelles. Ces processus peuvent là encore être d'origine naturelle comme anthropique. D'un point de vue naturel, les mécanismes principaux sont l'érosion physique et chimique (vent, eau ou activité biologique) et le transport atmosphérique (éruption volcanique, transport de poussière par le vent). Les composés majeurs régissant la composition chimique des eaux naturelles sont au nombre de 15 : H, C, N, O, Na, Mg, Al, Si, P, S, Cl, K, Ca, Mn et enfin Fe. Les ions majeurs, par exemple le Ca, le Mg et le K, sont présents à des

concentrations de l'ordre du mg/L. Les autres éléments, incluant les métaux, sont naturellement présents à l'état de trace, c'est-à-dire à de faibles concentrations, le plus souvent de l'ordre du µg/L ou du nmol/L (Shoreman-Ouimet & Kopnina, 2015). Comme ils sont liés à la géologie des sols, on parle alors de « fond géochimique ». Le défi est alors de bien dissocier le « bruit de fond » naturel d'une potentielle contamination anthropique. Les sources anthropiques sont souvent reliées aux rejets industriels (Lavoie *et al.*, 2012), urbains (Faburé *et al.*, 2015) et agricoles (Nagajyoti *et al.*, 2010). Les métaux peuvent alors être rejetés de manière ponctuelle dans l'environnement (exemple des effluents urbains/miniers ou rejets atmosphériques), ou de manière diffuse (exemple du lessivage ou de la percolation de sites industriels).

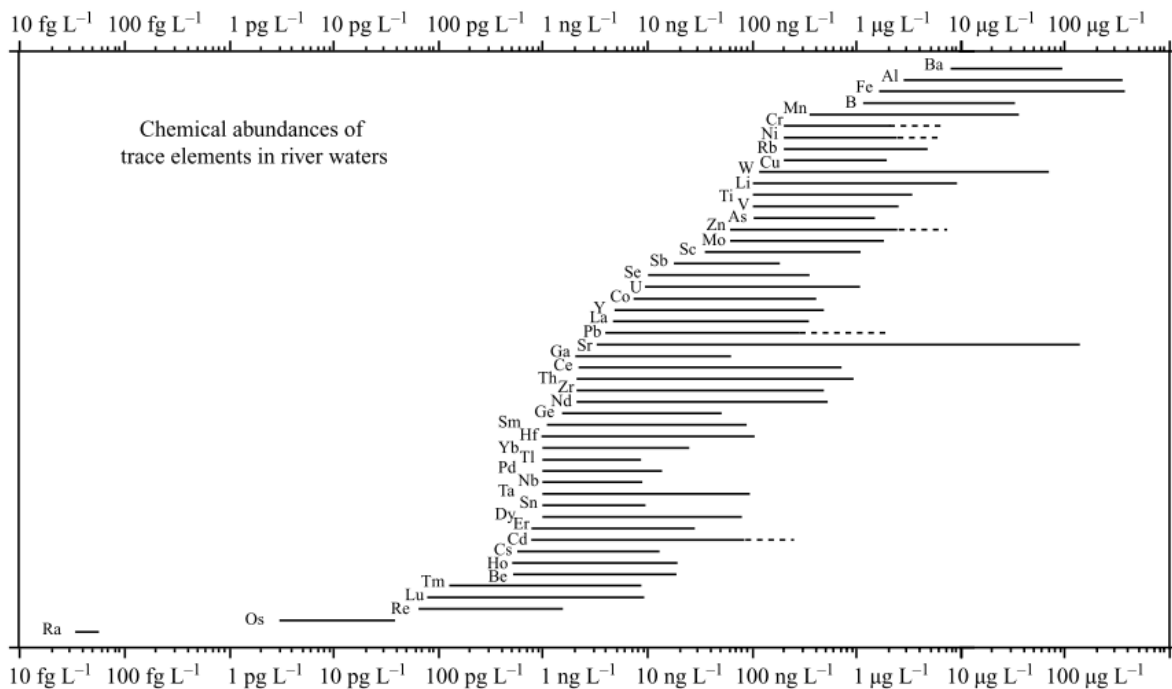


Figure 1-3 : Représentation graphique de l'ordre et de la magnitude des concentrations naturelles des éléments traces sous forme dissoute dans les milieux lotiques (valeurs moyennes mondiales). Tirée de Gaillardet *et al.* (2004).

De nombreuses études ont fait état de fortes contaminations métalliques en lien avec les activités anthropiques, et ceci aussi bien pour des pays en voie de développement (Islam *et al.*, 2015; Duan & Tan, 2013; Thi *et al.*, 2006) que pour des pays dits développés (Ancion *et al.*, 2013; Faburé *et al.*, 2015; Leguay *et al.*, 2016). Lorsque les concentrations en éléments traces sont

supérieures au fond géochimique, le cycle naturel des éléments peut être perturbé. Par exemple, Leguay *et al.* (2016) ont fait état de concentrations dissoutes en métaux divalents (Cu, Cd, Zn, Pb) supérieures aux recommandations du CCME dans des rivières adjacentes à des sites miniers abandonnés au Québec (Canada). Les auteurs ont en effet retrouvé des concentrations en Cu pouvant aller jusqu'à environ 2 mg/L. Le cuivre peut être d'origine géogénique avec des concentrations naturelles de l'ordre du ng/L au µg/L dans les eaux de surfaces (Gaillardet *et al.*, 2003). Une concentration de l'ordre du mg/L implique donc, dans la quasi-totalité des cas, des sources anthropiques qu'elles soient directes ou indirectes. Pour citer d'autres exemples, Mandal *et al.* (2002) ont retrouvé des concentrations avoisinant les 430 µg/L de Ni dans la région de Sudbury et plus spécifiquement dans la rivière Copper Cliff qui reçoit les rejets d'effluents de la mine Copper Cliff encore en activité aujourd'hui. Plus récemment, et dans la même région d'étude, Lavoie *et al.* (2018) ont montré des concentrations de l'ordre du mg/L au niveau de la rivière Frood Branch Creek, également réceptrice d'effluents miniers. En France, dans la rivière du Riou Mort, les concentrations retrouvées dans les eaux étaient bien supérieures au milieu de référence et pouvaient aller jusqu'à 49 µg/L de Cd et presque 3 mg/L de Zn (Morin *et al.*, 2008). Si des perturbations existent avec des concentrations dissoutes en métaux anormalement élevées, reste à savoir comment se comportent ces métaux dans les environnements aquatiques.

1.2.2.3 Concept de spéciation, de ligands et de biodisponibilité

Dans les eaux naturelles, les métaux ont la particularité d'être présents sous plusieurs formes chimiques en plus d'être infiniment persistants. Ces formes sont très variables et possèdent donc des caractéristiques de mobilité, de biodisponibilité et de toxicité différentes. Elles peuvent être regroupées en deux grandes familles : (1) le particulaire ; et (2) le dissous. Dans la première catégorie, se retrouvent : (a) les solides à l'exemple des oxydes comme (b) les métaux adsorbés sur les particules ($> 0,45 \mu\text{m}$). Dans la catégorie du dissous, les métaux peuvent être sous forme : (c) d'ions libres, (d) de complexes (c'est-à-dire liés à des ligands organiques ou inorganiques), ou encore (e) colloïdale (associés à un colloïde de taille comprise entre 1 nm et 0,45 µm). Une sixième catégorie pourrait cependant être ajoutée : la partie constitutive du vivant, c'est-à-dire présente à l'intérieur des organismes vivants (Tercier-Waeber *et al.*, 2012). Lorsque l'on s'intéresse au comportement d'un métal, le concept de spéciation est fondamental, car il régit autant le devenir que les impacts qu'un métal sera susceptible d'avoir dans son environnement et donc sur le vivant (Figure 1-4; Campbell *et al.*, 2002; Lavoie *et al.*, 2016; Zhao *et al.*, 2016).

Les composés majeurs (organiques comme inorganiques) régissent en grande partie la composition chimique des eaux naturelles. Ils contrôlent donc les réactions chimiques de base et par conséquent, le devenir des éléments traces dans les milieux naturels (Tercier-Waeber *et al.*, 2012; Zhao *et al.*, 2016).

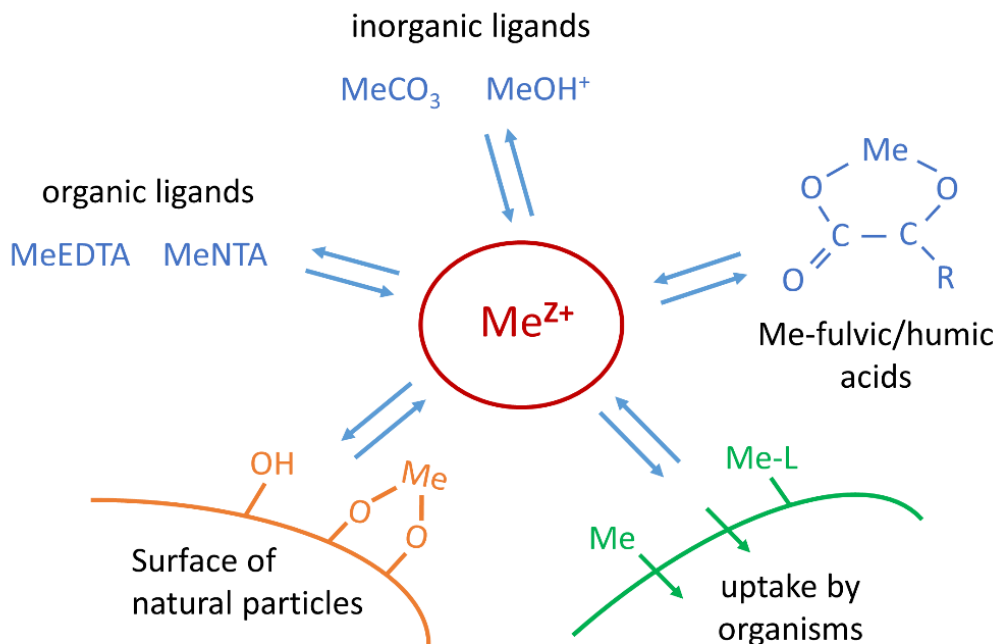


Figure 1-4 : Classification des interactions majeures entre les principaux composés et les métaux traces présents dans les écosystèmes aquatiques. Tirée de Wehrli & Behra (2015). Me = métal. EDTA = acide éthylènediaminetétraacétique. NTA = acide nitrilotriacétique.

L'ensemble des différentes formes chimiques se rapportent donc à la spéciation métallique et les processus impliqués sont divers. Certaines variables environnementales ou paramètres physico-chimiques agissent directement sur ces processus à l'exemple du pH qui influence la complexation des éléments métalliques (Tercier-Waeber *et al.*, 2009; Vidali *et al.*, 2010; Tercier-Waeber *et al.*, 2012). En effet, à pH acide, la quantité de protons H^+ dans le milieu augmente, accroissant ainsi la compétition avec des métaux sous forme libre pour des sites de complexation, notamment avec des ligands organiques comme inorganiques (Leguay *et al.*, 2016; Laderriere *et al.*, 2020). Les métaux auront alors une plus grande prévalence à se retrouver sous leur forme libre. De la même manière, un autre paramètre influençant les réactions chimiques dans les eaux de surface est la dureté de l'eau relative à la quantité de cations majeurs présents dans l'eau.

(exemple du Ca et du Mg). Les cations peuvent par exemple jouer un rôle de compétition envers les métaux pour certains sites de complexation tout comme les protons (Fortin *et al.*, 2007; Leguay *et al.*, 2016; Laderriere *et al.*, 2020). Les variables abiotiques comme la température ou la lumière (composition spectrale, photopériode ou intensité lumineuse) peuvent également jouer un rôle direct ou indirect sur la spéciation des métaux (Tercier-Waeber *et al.*, 2012; Worms *et al.*, 2015; Cheloni & Slaveykova, 2018). Par exemple, l'intensité lumineuse est susceptible d'avoir un effet d'altération sur la structure de certains ligands organiques, et notamment la matière organique dissoute (MOD), pouvant mener à une diminution de leur capacité de complexation (Worms *et al.*, 2015; Cheloni & Slaveykova, 2018).

Les ligands peuvent être de nature inorganique (carbonates, hydroxydes, etc.) ou organique (Figure 1-4 ; acides humiques, acides fulviques, acides aminés, etc). Comme dit précédemment, l'un des paramètres physico-chimiques les plus importants en relation avec la spéciation est le pH. À pH acide, les ligands complexant majoritairement les métaux seront les acides forts tels que les sulfates, les chlorures et les fluorures. À pH plus élevé, les acides faibles comme les carbonates et l'eau vont dominer les réactions de complexation des métaux. Si la spéciation dépend donc de paramètres physico-chimiques comme le pH, elle dépend aussi du type de ligands présents et de leur concentration (Sulzberger & Durisch-Kaiser, 2009; Tercier-Waeber *et al.*, 2012; Mueller *et al.*, 2012). À ce titre, la matière organique dissoute joue un rôle particulièrement important comme ligand. Elle correspond en effet à des molécules hétérogènes que ce soit sur le plan de la structure, de la charge ou des groupements fonctionnels. Elle est notamment riche en groupements carboxyliques et phénoliques qui sont connus pour lier les cations métalliques (Mueller *et al.*, 2012). Les ligands peuvent aussi découler du métabolisme des organismes. En effet, la synthèse de chélateurs ou de polymères extracellulaires, l'excrétion d'excréments et les débris biologiques sont autant de ligands potentiels susceptibles d'influencer la spéciation chimique des éléments (Tercier-Waeber *et al.*, 2012; Tonietto *et al.*, 2015; Loustau *et al.*, 2019). Enfin, les colloïdes et particules peuvent également jouer le rôle de ligand (par complexation ou adsorption).

Tous ces paramètres modifient la spéciation des métaux, mais influencent également l'accumulation de ces composés par les organismes vivants. Selon les multiples formes sous lesquels peuvent être présents les métaux, cela peut affecter la biodisponibilité et la toxicité. Le métal biodisponible est le métal susceptible d'être assimilé par les organismes. La réactivité du métal, c'est-à-dire l'activité des ions de métal libre, détermine l'étendue des réactions de celui-ci avec les sites cellulaires de surface et donc sa biodisponibilité (Campbell, 1995). La

biodisponibilité est un concept permettant de relier quantitativement les changements dans les concentrations et la spéciation des métaux avec l'intensité des effets biologiques induits sur le biote (Tercier-Waeber *et al.*, 2012). Dans la grande majorité des cas, la biodisponibilité et la toxicité dépendent de la concentration en ions libres (Campbell *et al.*, 2002). Pour provoquer un effet biologique, le métal doit d'abord réagir avec des sites récepteurs sur la membrane biologique, souvent (mais pas nécessairement) suivi d'un transport à travers la membrane. Une fois à l'intérieur de la cellule, les métaux interagissent avec différents composants intracellulaires et affectent ainsi les processus cellulaires (Campbell *et al.*, 2002; Tercier-Waeber *et al.*, 2012; Zhao *et al.*, 2016).

1.2.2.4 Métaux d'étude

Le projet s'est articulé autour d'un partenariat avec la mine *Nunavik Nickel* exploitée par *Canadian Royalties Inc* qui est une société minière privée basée à Montréal et appartenant à la compagnie chinoise *Jilin Jien Nickel Industry Co., Ltd.* La mine *Nunavik Nickel* exploite majoritairement le Cu et le Ni, c'est donc naturellement que le projet s'est intéressé à ces métaux. Étant des métaux divalents (M^{2+}), les autres métaux de même configuration électronique ayant une large gamme de variation de concentrations ont été étudiés, c'est le cas notamment du Cd.

Tableau 1-1 : Concentrations typiques en Cd, Cu et Ni dans des rivières déterminées après filtration (0.2 µm) et acidification (Gaillardet *et al.*, 2004, cités par Tercier-Waeber *et al.*, 2012).¹ Gamme de concentrations totales dissoutes mesurées (et moyenne mondiale). Adapté de Tercier-Waeber *et al.* (2012).

Métal	Concentrations (nM) ¹
Cd	0,009 – 1,6 (0,7)
Cu	3,6 – 40,9 (23,3)
Ni	3,4 – 85,2 (13,6)

Le Nickel (Ni)

Du point de vue de sa spéciation, le Ni est le plus souvent retrouvé dans les eaux naturelles sous sa forme libre Ni^{2+} ou hexahydratée $(\text{Ni}(\text{H}_2\text{O})_6)^{2+}$. Il peut néanmoins former des complexes avec des ligands comme les carbonates. Il peut également se lier avec des ligands organiques comme la matière organique dissoute, mais dans une moindre mesure que d'autres métaux à l'exemple du Cu (Mueller *et al.*, 2012; Macoustra *et al.* 2020; Macoustra *et al.* 2021). Il est connu comme étant un oligo-élément notamment pour certaines espèces de plantes, d'invertébrés, d'oiseaux et de mammifères (Ronald, 1990). Chez les procaryotes, il existe une famille de transporteurs *NicO* qui correspond à des transporteurs du Ni et du cobalt et qui permettent de fournir ces deux métaux aux organismes pour la biosynthèse de molécules comme la cobalamine (aussi connue sous le nom de vitamine B12), de la Ni-uréase, etc. (Blaby-Haas & Merchant, 2012). À l'inverse, les organismes ne possédant pas d'uréase (enzyme spécialisée dans la dégradation de l'urée) n'ont pas nécessairement besoin du Ni pour leur métabolisme et n'ont donc pas forcément de récepteurs spécifiques à son import. La présence de *NicO* dans les génomes des algues dépourvues d'enzymes dépendantes de Ni suggère soit qu'il existe une enzyme de Ni non identifiée, soit que *NicO* transporte également d'autres métaux (Blaby-Haas & Merchant, 2012).

Le cuivre (Cu)

Le premier état d'oxydation du cuivre Cu (I) tend à former des complexes plus stables que le Ni, en particulier avec les ligands organiques comme la MOD qui possèdent des groupements thiols (Lavoie *et al.*, 2016; Macoustra *et al.*, 2020a). Il a également une forte affinité pour les ions chlorures. Le Cu (II), lui, s'associe également à la MOD ainsi qu'aux ions hydroxydes et carbonates. Il se retrouve donc peu sous sa forme libre, il est en effet en grande proportion sous forme complexée (Fortin *et al.*, 2010). De plus, les paramètres physico-chimiques des eaux comme le pH ou la concentration en ligands influencent de manière importante sur la spéciation de ce métal et donc sur les proportions retrouvées sous sa forme libre (Fortin *et al.*, 2010). C'est également un oligo-élément, il a par conséquent des voies d'entrée dans les cellules qui lui sont dédiées. Plusieurs familles d'organismes de plantes (*Embryophyta*) ou d'algues (*Chlorophyta*, *Rhodophyta*, *Bacillariophyta*, etc.) possèdent des transporteurs CTR (*Copper Transporters*) ou des transporteurs Cu-ATPase (Blaby-Haas & Merchant, 2017). Les CTR sont des transporteurs spécifiques au Cu (I) impliqués dans l'import de celui-ci tandis que les Cu-ATPase gèrent l'export du Cu (I) hors des cellules. Ces systèmes de transport sont associés à des enzymes

membranaires qui sont connues comme réduisant le Cu(II) en Cu(I) en milieu aérobie permettant ainsi sa prise en charge en Cu(I) par les CTR (exemple de la réductase cuprique et de la réductase ferrique ; Blaby-Haas & Merchant, 2012; Lavoie *et al.*, 2016).

Le cadmium (Cd)

Le Cd est relativement stable dans les eaux douces naturelles et reste en très grande majorité sous forme ionique Cd²⁺. Cependant, dans certaines conditions basiques, il peut former des complexes avec des ligands organiques ou inorganiques en proportion notable (Lavoie *et al.*, 2016; Worms *et al.*, 2015). Cette tendance est bien moins moindre en comparaison d'autres métaux comme le Cu. Pour prendre un exemple d'étude en contexte minier, Fortin *et al.* (2010) ont déterminé que le Cd sous forme ionique (Cd²⁺) pouvait représenter jusqu'à 80 % de la proportion du Cd totale dans des rivières d'Abitibi (QC, Canada). À titre de comparaison, dans le cas du Cu, la proportion sous forme libre dans les zones étudiées ne dépassait pas les 30 %. De plus, le Cd est un métal qui a longtemps été considéré comme n'ayant aucune fonction biologique. Cependant, il semble y avoir des exceptions notamment avec l'exemple d'une diatomée marine *Thalassiosira weissflogii* qui peut utiliser le Cd (Lane & Morel, 2000). Il est néanmoins connu comme étant très toxique. Des études ont montré que le Cd sous forme ionique (Cd²⁺) pouvait emprunter les transporteurs membranaires du Zn²⁺ (Lavoie *et al.*, 2012a) chez l'algue verte *Chlamydomonas reinhardtii*, mais aussi ceux du Mn²⁺ (Sunda & Huntsman 2010) chez la diatomée *Thalassiosira oceanica*. Il est donc intéressant de noter ici que, selon l'organisme considéré, les voies d'exposition peuvent être différentes (importance du choix du modèle biologique) tout comme les voies d'entrée dans l'organisme (différents types de canaux impliqués selon les espèces).

1.2.2.5 Interaction des métaux avec le vivant et modèle du ligand biotique

Si certains métaux n'ont aucune fonction biologique connue à l'exemple, du Hg(II) et du Pb(II) (Arini *et al.*, 2013; Le Faucher *et al.*, 2014), d'autres sont essentiels à la vie (Cu(II), Zn(II), Fe(III), Mn(II), Co(II), Ni(II), Mo(IV), V(V), etc. ; Tercier-Waeber *et al.*, 2012; Blaby-Haas & Merchant, 2017). Ainsi, essentiel ou non, la question de la concentration de ces éléments est importante à l'exemple de la citation « Tout est poison et rien n'est poison ; c'est la dose qui fait le poison »

(Paracelse ; 1537). Ce concept, à la base de la pharmacologie, s'applique également pour les organismes aquatiques en milieu naturel. Ils peuvent ainsi induire une toxicité parfois même à de très faibles concentrations (Nagajyoti *et al.*, 2010).

Au cours de l'évolution, les cellules ont développé des moyens de réguler l'absorption des métaux essentiels tout en minimisant l'internalisation des métaux non essentiels qui pourraient interférer avec le métabolisme cellulaire (Pen *et al.*, 2006; Blaby-Haas & Merchant, 2012). À ce titre et comme mentionné précédemment, les membranes biologiques (dépendamment des espèces considérées) possèdent différentes familles de protéines impliquées dans le transport des métaux qui varient selon leurs fonctions et leurs structures (Campbell *et al.*, 2002). Ils permettent ainsi à ces organismes de subvenir à leurs besoins en métaux essentiels et ainsi d'éviter les phénomènes de carence et/ou de toxicité (Blaby-Haas & Merchant 2017). Cependant, ces systèmes n'étant pas totalement spécifiques aux oligo-éléments, certains éléments non essentiels peuvent passer à travers les membranes biologiques et potentiellement interférer avec l'homéostasie cellulaire. En effet, les cellules ne sont pas seulement limitées par la biodisponibilité de ces éléments mais aussi par leur abondance (Blaby-Haas & Merchant, 2012). Les mécanismes de transport d'import/d'export des métaux à travers les membranes biologiques peuvent donc être régulés selon les pressions géochimiques et ce, de manière non nécessairement spécifique. Par exemple, Lavoie *et al.* (2012a) ont montré que des variations de la concentration en Zn^{2+} pouvaient influer sur l'internalisation du Cd chez *Chlamydomonas reinhardtii*. À l'inverse, la concentration en Cd^{2+} influe sur l'internalisation du Zn^{2+} par un effet de rétrocontrôle en raison de la forte affinité de ces deux métaux pour les voies de transports du Zn.

La question de la concentration des possibles compétiteurs comme les cations majeurs (Ca^{2+} , Mg^{2+} , Na^+ , K^+ , etc.) est également un point très important dans l'évaluation de la toxicité des métaux, car ils vont jouer le rôle de protecteur par compétition ionique (Deleebeeck *et al.*, 2009; Leguay *et al.*, 2016; Laderriere *et al.*, 2020). Afin de bien comprendre l'interaction des métaux avec la surface des membranes biologiques et donc la biodisponibilité de ceux-ci, des modèles ont été développés, à l'exemple du modèle du ligand biotique (*Biotic Ligand Model*, BLM). Quand on fait référence au BLM, il est important de parler de son prédecesseur, le modèle de l'ion libre ou *free-ion activity model* (FIAM) (Lavoie *et al.*, 2016). Ce sont tous deux des modèles décrivant les processus de prise en charge des métaux par les organismes vivants. Dès les années 1970, le FIAM fut développé, principalement en milieu marin, sur le principe que la toxicité d'un métal ainsi que son internalisation sont proportionnelles à l'activité de l'ion libre M^{Z+} considéré. Beaucoup d'études ont suivi et ont démontré que la réponse biologique à la suite d'une

exposition en métaux était bel et bien proportionnelle à sa concentration sous forme libre (Lavoie *et al.*, 2016). Le BLM part également du principe très simple que pour qu'un métal soit毒ique, il doit au préalable interagir avec la surface biologique et par la suite être transporté à l'intérieur des cellules vivantes. Son objectif est donc de prédire au mieux comment les métaux dissous dans l'eau vont réagir et éventuellement affecter les organismes aquatiques (Erickson, 2013). Il continue également de considérer que la biodisponibilité et la toxicité d'un métal sont liées à sa concentration en ions libres dans l'eau, mais a l'avantage d'incorporer les effets compétitifs des ions en solution.

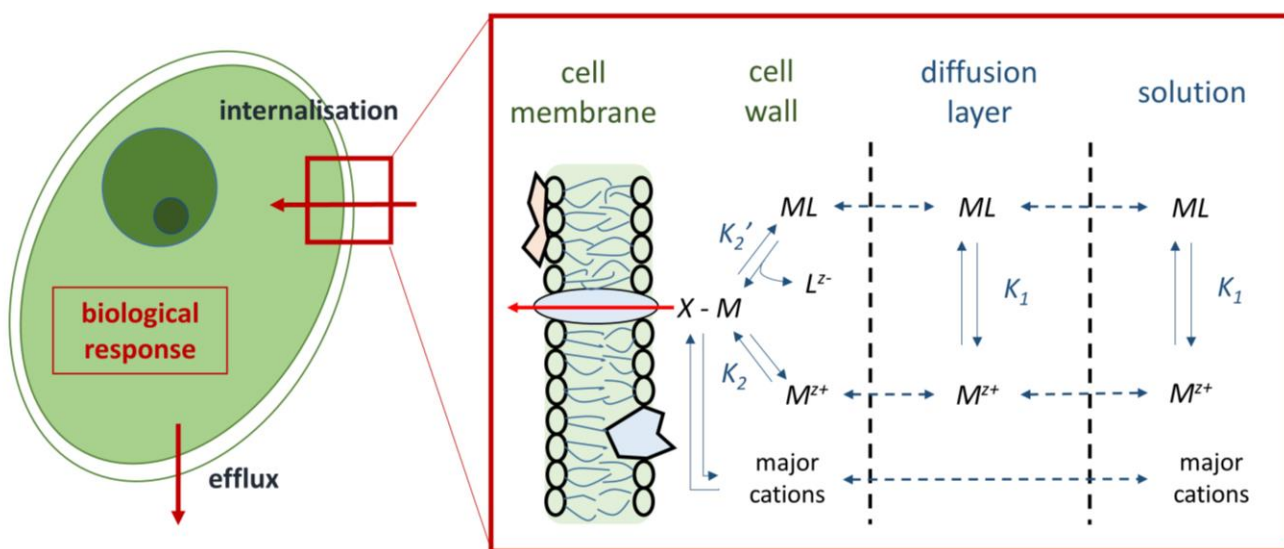


Figure 1-5 : Mode d'interaction d'un ion métallique à la surface biologique selon le modèle du ligand biotique.
 M^{2+} = ion métallique libre; ML = métal complexé; L^{2-} = ligand (acides aminés, citrate, $S_2O_3^{2-}$, CO_3^{2-} , Cl^- , etc.); X-M = métal complexé à la surface cellulaire. Adaptée de Lavoie *et al.* (2016).

Les différentes étapes nécessaires au métal pour accéder à la membrane biologique sont présentées dans la Figure 1-5. Selon la forme chimique sous laquelle est présent le métal M (forme complexée : ML ; forme libre : M^{2+}), plusieurs voies d'interactions sont possibles avec la membrane biologique des organismes. Le récepteur X représente ici le site clé permettant au métal M d'interagir physiologiquement avec la cellule. K_1 correspond à la constante d'équilibre décrivant la réaction de complexation du métal M avec un ligand L^{2-} (à noter que les charges pouvant être différentes entre M et L , celles-ci seront omises par souci de simplicité). Ces

réactions sont supposées à l'équilibre (Di Toro *et al.*, 2001). L'équation (1) ci-dessous permet de calculer K_1 .

$$K_1 = \frac{[ML]}{[M^{Z+}]. [L^{Z-}]} \quad (1)$$

Selon la Figure 1-5, deux possibilités se présentent : (1) le métal est sous sa forme libre M^{Z+} et diffuse jusqu'à atteindre la membrane plasmique avec laquelle il forme le complexe $X-M$; (2) le métal forme un complexe avec un ligand organique (MOD, acide aminé, etc.) ou inorganique (carbonates, sulfures, chlorures, etc.) et il interagit alors avec le site cellulaire X pour former le complexe $X-M$ en libérant ainsi son ligand sous la forme L^{Z-} .

L'équation (2) permet de décrire la complexation du métal sous sa forme libre M^{Z+} avec les transporteurs membranaires X . {} et [] indiquent respectivement les concentrations à la surface biologique et dans le milieu.

$$K_2 = \frac{\{cellule - X - M\}}{[M^{Z+}]. \{cellule - X^-\}} \quad (2)$$

L'équation (3) s'intéresse au deuxième cas décrivant l'interaction du métal cette fois sous sa forme complexée avec un ligand L et le récepteur membranaire noté X .

$$\{cellule - X - M\} = K'_2 \frac{\{cellule - X^-\}[ML]}{[L]} \quad (3)$$

L'équation (4) décrite ci-dessous nous montre que la concentration du complexe *cellule-X-M* est fonction de la concentration en métal libre dans le cas où le complexe ML réagirait avec le site cellulaire X par échange de ligands.

$$\{cellule - X - M\} = K_1 \cdot K'_2 \{cellule - X^-\}[M^{Z+}] \quad (4)$$

Dans tous les cas, la formation du complexe *cellule-X-M* dépend de la concentration en métal libre et ceci, que le métal soit initialement libre et donc sous la forme M^{Z+} ou sous sa forme complexée ML . La toxicité d'un métal pour les organismes aquatiques est donc proportionnelle à la portion du métal sous forme libre. Si ce modèle peut parfois ne pas s'appliquer dans certaines conditions très précises (voir (Zhao *et al.*, 2016) pour une discussion détaillée), il est aujourd'hui un des outils les plus complets pour prédire la toxicité des métaux sur les organismes vivants notamment pour les métaux divalents (Brix *et al.*, 2020; Adams *et al.*, 2020).

1.2.2.6 Mécanismes de toxicité des métaux

Les algues vertes unicellulaires ont beaucoup été utilisées afin d'appréhender le risque écotoxique des métaux : c'est en effet un modèle biologique simple et qui possède un cycle de vie court. Chez ces organismes, une des principales conséquences d'une exposition aux métaux est un stress oxydatif dû à la production d'espèces réactives à l'oxygène (*reactive oxygen species - ROS*) à l'exemple du peroxyde d'hydrogène (H_2O_2) ou de l'oxygène radicalaire (O_2^-) (Szivák *et al.*, 2009; Figure 1-6). Ces ROS peuvent interférer avec les activités enzymatiques liées à la photosynthèse ainsi qu'au niveau des photosystèmes, structures responsables de la photosynthèse (Corcoll *et al.*, 2012). Selon le type de contaminants et d'exposition (aiguë ou chronique), les systèmes antioxydants mis en place ne seront pas forcément les mêmes (Pinto *et al.*, 2003) avec la production par exemple de la superoxyde dismutase (SOD), de la catalase (CAT), du glutathion peroxydase (GPX), etc. (Bonet *et al.*, 2012; Bonnneau *et al.*, 2013; Bonet *et al.*, 2013). Il existe également des systèmes de défense non enzymatiques à l'exemple de la séquestration du métal dans des composés granulaires ou la synthèse de phytochélatines et de caroténoïdes qui sont respectivement des peptides et des pigments antioxydants (Pistocchi *et al.*, 2000; Le Faucheur *et al.*, 2005; Lavoie *et al.*, 2009). Si les mécanismes de gestion sont dépassés, les répercussions peuvent avoir une multitude d'effets en interférant avec la machinerie normale du métabolisme cellulaire (Nagajyoti *et al.*, 2010). Par exemple, la toxicité peut se manifester par une modification de l'intégrité structurelle de la cellule (perméabilité de la membrane, transports membranaires, etc. ; Lavoie *et al.*, 2012b) ou en perturbant les processus métaboliques (inhibition d'enzymes, interaction avec les acides aminés et les protéines, etc. ; Torres *et al.*, 2008). La composition biochimique de la cellule peut également être affectée (Okamoto *et al.*, 2001) tout comme l'expression de certains gènes (Moisset *et al.*, 2015; Kim Tiam *et al.*, 2018).

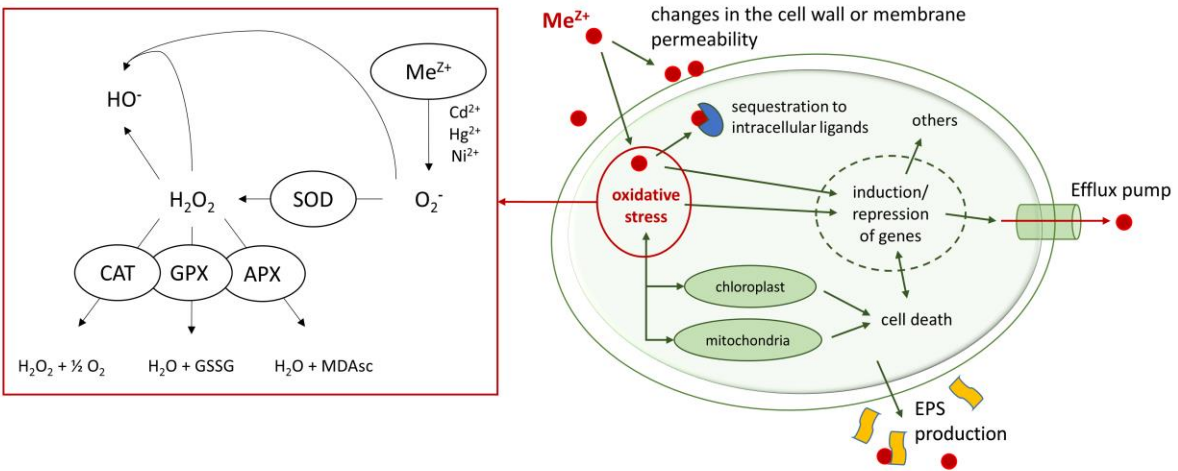


Figure 1-6 : Schéma illustrant la mobilité des métaux dans la cellule qui peut entraîner la production de formes réactives de l'oxygène. L'internalisation de métaux peut modifier la perméabilité membranaire et, une fois dans le milieu intracellulaire, induire un stress oxydatif. D'autres mécanismes peuvent être affectés comme le système photosynthétique de la cellule, l'activité mitochondriale, l'expression génétique, et éventuellement aboutir à la mort cellulaire. Il existe également des systèmes de défense comme la production d'EPS, la complexation des métaux par des ligands intracellulaires ou encore l'expulsion de ceux-ci hors de la cellule. Adapté de Pinto et al. (2003) et Morin et al. (2012).

Le biofilm étant un consortium d'organismes composé de plusieurs ordres du vivant, il apparaît important de raisonner également par rapport aux organismes qui ne possèdent pas de pigments photosynthétiques. En effet, les effets toxiques des métaux peuvent varier selon le paramètre structurel ou fonctionnel considéré. Plusieurs études ont en effet démontré que, suite à une exposition chronique en métaux, l'influence relative sur la vulnérabilité fonctionnelle des communautés microbiennes dépendait de la fonction étudiée à savoir phototrophe ou hétérotrophe (Tlili et al., 2011; Lambert et al., 2012; Pesce et al., 2018). Il apparaît donc important de considérer différents compartiments fonctionnels et différents descripteurs fonctionnels afin de pleinement appréhender la vulnérabilité des biofilms à des expositions aux éléments métalliques (Pesce et al., 2018). Par exemple, bien que le Cu est principalement utilisé comme fongicide,

celui-ci est connu pour affecter tous les règnes. En effet, une exposition chronique au Cu est connue pour entraîner une diminution de la biomasse globale, une modification de la répartition des classes algales ainsi qu'une modification des communautés diatomiques (Serra & Guasch, 2009; Lambert *et al.*, 2012; Morin *et al.*, 2017). Le Cd et le Ni ont été démontrés pour avoir des effets similaires (Morin *et al.*, 2008; Duong *et al.*, 2008; Lavoie *et al.*, 2018; Regenmortel *et al.*, 2018). Le Cu est également connu pour affecter les communautés bactériennes notamment par des effets indirects du fait d'une modification importante des ressources nutritives. Il a en effet été montré que le Cu entraînait des effets sur le rendement photosynthétique des organismes phototrophes (Serra *et al.*, 2009; Oukarroum *et al.*, 2012; Lambert *et al.*, 2017). Cette toxicité induite peut conduire à la sénescence de cellules phototrophes entraînant ainsi une plus forte disponibilité en MO pour les organismes hétérotrophes et donc à terme, induire des changements dans les communautés bactériennes (Massieux *et al.*, 2004; Tlili *et al.*, 2010; Proia *et al.*, 2012). Il a également été démontré qu'une exposition chronique au Cu pouvait diminuer significativement l'activité d'enzymes extracellulaires notamment impliquées dans la dégradation de la MO (Fechner *et al.*, 2011; Lambert *et al.*, 2012; Pesce *et al.*, 2018). D'autres études ont montré des effets des métaux sur les protozoaires de la microméiofaune (Ancion *et al.*, 2013; Balistrieri *et al.*, 2015; Mebane *et al.*, 2020) par des effets directs ou indirects. Par exemple, il existe une relation d'interdépendance du biofilm avec les protozoaires de la microméiofaune par effet de prédation (Ancion *et al.*, 2013; Mebane *et al.*, 2020; Neury-Ormanni *et al.*, 2020). En effet de nombreuses études ont mis en évidence le transfert trophique de métaux bioaccumulés par le biofilm vers les maillons supérieurs à l'exemple du Cd (Xie *et al.*, 2010), du Zn (Kim *et al.*, 2012) ou encore d'autres éléments (Scheibener *et al.*, 2017). De plus, une exposition au Ni peut modifier le profil en acides gras du biofilm (Fadhlaoui *et al.*, 2020). Cette modification peut avoir un impact sur les organismes de niveau trophique supérieur en changeant la qualité nutritionnelle du biofilm (Guo *et al.*, 2016). Les effets toxiques sur les consommateurs primaires peuvent donc entraîner un effet indirect des métaux sur le biofilm qu'ils soient synergiques ou antagonistes. Ces effets toxiques, de par leur effet sur le premier maillon de la chaîne trophique, sont donc susceptibles d'avoir des répercussions sur l'intégralité de l'écosystème.

1.2.3 Biosuivi à grande échelle : variables à prendre en compte pour comprendre la réponse des biofilms face aux métaux

1.2.3.1 Influence de variables biotiques : le concept du « PICT »

Les biofilms peuvent donc être utilisés comme indicateurs biologiques des contaminations métalliques en raison de leur sensibilité et de leur capacité à accumuler les métaux à partir de faibles concentrations dans les eaux de surfaces (Vendrell-Puigmitja *et al.*, 2020). Le concept du « PICT » traduit le fait qu'une communauté exposée de manière chronique à un contaminant devrait, par rapport à une communauté non exposée dite de référence, avoir subi une pression de sélection pour finalement présenter une tolérance accrue à ce contaminant (Blanck *et al.*, 1988; Blanck, 2002; Figure 1-7). En termes de composition taxonomique du biofilm, cette pression peut mener à la sélection d'espèces tolérantes au détriment d'espèces plus sensibles. Ces espèces plus tolérantes sont sélectionnées sur la base de mécanismes d'acclimatation voire d'adaptation et permettent à terme, une plus grande résilience de la communauté face à ce stress. Par exemple, il est bien connu que des contaminations métalliques entraînent des changements structuraux et fonctionnels chez les communautés phototrophiques et que certains de ces changements sont caractéristiques de la présence de hautes concentrations métalliques (Lavoie *et al.*, 2008; Morin *et al.*, 2012; Vendrell-Puigmitja *et al.*, 2020). Dans ce contexte, le concept du PICT vise donc à évaluer la pression de sélection exercée sur les communautés naturelles. Brièvement, il repose sur deux phases : (1) une phase de sélection et (2) une phase de détection (Tlili *et al.*, 2016a). Durant la phase de sélection, les communautés sont exposées de manière chronique au contaminant considéré conduisant à une sélection intra- et interspécifique. Cette sélection entraîne la restructuration de la communauté avec la disparition de certaines espèces au profit d'autres. Lors de la deuxième phase, il est possible de mesurer la tolérance de la communauté exposée et de la communauté non exposée au moyen de tests de toxicité aiguë utilisant différents paramètres fonctionnels. La comparaison des courbes dose-réponse des deux communautés et plus particulièrement des réponses de toxicité calculées telles que les concentrations effectives (EC_x), permet de mettre en évidence leur tolérance. La composition des deux communautés peut également être évaluée et comparée afin de vérifier l'hypothèse d'une sélection intra- et interspécifique.

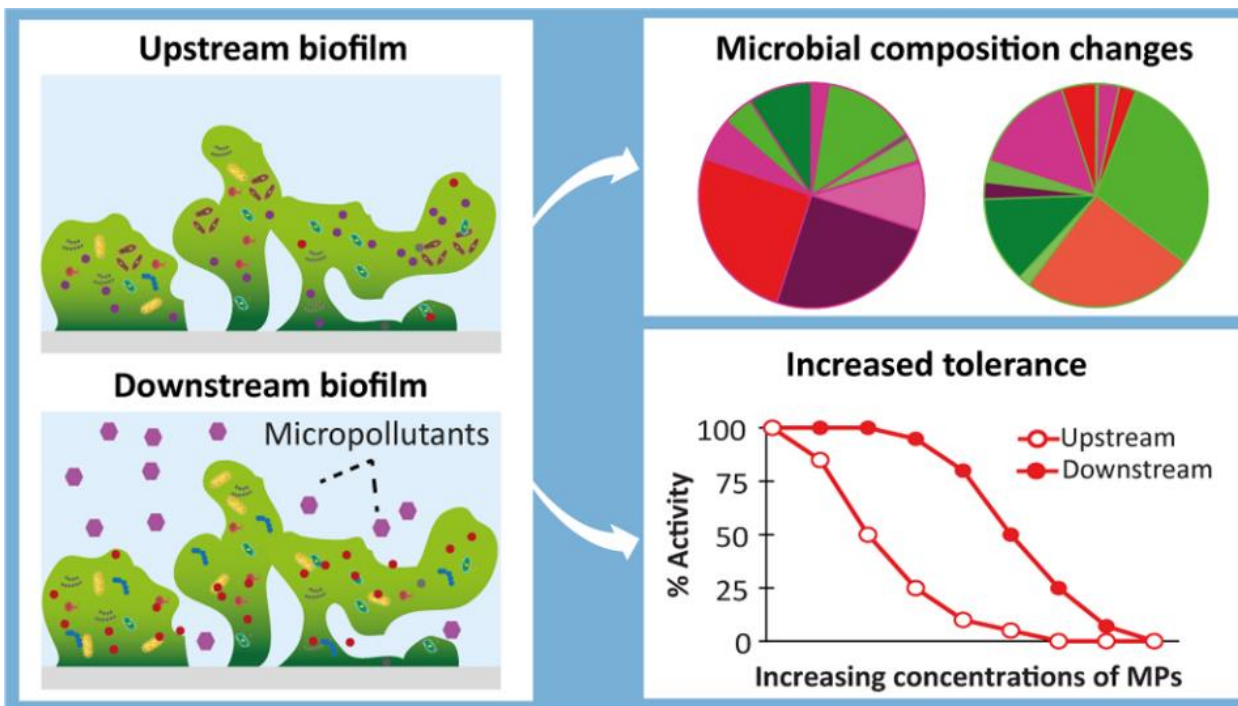


Figure 1-7 : Principe du concept du « PICT » (*Pollution Induced Community Tolerance*). La communauté « downstream » représente une communauté préalablement exposée à un contaminant, devenue plus tolérante, tandis que la communauté « upstream » correspond à une communauté de référence non préalablement exposée. Cette dernière se caractérise par une courbe dose-réponse avec une EC₅₀ plus faible par rapport au pourcentage d'activité du biomarqueur d'effet considéré. Tirée de Tlili *et al.* (2020).

Ainsi l'approche PICT permet de savoir si le biofilm est un bioindicateur pertinent en s'intéressant aux liens existants entre expositions aux contaminations et des changements significatifs (structure et diversité) conduisant à une tolérance accrue. Plusieurs études ont démontré l'acquisition de tolérance des communautés phototrophiques lorsque celles-ci étaient exposées de manière chronique aux contaminations métalliques. En effet, des marqueurs fonctionnels tels que le rendement photosynthétique ou les concentrations en chlorophylle-a se sont montrés efficaces dans ce type d'approche (Foulquier *et al.*, 2015; Lambert *et al.*, 2017; Pesce *et al.*, 2018; Tlili *et al.*, 2020). De manière similaire, d'autres études ont utilisé l'approche PICT avec succès sur le compartiment hétérotrophe du biofilm utilisant différents marqueurs fonctionnels à l'exemple de la respiration microbienne (Tlili *et al.*, 2011) ou encore de l'activité enzymatique de la β-glucosidase ou de la leucine-aminopeptidase (Fechner *et al.*, 2011; Fechner *et al.*, 2012; Pesce *et al.*, 2018; Tlili *et al.*, 2020). Toutes ces études, qui utilisent l'approche du PICT, ont permis de montrer que les changements dans les descripteurs utilisés traditionnellement en écotoxicologie peuvent fournir une information pertinente sur l'historique

d'exposition et les altérations résultantes pour les biofilms d'eau douce. Néanmoins, un défi majeur dans l'évaluation des risques environnementaux des contaminants est d'établir une relation causale entre exposition et effets au regard de la diversité fonctionnelle et structurelle des biofilms périphytiques d'eau douce (Tlili *et al.*, 2020). Ceci permettra à terme de distinguer l'effet spécifique des contaminants de ceux des facteurs environnementaux sur les communautés périphytiques d'eau douce.

1.2.3.2 Influence de variables abiotiques : du facteur environnemental au facteur de stress environnemental

Le biofilm étant en constante interaction avec son environnement, un point crucial en écotoxicologie est de démêler les effets d'une exposition aux contaminants de ceux dus à des différences dans des variables physiques, chimiques ou biologiques (qui peuvent conduire à un stress environnemental). En d'autres termes, la tolérance induite sur les communautés exposées ne peut pas toujours être attribuée uniquement à la présence de substances toxiques, car divers facteurs environnementaux peuvent également être impliqués (Holmstrup *et al.*, 2010; Laskowski *et al.*, 2010). Par exemple, Tercier-Waeber *et al.* (2009) ont montré des corrélations entre concentrations en métaux dissous, température et pH. En effet, au cours d'une journée, l'intensité lumineuse stimule l'activité photosynthétique entraînant une augmentation du pH tandis que la température peut varier avec l'ensoleillement (en particulier pour les cours d'eau à faible hauteur de colonne d'eau). Ainsi, au même titre que lorsque les métaux sont présents en mélange, ces facteurs peuvent avoir des effets indépendants, antagonistes ou synergiques (Nys *et al.*, 2018) et ainsi influencer la réponse du biofilm à des contaminations métalliques. Les facteurs environnementaux peuvent induire un stress comme être bénéfiques pour les microorganismes ce qui pourrait atténuer les effets négatifs des contaminants (Tlili *et al.*, 2020). Si l'on prend l'exemple de la lumière, la pénétration de celle-ci dans la colonne d'eau est influencée par la physico-chimie des eaux comme les concentrations en MOD ou la présence de particules. De son côté, la composition de la MOD est connue comme étant sous l'influence de la lumière, car ces molécules sont photodégradables (Sulzberger & Durisch-Kaiser, 2009; Vidali *et al.*, 2010). Cette photolyse peut devenir un facteur important dans les eaux naturelles, car elle peut conduire à une modification de la spéciation des éléments métalliques et donc de leur biodisponibilité (Worms *et al.*, 2015; Cheloni & Slaveykova, 2018). De plus, la spéciation des éléments métalliques est dépendante de paramètres tels que le pH ou le dioxygène dissous, ces derniers

étant associés aux réactions photosynthétiques de la production primaire (Tercier-Waeber *et al.*, 2009; Tercier-Waeber *et al.*, 2012; Macoustra *et al.*, 2020a). Ces paramètres variant au cours d'une journée (durée, intensité, etc.), ils sont donc susceptibles d'influencer les biofilms périphytiques tout comme leur exposition aux métaux. Si les facteurs environnementaux peuvent agir sur les conditions d'exposition, ils peuvent aussi directement influencer les biofilms d'eau douce. En effet, des études ont démontré que l'intensité lumineuse, la température ou les conditions hydrodynamiques du milieu influençaient significativement la structure et la diversité des biofilms de rivière ainsi que leurs réponses aux contaminations (Villeneuve *et al.*, 2010; Cheloni *et al.*, 2014; Lambert *et al.*, 2016; Chaumet *et al.*, 2019). Par exemple, Friesen *et al.* (2017) ont cultivé un biofilm naturel en microcosmes en présence de Se et pendant 21 jours sous différentes conditions de lumière et de nutriments, et ce, à partir du même inoculum. Les auteurs ont trouvé que les différentes conditions environnementales testées avaient abouti à des biofilms différents en termes de composition taxonomique. Cette modification d'assemblage entraînait des différences significatives dans les concentrations internalisées en Se suggérant que des facteurs autres que la concentration totale de Se dissous dans l'eau influencent l'accumulation de Se dans le biofilm, notamment la composition taxonomique et les caractéristiques physico-chimiques de l'eau. La question est donc de savoir si ces variables environnementales peuvent avoir des effets indépendants, antagonistes ou synergiques à ceux engendrés par une exposition chronique aux éléments métalliques (Cheloni & Slaveykova 2018).

Comme mentionné par Cheloni & Slaveykova (2018), si beaucoup d'études se sont intéressées aux effets combinés de la lumière (et en particulier des UV) sur des cultures algales monospécifiques, peu d'études se sont intéressées aux biofilms périphytiques. Navarro *et al.* (2008) ont étudié les changements induits par les rayons UV et la tolérance au Cd sur des biofilms d'eau douce. L'étude a montré des assemblages différents selon les traitements en UV. De plus, la communauté exposée sous fort rayonnement UV a augmenté sa tolérance aux effets toxiques des UV et a montré une co-tolérance au Cd. Les auteurs ont également démontré que même si l'accumulation de biomasse offrait une certaine protection contre les rayons UV et le Cd, les changements de communauté subis par la communauté à fort taux d'UV ont majoritairement contribué à la tolérance aux rayons UV. De manière similaire, Corcoll *et al.* (2012) a évalué la relation entre les changements d'intensité lumineuse (sans UV) à court terme et la toxicité chronique du Zn des biofilms périphytiques, et ce, après une photo-acclimatation à long terme à différentes conditions lumineuse (25, 100 et 500 $\mu\text{mol photons/m}^2/\text{s}$ respectivement). À l'issue de l'acclimatation, les biofilms présentaient là aussi des caractéristiques structurelles différentes (biomasse, concentrations en chlorophyll-a, EPS, taxonomie, rendement photosynthétique). De

plus, la toxicité du Zn était modulée selon le traitement de photo-acclimatation et les conditions lumineuses lors de l'exposition. En effet, les effets du Zn sur le rendement photosynthétique étaient plus importants lorsque l'exposition de biofilms acclimatés sous faible intensité lumineuse se faisait sous moyenne et haute intensité. Les auteurs ont ainsi mis en lumière le fait que des biofilms acclimatés à moyenne et haute intensité lumineuse montraient une sensibilité plus faible, probablement de par leurs différentes caractéristiques structurales (notamment un plus fort contenu en EPS et une composition taxonomique différente). Ces deux études soulignent le fait que la composition spectrale ou l'intensité de la lumière peuvent représenter des facteurs de stress suffisants pour entraîner une modification de structure qui peut mener à un effet de tolérance aux métaux. Ces résultats suggèrent donc l'importance de prendre en compte le stress environnemental dans une perspective de biosuivi, car ces stress sont susceptibles de modifier la réponse de ces communautés aux contaminations métalliques. L'effet combiné de la température et des métaux a reçu plus d'attention comme facteur environnemental. Par exemple, Lambert *et al.* (2017) ont exposé au Cu un biofilm cultivé à différentes températures et a mis en évidence l'influence de la température à la fois sur la capacité basale du périphyton phototrophe à tolérer une exposition ultérieure au Cu et sur sa capacité à acquérir une tolérance après une exposition chronique au Cu. Les auteurs ont ainsi conclu que la température devait être considérée pour établir des liens de causalité entre l'exposition chronique au Cu et les effets sur le biofilm phototrophique. D'une manière similaire, Pesce *et al.* (2018) se sont intéressés à la réponse du compartiment phototrophe comme hétérotrophe d'un biofilm exposé à plusieurs températures. Les auteurs soulignent que l'influence de la température sur la vulnérabilité des communautés microbiennes phototrophes et hétérotrophes à la toxicité du Cu peut varier fortement selon la fonction étudiée. Cette étude souligne donc l'importance d'étudier différents marqueurs fonctionnels afin d'évaluer au mieux la vulnérabilité du biofilm exposé à de multiples stress. Ce raisonnement reste valable pour d'autres facteurs environnementaux susceptibles d'avoir une influence directe sur le biofilm. D'autres études ont également mis en lumière des variations dans la réponse de toxicité en fonction des concentrations en nutriments dans les milieux aquatiques à l'exemple du phosphore (Serra *et al.*, 2010; Tlili *et al.*, 2010; Bonet *et al.*, 2013). En effet, les communautés phototrophes ont été décrites comme plus tolérantes en conditions riches en nutriments. De même, la tolérance induite des communautés hétérotrophes a été montrée comme positivement influencée par l'exposition du Cu ainsi que du gradient en P, avec une plus grande influence de l'un ou de l'autre selon l'activité enzymatique considérée (Tlili *et al.*, 2010). Les auteurs ont ainsi souligné la possible interaction entre les cycles du carbone comme du phosphore (de par l'activité de la β -glucosidase) et ceux du phosphore et de l'azote

(de par l'activité de la leucine-aminopeptidase) dans un contexte de contamination métallique. Leurs résultats suggèrent premièrement le rôle important que joue le biofilm dans les cycles biogéochimiques de ces éléments et donc dans l'écosystème. Deuxièmement, l'étude permet d'affirmer que la réponse des communautés hétérotrophes aux contaminations métalliques peut au moins en partie être influencée par les concentrations de P dans le milieu d'où l'importance d'une approche multimarqueur. De plus, sur le terrain, Bonet *et al.* (2013) ont montré que des variations saisonnières en concentrations de phosphore, mais aussi de température et d'intensité lumineuse influençaient la réponse de communautés exposées au Zn.

Ainsi, comme déjà mentionné par plusieurs études, la variabilité des facteurs environnementaux rend difficile l'établissement d'un lien de causalité entre l'exposition aux métaux et les effets biologiques observés (Bonet *et al.*, 2013; Faburé *et al.*, 2015; Lambert *et al.*, 2017). Mieux comprendre les interactions de ces différents facteurs de stress est aujourd'hui une des présentes perspectives à explorer en écotoxicologie. Néanmoins, les qualités du biofilm en font un outil prometteur en matière de biosurveillance pour le suivi des conditions stables, mais aussi pour les conditions changeantes, et ce pour tous types de contamination (Hobbs *et al.*, 2019; Bonnineau *et al.*, 2020; Pandey, 2020).

1.3 Structure de la thèse

Cette thèse s'articule autour de trois chapitres visant à comprendre les différents mécanismes influant sur la bioaccumulation des métaux par les biofilms périphytiques dans les écosystèmes d'eau douce. Le but de ce projet est donc d'identifier les paramètres et réponses clés afin d'utiliser le biofilm comme outil de biosuivi des contaminations métalliques dans les cours d'eau et ainsi à terme, mieux protéger les écosystèmes aquatiques des pressions anthropiques.

Les principales questions de recherche sont les suivantes :

1- Quel est le lien entre l'exposition et l'accumulation des métaux dans le biofilm?

L'objectif est de vérifier la capacité du biofilm à prédire la biodisponibilité des métaux et donc de connaître l'exposition du biote dans les milieux aquatiques. La relation entre les concentrations en métaux dans l'eau, leur spéciation (en s'intéressant particulièrement au métal dit « libre ») et

les concentrations retrouvées dans les biofilms a été examinée. Deux régions ayant des sites miniers en activité ont été échantillonnées : la ville de Sudbury en Ontario et le site minier Nunavik Nickel (*Canadian Royalties Inc.*). Ce premier chapitre a permis de mettre en lumière le rôle clé du pH et des effets de compétitions cationiques. Une fois ces paramètres pris en compte, les résultats ont montré qu'il existe une relation linéaire entre concentrations libres des métaux dans l'eau et les concentrations internalisées par le biofilm des deux régions, et ce malgré 1700 km de distance entre ces régions. Une extension de ce chapitre est le développement d'un modèle prédictif des quantités de métaux bioaccumulés se basant sur les caractéristiques biogéochimiques des sites d'étude.

Ce chapitre a fait l'objet d'une publication :

Laderriere V, Le Faucheur S, Fortin C (2021) Exploring the role of water chemistry on metal accumulation in biofilms from streams in mining areas. Sci Total Environ 784:146986
<https://doi.org/10.1016/j.scitotenv.2021.146986>

2- Quelle est la relation entre température, photopériode, accumulation et toxicité des métaux chez le biofilm?

Ce deuxième chapitre vise à explorer si des variations environnementales susceptibles de se produire au sein d'une même saison (ex. température ou photopériode) modifient la bioaccumulation des métaux par le biofilm. Par exemple, il est connu que la température peut modifier le métabolisme des organismes unicellulaires. Ce volet s'intéresse également à mieux caractériser les liens entre toxicité induite et accumulation. Des biofilms ont ainsi été cultivés en microcosmes dans une salle environnementale (à température et photopériode contrôlées) afin de subir des expositions chroniques au Ni. Le Ni a été choisi en fonction du manque de données concernant ce dernier en comparaison d'autres métaux primaires (ex. du Cu, Zn, Pb, Cd). Les résultats ont permis de montrer des réponses différentes selon les conditions environnementales testées. Ainsi, un biofilm ayant été exposé aux mêmes concentrations d'exposition, mais cultivé à plus haute température (20°C contre 14°C) a montré de plus hautes quantités internalisées tout en présentant une concentration effective à 50 % (EC₅₀) plus faible après 7 jours d'exposition. Une variation de la photopériode (cycle diurne/nocturne de 16/8 contre 10/14) n'a pas montré d'effet significatif sur les différents biomarqueurs suivis. Ces résultats nous permettent de mieux comprendre les relations complexes qui existent en milieu naturel dans une optique d'extrapolation des données obtenues du laboratoire vers le terrain.

Ce chapitre a fait l'objet d'une soumission d'article au journal *Environmental Toxicology and Chemistry* :

Laderriere V, Richard M, Morin S, Le Faucheur S, Fortin C (2021) Seasonal factors affect the sensitivity of biofilms to nickel and its accumulation

3- Quel est le lien causal entre la bioaccumulation et la composition taxonomique du biofilm?

Le but de ce troisième axe est d'explorer l'aspect communautaire du biofilm en s'intéressant aux différents compartiments qui le constituent à savoir le compartiment autotrophe et hétérotrophe. Des études ont en effet montré que la toxicité des métaux variait selon le compartiment considéré. Un biofilm naturel a donc été exposé de manière chronique à différentes concentrations en Ni et sa tolérance a été étudiée selon l'approche du PICT (*Pollution Induced Community Tolerance*). Ces données ont permis de mettre en lien toxicité, accumulation et composition structurale du biofilm. Le but était donc de mesurer compartiment par compartiment, la réponse aux métaux de biofilms exposés à différentes concentrations et de vérifier si la réponse de descripteurs classiques était modifiée en conséquence. Ce troisième chapitre a ainsi permis d'identifier les descripteurs qui restent pertinents en comparant une communauté devenue tolérante et une communauté dite de référence (définie comme non tolérante). Par exemple, ce chapitre a permis de comparer si ces deux communautés bioaccumulent autant les métaux pour une même concentration d'exposition selon des caractéristiques structurales différentes. Là encore, ces résultats nous permettent une meilleure compréhension des relations complexes qui existent dans les milieux naturels dans une perspective de biosuivi.

Ce chapitre a fait l'objet d'une ébauche d'article prête à soumettre :

Laderriere V, Morin S, Fortin C (2021) Role of seasonality in the vulnerability and tolerance of periphytic biofilms to nickel

2 BIBLIOGRAPHIE INTRODUCTION

- Adams, W., Blust, R., Dwyer, R., Mount, D., Nordheim, E., Rodriguez, P.H., Spry, D., 2020. Bioavailability assessment of metals in freshwater environments: a historical review. Environ. Toxicol. Chem. 39, 48–59. <https://doi.org/10.1002/etc.4558>
- Aguilera, A., Souza-Egipsy, V., San Martín-Uriz, P., Amils, R., 2008. Extracellular matrix assembly in extreme acidic eukaryotic biofilms and their possible implications in heavy metal adsorption. Aquat. Toxicol. 88, 257–266. <https://doi.org/10.1016/j.aquatox.2008.04.014>
- Álvarez, M., Peckarsky, B.L., 2005. How do grazers affect periphyton heterogeneity in streams? Oecologia 142, 576–587. <https://doi.org/10.1007/s00442-004-1759-0>
- Ancion, P.Y., Lear, G., Dopheide, A., Lewis, G.D., 2013. Metal concentrations in stream biofilm and sediments and their potential to explain biofilm microbial community structure. Environ. Pollut. 173, 117–124. <https://doi.org/10.1016/j.envpol.2012.10.012>
- Arini, A., Durant, F., Coste, M., Delmas, F., Feurtet-Mazel, A., 2013. Cadmium decontamination and reversal potential of teratological forms of the diatom *Planothidium frequentissimum* (*Bacillariophyceae*) after experimental contamination. J. Phycol. 49, 361–370. <https://doi.org/10.1111/jpy.12044>
- Balistrieri, L.S., Mebane, C.A., Schmidt, T.S., Keller, W. (Bill), 2015. Expanding metal mixture toxicity models to natural stream and lake invertebrate communities. Environ. Toxicol. Chem. 34, 761–776. <https://doi.org/10.1002/etc.2824>
- Battin, T.J., Besemer, K., Bengtsson, M.M., Romani, A.M., Packmann, A.I., 2016. The ecology and biogeochemistry of stream biofilms. Nat. Rev. Microbiol. 14, 251–263. <https://doi.org/10.1038/nrmicro.2016.15>
- Battin, T.J., Kaplan, L.A., Newbold, J.D., Hansen, C.M.E., 2003. Contributions of microbial biofilms to ecosystem processes in stream mesocosms. Nature 426, 439–442. <https://doi.org/10.1038/nature02152>
- Blaby-Haas, C.E., Merchant, S.S., 2017. Regulating cellular trace metal economy in algae. Curr. Opin. Plant Biol. 39, 88–96. <https://doi.org/10.1016/j.pbi.2017.06.005>
- Blaby-Haas, C.E., Merchant, S.S., 2012. The ins and outs of algal metal transport. Biochim. Biophys. Acta 1823, 1531–1552. <https://doi.org/10.1016/j.bbamcr.2012.04.010>

- Blanck, H., 2002. A critical review of procedures and approaches used for assessing Pollution-Induced Community Tolerance (PICT) in biotic communities. *Hum. Ecol. Risk Assess.* 8, 1003–1034. <https://doi.org/10.1080/1080-700291905792>
- Blanck, H., Wängberg, S., Molander, S., 1988. Pollution-Induced Community Tolerance — A new ecotoxicological tool, eds J. Cai. ed, *Functional Testing of Aquatic Biota for Estimating Hazards of Chemicals*. <https://doi.org/10.1520/STP26265S>
- Bonet, B., Corcoll, N., Acuña, V., Sigg, L., Behra, R., Guasch, H., 2013. Seasonal changes in antioxidant enzyme activities of freshwater biofilms in a metal polluted Mediterranean stream. *Sci. Total Environ.* 444, 60–72. <https://doi.org/10.1016/j.scitotenv.2012.11.036>
- Bonet, B., Corcoll, N., Guasch, H., 2012. Antioxidant enzyme activities as biomarkers of Zn pollution in fluvial biofilms. *Ecotoxicol. Environ. Saf.* 80, 172–178. <https://doi.org/10.1016/j.ecoenv.2012.02.024>
- Bonnineau, C., Artigas, J., Chaumet, B., Dabrin, A., Faburé, J., Ferrari, B.J.D., Lebrun, J.D., Margoum, C., Mazzella, N., Miège, C., Morin, S., Uher, E., Babut, M., Pesce, S., 2020. Role of biofilms in contaminant bioaccumulation and trophic transfer in aquatic ecosystems: current state of knowledge and future challenges. *Rev. Environ. Contam. Toxicol.* 253, 115–153. https://doi.org/10.1007/398_2019_39
- Bonnineau, C., Tlili, A., Faggiano, L., Montuelle, B., Guasch, H., 2013. The use of antioxidant enzymes in freshwater biofilms: Temporal variability vs. toxicological responses. *Aquat. Toxicol.* 136–137, 60–71. <https://doi.org/10.1016/j.aquatox.2013.03.009>
- Bricheux, G., Morin, L., Le Moal, Gwenael Coffe, Gérard Balestrino, Damien Charbonnel, N., Bohatier, J., Forestier Christiane, 2013. Pyrosequencing assessment of prokaryotic and eukaryotic diversity in biofilm communities from a French river. *Microbiologyopen* 2, 402–414. <https://doi.org/10.1002/mbo3.80>
- Brix, K. V., DeForest, D.K., Tear, L., Peijnenburg, W., Peters, A., Middleton, E.T., Erickson, R., 2020. Development of empirical bioavailability models for metals. *Environ. Toxicol. Chem.* 39, 85–100. <https://doi.org/10.1002/etc.4570>
- Buffel, J., Wilkinson, K.J., Van Leeuwen, H.P., 2009. Chemodynamics and bioavailability in natural waters. *Environ. Sci. Technol.* 43, 7170–7174. <https://doi.org/10.1021/es9013695>

- Campbell, P.G.C., 1995. Interactions between trace metals and aquatic organisms: A critique of the free-ion activity mode, In: Tessier, A., Turner, D.R. (Eds.), Metal Speciation and Bioavailability in Aquatic Systems. New York, NY, États-Unis, pp. 45–102.
- Campbell, P.G.C., Errécalde, O., Fortin, C., Hiriart-Baer, V.P., Vigneault, B., 2002. Metal bioavailability to phytoplankton--applicability of the biotic ligand model. *Comp. Biochem. Physiol. C. Toxicol. Pharmacol.* 133, 189–206. [https://doi.org/10.1016/S1532-0456\(02\)00104-7](https://doi.org/10.1016/S1532-0456(02)00104-7)
- Campbell, P.G.C., Hare, L., 2009. Metal detoxification in freshwater animals. Roles of metallothioneins, Metallothioneins and Related Chelators: Metal Ions in Life Sciences. <https://doi.org/10.1039/9781847558992-00239>
- Ressources Naturelles Canada, 2016. Cahier d'information sur les minéraux et les métaux – 2016. https://www.rncan.gc.ca/sites/www.nrcan.gc.ca/files/mineralsmetals/pdf/mms-smm/Minerals%20and%20Metals_factbook_Fr.pdf
- Characklis, W.G., Wilderer, P.A. (Eds.), 1990. Structure and Function of Biofilms. Wiley-Blackwell.
- Chaumet, B., Morin, S., Hourtané, O., Artigas, J., Delest, B., Eon, M., Mazzella, N., 2019. Flow conditions influence diuron toxicokinetics and toxicodynamics in freshwater biofilms. *Sci. Total Environ.* 652, 1242–1251. <https://doi.org/10.1016/j.scitotenv.2018.10.265>
- Cheloni, G., Cosio, C., Slaveykova, V.I., 2014. Antagonistic and synergistic effects of light irradiation on the effects of copper on *Chlamydomonas reinhardtii*. *Aquat. Toxicol.* 155, 275–282. <https://doi.org/10.1016/j.aquatox.2014.07.010>
- Cheloni, G., Slaveykova, V.I., 2018. Combined effects of trace metals and light on photosynthetic microorganisms in aquatic environment. *Environments* 5, 1–19. <https://doi.org/10.3390/environments5070081>
- Conseil Canadien des Ministres de l'Environnement, 2018. Recommandations pour la qualité des eaux et la protection de la vie aquatique 1–14.
- Corcoll, N., Bonet, B., Leira, M., Guasch, H., 2011. Chl-a fluorescence parameters as biomarkers of metal toxicity in fluvial biofilms: An experimental study. *Hydrobiologia* 673, 119–136. <https://doi.org/10.1007/s10750-011-0763-8>
- Corcoll, N., Bonet, B., Leira, M., Montuelle, B., Tlili, A., Guasch, H., 2012a. Light history influences the response of fluvial biofilms to Zn exposure. *J. Phycol.* 48, 1411–1423. <https://doi.org/10.1111/j.1529-8817.2012.01223.x>

- Corcoll, N., Ricart, M., Franz, S., Sans-Piché, F., Schmitt-Jansen, M., Guasch, H., 2012b. The use of photosynthetic fluorescence parameters from autotrophic biofilms for monitoring the effect of chemicals in river ecosystems, in: Guasch, H, Ginebreda, A., Geiszinger, A. (Eds.), Emerging and Priority Pollutants in Rivers. Springer-Verlag Berlin Heidelberg, pp. 85–116. https://doi.org/10.1007/978-3-642-25722-3_4
- Crémazy, A., Brix, K. V., Wood, C.M., 2019. Using the Biotic Ligand Model framework to investigate binary metal interactions on the uptake of Ag, Cd, Cu, Ni, Pb and Zn in the freshwater snail *Lymnaea stagnalis*. Sci. Total Environ. 647, 1611–1625. <https://doi.org/10.1016/j.scitotenv.2018.07.455>
- D'Abzac, P., Bordas, F., Joussein, E., 2013. Metal binding properties of extracellular polymeric substances extracted from anaerobic granular sludges. Environ. Sci. Pollut. Res. 20, 4509–4519. <https://doi.org/10.1007/s11356-012-1401-3>
- Defo, M.A., Spear, P.A., Couture, P., 2014. Consequences of metal exposure on retinoid metabolism in vertebrates: A review. Toxicol. Lett. 225, 1–11. <https://doi.org/10.1016/j.toxlet.2013.11.024>
- Deleebeeck, N.M.E., De Schamphelaere, K.A.C., Janssen, C.R., 2009. Effects of Mg²⁺ and H⁺ on the toxicity of Ni²⁺ to the unicellular green alga *Pseudokirchneriella subcapitata*: Model development and validation with surface waters. Sci. Total Environ. 407, 1901–1914. <https://doi.org/10.1016/j.scitotenv.2008.11.052>
- Di Toro, D.M., Allen, H.E., Bergman, H.L., Meyer, J.S., Paquin, P.R., Santore, R.C., 2001. Biotic ligand model of the acute toxicity of metals. 1. Technical basis. Environ. Toxicol. Chem. 20, 2383–2396. <https://doi.org/10.1002/etc.5620201034>
- Dranguet, P., Slaveykova, V.I., Le Faucheur, S., 2017. Kinetics of mercury accumulation by freshwater biofilms. Environ. Chem. 14, 458–467. <https://doi.org/10.1071/EN17073>
- Duan, J., Tan, J., 2013. Atmospheric heavy metals and Arsenic in China: Situation, sources and control policies. Atmos. Environ. 74, 93–101. <https://doi.org/10.1016/j.atmosenv.2013.03.031>
- Duong, T.T., Morin, S., Herlory, O., Feurtet-Mazel, A., Coste, M., Boudou, A., 2008. Seasonal effects of cadmium accumulation in periphytic diatom communities of freshwater biofilms. Aquat. Toxicol. 90, 19–28. <https://doi.org/10.1016/j.aquatox.2008.07.012>
- Edwards, S.J., Kjellerup, B. V., 2013. Applications of biofilms in bioremediation and biotransformation of persistent organic pollutants, pharmaceuticals/personal care products,

and heavy metals. *Appl. Microbiol. Biotechnol.* 97, 9909–9921.
<https://doi.org/10.1007/s00253-013-5216-z>

Erickson, R.J., 2013. The biotic ligand model approach for addressing effects of exposure water chemistry on aquatic toxicity of metals: Genesis and challenges. *Environ. Toxicol. Chem.* 32, 1212–1214. <https://doi.org/10.1002/etc.2222>

Faburé, J., Dufour, M., Autret, A., Uher, E., Fechner, L.C., 2015. Impact of an urban multi-metal contamination gradient: Metal bioaccumulation and tolerance of river biofilms collected in different seasons. *Aquat. Toxicol.* 159, 276–289.
<https://doi.org/10.1016/j.aquatox.2014.12.014>

Fadhloui, M., Laderriere, V., Lavoie, I., Fortin, C., 2020. Influence of temperature and nickel on algal biofilm fatty acid composition. *Environ. Toxicol. Chem.* 39, 1566–1577.
<https://doi.org/10.1002/etc.4741>

Fechner, L.C., Gourlay-Francé, C., Bourgeault, A., Tusseau-Vuillemin, M.H., 2012. Diffuse urban pollution increases metal tolerance of natural heterotrophic biofilms. *Environ. Pollut.* 162, 311–318. <https://doi.org/10.1016/j.envpol.2011.11.033>

Fechner, L.C., Gourlay-Francé, C., Tusseau-Vuillemin, M.H., 2011. Low exposure levels of urban metals induce heterotrophic community tolerance: A microcosm validation. *Ecotoxicology* 20, 793–802. <https://doi.org/10.1007/s10646-011-0630-4>

Fernandes, G., Bastos, M.C., de Vargas, J.P.R., Le Guet, T., Clasen, B., dos Santos, D.R., 2020. The use of epilithic biofilms as bioaccumulators of pesticides and pharmaceuticals in aquatic environments. *Ecotoxicology* 29, 1293–1305. <https://doi.org/10.1007/s10646-020-02259-4>

Findlay, S.E.G., Sinsabaugh, R.L., Sobczak, W. V., Hoostal, M., 2003. Metabolic and structural response of hyporheic microbial communities to variations in supply of dissolved organic matter. *Limnol. Oceanogr.* 48, 1608–1617. <https://doi.org/10.4319/lo.2003.48.4.1608>

Flemming, H.C., Neu, T.R., Wozniak, D.J., 2007. The EPS matrix: The “house of biofilm cells.” *J. Bacteriol.* 189, 7945–7947. <https://doi.org/10.1128/JB.00858-07>

Flemming, H.C., Wingender, J., 2010. The biofilm matrix. *Nat. Rev. Microbiol.* 8, 623–633.
<https://doi.org/10.1038/nrmicro2415>

Flemming, H.C., Wingender, J., Szewzyk, U., Steinberg, P., Rice, S.A., Kjelleberg, S., 2016. Biofilms: An emergent form of bacterial life. *Nat. Rev. Microbiol.* 14, 563–575.
<https://doi.org/10.1038/nrmicro.2016.94>

- Fortin, C., Couillard, Y., Vigneault, B., Campbell, P.G.C., 2010. Determination of free Cd, Cu and Zn concentrations in lake waters by in situ diffusion followed by column equilibration ion-exchange. *Aquat. Geochemistry* 16, 151–172. <https://doi.org/10.1007/s10498-009-9074-3>
- Fortin, C., Denison, F.H., Garnier-Laplace, J., 2007. Metal-phytoplankton interactions: Modeling the effect of competing ions (H^+ , Ca^{2+} , and Mg^{2+}) on uranium uptake. *Environ. Toxicol. Chem.* 26, 242–248. <https://doi.org/10.1897/06-298R.1>
- Foulquier, A., Morin, S., Dabrin, A., 2015. Effects of mixtures of dissolved and particulate contaminants on phototrophic biofilms : new insights from a PICT approach combining toxicity tests with passive samplers and model substances. *Environ. Sci. Pollut. Res.* 22, 4025–4036. <https://doi.org/10.1007/s11356-014-3289-6>
- Friesen, V., Doig, L.E., Markwart, B.E., Haakensen, M., Tissier, E., Liber, K., 2017. Genetic characterization of periphyton communities associated with selenium bioconcentration and trophic transfer in a simple food chain. *Environ. Sci. Technol.* 51, 7532–7541. <https://doi.org/10.1021/acs.est.7b01001>
- Gaillardet, J., Viers, J., Dupre, B., 2003. Trace elements in river waters. *Treatise geochemistry* Surf. Gr. water, Weather. soils 225–272. <https://doi.org/10.1016/B0-08-043751-6/05165-3>
- Giguère, A., Campbell, P.G.C., Hare, L., Cossu-leguille, C., 2005. Metal bioaccumulation and oxidative stress in yellow perch (*Perca flavescens*) collected from eight lakes along a metal contamination gradient (Cd, Cu, Zn, Ni). *Can. J. Fish. Aquat. Sci.* 577, 563–577. <https://doi.org/10.1139/f04-224>
- Gonçalves, S., Kahlert, M., Almeida, S.F.P., Figueira, E., 2018. Assessing Cu impacts on freshwater diatoms : biochemical and metabolomic responses of *Tabellaria flocculosa* (Roth) Kützing. *Sci. Total Environ.* 625, 1234–1246. <https://doi.org/10.1016/j.scitotenv.2017.12.320>
- Graedel, T.E., Cao, J., 2010. Metal spectra as indicators of development. *Proc. Natl. Acad. Sci.* 107, 20905–20910. <https://doi.org/10.1073/pnas.1011019107>
- Guasch, H., Artigas, J., Bonet, B., Bonnneau, C., Canals, O., Corcoll, N., 2016a. The use of biofilms to assess the effects of chemicals on freshwater ecosystems, in: Romaní, A.M., Guasch, H., Balaguer, M.D. (Eds.), *In Aquatic Biofilms: Ecology, Water Quality and Wastewater Treatment*. Caister Academic Press, Spain, pp. 125–144. <https://doi.org/10.21775/9781910190173.06>

- Guasch, H., Ricart, M., López-Doval, J., Bonnneau, C., Proia, L., Morin, S., Muñoz, I., Romaní, A.M., Sabater, S., 2016b. Influence of grazing on triclosan toxicity to stream periphyton. Freshw. Biol. 61, 2002–2012. <https://doi.org/10.1111/fwb.12797>
- Guo, F., Kainz, M.J., Sheldon, F., Bunn, S.E., 2016. The importance of high-quality algal food sources in stream food webs - current status and future perspectives. Freshw. Biol. 61, 815–831. <https://doi.org/10.1111/fwb.12755>
- Hobbs, W.O., Collyard, S.A., Larson, C., Carey, A.J., O'Neill, S.M., 2019. Toxic burdens of freshwater biofilms and use as a source tracking tool in rivers and streams. Environ. Sci. Technol. 53, 11102–11111. <https://doi.org/10.1021/acs.est.9b02865>
- Holmstrup, M., Bindesbøl, A.M., Oostingh, G.J., Duschl, A., Scheil, V., Köhler, H.R., Loureiro, S., Soares, A.M.V.M., Ferreira, A.L.G., Kienle, C., Gerhardt, A., Laskowski, R., Kramarz, P.E., Bayley, M., Svendsen, C., Spurgeon, D.J., 2010. Interactions between effects of environmental chemicals and natural stressors: A review. Sci. Total Environ. 408, 3746–3762. <https://doi.org/10.1016/j.scitotenv.2009.10.067>
- Islam, S., Ahmed, K., Raknuzzaman, M., 2015. Heavy metal pollution in surface water and sediment: A preliminary assessment of an urban river in a developing country. Ecol. Indic. 48, 282–291. <https://doi.org/10.1016/j.ecolind.2014.08.016>
- Jang, A., Kim, S.M., Kim, S.Y., Lee, S.G., Kim, I.S., 2001. Effects of heavy metals (Cu, Pb, and Ni) on the compositions of EPS in biofilms. Water Sci. Technol. 43, 41–48. <https://doi.org/10.2166/wst.2001.0336>
- Minister of Justice, M. of, 2012. Canadian Environmental Assessment Act (S.C. 2012, c. 19, s. 52). Canada.
- Kim, K.S., Funk, D.H., Buchwalter, D.B., 2012. Dietary (periphyton) and aqueous Zn bioaccumulation dynamics in the mayfly *Centroptilum triangulifer*. Ecotoxicology 21, 2288–2296. <https://doi.org/10.1007/s10646-012-0985-1>
- Kim Tiam, S., Laviale, M., Feurtet-Mazel, A., Jan, G., Gonzalez, P., Mazzella, N., Morin, S., 2015. Herbicide toxicity on river biofilms assessed by pulse amplitude modulated (PAM) fluorometry. Aquat. Toxicol. 165, 160–171. <https://doi.org/10.1016/j.aquatox.2015.05.001>
- Kim Tiam, S., Lavoie, I., Doose, C., Hamilton, P.B., Fortin, C., Tiam, S.K., 2018. Morphological, physiological and molecular responses of *Nitzschia palea* under cadmium stress. Ecotoxicology 675–688. <https://doi.org/10.1007/s10646-018-1945-1>

- Kochoni, E., Fortin, C., 2019. Iron modulation of copper uptake and toxicity in a green alga (*Chlamydomonas reinhardtii*). Environ. Sci. Technol. 53, 6539–6545. <https://doi.org/10.1021/acs.est.9b01369>
- Laderriere, V., Paris, L.E., Fortin, C., 2020. Proton competition and free ion activities drive cadmium, copper, and nickel accumulation in river biofilms in a nordic ecosystem. Environments 7, 1–13. <https://doi.org/10.3390/environments7120112>
- Lagadic, L., Caquet, T., Amiard, J., Ramade, F., 1997. Biomarqueurs en écotoxicologie : aspects fondamentaux.
- Lambert, A., Morin, S., Artigas, J., Volat, B., Coquery, M., Neyra, M., Pesce, S., 2012. Structural and functional recovery of microbial biofilms after a decrease in copper exposure : Influence of the presence of pristine communities. Aquat. Toxicol. 109, 118–126. <https://doi.org/10.1016/j.aquatox.2011.12.006>
- Lambert, A.S., Dabrin, A., Foulquier, A., Morin, S., Rosy, C., Coquery, M., Pesce, S., 2017. Influence of temperature in pollution-induced community tolerance approaches used to assess effects of copper on freshwater phototrophic periphyton. Sci. Total Environ. 607–608, 1018–1025. <https://doi.org/10.1016/j.scitotenv.2017.07.035>
- Lambert, A.S., Dabrin, A., Morin, S., Gahou, J., Foulquier, A., Coquery, M., Pesce, S., 2016. Temperature modulates phototrophic periphyton response to chronic copper exposure. Environ. Pollut. 208, 821–829. <https://doi.org/10.1016/j.envpol.2015.11.004>
- Lane, T.W., Morel, F.M.M., 2000. A biological function for cadmium in marine diatoms. Proc. Natl. Acad. Sci. U. S. A. 97, 4627–4631. <https://doi.org/10.1073/pnas.090091397>
- Laskowski, R., Bednarska, A.J., Kramarz, P.E., Loureiro, S., Scheil, V., Kudłek, J., Holmstrup, M., 2010. Interactions between toxic chemicals and natural environmental factors - A meta-analysis and case studies. Sci. Total Environ. 408, 3763–3774. <https://doi.org/10.1016/j.scitotenv.2010.01.043>
- Lavoie, I., Campeau, S., Darchambeau, F., Cabana, G., Dillon, P.J., 2008. Are diatoms good integrators of temporal variability in stream water quality? Freshw. Biol. 53, 827–841. <https://doi.org/10.1111/j.1365-2427.2007.01935.x>
- Lavoie, I., Campeau, S., Zugic-Drakulic, N., Winter, J.G., Fortin, C., 2014. Using diatoms to monitor stream biological integrity in Eastern Canada: An overview of 10 years of index

development and ongoing challenges. Sci. Total Environ. 475, 187–200. <https://doi.org/10.1016/j.scitotenv.2013.04.092>

Lavoie, I., Lavoie, M., Fortin, C., 2012. A mine of information: Benthic algal communities as biomonitor of metal contamination from abandoned tailings. Sci. Total Environ. 425, 231–241. <https://doi.org/10.1016/j.scitotenv.2012.02.057>

Lavoie, I., Morin, S., Laderriere, V., Fortin, C., 2018. Freshwater diatoms as indicators of Combined long-term mining and urban stressors in Junction Creek (Ontario, Canada). Environments 5, 30. <https://doi.org/10.3390/environments5020030>

Lavoie, M., Campbell, P.G.C., Fortin, C., 2016. Importance de mieux connaître les mécanismes de transport des métaux pour la prédition de l'accumulation et de la toxicité des métaux dissous chez le phytoplancton : récentes avancées et défis pour le développement du modèle du ligand biotique. Rev. des Sci. l'Eau 292 29, 119–147.

Lavoie, M., Campbell, P.G.C., Fortin, C., 2012a. Extending the biotic ligand model to account for positive and negative feedback interactions between cadmium and zinc in a freshwater alga. Environ. Sci. Technol. 46, 12129–12136. <https://doi.org/10.1021/es302512r>

Lavoie, M., Le Faucheur, S., Boullemand, A., Fortin, C., Campbell, P.G.C., 2012b. The influence of pH on algal cell membrane permeability and its implications for the uptake of lipophilic metal complexes. J. Phycol. 48, 293–302. <https://doi.org/10.1111/j.1529-8817.2012.01126.x>

Lavoie, M., Le Faucheur, S., Fortin, C., Campbell, P.G.C., 2009. Cadmium detoxification strategies in two phytoplankton species: Metal binding by newly synthesized thiolated peptides and metal sequestration in granules. Aquat. Toxicol. 92, 65–75. <https://doi.org/10.1016/j.aquatox.2008.12.007>

Le Faucheur, S., Behra, R., Sigg, L., 2005a. Thiol and metal contents in periphyton exposed to elevated copper and zinc concentrations : A field and microcosm study. Environ. Sci. Technol. 39, 8099–8107. <https://doi.org/10.1021/es050303z>

Le Faucheur, S., Behra, R., Sigg, L., 2005b. Phytochelatin induction, cadmium accumulation, and algal sensitivity to free Cadmium ion in *Scenedesmus vacuolatus*. Environ. Toxicol. Chem. 24, 1731–1737. <https://doi.org/10.1897/04-394R.1>

Le Faucheur, S., Campbell, P.G.C., Fortin, C., Slaveykova, V.I., 2014. Interactions between mercury and phytoplankton: speciation, bioavailability, and internal handling. Environ. Toxicol. Chem. 33, 1211–1224. <https://doi.org/10.1002/etc.2424>

- Le Faucher, S., Tremblay, Y., Fortin, C., 2011. Acidification increases mercury uptake by a freshwater alga, *Chlamydomonas reinhardtii*. Environ. Chem. 8, 612–622. <https://doi.org/http://dx.doi.org/10.1071/EN11006>
- Lebrun, J.D., Geffard, O., Urien, N., François, A., Uher, E., Fechner, L.C., 2015. Seasonal variability and inter-species comparison of metal bioaccumulation in caged gammarids under urban diffuse contamination gradient: Implications for biomonitoring investigations. Sci. Total Environ. 511, 501–508. <https://doi.org/10.1016/j.scitotenv.2014.12.078>
- Leguay, S., Lavoie, I., Levy, J.L., Fortin, C., 2016. Using biofilms for monitoring metal contamination in lotic ecosystems: The protective effects of hardness and pH on metal bioaccumulation. Environ. Toxicol. Chem. 35, 1489–1501. <https://doi.org/10.1002/etc.3292>
- Liu, F., Tan, Q.G., Weiss, D., Crémazy, A., Fortin, C., Campbell, P.G.C., 2020. Unravelling metal speciation in the microenvironment surrounding phytoplankton cells to improve predictions of metal bioavailability. Environ. Sci. Technol. 54, 8177–8185. <https://doi.org/10.1021/acs.est.9b07773>
- Loustau, E., Ferriol, J., Koteiche, S., Gerlin, L., Leflaise, J., Moulin, F., 2019. Physiological responses of three mono-species phototrophic biofilms exposed to copper and zinc. Environ. Sci. Pollut. Res. 26, 35107–35120. <https://doi.org/10.1007/s11356-019-06560-6>
- Macoustra, G.K., Jolley, D.F., Stauber, J.L., Koppel, D.J., Holland, A., 2021. Speciation of nickel and its toxicity to *Chlorella sp.* in the presence of three distinct dissolved organic matter (DOM). Chemosphere 273, 128454. <https://doi.org/10.1016/j.chemosphere.2020.128454>
- Macoustra, G.K., Jolley, D.F., Stauber, J.L., Koppel, D.J., Holland, A., 2020. Amelioration of copper toxicity to a tropical freshwater microalga: Effect of natural DOM source and season. Environ. Pollut. 115–141. <https://doi.org/10.1016/j.envpol.2020.115141>
- Mandal, R., Hassan, N.M., Murimboh, J., Chakrabarti, C.L., Back, M.H., Rahayu, U., Lean, D.R.S., 2002. Chemical speciation and toxicity of nickel species in natural waters from the Sudbury area (Canada). Environ. Sci. Technol. 36, 1477–1484. <https://doi.org/10.1021/es015622e>
- Martyniuk, M.A.C., Couture, P., Tran, L., Beaupré, L., Urien, N., Power, M., 2020. A seasonal comparison of trace metal concentrations in the tissues of Arctic char (*Salvelinus alpinus*) in Northern Québec, Canada. Ecotoxicology 29, 1327–1346. <https://doi.org/10.1007/s10646-020-02248-7>

- Massieux, B., Boivin, M.E.Y., Van Den Ende, F.P., Langenskiöld, J., Marvan, P., Barranguet, C., Admiraal, W., Laanbroek, H.J., Zwart, G., 2004. Analysis of structural and physiological profiles to assess the effects of Cu on biofilm microbial communities. *Appl. Environ. Microbiol.* 70, 4512–4521. <https://doi.org/10.1128/AEM.70.8.4512-4521.2004>
- Mebane, C.A., Schmidt, T.S., Miller, J.L., Balistrieri, L.S., 2020. Bioaccumulation and toxicity of cadmium, copper, nickel, and zinc and their mixtures to aquatic insect communities. *Environ. Toxicol. Chem.* 39, 812–833. <https://doi.org/10.1002/etc.4663>
- Moisset, S., Tiam, S.K., Morin, S., 2015. Genetic and physiological responses of three freshwater diatoms to realistic diuron exposures. *Environ. Sci. Pollut. Res.* 22, 4046–4055. <https://doi.org/10.1007/s11356-014-3523-2>
- Morin, S., Cordonier, A., Lavoie, I., Arini, A., Blanco, S., Duong, T.T., Tornés, E., Bonet, B., Corcoll, N., Faggiano, L., Laviale, M., Pérès, F., Becares, E., Coste, M., Feurter-Mazel, A., Fortin, C., Guasch, Helena, Sabater, S., 2012. Consistency in diatom response to metal-contaminated environments, in: Guasch, H., Ginebreda, A., Geiszinger, A. (Eds.), Emerging and Priority Pollutants in Rivers. Springer-Verlag Berlin Heidelberg, pp. 117–146. https://doi.org/10.1007/978-3-642-25722-3_5
- Morin, S., Duong, T.T., Dabrin, A., Coynel, A., Herlory, O., Baudrimont, M., Delmas, F., Durrieu, G., Schäfer, J., Winterton, P., Blanc, G., Coste, M., 2008. Long-term survey of heavy-metal pollution, biofilm contamination and diatom community structure in the Riou Mort watershed, South-West France. *Environ. Pollut.* 151, 532–542. <https://doi.org/10.1016/j.envpol.2007.04.023>
- Morin, Soizic, Duong, T.T., Herlory, O., Feurtet-Mazel, A., Coste, M., 2008. Cadmium toxicity and bioaccumulation in freshwater biofilms. *Arch. Environ. Contam. Toxicol.* 54, 173–186. <https://doi.org/10.1007/s00244-007-9022-4>
- Morin, S., Lambert, A.S., Rodriguez, E.P., Dabrin, A., Coquery, M., Pesce, S., 2017. Changes in copper toxicity towards diatom communities with experimental warming. *J. Hazard. Mater.* 334, 223–232. <https://doi.org/10.1016/j.jhazmat.2017.04.016>
- Mueller, K.K., Loftis, S., Fortin, C., Campbell, P.G.C., 2012. Trace metal speciation predictions in natural aquatic systems: Incorporation of dissolved organic matter (DOM) spectroscopic quality. *Environ. Chem.* 9, 356–368. <https://doi.org/10.1071/EN11156>

- Murguía, D.I., Bringezu, S., Schaldach, R., 2016. Global direct pressures on biodiversity by large-scale metal mining: Spatial distribution and implications for conservation. *J. Environ. Manage.* 180, 409–420. <https://doi.org/10.1016/j.jenvman.2016.05.040>
- Nadell, C.D., Drescher, K., Foster, K.R., 2016. Spatial structure, cooperation and competition in biofilms. *Nat. Rev. Microbiol.* 14, 589–600. <https://doi.org/10.1038/nrmicro.2016.84>
- Nagajyoti, P.C., Lee, K.D., Sreekanth, T.V.M., 2010. Heavy metals, occurrence and toxicity for plants: A review. *Environ. Chem. Lett.* 8, 199–216. <https://doi.org/10.1007/s10311-010-0297-8>
- Namba, H., Iwasaki, Y., Heino, J., Matsuda, H., 2020. What to survey? A systematic review of the choice of biological groups in assessing ecological impacts of metals in running waters. *Environ. Toxicol. Chem.* 39, 1964–1972. <https://doi.org/10.1002/etc.4810>
- Nations-Unies, 2018. Rapport mondial des Nations Unies sur la mise en valeur des ressources en eau 2018 : Les solutions fondées sur la nature pour la gestion de l'eau. Paris, UNESCO. WWAP (Le Programme mondial des Nations Unies pour l'évaluation des ressources en eau)/ONU-Eau.
- Navarro, E., Robinson, C.T., Behra, R., 2008. Increased tolerance to ultraviolet radiation (UVR) and cotolerance to cadmium in UVR-acclimatized freshwater periphyton. *Limnol. Oceanogr.* 53, 1149–1158. <https://doi.org/10.4319/lo.2008.53.3.1149>
- Neury-Ormanni, J., Doose, C., Majdi, N., Vedrenne, J., Traunspurger, W., Morin, S., 2020. Selective grazing behaviour of chironomids on microalgae under pesticide pressure. *Sci. Total Environ.* 730, 138673. <https://doi.org/10.1016/j.scitotenv.2020.138673>
- Nys, C., Van Regenmortel, T., Janssen, C.R., Oorts, K., Smolders, E., De Schampheleire, K.A.C., 2018. A framework for ecological risk assessment of metal mixtures in aquatic systems. *Environ. Toxicol. Chem.* 37, 623–642. <https://doi.org/10.1002/etc.4039>
- Okamoto, O.K., Pinto, E., Latorre, L.R., Bechara, E.J.H., Colepicolo, P., 2001. Antioxidant modulation in response to metal-induced oxidative stress in algal chloroplasts. *Arch. Environ. Contam. Toxicol.* 40, 18–24. <https://doi.org/10.1007/s002440010144>
- Oukarroum, A., Perreault, F., Popovic, R., 2012. Interactive effects of temperature and copper on photosystem II photochemistry in *Chlorella vulgaris*. *J. Photochem. Photobiol. B Biol.* 110, 9–14. <https://doi.org/10.1016/j.jphotobiol.2012.02.003>

Pandey, L.K., 2020. In situ assessment of metal toxicity in riverine periphytic algae as a tool for biomonitoring of fluvial ecosystems. Environ. Technol. Innov. 18, 100675. <https://doi.org/10.1016/j.eti.2020.100675>

Pandey, L.K., Bergey, E.A., Lyu, J., Park, J., Choi, S., Lee, H., Depuydt, S., Oh, Y.T., Lee, S.M., Han, T., 2017. The use of diatoms in ecotoxicology and bioassessment: Insights, advances and challenges. Water Res. 118, 39–58. <https://doi.org/10.1016/j.watres.2017.01.062>

Parlement européen et Conseil de l'Union Européenne, 2013. Directive 2013/39/UE du Parlement européen et du Conseil du 12 août 2013 modifiant les directives 2000/60/CE et 2008/105/CE en ce qui concerne les substances prioritaires pour la politique dans le domaine de l'eau. J. Off. des Communautés Eur. du 24.8.2013 (JO L 226/1). 2013, 1–17.

Pen, M., Perales-vela, H.V., Can, R.O., 2006. Heavy metal detoxification in eukaryotic microalgae. Chemosphere 64, 1–10. <https://doi.org/10.1016/j.chemosphere.2005.11.024>

Pesce, S., Lambert, A.-S., Morin, S., Foulquier, A., Coquery, M., Dabrin, A., 2018. Experimental warming differentially influences the vulnerability of phototrophic and heterotrophic periphytic communities to copper toxicity. Front. Microbiol. 9, 1424. <https://doi.org/10.3389/fmicb.2018.01424>

Pinto, E., Sigaud- Kutner, T.C.S., Leitao, M.A.S., Okamoto, O.K., Morse, D., Calepicolo, P., 2003. Heavy metal-induced oxidatives stress in algae. J. Phycol. 39, 1008–1018. <https://doi.org/10.1111/j.0022-3646.2003.02-193.x>

Pistocchi, R., Mormile, A.M., Guerrini, F., Isani, G., Boni, L., 2000. Increased production of extra- and intracellular metal-ligands in phytoplankton exposed to copper and cadmium. J. of Applied Phycol. 469–477. <https://doi.org/10.1023/A>

Proia, L., Cassio, F., Pascoal, C., Tlili, A., Romani, A.M., 2012. The use of attached microbial communities to assessecological risks of pollutants in river ecosystems : The role of heterotrophs, in: Guasch, H., Ginebreda, A., Geiszinger, A. (Eds.), Emerging and Priority Pollutants in Rivers. Springer-Verlag Berlin Heidelberg, pp. 55–84. https://doi.org/10.1007/978-3-642-25722-3_3

Gouvernement du Québec, 2017. Chapitre Q2 - Loi sur la qualité de l'environnement (2017, c. 4, a. 1; 2017, c. 14, a. 26). Éditeur Officiel du Québec 1–176.

Gouvernement du Québec, 1988. Chapitre M13 - Loi sur les mines (1987, c.64, a.324). Éditeur Officiel du Québec 1–24.

- Van Regenmortel, T., Van De Perre, D., Janssen, C.R., De Schamphelaere, K.A.C., 2018. The effects of a mixture of copper, nickel, and zinc on the structure and function of a freshwater planktonic community. *Environ. Toxicol. Chem.* 37, 2380–2400. <https://doi.org/10.1002/etc.4185>
- Roeselers, G., Loosdrecht, M.C.M.V., Muyzer, G., 2008. Phototrophic biofilms and their potential applications. *J. Appl. Phycol.* 20, 227–235. <https://doi.org/10.1007/s10811-007-9223-2>
- Romaní, A.M., 2010. Freshwater Biofilms, in: Durr, S., Thomason, J.C. (Eds.), *Biofouling*. Wiley-Blackwell, pp. 137–153. <https://doi.org/10.1002/9781444315462.ch10>
- Romaní, A.M., Fund, K., Artigas, J., Schwartz, T., Sabater, S., Obst, U., 2008. Relevance of polymeric matrix enzymes during biofilm formation. *Microb. Ecol.* 56, 427–436. <https://doi.org/10.1007/s00248-007-9361-8>
- Ronald, E., 1990. Boron hazards to fish, wildlife, and invertebrates: A synoptic review, Contaminant Hazard Reviews. <https://doi.org/10.5962/bhl.title.11357>
- Sabater, S., Guasch, H., Ricart, M., Romaní, A., Vidal, G., Klünder, C., Schmitt-Jansen, M., 2007. Monitoring the effect of chemicals on biological communities. The biofilm as an interface. *Anal. Bioanal. Chem.* 387, 1425–1434. <https://doi.org/10.1007/s00216-006-1051-8>
- Scheibener, S.A., Rivera, N.A., Hesterberg, D., Duckworth, O.W., Buchwalter, D.B., 2017. Periphyton uptake and trophic transfer of coal fly-ash-derived trace elements. *Environ. Toxicol. Chem.* 36, 2991–2996. <https://doi.org/10.1002/etc.3864>
- Schneck, F., Schwarzböld, A., Melo, A.S., 2013. Substrate roughness, fish grazers, and mesohabitat type interact to determine algal biomass and sediment accrual in a high-altitude subtropical stream. *Hydrobiologia* 711, 165–173. <https://doi.org/10.1007/s10750-013-1477-x>
- Serra, A., Corcoll, N., Guasch, H., 2009. Copper accumulation and toxicity in fluvial periphyton: The influence of exposure history. *Chemosphere* 74, 633–641. <https://doi.org/10.1016/j.chemosphere.2008.10.036>
- Serra, A., Guasch, H., 2009. Effects of chronic copper exposure on fluvial systems: Linking structural and physiological changes of fluvial biofilms with the in-stream copper retention. *Sci. Total Environ.* 407, 5274–5282. <https://doi.org/10.1016/j.scitotenv.2009.06.008>
- Serra, A., Guasch, H., Admiraal, W., Van Der Geest, H.G., Van Beusekom, S.A.M., 2010. Influence of phosphorus on copper sensitivity of fluvial periphyton: The role of chemical,

- physiological and community-related factors. *Ecotoxicology* 19, 770–780. <https://doi.org/10.1007/s10646-009-0454-7>
- Shoreman-Ouimet, E., Kopnina, H., 2015. Reconciling ecological and social justice to promote biodiversity conservation. *Biol. Conserv.* 184, 320–326. <https://doi.org/10.1016/j.biocon.2015.01.030>
- Stewart, T.J., Behra, R., Sigg, L., 2015. Impact of chronic lead exposure on metal distribution and biological effects to periphyton. *Environ. Sci. Technol.* 49, 5044–5051. <https://doi.org/10.1021/es505289b>
- Sulzberger, B., Durisch-Kaiser, E., 2009. Chemical characterization of dissolved organic matter (DOM): A prerequisite for understanding UV-induced changes of DOM absorption properties and bioavailability. *Aquat. Sci.* 71, 104–126. <https://doi.org/10.1007/s00027-008-8082-5>
- Sunda, W.G., Huntsman, S.A., 2000. Effect of Zn, Mn, and Fe on Cd accumulation in phytoplankton : implications for oceanic Cd cycling. *Am. Soc. Limnol. Oceanogr.* 45, 1501–1516. <https://doi.org/10.4319/lo.2000.45.7.1501>
- Szivák, I., Behra, R., Sigg, L., 2009. Metal-induced reactive oxygen species production in *Chlamydomonas reinhardtii* (chlorophyceae). *J. Phycol.* 45, 427–435. <https://doi.org/10.1111/j.1529-8817.2009.00663.x>
- Tercier-Waeber, M. Lou, Hezard, T., Masson, M., Schäfer, J., 2009. In situ monitoring of the diurnal cycling of dynamic metal species in a stream under contrasting photobenthic biofilm activity and hydrological conditions. *Environ. Sci. Technol.* 43, 7237–7244. <https://doi.org/10.1021/es900247y>
- Tercier-Waeber, M.-L., Stoll, S., Slaveykova, V.I., 2012. Trace metal behavior in surface waters: Emphasis on dynamic speciation, sorption processes and bioavailability. *Arch. des Sci.* 65, 119–142. <https://archive-ouverte.unige.ch/unige:27739>
- Thi, T.D., Coste, M., Feurtet-Mazel, A., Dinh, K.D., Gold, C., Young, S.P., Boudou, A., 2006. Impact of urban pollution from the Hanoi area on benthic diatom communities collected from the Red, Nhue and Tolich rivers (Vietnam). *Hydrobiologia* 563, 201–216. <https://doi.org/10.1007/s10750-005-0005-z>
- Tlili, A., Berard, A., Blanck, H., Bouchez, A., Cássio, F., Eriksson, K.M., Morin, S., Montuelle, B., Navarro, E., Pascoal, C., Pesce, S., Schmitt-Jansen, M., Behra, R., 2016. Pollution-induced

community tolerance (PICT): towards an ecologically relevant risk assessment of chemicals in aquatic systems. *Freshw. Biol.* 61, 2141–2151. <https://doi.org/10.1111/fwb.12558>

Tlili, A., Bérard, A., Roulier, J.L., Volat, B., Montuelle, B., 2010. PO₄³⁻ dependence of the tolerance of autotrophic and heterotrophic biofilm communities to copper and diuron. *Aquat. Toxicol.* 98, 165–177. <https://doi.org/10.1016/j.aquatox.2010.02.008>

Tlili, A., Corcoll, N., Arrhenius, Å., Backhaus, T., Hollender, J., Creusot, N., Wagner, B., Behra, R., 2020. Tolerance patterns in stream biofilms link complex chemical pollution to ecological impacts. *Environ. Sci. Technol.* 54, 10745–10753. <https://doi.org/10.1021/acs.est.0c02975>

Tlili, A., Maréchal, M., Bérard, A., Volat, B., Montuelle, B., 2011. Enhanced co-tolerance and co-sensitivity from long-term metal exposures of heterotrophic and autotrophic components of fluvial biofilms. *Sci. Total Environ.* 409, 4335–4343. <https://doi.org/10.1016/j.scitotenv.2011.07.026>

Tonietto, A.E., Lombardi, A.T., Choueri, R.B., Vieira, A.A.H., 2015. Chemical behavior of Cu, Zn, Cd, and Pb in a eutrophic reservoir: speciation and complexation capacity. *Environ. Sci. Pollut. Res.* 22, 15920–15930. <https://doi.org/10.1007/s11356-015-4773-3>

Torres, M.A., Barros, M.P., Campos, S.C.G., Pinto, E., Rajamani, S., Sayre, R.T., Colepicolo, P., 2008. Biochemical biomarkers in algae and marine pollution: A review. *Ecotoxicol. Environ. Saf.* 71, 1–15. <https://doi.org/10.1016/j.ecoenv.2008.05.009>

Vendrell-Puigmitja, L., Abril, M., Proia, L., Espinosa Angona, C., Ricart, M., Oatley-Radcliffe, D.L., Williams, P.M., Zanain, M., Llenas, L., 2020. Assessing the effects of metal mining effluents on freshwater ecosystems using biofilm as an ecological indicator: Comparison between nanofiltration and nanofiltration with electrocoagulation treatment technologies. *Ecol. Indic.* 113. <https://doi.org/10.1016/j.ecolind.2020.106213>

Vidali, R., Remoundaki, E., Tsezos, M., 2010. Humic acids copper binding following their photochemical alteration by simulated solar light. *Aquat. Geochemistry* 16, 207–218. <https://doi.org/10.1007/s10498-009-9080-5>

Villeneuve, A., Montuelle, B., Bouchez, A., 2010. Influence of slight differences in environmental conditions (light, hydrodynamics) on the structure and function of periphyton. *Aquat. Sci.* 72, 33–44. <https://doi.org/10.1007/s00027-009-0108-0>

Vörösmarty, C.J., McIntyre, P.B., Gessner, M.O., Dudgeon, D., Prusevich, A., Green, P., Glidden, S., Bunn, S.E., Sullivan, C.A., Liermann, C.R., Davies, P.M., 2010. Global threats to human

water security and river biodiversity. *Nature* 467, 555–561.
<https://doi.org/10.1038/nature09440>

Vu, B., Chen, M., Crawford, R.J., Ivanova, E.P., 2009. Bacterial extracellular polysaccharides involved in biofilm formation. *Molecules* 14, 2535–2554.
<https://doi.org/10.3390/molecules14072535>

Wehrli, B., Behra, P., 2015. Laura Sigg: Investigating the speciation, bioavailability and ecotoxicology of trace metals in natural waters. *Aquat. Geochemistry* 21, 59–64.
<https://doi.org/10.1007/s10498-015-9263-1>

Weitere, M., Erken, M., Majdi, N., Arndt, H., Norf, H., Reinshagen, M., Traunspurger, W., Walterscheid, A., Wey, J.K., 2018. The food web perspective on aquatic biofilms. *Ecol. Monogr.* 88, 543–559. <https://doi.org/10.1002/ecm.1315>

Wetzel, R.G. (Ed.), 1983. Periphyton of freshwater ecosystems. Dr W. Junk Publishers, The Hague. <https://doi.org/10.1007/978-94-009-7293-3>

Worms, I.A.M., Adenmatten, D., Miéville, P., Traber, J., Slaveykova, V.I., 2015. Photo-transformation of pedogenic humic acid and consequences for Cd(II), Cu(II) and Pb(II) speciation and bioavailability to green microalga. *Chemosphere* 138, 908–915.
<https://doi.org/10.1016/j.chemosphere.2014.10.093>

Xie, L., Funk, D.H., Buchwalter, D.B., 2010. Trophic transfer of Cd from natural periphyton to the grazing mayfly *Centropilum triangulifer* in a life cycle test. *Environ. Pollut.* 158, 272–277.
<https://doi.org/10.1016/j.envpol.2009.07.010>

Zhao, C.M., Campbell, P.G.C., Wilkinson, K.J., 2016. When are metal complexes bioavailable? *Environ. Chem.* 13, 425–433. <https://doi.org/10.1071/EN15205>

Zou, K., Thébault, E., Lacroix, G., Barot, S., 2016. Interactions between the green and brown food web determine ecosystem functioning. *Funct. Ecol.* 30, 1454–1465.
<https://doi.org/10.1111/1365-2435.12626>

3 EXPLORING THE ROLE OF WATER CHEMISTRY ON METAL ACCUMULATION IN BIOFILMS FROM STREAMS IN MINING AREAS

EXPLORATION DU RÔLE DE LA CHIMIE DE L'EAU SUR L'ACCUMULATION DES MÉTAUX PAR DES BIOFILMS DE COURS D'EAU EN RÉGIONS MINIÈRES

Auteurs : Vincent Laderriere¹, Séverine Le Faucheur², Claude Fortin¹

Affiliations :

¹ Institut national de la recherche scientifique, Centre Eau Terre Environnement, 490 rue de la Couronne, Québec, Canada

² Université de Pau et des Pays de l'Adour, e2s-UPPA, IPREM, 2 avenue Pierre Angot, Pau, France

Titre de la revue ou de l'ouvrage :

Science of the Total Environment

Publié le 09 avril 2021

<https://doi.org/10.1016/j.scitotenv.2021.146986>

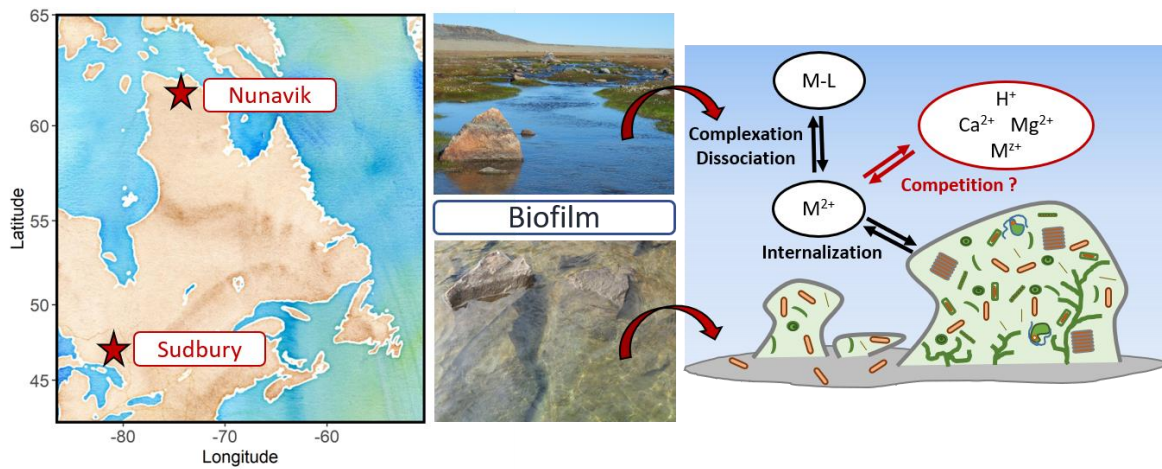
Contribution des auteurs :

Vincent Laderriere: Methodology, Software, Formal analysis, Investigation, Data curation, Writing – original draft, Visualization.

Séverine Le Faucheur: Writing – review & editing, Supervision.

Claude Fortin: Conceptualization, Methodology, Writing – review & editing, Supervision, Project administration, Funding acquisition.

3.1 Graphical abstract



3.2 Abstract

Biofilms play a key role in aquatic ecosystems. They are ubiquitous, even in the most contaminated ecosystems, and have great potential as bioindicators of exposure to contaminants such as metals. Freshwater biofilms and surface waters were sampled in two active mining areas of Canada: in the northern part of Nunavik (Quebec) and in the Greater Sudbury area (Ontario). Significant linear relationships were found between both total dissolved and free metal ion concentrations with biofilm metal contents for Cu and Ni, but not for Cd. When pH was below 6, biofilms accumulated less metals than at higher pHs. These results confirm that protons have a protective effect, leading to lower internalized metal concentrations. When considering only the sites where pH was above 6, the linear relationships between metal concentrations in water and in biofilms were improved for all three studied metals. The presence of metal ions could also modify the internalization of a given metal. To further study the role of cations as competitors to Cu, Ni and Cd uptake, relationships between the ratio of biofilm metal contents (Cu, Ni and Cd) on the ambient free metal ion concentrations were built as a function of potential cation

competitors, such as major cations and metals. Surprisingly, our data suggest that calcium plays a minor role in preventing metal accumulation as compared to magnesium and possibly other metals. At a global scale, metal accumulation remained highly consistent between the two studied regions and over the sampling period, despite differences in ambient physicochemical water characteristics, climate or types of ecosystems. Metal bioaccumulation is thus a promising biomarker to assess metal bioavailability in a mining context. Nevertheless, more data are still required to further highlight the contribution of each competitor in metal accumulation by biofilms and to be able to build a unifying predictive model.

Keywords: Biotic ligand model, Metal speciation, Biomonitoring, Nickel, Copper, Cadmium

3.3 Introduction

Human activities, such as mining operations, release significant amounts of metals into aquatic environments, which may exert pressures on aquatic ecosystems (Tercier-Waeber *et al.*, 2012). Measuring the total dissolved concentration can identify the level of exposure to living organisms but it does not provide information on the bioavailability of metals. Total metal concentrations are thus not always representative of ecotoxicological risk. Indeed, metals are present under several chemical forms in natural waters, which influence their bioavailability (Erickson, 2013; Adams *et al.*, 2020). Sites with similar total metal concentrations may result in different rates of bioaccumulation in aquatic organisms. For instance, Lopez *et al.* (2017) demonstrated that the accumulation of arsenic in benthic invertebrates varied significantly with pH for exposures to similar concentrations.

While high concentrations of metals can have direct toxic effects, mining activities often result in additional changes to water quality (Cadmus *et al.*, 2016). For instance, these operations can generate acid mine drainage, which can cause acidification when introduced to aquatic systems. This acidic byproduct is often neutralized by the addition of CaO, however, this subsequently yields high concentrations of cations that influence hardness (i.e. Ca) within receiving waters (Kalin *et al.*, 2006). Similar to the pH of water, changes in water hardness have been shown to modify metal bioavailability. As explained by Tercier-Waeber *et al.* (2012) competition of H⁺, Mg²⁺ and Ca²⁺ occurs at the transport binding sites of a metal. Additionally, competition between H⁺ and metals for binding ligands in ambient water can change metal speciation and thus bioavailability. In recent decades, models have been developed to describe the interaction of metals with biological membranes, such as the Free Ion Activity Model (FIAM) and later on, the Biotic Ligand Model (BLM; Morel, 1983; Campbell & Fortin, 2013). These two models predict that the biological response to metal exposure is mainly proportional to its free ion concentration, with the BLM incorporating the competitive effects of ions at the membrane surface. Applying such

models to field data can be challenging, however, as metal interactions to exposed organisms differ with the physicochemical composition of the medium and biotic factors specific to each organism.

The biomonitoring approach has proven to be very useful as a proxy for the bioavailability of metals in the field. In recent years, many biological models have been used in natural waters, such as fish (Weber *et al.*, 2008; Martyniuk *et al.*, 2020), invertebrates (Lebrun *et al.*, 2015; Mebane *et al.*, 2020) or freshwater periphytic biofilms (Xie *et al.*, 2010; Faburé *et al.*, 2015). The latter are particularly useful for a biomonitoring approach in natural waters; they are sedentary, ubiquitous and at the base of the trophic chain. Biofilms (or periphyton) are a community constituted of a variety of autotrophic and heterotrophic microorganisms (such as bacteria, microalgae, fungi and micromeiofauna) included in a self-produced matrix of extracellular polymeric substances (EPS; Flemming & Wingender, 2010; Battin *et al.*, 2016). Because biofilms are an assemblage of many organisms, some studies use one group inside the biofilm, such as diatom communities, as a bio-indicator of contaminants by their presence or absence (Morin *et al.*, 2012; Morin *et al.*, 2016; Tolotti *et al.*, 2019). Biological interactions (e.g. mobility, predation or food selection behavior) within the biofilm community can also be modified by contaminants, and thus can be used as a marker of direct or indirect effect (Neury-Ormanni *et al.*, 2020). Numerous studies successfully used biofilms as biomonitorors because they are known to respond quickly to organic or metal contaminants (Chaumet *et al.*, 2019; Bradac *et al.*, 2010; Lavoie *et al.*, 2012a). Furthermore, some studies have demonstrated that diet is a predominant exposure route and that metals can be transferred from biofilm to grazers (Xie *et al.*, 2010; Kim *et al.*, 2012). Freshwater biofilms seem therefore suitable for long-term monitoring and allow for metal toxicity to be assessed at a community level.

Statistically significant relationships between free metal ion concentrations in surface waters and intracellular metal concentrations in biofilms (for Cd, Cu Ni, Pb and Zn) were previously

observed from samples collected in the vicinity of mine tailings and operations (Lavoie *et al.*, 2012; Laderriere *et al.*, 2020). This suggests that metal content in biofilms could be used as a proxy of metal exposure and could play the role of a natural "passive sampler". In addition, the authors demonstrated that accumulation of metals by biofilms was modulated by major cations and protons, in agreement with the BLM principles. It was suggested that the biofilm response is robust over time and coherent over large geographical areas (Leguay *et al.*, 2016; Laderriere *et al.*, 2020) for Cd, Cu, Pb and Zn but additional data were needed for Ni. In the present study, we compared two different types of ecosystems (nordic and temperate areas) impacted by Ni mining. This also provided an opportunity to further test the response of this biomonitoring tool for Cd and Cu. To characterize the anthropogenic pressure in these two mining areas, the biofilm metal content, as well as the dissolved metal concentrations, were measured and the free metal ion concentrations were subsequently estimated. For both regions, metal accumulation data were assessed as a function of protons, major cations or other metals to characterize potential competing effects and to identify parameters needed to be considered in the development of a predictive tool for metal bioavailability using freshwater biofilms.

3.4 Materials & methods

3.4.1 Study area

The present study sites were located in two different mining regions of Canada: the northern part of Nunavik in Quebec and the Greater Sudbury area in Ontario. Both regions are characterized by an intensive extraction of Ni, Cu and precious metals. However, both areas are different in terms of geology, climate and ecosystem. The sampling was designed to capture a representative metal contamination gradient of these two regions as well as different

physicochemical conditions. The detailed sampling map of both regions is presented in Figure 3-1.

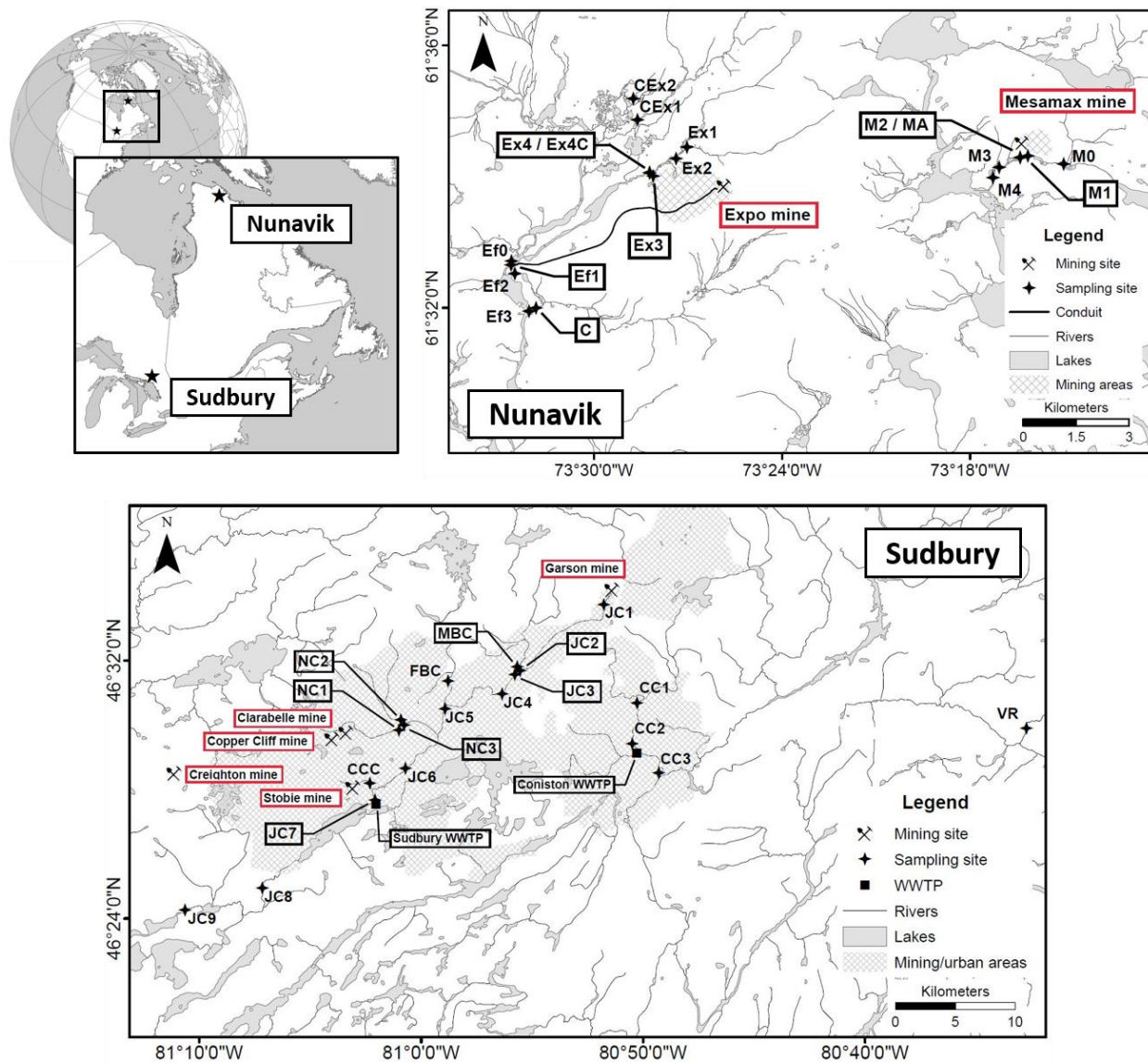


Figure 3-1 : Sampling sites in Nunavik (QC) and in the Sudbury area (ON) in Canada. The shaded zones (light gray) represent in both cases the mining or urban areas. WWTP = wastewater treatment plant; JC = Junction Creek; MBC = Maley Branch Creek; VR = Veuve River; FBC = Frood Branch Creek; CC = Coniston Creek; NC = Nolin Creek; CCC = Copper Cliff Creek.

3.4.1.1 Northern Nunavik region

Nunavik is the largest administrative region of Quebec and is located north of the 60th parallel. Although sparsely populated, this vast area is the home of indigenous populations and is thought to hold large metal reserves. Located on the Canadian Shield, it has a metal-rich geological composition. Two field campaigns were undertaken during the summer of 2016 (July and August) in the vicinity of the Nunavik Nickel mine (*Canadian Royalties Inc.*) operated by *Jilien Jien Nickel Industry Co., Ltd.* Currently, this mine extracts primary metals such as Cu and Ni, but also lanthanides and precious metals such as Au, Ag and Co. It is an open-pit mine located 400 km north of the boreal forest northern limit and 59 km west of the Inuit village of Kangiqsujuaq. The mine discharges its treated effluents into the Puvirnituq River. This river is the main source of drinking water for the village of Puvirnituq, which is located 260 km downstream from the effluent discharge site. The treated effluents are discharged between June and September and sampling dates were chosen accordingly to capture any potential metal contamination. During the sampling campaigns, the mine had two main operating sites, the Expo site (in operation since 2012) and the Mesamax site (since 2013). In total, 18 sites were sampled in the vicinity of these two operating sites. For a more detailed description of the study sites, the reader is referred to a previous publication (Lavoie *et al.*, 2018). Data on biofilm metal content from sampling expeditions in 2014 and 2015 have also been the focus of a previous publication (Laderriere *et al.*, 2020).

3.4.1.2 Southern Ontario region

The second study area is located further south in the Greater Sudbury area in Ontario. This area has a long mining history and hosts a population of 160 000. Ontario is the most active mining province in Canada, and is one of the world's largest producers of Ni and Cu. The first smelter was built in 1888 and six mines were in operation within a 20-km radius of Sudbury:

Garson (*Valve Canada Limited*), Stobie (*Valve Canada Limited*), Clarabelle (*Valve Canada Limited*), Copper Cliff North (*Valve Canada Limited*), Creighton (*Valve Canada Limited*) and Nickel Rim South (*Glencore Canada Corporation*). In September 2016, nine sites were sampled along the Junction Creek River. This is the main river flowing through the City of Sudbury, which receives the city's discharged effluent as well as effluents from nearby mines. In addition, ten sites were also sampled from tributaries of the Junction Creek River (Maley Branch Creek, Frood Branch Creek, Nolin Creek, Copper Cliff Creek), Coniston Creek and the North Veuve river. For more historical details on the region, the reader is referred to our previous study (Lavoie *et al.*, 2018) in which the general water chemistry is presented.

3.4.2 Surface water collection and analyses

Each site was sampled for water chemistry in triplicate ($n = 3$). Unless otherwise mentioned, all plasticware to be used for cation work was previously soaked in 10% (v/v) HNO_3 (ACS grade; Fisher Scientific) for 24 h, thoroughly rinsed three times with distilled water and three times with ultrapure water (18 $\text{M}\Omega\cdot\text{cm}$), and dried under a laminar flow hood. Sampling bottles (15 mL; HDPE; Nalgene) were pre-acidified to 0.2% (v/v) HNO_3 (trace metal grade; Fisher) before sampling. Plasticware for anion and dissolved organic carbon (DOC) work was rinsed six times using ultrapure water and dried under a laminar flow hood. For total phosphorus samples, unwashed new tubes (50 mL; polypropylene (PP); Sarstedt) were used and were pre-acidified to 0.2% (v/v) H_2SO_4 (Fisher Scientific) before sampling. In the field, syringes (20 mL; PP; Fisher Scientific) were used and fully rinsed three times on-site with surface water. Affixed disposable polysulfonate encapsulated filters (0.45 μm porosity; VWR International) were purged prior to use with 5 mL of surface water before sampling. Triplicate 15 mL filtered samples were obtained for the subsequent analyses of major cations and metals. This was repeated to obtain triplicate filtered samples for the analyses of major anions and DOC. Bulk unfiltered water samples were

also taken for total phosphorus analysis. After sampling, all bottles were kept on ice in a cooler for transport and later stored at 4°C. Additionally, at each site, blanks were generated using ultra-pure water which underwent the same manipulations as field samples for the purpose of investigating possible procedural contamination (blanks were prepared for cations, anions and DOC analyses).

3.4.3 Biofilm collection and metal content

The biofilm considered in the present study corresponds to a periphytic biofilm collected using toothbrushes by scraping several benthic rocks. A new toothbrush was used at each site and rinsed with ambient surface water before use. The collected biofilms were composite samples of four randomly selected rocks. Each sampled biofilm was collected in trace metal grade unwashed new tube (50 mL; PP; Sarstedt) and re-suspended with site water. All samples were centrifuged (5 min, 4000g) at the end of each day. The pellet was resuspended in 15 mL of 10 mM ethylenediaminetetraacetic acid (EDTA) solution at pH 7. The chelator EDTA was used to extract adsorbed metals in order to differentiate between intra- and extracellular contents (Meylan *et al.*, 2004; Lavoie *et al.*, 2012b; Crémazy *et al.*, 2013). The EDTA solution was withdrawn and the pellet was kept frozen prior to freeze-drying for 48 h (Dura-Top/Dura-dry MP; FTS SYSTEMS). A cold, partial digestion of 30 mg of dry mass (precisely weighed) was performed with the addition of 0.8 mL of concentrated HNO₃ (Trace Metal Grade; Fisher Scientific) for 48 h. Then, 0.2 mL of concentrated H₂O₂ (Optima Grade; Fisher Scientific) was added and allowed to stand for another 48 h. An aliquot of 0.8 mL of mineralization supernatant was collected and transferred to a new 13 mL tube (PP; Sarstedt) containing 7.2 mL of milli-Q water for a final volume of 8 mL resulting in a 10% of HNO₃ matrix (v/v). The solutions were then stored in the refrigerator (4°C) prior to analysis. Digestions were also performed on certified materials of lichen and algae from the International Atomic Energy Agency (IAEA-336, IAEA-413 and IAEA-450). Measured metal

contents of certified material were all higher than 80% of certified values ($80.5 \pm 0.6\%$ Cu, $81 \pm 0.5\%$ Ni, $85.7 \pm 0.6\%$ Cd; n = 3).

3.4.4 Analyses

For water and biofilm samples, cations (Na, Mg, Al, Si, K, Ca, Mn, Fe) and metals (Ni, Cu, Zn, Cd, Pb) were measured by inductively coupled plasma–atomic emission spectrometry (ICP-AES; Varian Vista AX CCD), and anions (Cl⁻, F⁻, SO₄²⁻ and NO₃⁻) were measured by ion chromatography (Dionex Autolon; System DX300). Trace element (Zn, Cu, Cd, and Pb) concentrations in water and biofilm were also determined by ICP-mass spectrometry (Thermo instrument model X7). The DOC samples were analyzed using a total organic carbon analyzer (TOC-500A; Shimadzu) and total phosphorus concentrations were determined using persulfate digestion colorimetry (SM 4500-PB). For several sites, Zn measured concentrations as well as those of Pb were sometimes lower than field background blank samples. Because of the overall very low Zn and Pb concentrations observed at our sampling sites, we focused our data analyses on Cd, Cu and Ni.

3.4.5 Metal speciation

The Windermere Humic Acid Model VII (WHAM) was used to estimate metal speciation in natural waters (Lofts & Tipping, 2011). This software allows for calculating the concentrations of metal species at equilibrium using input parameters such as the measured concentrations of cations, anions and DOC as well as pH. Total carbonates were assumed to be at equilibrium with the atmosphere (3.09×10^{-4} atm) and the default thermodynamic database was used. The concentrations of fulvic (FA) and humic (HA) acids were required for modelling purposes, which were estimated from the concentrations of dissolved organic carbon (DOC). The proportion of FA

to HA was assumed to be at a 3:1 ratio and metal binding DOC to represent 60% of the dissolved organic matter, which is made of 50% C (Perdue & Ritchie, 2003).

3.4.6 Metal accumulation model

The BLM is a conceptual model developed to explain how dissolved metals interact with biological membranes and thus, eventually enter aquatic organisms (Campbell & Fortin, 2013). The biological response to a metal is assumed to be proportional to its internalization and subsequent binding to sensitive intracellular sites. If we consider that a cell membrane receptor (noted as $\{\equiv X^-\}$) could interact with a proton (H^+), a cation (Cat^{z+}), or a metal (M^{z+}) with equilibrium constants K_H , K_C and K_M , respectively, we can write:



We assumed that $\{\equiv X - M\} < \{\equiv X^-\}$ because of the relatively low concentrations of trace elements in freshwaters, which allows us to consider the following as described by Leguay *et al.* (2016):

$$\{\equiv X\}_{Tot} = \{\equiv X^-\} + \{\equiv X - H\} + \{\equiv X - Cat\} + \{\equiv X - M\} \quad (4)$$

If we combine Eq 4 with Eqs 1, 2 and 3, we obtain:

$$[\equiv X - M] = \frac{K_M[M^{z+}] \times [\equiv X]_{Tot}}{1 + K_H[H^+] + \sum_i (K_C[Cat_i^{z+}])} \quad (5)$$

Note that a proportionality constant a is inserted to link metal binding to steady-state metal content in biofilms ($[M_{Bio}]$):

$$[M_{Bio}] = \frac{a \times K_M[M^{z+}] \times [\equiv X]_{Tot}}{1 + K_H[H^+] + \sum_i (K_C[Cat_i^{z+}])} \quad (6)$$

3.4.7 Data treatment

Unless otherwise indicated, results are given as the mean \pm one standard deviation for a minimum of three replicates. Statistical analyses and figures were performed using R software (v. 4.0; <https://cran.r-project.org>). No outlier treatment was applied.

3.5 Results & discussions

3.5.1 General water chemistry

Physicochemical parameters measured for both regions are presented in Figure 3-2. The mean values and standard deviations of the physicochemical parameters of the surface water sampled at each site and for both regions are publicly available (<https://doi.org/10.5683/SP2/RBIM04>). Among the measured parameters, only T, Fe, Mn, Ni and Pb did not show significant differences between the two studied regions.

In Nunavik, very low pH values were measured near the extraction sites. The closest sampling sites, *i.e.* Expo sites (EX2, EX3, EX4 and EX4C), had pH values below 5, or even 4 in the case of EX3. In Sudbury, only the CCC site situated downstream of wastewater releases from the Copper Cliff mine was slightly acidic, with a pH value below 6 (pH = 5.75). From the 18 sampling sites in Nunavik, 12 were acidic (pH < 6) whereas in Sudbury, only one site out of the 19 sampled had a pH value below 6. Excluding these sites, the average pH values were around 6.5 ± 0.4 for the Nunavik region and 7.2 ± 0.5 for the Sudbury area. Moreover, the Sudbury area is characterized by average DOC values of 4.3 ± 2.4 mg/L compared to 1.9 ± 0.7 mg/L for Nunavik, these values being statistically different (Figure 3-2). This difference can be explained by the higher biological productivity in the Sudbury area compared to Nunavik. Indeed, the Sudbury area in southern Ontario is characterized by an important forest cover with a mixture of coniferous and deciduous trees. In contrast, Nunavik has a polar climate with an ecosystem corresponding to

herbaceous tundra. The acidic pHs found in Nunavik may also contribute to the observed low concentrations of organic matter since the solubility of humic acids decrease with acidity (Perdue & Ritchie, 2003). Lower phosphate concentrations in Nunavik are another significant difference between the two regions. Note that the Nunavik data were consistent over time for the two sampling periods (July and August) and with the data obtained in 2014 and 2015 (Laderriere *et al.*, 2020).

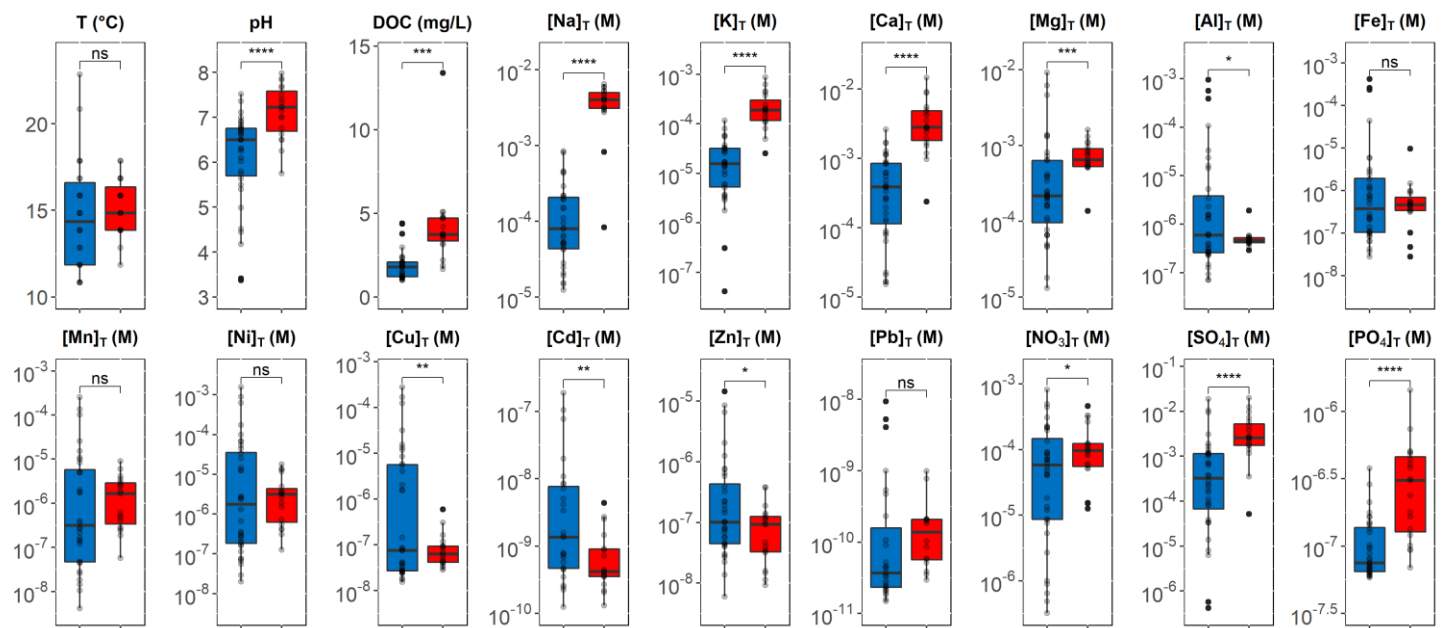


Figure 3-2 : Box plots of major physicochemical parameters for the surface waters sampled in July and August for Nunavik (blue), and in September for Sudbury (red). Except for temperature and DOC, data are presented on a log scale. A t-test was performed on means for comparison with significance thresholds of: $p \leq 0.0001$ “**”; $p \leq 0.001$ “**”; $p \leq 0.01$ “*”; $p \leq 0.05$ “*”; $p > 0.05$ “ns”.**

3.5.2 Dissolved metal concentrations

High concentrations of dissolved metals (Ni, Cu and Cd) were found in mining impacted surface waters for both regions. The most contaminated sites were characterized by metal concentrations that were one to several orders of magnitude higher than the reference sites in

both the Sudbury area (MBC and VR) and in Nunavik (CEx1, CEx2, C and M0). The Sudbury reference sites MBC and VR had concentrations below 310 nM, 31 nM and 0.3 nM for Ni, Cu and Cd, respectively. In the case of Nunavik, the control sites had concentrations below 250 nM, 30 nM and 0.6 nM for Ni, Cu and Cd, respectively. Overall, higher background concentrations of dissolved metals were found in Sudbury. Although the total dissolved Ni concentrations were not statistically different between the two regions, the range of Ni concentrations was much greater in Nunavik ($10^{-8} - 10^{-3}$ M) than in Sudbury ($10^{-7} - 10^{-5}$ M). Similarly, Cu and Cd concentrations spanned over a larger range of values in Nunavik than in Sudbury, and showed statistical differences between the two regions (Figure 3-2).

The sites with the highest concentrations were sampling points located near the operating sites; the Expo sites in the case of Nunavik (EX1, EX2, EX3, EX4 and EX4C) and the Nolin Creek sites (NC1, NC2 and NC3) in the case of the Sudbury area. Indeed, the EX3 site was characterized by the highest concentrations of dissolved metals reported, with 1.2 ± 0.4 mM Ni, 0.22 ± 0.06 mM Cu and 0.15 ± 0.05 μ M Cd. The Mesamax sites (M0, M1, M2, M3, M4 and MA) and effluent sites (EF0, EF1, EF2, EF3) located further away from the mine (~6 km) showed concentrations in the μ M range. In the Sudbury area, the tributaries receiving mining effluents had the highest concentrations. For example, Frood Branch Creek (FBC) and Nolin Creek (NC1, NC2 and NC3) were the most contaminated with concentrations in the μ M range for Ni and Cu, and nM for Cd. These rivers receive effluents from the Frood and Nolin mines, respectively. The highest observed concentrations were at the NC1 for Ni with concentrations of 17.7 ± 0.05 μ M, and at the NC2 for Cu and Cd with concentrations of 0.60 ± 0.04 μ M and 4.37 ± 0.05 nM, respectively. Frood branch and Nolin creeks are both tributaries of the Junction Creek (JC) River and flow into it between JC5 and JC6 sampling sites. Additional sampling points were selected along Junction Creek and the JC7 site had the highest dissolved Ni concentration (4.95 ± 0.01 μ M) among the JC sites; the JC7 site is located just after the discharge of the Sudbury municipal

wastewater treatment facilities. The concentrations found at sites JC1 to JC3 remained high ($> 3 \mu\text{M Ni}$), which is due to the Garson mine located upstream from JC1 where effluents are discharged. As mentioned in previous studies (Lavoie *et al.*, 2018; Lavoie *et al.*, 2019), these two regions are strongly affected by mining activities with metal concentrations exceeding the recommended values of the Canadian Council of Ministers of the Environment in many cases (Canadian Council of Ministers of the Environment, 2014). Based on an average water hardness (142 mg CaCO₃/L for Nunavik and 478 mg CaCO₃/L for Sudbury), the chronic exposure criteria were 0.055 $\mu\text{M Cu}$, 2.1 $\mu\text{M Ni}$ and 1.9 nM Cd for Nunavik, and 0.063 $\mu\text{M Cu}$, 2.6 $\mu\text{M Ni}$ and 3.3 nM Cd for Sudbury. In the most contaminated sites for both regions, dissolved Cu, Ni and Cd concentrations were highly above these criteria. In the case of EX3 in Nunavik, this difference represents a factor of 4100, 580 and 77 for Cu, Ni and Cd, respectively. In Sudbury, dissolved concentrations were slightly above the criteria for Ni (7x) at NC1 and for Cu (9x) and Cd (1.3x) at NC2.

3.5.3 Biofilm metal contents as a function of total dissolved and free ion concentrations

Several studies have found tight relationships between metal concentrations (labile or free metal ion) in ambient media and periphytic biofilm metal content (Bonneau *et al.*, 2020). These results were obtained based on both field and laboratory approaches: using microcosm experiments in the laboratory (Meylan *et al.*, 2004; Mebane *et al.*, 2020) or through field sampling at the river scale (Bonet *et al.*, 2013; Faburé *et al.*, 2015), at the watershed scale (Morin *et al.*, 2008; Lavoie *et al.*, 2012b) or at the inter-regional scale (Leguay *et al.*, 2016; Laderriere *et al.*, 2020). Correlation coefficients obtained through linear regression analyses of biofilm metal contents as a function of both dissolved concentrations and free metal concentrations are shown in Table 3-1. Except for Cd, taking into account Sudbury and Nunavik data at all pHs, statistically

significant linear relationships were found between biofilm metal contents and their concentrations.

Table 3-1 : Coefficients of determination (R^2 values) from linear regression analyses of accumulated metals ($[M]_{Bio}$) as a function of dissolved or free metal concentration. Significance threshold values are: $p \leq 0.0001$ "**"; $p \leq 0.001$ "****"; $p \leq 0.01$ "**"; $p \leq 0.05$ "*"; $p > 0.05$ "ns". All data refers to data from Nunavik and Sudbury together.**

Metal form	All data	Nunavik	Sudbury			
All pHs						
Dissolved Cu	0.35	****	0.48	****	0.77	****
Free Cu ²⁺	0.41	****	0.58	****	0.62	****
Dissolved Ni	0.16	**	0.24	**	0.54	***
Free Ni ²⁺	0.14	**	0.27	**	0.50	***
Dissolved Cd	1.9×10^{-4}	ns	2.6×10^{-3}	ns	0.35	**
Free Cd ²⁺	7.1×10^{-5}	ns	2.3×10^{-5}	ns	0.33	**
Only pH > 6						
Dissolved Cu	0.63	****	0.71	****	0.79	****
Free Cu ²⁺	0.57	****	0.74	****	0.60	***
Dissolved Ni	0.62	****	0.54	****	0.70	****
Free Ni ²⁺	0.55	****	0.56	****	0.70	****
Dissolved Cd	0.38	****	0.37	**	0.35	**
Free Cd ²⁺	0.30	***	0.37	**	0.38	**

Coefficients of determination (R^2 values) were comparable whether the biofilm metal content was expressed as a function of free metal concentrations or total dissolved metal concentrations.

In the merged data set, the average ratio of M^{2+}/M_T was $18 \pm 30\%$, $76 \pm 17\%$ and $71 \pm 16\%$ for Cu, Ni and Cd, respectively. For each region, these ratios were $26 \pm 34\%$, $81 \pm 17\%$ and $76 \pm 17\%$ for Nunavik, and $3 \pm 5\%$, $68 \pm 13\%$ and $62 \pm 8\%$ for Sudbury. Nickel and Cd were mainly present as free ion species, reflecting their poor affinity for natural organic ligands (Mueller *et al.*, 2012). The remaining predicted Ni complexes are mainly with carbonates (~3%), sulfates (~10%) and DOM (~9%), whereas Cd binds to sulfates (~12%), chlorides (~7%) and DOM (~11%). Conversely, Cu is known to have a strong affinity for organic ligands and only a small proportion of Cu is usually present as the free ion (Mueller *et al.*, 2012). Indeed, about $76 \pm 37\%$ were calculated to bind to DOM in our samples. The remaining was principally bound by sulfates (~4%), carbonates (~1%) or present in the free form (~18%). However, in the case of Nunavik, these ratios are strongly affected by pH. With decreasing pHs, protons progressively bind to ligand functional groups which decreases binding site availability for metals and subsequently leads to an increase in the percentage of free metal ions. This point is important because, for Cu in the Nunavik data set, by excluding sites with pHs below 6, the percentages of free and DOM-bound Cu become $5 \pm 11\%$ and $91 \pm 17\%$, respectively. At circumneutral pHs, Cu is therefore scarcely present in its free form. Studies comparing field speciation to those predicted by WHAM in freshwaters report good agreements for metals that are known to weakly bind to DOM such as Ni and Cd (Unsworth *et al.*, 2006; Loft & Tipping, 2011; Mueller *et al.*, 2012). However, depending on the analytical method used to measure the free ion concentration, the speciation of metals that have high affinity for DOM (such as Cu) were predicted with less accuracy. It was also observed that agreement between *in situ* measurements and WHAM predictions of the free metal ion tend to improve in lakes that had high total Cu concentrations. Additionally it was observed that there was excellent agreement when free copper concentrations were higher than 10^{-9} M (Mueller *et al.*, 2012). In the present study, free copper concentrations were calculated to be ranging between $\sim 10^{-12}$ to $\sim 10^{-4}$ M.

Despite these differences between total and free ion concentrations, these two concentrations are strongly correlated for Cu, Ni and Cd, with R^2 values of 0.93, 0.98 and 0.97, respectively (data not shown). As such, using the free metal ion concentrations do not improve the relationships between metal concentration in ambient media and bioaccumulated metal (Table 3-1), suggesting that there are no advantages of using the free ion concentration to predict metal accumulation in our samples. Such a result does not apply for all rivers. For instance, Lavoie *et al.* (2012) reported significant relationships between biofilm Cu content and free Cu concentrations, but not with total dissolved Cu concentrations. Indeed, despite total Cu concentrations being comparable across sampling sites (15 to 46 nM), a clear gradient of free ion concentrations was observed (~10 pM to ~3 nM). The authors explained this result by the presence of a concentration gradient in DOC (1.9 to 5.8 mg C/L), resulting in an increase in Cu binding downstream of the mine tailings, which resulted in a decrease in Cu accumulation in biofilms. Because free metal ion concentrations are not always correlated to total dissolved metal concentrations, as it is the case in our study, using free metal concentration ensures that the present approach can be generalized on a larger geographical scale and therefore under various water chemistry conditions.

3.5.4 Relationships between metal accumulation and free metal ion concentration on a regional scale

Linear regressions were plotted for biofilm metal content as a function of free metal ion concentrations for the two sampled regions (Figure 3-3). Using an analysis of covariance (ANCOVA), the obtained slopes were found to be statistically different between the two regions and for the three metals studied (p-values of 0.0005, 0.038, 0.013 for Cu, Ni and Cd, respectively).

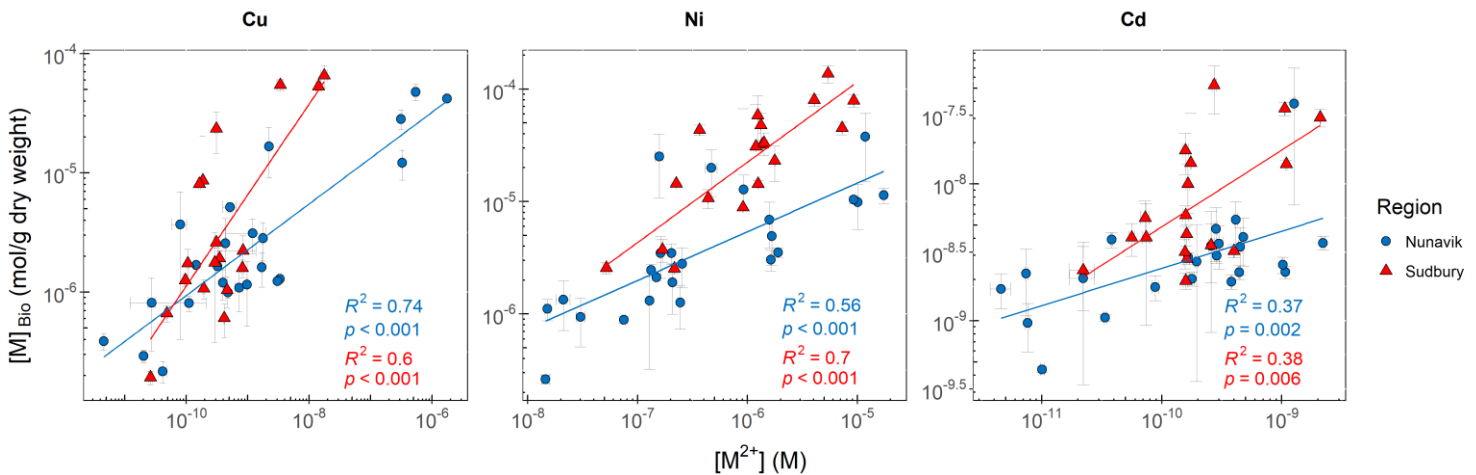


Figure 3-3 : Regressions of biofilm metal contents (Cu, Ni and Cd) as a function of free metal species (Cu^{2+} , Ni^{2+} , Cd^{2+}) for sites where $\text{pH} > 6$. Nunavik data are represented as blue circles and Sudbury data as red triangles.

It is well known that environmental factors such as light or temperature are two of the main environmental parameters influencing primary production (Staehr & Sand-Jensen, 2006). Several studies have been conducted to assess the role of environmental fluctuations of parameters such as temperature (Morin *et al.*, 2017), light duration (Corcoll *et al.*, 2012a), light intensity (Cheloni & Slaveykova, 2018) or, more generally, seasonal variability (Faburé *et al.*, 2015) on the effects of metals upon biofilms. All of these studies highlight the fact that environmental parameters are likely to modify biofilm composition and thus potentially its response to metal exposure. Although no significant differences were observed in temperature (see Figure 3-2), it should be noted that the Sudbury area has significant forest cover, which can influence the amount of warming caused by solar radiation received at the water's surface. In contrast, the tundra of Nunavik has minimal shade coverage and the streams are very shallow. Significant temperature variations can therefore occur between a sunny or overcast day, or between day and night. Daily variation could thus occur and a single temperature measurement may not be sufficient to make accurate conclusions. Furthermore, these two regions are at different latitudes and light (intensity or spectral composition), which can modify the response of phototrophic aquatic organisms to metal

exposure. Light can either directly affect the interactions between trace metals and photosynthetic microorganisms (i.e., metal toxicokinetics and toxicodynamics) or indirectly change ambient medium characteristics (Cheloni & Slaveykova, 2018). For instance, Cheloni *et al.* (2014) reported a change in Cu accumulation by *Chlamydomonas reinhardtii* when exposed to an altered ratio of PAR/UVR (photosynthetically active radiation/ultra-violet radiation) although no subcellular effects or growth inhibition were observed. The mine in Nunavik is located north of the 60th parallel and this high latitude means that the biofilm could receive a light with a different PAR/UVR ratio than in the Sudbury region. Furthermore, the region has a photoperiod of approximately 19/5 (day/night) at the summer solstice, compared to 15/9 for the city of Greater Sudbury (46° of latitude). Biofilms from Nunavik thus benefit from a greater photoperiod and a slightly different light spectral composition than biofilms from Sudbury. However, as mentioned by Cheloni & Slaveykova (2018), we still lack knowledge about these interactions and better understanding the mechanisms driving trace metal effects in aquatic environments and light irradiation will enable relevant lab-to-field extrapolation of metal exposure data.

The question is therefore whether a difference in communities induces a different bioaccumulation response. For instance, Pesce *et al.* (2018) exposed natural biofilms for 4 weeks to three different temperatures (18, 23, and 28°C) in microcosms enriched with Cu (0.24 µM). Using different biomarkers, the authors studied the metal response of heterotrophic and autotrophic compartments of the biofilm (including microalgae, bacteria, fungi, and heterotrophic protists). They postulated that both the increase in temperature and the chronic Cu exposure modify microbial community structure, leading to changes in the capacity of phototrophic and heterotrophic communities to tolerate subsequent acute exposure to Cu. However, although the authors highlighted the fact that the toxic response to Cu can vary greatly depending on the considered endpoint, they found no significant differences in internalized Cu concentrations, regardless of temperature and community changes. A similar conclusion was reached by Stewart

et al. (2015) who exposed two different biofilm communities to Pb (97 nM) for 3 weeks to relate Pb distribution to biological effects in biofilm. The study concluded that Pb accumulation was independent of the community composition, with field data suggesting a similar conclusion. Indeed, both areas of the present study have been the subject of previous publications by Lavoie *et al.* (2018, 2019) on diatom assemblage structures. These studies demonstrated different diatom assemblage structures depending on the level and the type of contamination inside the same area and between the two regions. However, some similar species were found in both areas as *Achnanthidium minutissimum*, a species known to be tolerant to high metal concentrations (Luís *et al.*, 2011; Morin *et al.*, 2012; Leguay *et al.*, 2016). In earlier work, Lavoie *et al.* (2012) collected water and biofilm samples in a single river once a month from May to October. Results showed similar accumulation of metals over time, despite the large variations in diatom species composition observed. Moreover, Leguay et al., (2016) demonstrated complementary findings with observed metal accumulation in biofilms from different regions (sites over 500 km apart) and among rivers with different physicochemical characteristics. In other words, field data suggest that, while environmental fluctuations or exposure to metals may alter the biofilm composition, metal content represents a robust biomarker for quantifying the metal exposure of biological communities.

3.5.5 Relationships between metal accumulation and free metal ion concentration on a global scale

For a similar free metal concentration, the biofilm metal concentrations were of the same order of magnitude in Sudbury and Nunavik, despite the distance (~1700 km apart) and the different physicochemical parameters of ambient surface waters. This result suggests that metal accumulation by biofilm in rivers can be compared between different ecosystems and ranges of

free metal concentrations, although differences in uptake can be observed on a finer scale. Henceforth, we have combined the data from both regions to seek further trends.

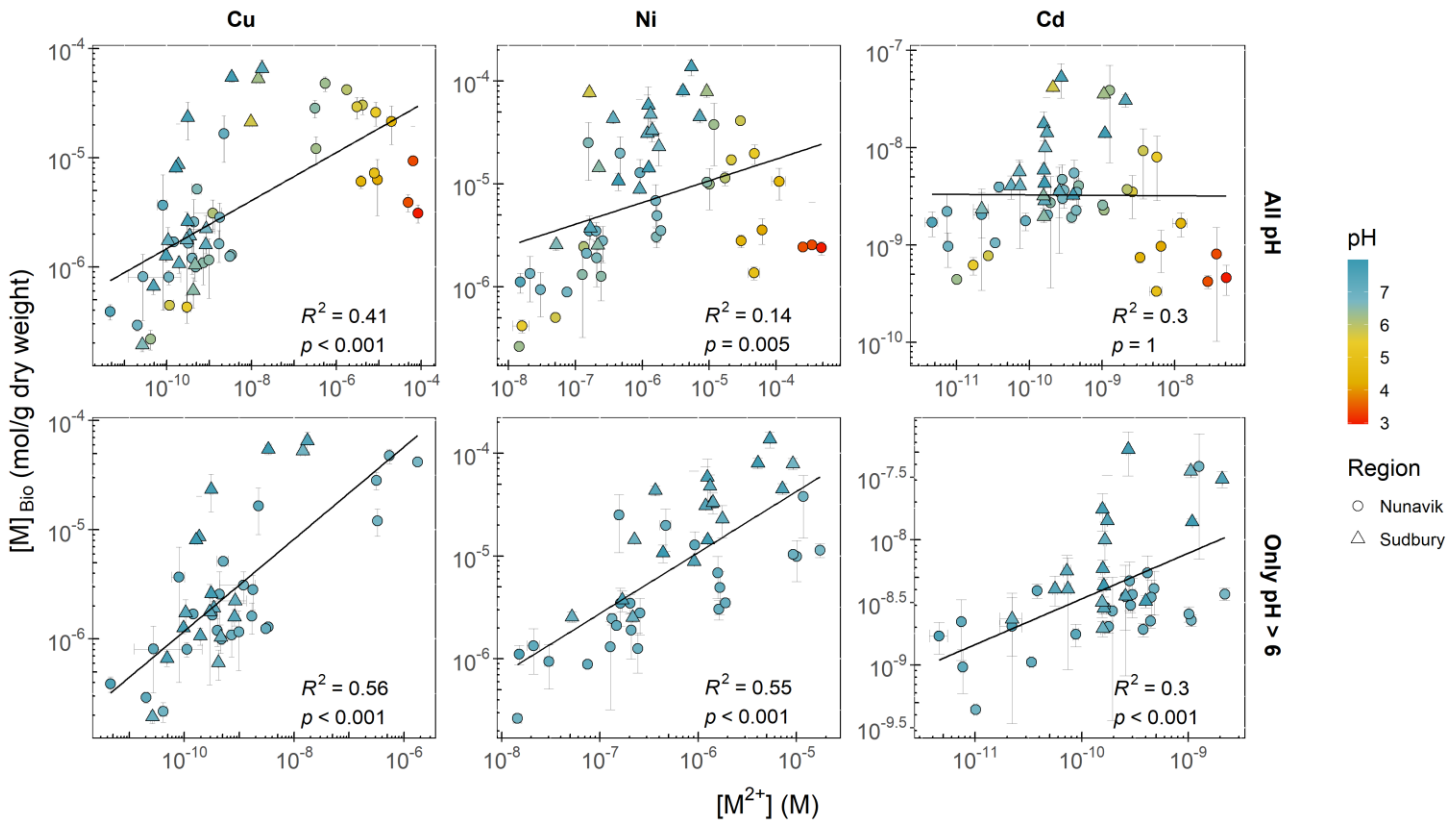


Figure 3-4 : Linear regression analyses of biofilm metal contents (Cu, Ni and Cd) as a function of free metal species (Cu^{2+} , Ni^{2+} , Cd^{2+}) for all samples from Nunavik (circles) and Sudbury (triangles) in 2016. The color gradient represents the observed pH values for each site. Upper figures represent data for biofilms collected at all sites and lower figures correspond to biofilms collected at sites with a pH higher than 6.

Sites with the highest free metal concentrations are characterized by low pHs and show internalized metal concentrations that do not follow the overall trend of the data (see yellow and red data in Figure 3-4). On the lower panel of Figure 3-4, the regressions statistically improve by excluding data with $\text{pH} < 6$ (higher R^2 values) whereas the linear relationship between biofilm Cd content and free Cd ion concentration became significant ($p = 0.0002$). These results are in

agreement with those published by Leguay *et al.* (2016) and Laderriere *et al.* (2020). The lower biofilm metal content at low pHs confirms the important role of pH and suggests an inhibition of metal uptake at high proton concentrations as highlighted in the BLM. A competitive effect is usually observed between H⁺ ions and metals (Sánchez-Marín *et al.*, 2018), which tends to decrease metal bioavailability and thus, toxicity. The possible effect of competing cations will be discussed below. Furthermore, acidity could also affect biofilm composition which may explain the lower biofilm metal content at pH < 6. For instance, Luís *et al.* (2014) showed a co-tolerance to metals and acidity of biofilms exposed to acidic treatments, contrasting with the higher sensitivity observed in biofilms exposed to alkaline treatments. In other words, the authors conclude that acidic environment exerts a selection pressure on the community composition which led to a greater tolerance to metal exposure. An acidic pH could therefore ameliorate the metal tolerance of a biofilm if the community has been pre-exposed (and has thus acclimated) to a complex chemical environment similar to what can be found in the vicinity of an operating mine. More recently, Luís *et al.* (2019) observed that biofilm communities affected by acid mine drainage and metal contamination had a greater ability to call upon antioxidant processes. This suggests that the adaptability of the biofilm communities to extreme acidic conditions may explain the low metal bioaccumulation at low pH levels. Nevertheless, these results obtained in the field confirm the universal potential of biofilm metal content to be used as a biomonitor at circumneutral pHs over time, on a large geographical scale.

3.5.6 Competing effects

Besides pH, hardness is also known to modulate metal accumulation with high Ca²⁺ concentration, typically providing a protective effect (Deleebeeck *et al.*, 2008). Moreover, trace metals can also show competitive effects between each other for uptake in algae as shown for Cu²⁺ (Flouty & Khalaf, 2015), Ni²⁺ (Worms & Wilkinson, 2007) and Cd²⁺ (Lavoie *et al.*, 2012b). As

presented in Eq. (6), the possible effect of competing cations can be evaluated by plotting the ratio of biofilm metal content to free metal ion concentration ($[M]_{\text{Bio}}/[M^{2+}]$), as a function of competing cation concentrations. For an element with no expected competing effect, the $[M]_{\text{Bio}}/[M^{2+}]$ ratio will be constant as a function of the competing cation concentration (a slope of zero). However, if the ratio decreases when a competing ion concentration increases (continuous decreasing trend), this would suggest that this ion may be modulating the biofilm metal accumulation.

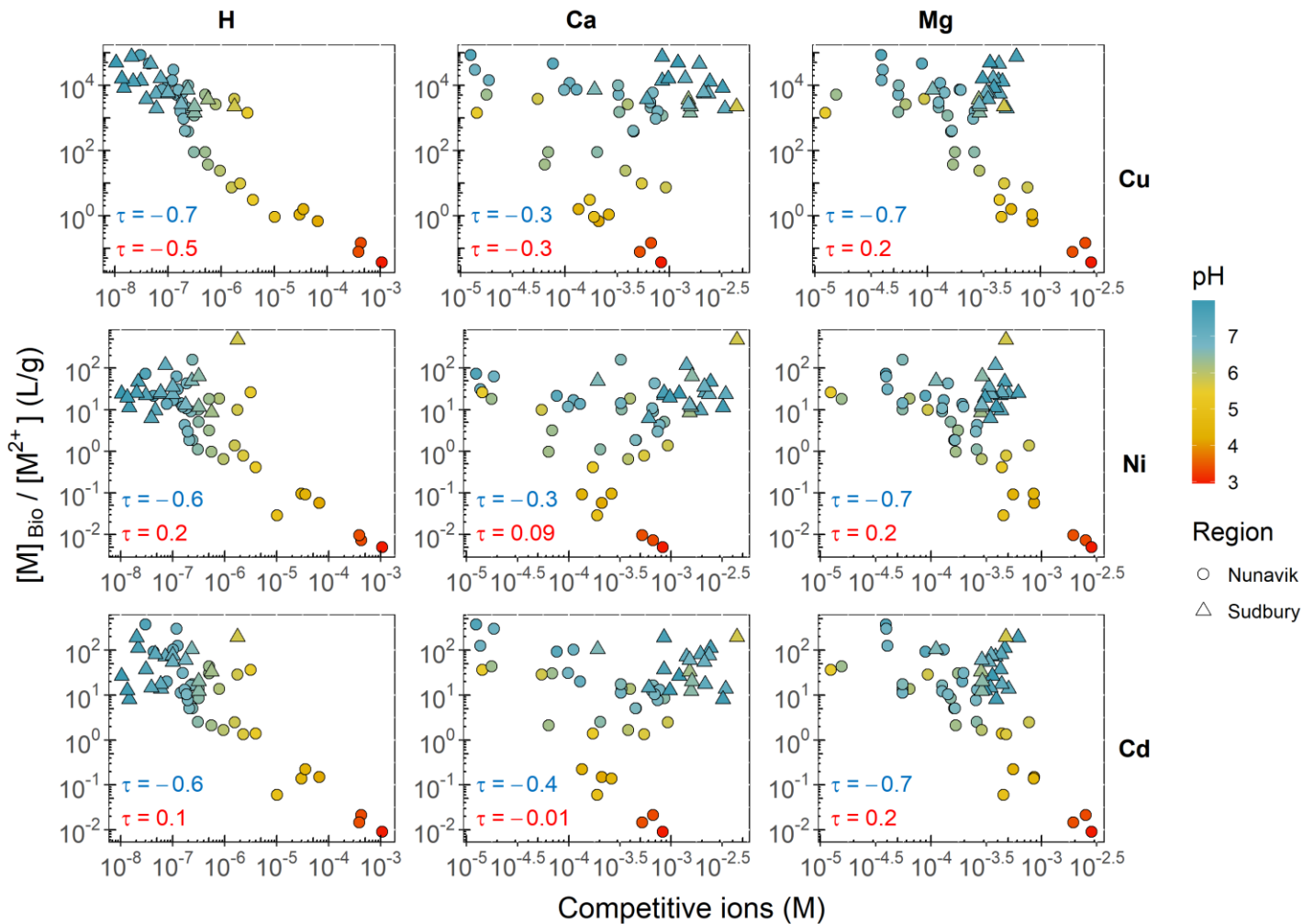


Figure 3-5 : Ratio of biofilm metal contents to free metal ion concentrations for Cu, Ni and Cd as a function of free proton, calcium, and magnesium concentrations. Symbols are identical to those used in Figures 3-3 and 3-4. Kendall's coefficients (τ) are presented for each region (blue for Nunavik and red for Sudbury).

The ratio of biofilm metal contents to free metal ion concentrations was then plotted as a function of the concentration of proton, calcium and magnesium ions for both regions (Figure 3-5). We used a Kendall's coefficient approach to measure the correlation of ratios ($[M]_{\text{Bio}}/[M^{2+}]$) with the different ions in the water column. Kendall's correlation (coefficient marked as τ) measures the dependence between two variables by ordinal association (based on rank correlation with values ranging from -1 to 1), and not only considering linear regression. The plots built as a function of proton concentration reveal the same trends for the three metals with ratio values relatively comparable for a proton concentration below 10^{-6} M. Beyond this concentration of H^+ , the three ratios follow a decreasing trend suggesting an important competing effect. This effect was more evident in the case of Nunavik compared to Sudbury, which is due to the quasi-absence of acidic pHs in the Sudbury data set. When plotted as a function of calcium, no uniform trend can be observed, although a plateau appears over the entire range of $[Ca^{2+}]$ for data where $pH > 6$. In other words, Ca^{2+} appears to have no notable competing effect at neutral pHs. However, the three ratios decrease when pH becomes acidic, reconfirming the key role of pH. This trend is particularly evident for the Nunavik data set (τ values of -0.3, -0.3 and -0.4 for Cu, Ni and Cd, respectively). With respect to the Sudbury data set, $[Ca^{2+}]$ remains stable around 10^{-3} M, which makes it difficult to observe a trend. The calculated τ values are close to 0 except for Cu ratio ($\tau = -0.3$), but no vertical trend is visible suggesting no competing effect despite important Ca^{2+} concentrations. These results are surprising because calcium is usually described as a key protective cation. For Mg^{2+} , the ratios decrease when its concentration increase in the water column. The pattern is particularly marked in Nunavik ($\tau = -0.7$ for the three metals studied) suggesting a protective effect. In the Sudbury data set, and as noticed for Ca^{2+} concentrations, the range of concentration is narrow resulting of τ values of 0.2 but with a variation of $[M]_{\text{Bio}}/[M^{2+}]$ between 10^1 and 10^2 L/g. Nevertheless, for a Ca^{2+} concentration between $10^{-3.5}$ and $10^{-2.5}$ M, a difference in ratio is observed between the two regions. Indeed, for these concentrations, the Sudbury data set shows a ratio of approximately 10^4 L/g for Cu and 10^1 L/g for Ni and Cd.

compared to 10^{-2} and 10^{-1} L/g in Nunavik. Nonetheless, sites with these low ratios are characterized by acidic pHs. It is therefore difficult to distinguish whether these values can be explained by low pH values or by the fact that elements are correlated with each other, especially at low pHs. In Leguay *et al.* (2016), $[M]_{\text{Bio}}/[M^{2+}]$ ratios showed a strong negative correlation with $[\text{H}^+]$, $[\text{Ca}^{2+}]$ and $[\text{Mg}^{2+}]$, demonstrating a competitive effect in the case of Cd and Zn. Moreover, for Cu and Pb, they observed a plateau followed by a continuously decreasing trend for both cations suggesting a competitive effect from a threshold concentration. However, for the range of Ca^{2+} concentrations found in Leguay *et al.* (2016), i.e. below 10^{-2} M of magnitude, our findings are in agreement. In addition, we reported similar relationships in the same area of Nunavik in 2014 and 2015 (Laderriere *et al.*, 2020). Indeed, results showed a gradual decrease in the ratio of Cu, Ni and Cd biofilm contents when the concentrations of protons and magnesium ions increased in the water column. However, for calcium, data was quite scattered and no clear trend was observed as we also observed here. Interestingly, for metals common to these studies, the ratios have the same values of $[M]_{\text{Bio}}/[M^{2+}]$ for circumneutral pHs, reaffirming the robustness of biofilm content as a pertinent biomarker of exposure despite large geographical scales, differences in type of ecosystem or biofilm characteristics.

In Figure 3-6, we analyzed the degree of association of each surface water parameter with the ratio of biofilm metal contents to its free metal concentrations for each region, independently. The upper panel presents three examples of opposing trends. In the case of $[\text{Cu}]_{\text{Bio}}/[\text{Cu}^{2+}]$ as a function of $[\text{Ni}^{2+}]$ (Nunavik data set), τ value is near -1 ($\tau = -0.7$) with data having a continuously decreasing trend. In other words, the ratio $[\text{Cu}]_{\text{Bio}}/[\text{Cu}^{2+}]$ is decreasing as the $[\text{Ni}^{2+}]$ is increasing. This indicates that Ni potentially acts as a strong competitor of Cu uptake in biofilm. With $[\text{Ni}]_{\text{Bio}}/[\text{Ni}^{2+}]$ as a function of $[\text{Ca}^{2+}]$ (Sudbury data set), τ value is near 0 indicating no trend and thus, no competing effect. The last case presents $[\text{Cd}]_{\text{Bio}}/[\text{Cd}^{2+}]$ as a function of $[\text{PO}_4^{3-}]$ (Nunavik

data set). Data follow an increasing trend, which leads to a positive τ value (0.6). Biofilm metal content is thus positively correlated with this element.

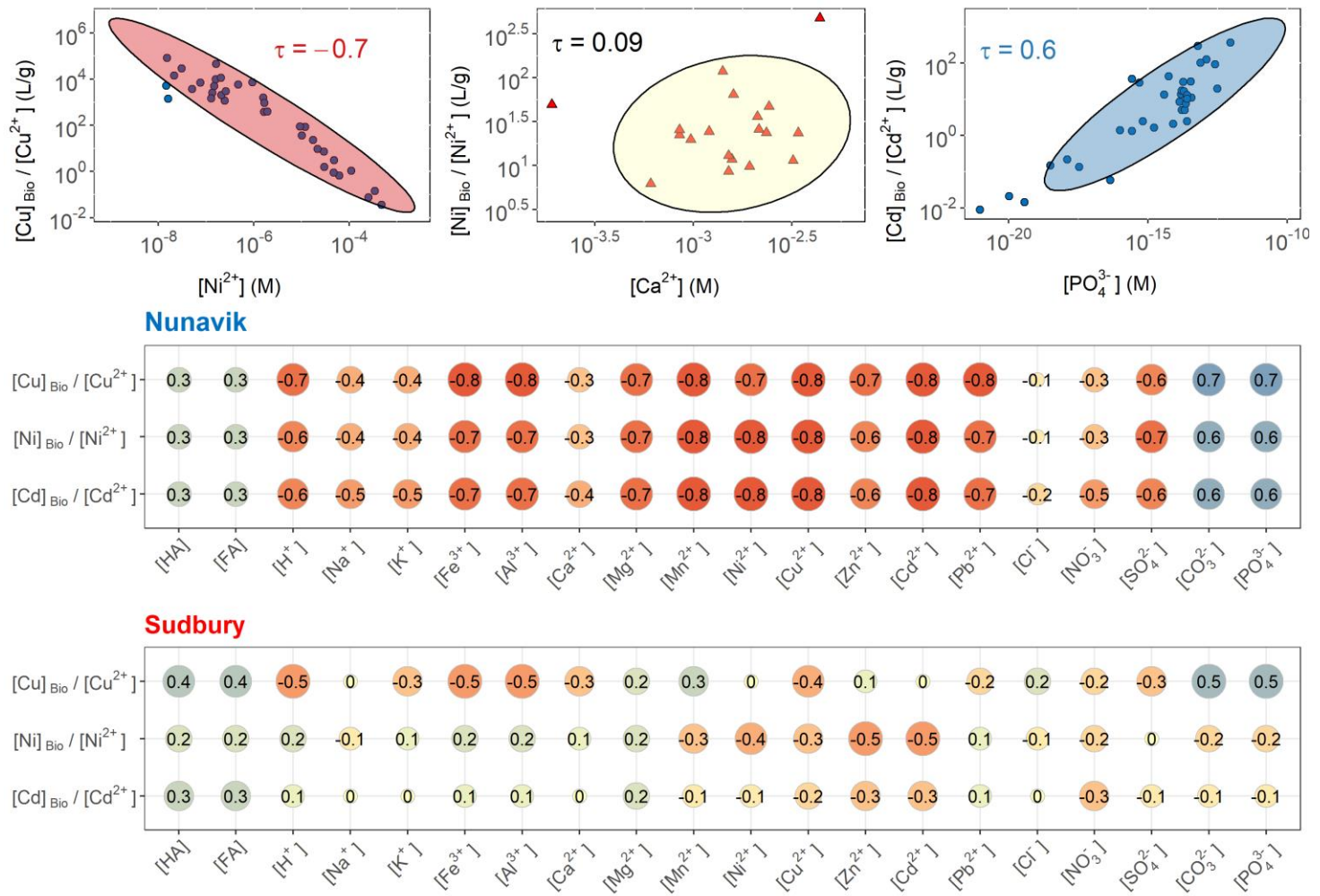


Figure 3-6 : The upper panel presents three examples of correlations, with a lower the Kendall coefficient indicating a greater effect of competition upon biofilm metal content (circles for Nunavik data and triangles for Sudbury data). The middle and lower panel presents, for each region, the ratio of biofilm metal content to free metal ion concentration for Cu, Ni and Cd as a function of the free species. The values represent the Kendall's correlation coefficient.

Despite our large number of samples, a greater variety of sampling sites incorporating physicochemical characteristics and the degree of anthropogenic pressure is needed to complete the analyses. Indeed, the Nunavik data set shows many auto-correlations between parameters,

which impede the correct distinction between interactions. For example, if one site had a high concentration of dissolved Cu, which occurs in many cases in the Nunavik data set, the dissolved competitor concentrations were also high. This point makes interpretation difficult because, using copper as an example, the copper concentrations ($[Cu]_T$ or $[Cu^{2+}]$) show a strong correlation with other metals. The biofilm metal content $[Cu]_{Bio}$ is thus correlated to $[Cu^{2+}]$, but also to other $[M^{z+}]$. As such, in the case of auto-correlated metals, ratios only indicate the correlation between the metals themselves. This explains why in the Nunavik data set, $[Ni]_{Bio}/[Ni^{2+}]$ shows a Kendall's coefficient equal ($\tau = -0.8$) with $[Cu^{2+}]$, $[Mn^{2+}]$, $[Cd^{2+}]$, and to major cation concentrations ($\tau = -0.7$ with $[Ca^{2+}]$ or $[Mg^{2+}]$). In 2014 and 2015, data collected at the same sites in Nunavik showed similar patterns and auto-correlations (Laderriere *et al.*, 2020). However, the results found in the present study confirm that the biofilm metal content is consistent over several years. The Sudbury data set is more appropriate to model competitive interactions and extract binding constants for biofilm using a BLM approach. Indeed, despite important mining activities, this data set incorporates more variability in stressors (e.g. urban context) and conditions (e.g. input of other rivers along the Junction Creek). Therefore, this region is less exposed to conditions specific to mining activities, such as acidic pH or very high concentrations of several metals at the same time. We will thus focus the rest of the discussion on the correlation matrix of the Sudbury data set. However, it is important to keep in mind that a τ value between -0.2 and 0.2 could represent data that do not necessarily form a decreasing pattern on an interesting range of concentrations. For instance, $[Mg]$ are tightly grouped around 10^{-3} M (see Figure 3-2) and $[Cu]_{Bio}/[Cu^{2+}]$ only vary by two orders of magnitude in Sudbury, which represents narrow ranges of variation lacking in heterogeneity in our sampling sites (see Figure 3-5). All the competitive effects discussed in the rest of this section showed a decreasing trend of $[M]_{Bio}/[M^{z+}]$ as a function of the competitor with τ values between -0.3 and -1.

On the lower panel of Figure 3-6, a matrix correlation approach was used to simplify the representation. With respect to divalent metals, the ratio $[Cu]_{Bio}/[Cu^{2+}]$ has a negative τ value with Ca ($\tau = -0.3$), indicating a slight competing effect. Moreover, the $[Cu]_{Bio}/[Cu^{2+}]$ ratio is not negatively correlated to $[Ni^{2+}]$ and $[Cd^{2+}]$ ($\tau = 0$) or other divalent metals (except for Pb but the τ value is superior to -0.3). On the other hand, $[Ni]_{Bio}/[Ni^{2+}]$ shows a negative τ value (inferior to -0.3) with $[Mn^{2+}]$, $[Cu^{2+}]$, $[Zn^{2+}]$ and $[Cd^{2+}]$. These results are in agreement with the observations of Flouty & Khalaf (2015). The authors measured the uptake of Ni, Pb and Cu by the unicellular green alga *Chlamydomonas reinhardtii* in the presence of various concentrations of Pb^{2+} and Cu^{2+} . Cu was shown to strongly compete with Ni uptake and Cu^{2+} was shown to have a high binding affinity for both Ni and Cu transport sites. Furthermore, internalization fluxes of Cu remained constant in the absence and presence of Ni^{2+} , implying that Ni had no effect on the uptake of Cu. This is consistent with our results with $[Cu]_{Bio}/[Cu^{2+}]$ as a function of $[Ni^{2+}]$ having a $\tau = 0$. Furthermore, Worms & Wilkinson (2007) observed that the Ni uptake by *C. reinhardtii* was strongly affected by Zn^{2+} and Cu^{2+} but only slightly by Mn^{2+} and Cd^{2+} . They showed that Ni uptake decreased by 70% with a 5-fold greater concentration of Cu, while the same concentration of Zn decreased Ni uptake by 60%. Conversely, Cd^{2+} had only a small effect on Ni uptake (10% decrease) while Mn^{2+} had no significant effect. Our results are in agreement ($\tau = -0.3$, -0.5, -0.5 for Cu^{2+} , Zn^{2+} and Cd^{2+} , respectively), although Mn^{2+} seems to have a slight competing effect according to our data ($\tau = -0.3$). Finally, the Cd ratio shows negative τ values with $[Cu^{2+}]$ ($\tau = -0.3$) and $[Zn^{2+}]$ but the value in the case of the latter remains relatively low ($\tau = -0.2$). Lavoie *et al.* (2012) confirmed the strong protective effect of Zn^{2+} on Cd accumulation in *C. reinhardtii*. Regarding trivalent metals, the Sudbury data set shows too narrow a range of Al variation in terms of free concentrations to make conclusions (Figure 3-2). For Fe, only $[Cu]_{Bio}/[Cu^{2+}]$ ratios show a trend ($\tau = -0.5$). Indeed, $[Ni]_{Bio}/[Ni^{2+}]$ and $[Cd]_{Bio}/[Cd^{2+}]$ were not correlated to Fe. This suggests a possible competing effect for Cu. Kochoni & Fortin (2019) suggested that low concentrations of Fe^{3+} (from $10^{-19.0}$ to $10^{-17.6}$ M) could increase Cu^{2+} uptake and toxicity in *C. reinhardtii*. Calculated

free Fe³⁺ ion concentrations were ranging from 10⁻²¹ to 10⁻¹⁵ M in our Sudbury data set. On the other hand, for Ni and Cd, and again with *C. reinhardtii*, Worms & Wilkinson (2007) showed that high concentrations of Fe (0.25 µM) had no effect on Ni uptake, and Lavoie *et al.* (2012) demonstrated that a 100-fold increase in free Fe³⁺ did not affect Cd uptake or toxicity. Overall, the relationships observed in the field are coherent with those obtained in the laboratory with model organisms. However, further investigations will be necessary to clarify the effect of each competitor while incorporating a greater variety of exposure conditions and not necessarily in a mining context, to avoid or reduce auto-correlations. Indeed, if the Sudbury data set had less auto-correlations than observed for the Nunavik data, the dynamic range of concentrations was smaller for almost all elements present in the water column (Figure 3-2). Moreover, this auto-correlation in the Nunavik data set did not allow us to compare the effects of ion competition between the two regions. Indeed, a difference at this level could explain the differences in bioaccumulation slopes observed between regions.

3.6 Conclusions

This study investigated the robustness of biofilm metal content as a tool for the biomonitoring of metal exposure over large geographical scales. Our results confirm that the concentration of free metals in the water explains a large amount of the metal concentrations in biofilms at circumneutral pHs. Significant linear relationships were also found with dissolved metal concentrations. However, this finding could be related to our specific mining context leading to auto-correlation between total and free metal concentrations. Using free metal concentrations ensures that the approach can be generalized to various water chemistry conditions. Furthermore, pH appears to play a key role in the metal accumulation response of biofilm. Results were highly consistent from one month to the other in the case of Nunavik, and between the two regions studied, despite the ~1700 km distance between them. Indeed, biofilm metal contents normalized

to ambient metal ion concentrations were consistent despite differences in climate, ecosystems and anthropogenic pressures. On one hand, the results suggest that the accumulation of metals by biofilm is sensitive to the protective effect of magnesium and protons. On the other hand, we did not observe any evidence of the effect of calcium as a competitor for Ni, Cu and Cd bioaccumulation, with its effect being pH related. The auto-correlation of metals within the Nunavik data set made it difficult to analyze the interactions between elements in the water column with the internalization of metals. Despite a lower range of observed metal concentrations as compared to those in Nunavik, the Sudbury data set allowed for comparing the protective effects of competitive ions with those found in the literature, notably in studies using unicellular algae in single or mixture exposures. However, we were unable to tease out the effects of ionic competition between the two regions, which could have explained the differences in slopes observed in bioaccumulation regressions. A greater variety in terms of physicochemical characteristics and degree of anthropogenic pressure will be necessary to distinguish interactions correctly. Finally, results found in the present study were highly consistent with those already published with similar normalized biofilm metal contents for the three metals studied at neutral pH values. This finding is important because it suggests the universal potential of biofilm metal content as a proxy for metal bioavailability, despite large geographical scales in lotic ecosystems.

Future work will need to focus on having a wider range of physicochemical conditions to avoid auto-correlation of data found here due to the typical water composition found in a mining context. This will allow for better discrimination of interactions between biofilm metal content and elements in the water column. This will be helpful to predict biofilm metal content by integrating some of the complexity of natural waters in a BLM based model. A multi-metric approach that would include the inherent characteristics of the biofilm (structure, community, tolerance) could also be useful to predict the degree of stress caused by metal exposure as well as the effects of environmental factors in a biomonitoring perspective.

3.7 Acknowledgements

We acknowledge the helpful assistance of Louise-Emmanuelle Paris and Sandra Kim Tiam during field work. We also thank the Nunavik Nickel mine staff for their participation and access to their facilities. Special thanks to Emmanuel Demard and Jimmy Poulin for their help in preparing the maps and Scott Hepditch for language assistance. This study was funded by the *Fonds de recherche du Québec - Nature et technologies* (FRQNT; grant number 2014-MI-183237). Claude Fortin is supported by the Canada Research Chair Program (grant number 950-231107). Séverine Le Faucher is supported by the Research Partnership Chair E2S-UPPA-Total-Rio Tinto (ANR-16-IDEX-0002). Finally, we thank the Institut National de la Recherche Scientifique (INRS) laboratory technicians for their help in performing chemical analyses of water samples.

4 BIBLIOGRAPHIE 1^{ER} ARTICLE

- Adams, W., Blust, R., Dwyer, R., Mount, D., Nordheim, E., Rodriguez, P.H., Spry, D., 2020. Bioavailability assessment of metals in freshwater environments: a historical review. Environ. Toxicol. Chem. 39, 48–59. <https://doi.org/10.1002/etc.4558>
- Battin, T.J., Besemer, K., Bengtsson, M.M., Romani, A.M., Packmann, A.I., 2016. The ecology and biogeochemistry of stream biofilms. Nat. Rev. Microbiol. 14, 251–263. <https://doi.org/10.1038/nrmicro.2016.15>
- Bonet, B., Corcoll, N., Acuña, V., Sigg, L., Behra, R., Guasch, H., 2013. Seasonal changes in antioxidant enzyme activities of freshwater biofilms in a metal polluted Mediterranean stream. Sci. Total Environ. 444, 60–72. <https://doi.org/10.1016/j.scitotenv.2012.11.036>
- Bonnineau, C., Artigas, J., Chaumet, B., Dabrin, A., Faburé, J., Ferrari, B.J.D., Lebrun, J.D., Margoum, C., Mazzella, N., Miège, C., Morin, S., Uher, E., Babut, M., Pesce, S., 2020. Role of biofilms in contaminant bioaccumulation and trophic transfer in aquatic ecosystems: current state of knowledge and future challenges. Rev. Environ. Contam. Toxicol. 253, 115–153. https://doi.org/10.1007/398_2019_39
- Bradac, P., Wagner, B., Kistler, D., Traber, J., Behra, R., Sigg, L., 2010. Cadmium speciation and accumulation in periphyton in a small stream with dynamic concentration variations. Environ. Pollut. 158, 641–648. <https://doi.org/10.1016/j.envpol.2009.10.031>
- Cadmus, P., Clements, W.H., Williamson, J.L., Ranville, J.F., Meyer, J.S., Gutiérrez Ginés, M.J., 2016. The use of field and mesocosm experiments to quantify effects of physical and chemical stressors in mining-contaminated streams. Environ. Sci. Technol. 50, 7825–7833. <https://doi.org/10.1021/acs.est.6b01911>
- Campbell, P.G.C., Fortin, C., 2013. Biotic Ligand Model. J.-F. Férand, C. Blaise (eds.), Encycl. Aquat. Ecotoxicol. 2, 237–245. <https://doi.org/10.1007/978-94-007-5704-2>
- Canadian Council of Ministers for the Environment, 2014. Canadian water quality guidelines for the protection of aquatic life. [WWW Document]. URL <https://www.ccme.ca/en/about/index.html>
- Chaumet, B., Morin, S., Hourtané, O., Artigas, J., Delest, B., Eon, M., Mazzella, N., 2019. Flow conditions influence diuron toxicokinetics and toxicodynamics in freshwater biofilms. Sci. Total Environ. 652, 1242–1251. <https://doi.org/10.1016/j.scitotenv.2018.10.265>

- Cheloni, G., Cosio, C., Slaveykova, V.I., 2014. Antagonistic and synergistic effects of light irradiation on the effects of copper on *Chlamydomonas reinhardtii*. Aquat. Toxicol. 155, 275–282. <https://doi.org/10.1016/j.aquatox.2014.07.010>
- Cheloni, G., Slaveykova, V.I., 2018. Combined effects of trace metals and light on photosynthetic microorganisms in aquatic environment. Environments 5, 1–19. <https://doi.org/10.3390/environments5070081>
- Corcoll, N., Bonet, B., Leira, M., Montuelle, B., Tlili, A., Guasch, H., 2012. Light history influences the response of fluvial biofilms to Zn exposure. J. Phycol. 48, 1411–1423. <https://doi.org/10.1111/j.1529-8817.2012.01223.x>
- Crémazy, A., Campbell, P.G.C., Fortin, C., 2013. The biotic ligand model can successfully predict the uptake of a trivalent ion by a unicellular alga below pH 6.50 but not above: Possible role of hydroxo-species. Environ. Sci. Technol. 47, 2408–2415. <https://doi.org/10.1021/es3038388>
- Deleebeeck, N.M.E., Schamphelaere, K.A.C.D., Janssen, C.R., 2008. A novel method for predicting chronic nickel bioavailability and toxicity to *Daphnia magna* in artificial and natural waters. Environ. Toxicol. Chem. 27, 2097–2107. <https://doi.org/10.1897/07-579.1>
- Erickson, R.J., 2013. The biotic ligand model approach for addressing effects of exposure water chemistry on aquatic toxicity of metals: Genesis and challenges. Environ. Toxicol. Chem. 32, 1212–1214. <https://doi.org/10.1002/etc.2222>
- Faburé, J., Dufour, M., Autret, A., Uher, E., Fechner, L.C., 2015. Impact of an urban multi-metal contamination gradient: Metal bioaccumulation and tolerance of river biofilms collected in different seasons. Aquat. Toxicol. 159, 276–289. <https://doi.org/10.1016/j.aquatox.2014.12.014>
- Flemming, H.C., Wingender, J., 2010. The biofilm matrix. Nat. Rev. Microbiol. 8, 623–633. <https://doi.org/10.1038/nrmicro2415>
- Flouty, R., Khalaf, G., 2015. Role of Cu and Pb on Ni bioaccumulation by *Chlamydomonas reinhardtii*: validation of the biotic ligand model in binary metal mixtures. Ecotoxicol. Environ. Saf. 113, 79–86. <https://doi.org/10.1016/j.ecoenv.2014.11.022>
- Guasch, H., Artigas, J., Bonet, B., Bonnneau, C., Canals, O., Corcoll, N., 2016. The use of biofilms to assess the effects of chemicals on freshwater ecosystems, in: Romaní, A.M., Guasch, H., Balaguer, M.D. (Eds.), In Aquatic Biofilms: Ecology, Water Quality and

- Wastewater Treatment. Caister Academic Press, Spain, pp. 125–144.
<https://doi.org/10.21775/9781910190173.06>
- Guasch, H., Ginebreda, A., Geiszinger, A., 2012. Emerging and priority pollutants in river, In Handboo. ed, The Handbook of Environmental Chemistry. Springer.
[https://doi.org/10.1016/0143-1471\(82\)90111-8](https://doi.org/10.1016/0143-1471(82)90111-8)
- Kalin, M., Fyson, A., Wheeler, W.N., 2006. The chemistry of conventional and alternative treatment systems for the neutralization of acid mine drainage. Sci. Total Environ. 366, 395–408. <https://doi.org/10.1016/j.scitotenv.2005.11.015>
- Kim, K.S., Funk, D.H., Buchwalter, D.B., 2012. Dietary (periphyton) and aqueous Zn bioaccumulation dynamics in the mayfly *Centroptilum triangulifer*. Ecotoxicology 21, 2288–2296. <https://doi.org/10.1007/s10646-012-0985-1>
- Kochoni, E., Fortin, C., 2019. Iron modulation of copper uptake and toxicity in a green alga (*Chlamydomonas reinhardtii*). Environ. Sci. Technol. 53, 6539–6545. <https://doi.org/10.1021/acs.est.9b01369>
- Laderriere, V., Paris, L.E., Fortin, C., 2020. Proton competition and free ion activities drive cadmium, copper, and nickel accumulation in river biofilms in a nordic ecosystem. Environments 7, 1–13. <https://doi.org/10.3390/environments7120112>
- Lavoie, I., Lavoie, M., Fortin, C., 2012. A mine of information: Benthic algal communities as biomonitor of metal contamination from abandoned tailings. Sci. Total Environ. 425, 231–241. <https://doi.org/10.1016/j.scitotenv.2012.02.057>
- Lavoie, I., Morin, S., Laderriere, V., Fortin, C., 2018. Freshwater diatoms as indicators of Combined long-term mining and urban stressors in Junction Creek (Ontario, Canada). Environments 5, 30. <https://doi.org/10.3390/environments5020030>
- Lavoie, I., Morin, S., Laderriere, V., Paris, L.-E., Fortin, C., 2019. Assessment of diatom assemblages in close proximity to mining activities in Nunavik, Northern Quebec (Canada). Environments 6, 74. <https://doi.org/10.3390/environments6060074>
- Lavoie, M., Campbell, P.G.C., Fortin, C., 2012a. Extending the biotic ligand model to account for positive and negative feedback interactions between cadmium and zinc in a freshwater alga. Environ. Sci. Technol. 46, 12129–12136. <https://doi.org/10.1021/es302512r>

- Lavoie, M., Fortin, C., Campbell, P.G.C., 2012b. Influence of essential elements on cadmium uptake and toxicity in a unicellular green alga: the protective effect of trace zinc and cobalt concentrations. Environ. Toxicol. Chem. 31, 1445–1452. <https://doi.org/10.1002/etc.1855>
- Lebrun, J.D., Geffard, O., Urien, N., François, A., Uher, E., Fechner, L.C., 2015. Seasonal variability and inter-species comparison of metal bioaccumulation in caged gammarids under urban diffuse contamination gradient: Implications for biomonitoring investigations. Sci. Total Environ. 511, 501–508. <https://doi.org/10.1016/j.scitotenv.2014.12.078>
- Leguay, S., Lavoie, I., Levy, J.L., Fortin, C., 2016. Using biofilms for monitoring metal contamination in lotic ecosystems: The protective effects of hardness and pH on metal bioaccumulation. Environ. Toxicol. Chem. 35, 1489–1501. <https://doi.org/10.1002/etc.3292>
- Lofts, S., Tipping, E., 2011. Assessing WHAM / Model VII against field measurements of free metal ion concentrations : model performance and the role of uncertainty in parameters and inputs. Environ. Chem. 8, 501–516. <https://doi.org/10.1071/EN11049>
- Lopez, A.R., Funk, D.H., Buchwalter, D.B., 2017. Arsenic (V) bioconcentration kinetics in freshwater macroinvertebrates and periphyton is influenced by pH. Environ. Pollut. 224, 82–88. <https://doi.org/10.1016/j.envpol.2016.12.066>
- Luís, A.T., Bonet, B., Corcoll, N., Almeida, S.F.P., Da Silva, E.F., Figueira, E., Guasch, H., 2014. Experimental evaluation of the contribution of acidic pH and Fe concentration to the structure, function and tolerance to metals (Cu and Zn) exposure in fluvial biofilms. Ecotoxicology 23, 1270–1282. <https://doi.org/10.1007/s10646-014-1270-2>
- Luís, A.T., Teixeira, M., Durães, N., Pinto, R., Almeida, S.F.P., da Silva, E.F., Figueira, E., 2019. Extremely acidic environment: Biogeochemical effects on algal biofilms. Ecotoxicol. Environ. Saf. 177, 124–132. <https://doi.org/10.1016/j.ecoenv.2019.04.001>
- Luís, A.T., Teixeira, P., Almeida, S.F.P., Matos, J.X., Da Silva, E.F., 2011. Environmental impact of mining activities in the Lousal area (Portugal): Chemical and diatom characterization of metal-contaminated stream sediments and surface water of Corona stream. Sci. Total Environ. 409, 4312–4325. <https://doi.org/10.1016/j.scitotenv.2011.06.052>
- Martyniuk, M.A.C., Couture, P., Tran, L., Beaupré, L., Urien, N., Power, M., 2020. A seasonal comparison of trace metal concentrations in the tissues of Arctic charr (*Salvelinus alpinus*) in Northern Québec, Canada. Ecotoxicology 29, 1327–1346. <https://doi.org/10.1007/s10646-020-02248-7>

- Mebane, C.A., Schmidt, T.S., Miller, J.L., Balistrieri, L.S., 2020. Bioaccumulation and toxicity of cadmium, copper, nickel, and zinc and their mixtures to aquatic insect communities. Environ. Toxicol. Chem. 39, 812–833. <https://doi.org/10.1002/etc.4663>
- Meylan, S., Behra, R., Sigg, L., 2004. Influence of metal speciation in natural freshwater on bioaccumulation of copper and zinc in periphyton: A microcosm study. Environ. Sci. Technol. 38, 3104–3111. <https://doi.org/10.1021/es034993n>
- Morel, F.M.M., 1983. Principles and applications of aquatic chemistry, John Wiley & Sons, Inc.: Somerset, N.J.
- Morin, S., Duong, T.T., Dabrin, A., Coynel, A., Herlory, O., Baudrimont, M., Delmas, F., Durrieu, G., Schäfer, J., Winterton, P., Blanc, G., Coste, M., 2008. Long-term survey of heavy-metal pollution, biofilm contamination and diatom community structure in the Riou Mort watershed, South-West France. Environ. Pollut. 151, 532–542. <https://doi.org/10.1016/j.envpol.2007.04.023>
- Morin, S., Lambert, A.S., Rodriguez, E.P., Dabrin, A., Coquery, M., Pesce, S., 2017. Changes in copper toxicity towards diatom communities with experimental warming. J. Hazard. Mater. 334, 223–232. <https://doi.org/10.1016/j.jhazmat.2017.04.016>
- Mueller, K.K., Loftis, S., Fortin, C., Campbell, P.G.C., 2012. Trace metal speciation predictions in natural aquatic systems: Incorporation of dissolved organic matter (DOM) spectroscopic quality. Environ. Chem. 9, 356–368. <https://doi.org/10.1071/EN11156>
- Neury-Ormanni, J., Doose, C., Majdi, N., Vedrenne, J., Traunspurger, W., Morin, S., 2020. Selective grazing behaviour of chironomids on microalgae under pesticide pressure. Sci. Total Environ. 730, 138673. <https://doi.org/10.1016/j.scitotenv.2020.138673>
- Perdue, E.M., Ritchie, J.D., 2003. Dissolved organic matter in freshwaters, in: Heinrich D.H., Turekian, K.K. (Eds.), Treatise on Geochemistry. Elsevier, pp. 273–318. <https://doi.org/10.1016/B0-08-043751-6/05080-5>
- Pesce, S., Lambert, A.-S., Morin, S., Foulquier, A., Coquery, M., Dabrin, A., 2018. Experimental warming differentially influences the vulnerability of phototrophic and heterotrophic periphytic communities to copper toxicity. Front. Microbiol. 9, 1424. <https://doi.org/10.3389/fmicb.2018.01424>
- Sánchez-Marín, P., Liu, F., Chen, Z., Fortin, C., Campbell, P.G.C., 2018. Microalgal-driven pH changes in the boundary layer lead to apparent increases in Pb internalization by a unicellular

alga in the presence of citrate. Limnol. Oceanogr. 63, 1328–1339. <https://doi.org/10.1002/lno.10774>

Staehr, P.A., Sand-Jensen, K.A.J., 2006. Seasonal changes in temperature and nutrient control of photosynthesis, respiration and growth of natural phytoplankton communities. Freshw. Biol. 51, 249–262. <https://doi.org/10.1111/j.1365-2427.2005.01490.x>

Stewart, T.J., Behra, R., Sigg, L., 2015. Impact of chronic lead exposure on metal distribution and biological effects to periphyton. Environ. Sci. Technol. 49, 5044–5051. <https://doi.org/10.1021/es505289b>

Tercier-Waeber, M.-L., Stoll, S., Slaveykova, V.I., 2012. Trace metal behavior in surface waters: Emphasis on dynamic speciation, sorption processes and bioavailability. Arch. des Sci. 65, 119–142. <https://archive-ouverte.unige.ch/unige:27739>

Tolotti, R., Consani, S., Carbone, C., Vagge, G., Capello, M., Cutroneo, L., 2019. Benthic diatom community response to metal contamination from an abandoned Cu mine: Case study of the Gromolo Torrent (Italy). J. Environ. Sci. (China) 75, 233–246. <https://doi.org/10.1016/j.jes.2018.03.034>

Unsworth, E.R., Warnken, K.W., Zhang, H., Davison, W., Black, F., Buffle, J., Cao, J., Cleven, R., Galceran, J., Gunkel, P., Kalis, E., Kistler, D., Van Leeuwen, H.P., Martin, M., Noël, S., Nur, Y., Odzak, N., Puy, J., Van Riemsdijk, W., Sigg, L., Temminghoff, E., Tercier-Waeber, M. Lou, Toepperwien, S., Town, R.M., Weng, L., Xue, H., 2006. Model predictions of metal speciation in freshwaters compared to measurements by in situ techniques. Environ. Sci. Technol. 40, 1942–1949. <https://doi.org/10.1021/es051246c>

Weber, L.P., Dubé, M.G., Rickwood, C.J., Driedger, K., Portt, C., Brereton, C., Janz, D.M., 2008. Effects of multiple effluents on resident fish from Junction Creek, Sudbury, Ontario. Ecotoxicol. Environ. Saf. 70, 433–445. <https://doi.org/10.1016/j.ecoenv.2007.08.001>

Worms, I.A.M., Wilkinson, K.J., 2007. Ni uptake by a green alga. 2. Validation of equilibrium models for competition effects. Environ. Sci. Technol. 41, 4264–4270. <https://doi.org/10.1021/es0630341>

Xie, L., Funk, D.H., Buchwalter, D.B., 2010. Trophic transfer of Cd from natural periphyton to the grazing mayfly *Centroptilum triangulifer* in a life cycle test. Environ. Pollut. 158, 272–277. <https://doi.org/10.1016/j.envpol.2009.07.010>

5 SEASONAL FACTORS AFFECT THE SENSITIVITY OF BIOFILMS TO NICKEL AND ITS ACCUMULATION

LES FACTEURS SAISONNIERS AFFECTENT LA SENSIBILITÉ DES BIOFILMS AU NICKEL AINSI QUE SON ACCUMULATION

Auteurs : Vincent Laderriere¹, Maxime Richard¹, Soizic Morin², Séverine Le Faucheur³, Claude Fortin¹

Affiliations :

¹ Institut national de la recherche scientifique, Centre Eau Terre Environnement, 490 rue de la Couronne, Québec, Canada

² Institut national de recherche pour l'agriculture, l'alimentation et l'environnement, EABX, 50 avenue de Verdun, Cestas, France

³ Université de Pau et des Pays de l'Adour, IPREM, 2 avenue Pierre Angot, Pau, France

Titre de la revue ou de l'ouvrage :

Environmental Toxicology and Chemistry

Soumis le 02 août 2021

Contribution des auteurs :

Vincent Laderriere: methodology, software, formal analysis, investigation, data curation, writing – original draft, visualization.

Maxime Richard: methodology, formal analysis, data curation.

Soizic Morin: writing – review & editing, supervision.

Séverine Le Faucheur: writing – review & editing, supervision.

Claude Fortin: conceptualization, methodology, writing – review& editing, supervision, project administration, funding acquisition.

5.1 Abstract

While metal impacts on fluvial communities have been extensively investigated, effects of abiotic parameters on community responses to contaminants are poorly documented. Variations of photoperiod and temperature commonly occurs over the course of a season and could affect aquatic biofilm communities and their responses to contaminants. The objective of this study was to characterise the influence of environmental conditions (photoperiod and temperature) on Ni bioaccumulation and toxicity using a laboratory-grown biofilm. Environmental parameters were chosen to represent variations that can occur over the summer season. Biofilms were exposed for 7 days to six dissolved Ni treatments (ranging from 6 to 115 µM) at two temperatures (14°C and 20°C) using two photoperiods (16/8 and 12/12 light/dark cycle). Under these different scenarios, structural (dry weight biomass, chlorophyll-a) and functional biomarkers (photosynthetic yield and Ni content) were analysed at four sampling dates allowing us to evaluate Ni sensitivity of biofilms over time. The results highlight the effects of temperature on Ni accumulation and tolerance for biofilms. Indeed, biofilms exposed at 20°C accumulated 1.6 to 4.2-fold higher concentrations of Ni and were characterized by a lower EC₅₀ value using photosynthetic yield as compared to those exposed at 14°C. Regarding the photoperiod, significantly greater rates of Ni accumulation were observed at the highest tested Ni concentration for biofilms exposed to a 12/12 compared to 16/8 cycle light/dark cycle. Our study demonstrates the influence of the temperature on biofilm metabolism and illustrates that environmental factors may influence Ni accumulation response and thus, Ni sensitivity of phototrophic biofilms.

Keywords: Biomonitoring, Metal speciation, Bioaccumulation, Freshwater periphyton, Temperature, Photoperiod

5.2 Introduction

Freshwater biofilms are a complex assemblage composed of eukaryotic (e.g., microalgae, fungi, protozoa) and prokaryotic (e.g., bacteria, cyanobacteria) microorganisms living encapsulated in an polysaccharide matrix and growing on submerged substratum surfaces (Flemming and Wingender, 2010; Battin et al., 2016). These communities are at the basis of aquatic trophic chains and are fundamental in their contributions to energy flow, nutrient cycling and global biogeochemical fluxes (Battin et al., 2016). Moreover, they are known to respond rapidly to physicochemical or environmental stress, and have been shown to tolerate environmental stresses over extended periods of time (Guasch et al., 2016; Hobbs et al., 2019). Therefore, due to the known potential for periphytic biofilms to accumulate contaminants, they are likely to influence the fate of metals in freshwater ecosystems, which makes them particularly interesting for contamination assessment studies (Hobbs et al., 2019; Bonnneau et al., 2020).

Metals are naturally present in freshwater ecosystems but many anthropogenic activities are significant sources of releases into aquatic environments (e.g. agriculture, mining, urbanization, etc; Lavoie et al., 2012; Faburé et al., 2015). In this context, biological communities are exposed to multiple stresses and periphytic biofilms have been pointed out as promising bio-indicators of the effects of contaminants such as metals on aquatic systems (Guasch et al., 2016). For instance, because biofilms are at the base of the food chain, they can be used as a proxy of the transfer of contaminants through the trophic chain. Several studies investigated the direct or indirect effects of metals on relationships between biofilms and various consumers including micro/macrofauna or fish (Namba et al., 2020). Furthermore, Chl-a fluorescence (Corcoll et al., 2011), diatom assemblages (Lavoie et al., 2012), antioxidant enzymes activities (Bonet et al., 2013), photosystem II photochemistry (Lambert et al., 2016) and fatty acid composition (Fadhloui et al., 2020) are all markers of contaminant effects which can be used with biofilms. Metal accumulation in periphytic biofilms has been shown to be a robust indicator of exposure (Ancion et al., 2010; Leguay et al., 2016; Laderriere et al., 2020). Although some metals have been extensively studied, such as Cu (Morin et al., 2017; Pesce et al., 2018), Zn (Corcoll et al., 2012; Lavoie et al., 2012), or Pb (Ancion et al., 2010; Stewart et al., 2015), others like Ni have been poorly examined (Bonnneau et al., 2020). Nickel is often associated geochemically with other metals (e.g. iron, cobalt, copper), therefore soils with a high concentration of these elements generally contain large amounts of Ni (Harasim and Filipek, 2015). Due to the intrusive nature of extraction and processing techniques, Ni-producing countries such as Indonesia, Philippines,

New Caledonia and Canada have reported abundant levels of environmental contamination (Gillmore et al., 2021). As an example, concentrations of Ni in surface waters have been shown to be high due to mining and metallurgical activities within regions of the Canadian provinces of Ontario (Lavoie et al., 2018) and Quebec (Leguay et al., 2016; Laderriere et al., 2020).

In aquatic environments, characterizing the interactions between metals and living organisms can be challenging. For example, accumulation is a dynamic process that is influenced by a multitude of factors, many of which can experience diurnal, daily and seasonal variations, such as nutrient concentrations or flow conditions (Serra et al., 2010; Chaumet et al., 2019; Tlili et al., 2020). Metal speciation (e.g. metal binding by dissolved ligands such as organic matter) is known to determine the bioavailability of these contaminants, and subsequently their uptake (Tercier-Waeber et al., 2012). It is difficult to quantify the impact of natural environmental variables on the fate and behaviour of toxicants, especially in the context of a changing climate. Ecotoxicologists are challenged with predicting how environmental factors will affect the response of toxic substances at the individual or the community level (Moe et al., 2013). Environmental conditions, such as temperature (Lambert et al., 2016; Morin et al., 2017; Pesce et al., 2018) or incident light characteristics (Cheloni and Slaveykova, 2018; Chaumet et al., 2020), are known to directly influence aquatic organisms, but also indirectly by modifying physicochemical parameters of the aquatic media. To be specific, Lambert et al. (2016) and Pesce et al. (2018) showed the ubiquitous findings that the bioaccumulation of Cu was reduced at higher temperatures. Therefore, changes in temperature and light conditions may alter metal toxicity. Better understandings of the mechanisms driving trace metal effects in association with environmental factors such as light and temperature will reduce the uncertainties associated with the extrapolation of laboratory data to the natural environment and possibly integrate site-specific conditions in risk assessment.

In a previous study, we found that biofilm metal content was consistent over large geographical scales and in different types of ecosystems (Laderriere et al., 2021). However, some differences in regression slopes observed between free metal ions and biofilm metal concentrations were found between the different regions studied. It was hypothesized that environmental factors could explain the differences of metal accumulation concentrations in biofilms. The aim of the present study was to evaluate if seasonal variability could modify Ni accumulation by periphytic biofilm in the perspective of using the internalized concentration as a biomarker of metal contamination in surface waters. The experiments were designed to identify the possible effects of temperature and photoperiod variations in biofilm metal accumulation and tolerance. Variations in temperature and photoperiod were chosen to represent daily or seasonal

variations. For this purpose, natural river biofilms were collected on a site free of metal contamination and cultivated in the laboratory before subsequent experiments. Biofilm characterization, toxicity induced by Ni, metal accumulation and environmental parameters (including metal contamination levels) were monitored.

5.3 Materials & methods

5.3.1 Biofilm culture

Natural biofilms were collected from the Cap-Rouge River near Quebec City by scraping several rocks with a toothbrush. This river was chosen due to its low metal concentrations, with Ni and other metal concentrations near or less than 0.01 µM (see Table 12-2 in Appendix II) for the physico-chemistry of the Cap-Rouge River). Biofilms were resuspended in river water to form a periphytic homogenate, which was used to inoculate a recirculating laboratory culture channel (Volume: 60 L; Length: 40 cm, Width: 20 cm, Height: 12 cm; plexiglass). Unglazed ceramic tiles (surface of 23 cm²) were placed at the bottom of the channel as growth substrate and Fraquil medium was used as a culture medium (see Table 12-1 in Appendix II for Fraquil medium composition). A submersible pump (capacity of 4350 L/h; PC1150; BASIN+) placed in a 40-L bucket was used to maintain a continuous flow, to provide oxygenation and to simulate a riffle environment. Biofilms were cultivated under controlled light intensity (approximately 70 to 80 µmol·photon·m⁻²·s⁻¹) with a light/dark photoperiod of 16/8 and temperature (14°C) in an environmental chamber for a period of approximately 35 days prior to exposure experiments.

5.3.2 Biofilm exposure experiments

Three independent experiments were performed, at two light/dark photoperiods (16/8 or 12/12) and two temperatures (14 or 20°C) in order to mimic different conditions occurring within summer. The combination of experiments is therefore focusing on first, a variation of photoperiod and second, a variation of temperature. The light intensity was not changed and was maintained between 70 to 80 µmol·photon·m⁻²·s⁻¹ for all experiments conducted. The condition at 14°C with a light/dark photoperiod of 16/8 was defined as reference for comparison. Biofilms were acclimated to the studied light/temperature conditions for two weeks prior Ni-exposure. The

different exposure experiments were carried out one after another, leaving a two-week period between each experiment to allow for the acclimation of the biofilm to the modified environmental conditions. After this two-week period, the Ni exposures were performed over 7 days. Before each Ni exposure, 144 tiles were randomly selected from the culture channel and placed in the 12 exposure channels. A total of 12 tiles were placed in each unit allowing for 3 pseudo-replicates per exposure channel for each sampling date.

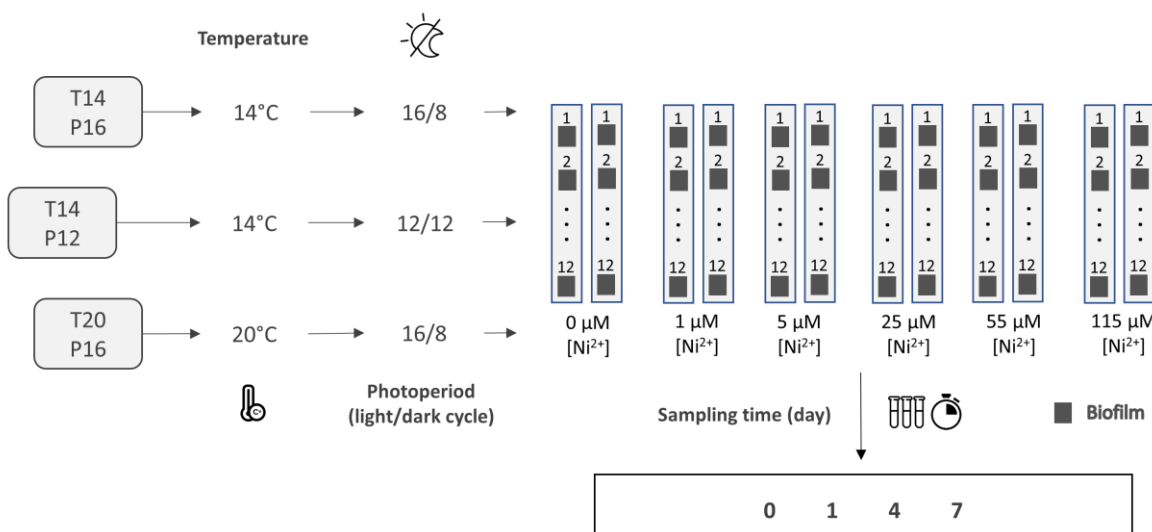


Figure 5-1 : Graphical representation of the experimental design. The rectangles represent the microcosms and each square, a biofilm tile. Calculated free nickel ion concentrations [Ni²⁺] are presented.

The experimental setup is presented in Figure 5-1. It was composed of twelve independent exposure channels (volume: 6 L; length: 100 cm, width: 20 cm, height: 10 cm; plexiglass). Each unit was independently supplied with recirculating Fraquil medium at a pH of 6.9 ± 0.1 with a submersible pump (capacity of 454 L/h; Laguna) placed in a 10 L plastic bucket to ensure a continuous circulating medium. Six Ni treatments were tested: one control (0 μM of total Ni) and five different total Ni concentrations (6, 10, 30, 60 and 120 μM Ni). Exposure solutions were prepared from a Ni stock solution (ICP standard solution of 10 g/L of Ni in 4% HNO₃ (v/v); SCP Science). For each treatment, two independent microcosms were assigned. Before each experiment, all units as well as their buckets, pipes and pumps were pre-washed with 10% nitric acid ACS grade (v/v; Fisher Scientific). The water circulation in all exposure units was initiated 24

h before the tiles covered with biofilm were put in place, allowing the exposure medium to equilibrate. No change of water was made during each exposure and experiments were carried out for seven days, with four sampling times (0, 1, 4 and 7 days). The first sampling time (t_0) was done before Ni addition in the different exposure channels. This time thus allowed to obtain the inter-channel variability before the appearance of Ni effects on biofilms by its addition in the culture medium. Water and biofilm samples were collected at each sampling time, along with in-situ measurements of pH and temperature by a multi-parametric probe (Orion Star A220; ThermoFisher Scientific).

In order to simplify the comparison of the different conditions of temperature and light/dark cycle tested, we established the following code: T14P16 = 14°C in 16/8; T14P12 = 14°C in 12/12; and T20P16 = 20°C in 16/8. The combination of experiments T14P16 and T14P12 are therefore focusing on a variation of photoperiod while experiments T14P16 and T20P16 investigate temperature effect. In terms of water temperatures, each microcosm was close to the target temperature with mean values of T14P16 = $14.4 \pm 0.2^\circ\text{C}$, T14P12 = $14.8 \pm 0.1^\circ\text{C}$ and T20P16 = $19.3 \pm 0.4^\circ\text{C}$ ($n = 48$; one measure per microcosm per sampling date).

5.3.3 Biofilm sampling and analysis

The three replicates of biofilm from each channel were sampled and prepared as described below. Biofilm was scraped from the top of one tile using a razor blade and collected in a large polypropylene tube (50 mL; Sarstedt). Biomass was then resuspended in 10 mL of fresh Fraquil media and the homogenized solution was promptly divided for the different parameter analyses. From this volume, 4 mL was collected to measure Ni bioaccumulation and 3 mL to measure the photosynthetic yield and chlorophyll-a concentration.

In order to measure bioaccumulation, the 4 mL of resuspended biofilms were concentrated by removing the supernatant using a centrifugation step of 5 min at 6000 rpm. A volume of 10 mL of ethylenediaminetetraacetic acid (EDTA; 10 mM; pH 7) was then added to the pellets, vigorously shaken, and the centrifugation process was repeated after 5 min to eliminate the EDTA solution. The EDTA was used to distinguish adsorbed metals from intracellular contents (Hassler et al., 2004). The final pellets were kept in a freezer at -20°C before lyophilization for 48 h (Dura-Top/Dura-dry MP; FTS SYSTEMS). The dry biofilm was subsequently mineralized: 800 μL of HNO_3 (trace metal grade; Fisher Scientific) were added for 48 h and then 200 μL of H_2O_2 (optima

grade; Fisher Scientific) were added for another 48 h. Finally, 800 µL of the digested biomass were diluted in 7.2 mL of ultrapure water (18 MΩ·cm) in a polyethylene tube (15 mL; Fisher Scientific) to reach 10% HNO₃ (v/v). All samples were kept at 4°C before subsequent analyses. Bioaccumulated Ni was measured by inductively coupled plasma–atomic emission spectrometry (ICP-AES; Varian Vista AX CCD). Certified reference material (IAEA-450; algae) was analyzed to determine the efficiency of the digestion method (mean Ni recovery of 81.5 ± 0.5%; n = 3).

In order to measure the Ni induced toxicity on the phototrophic compartment of the biofilm, we used the effective photosynthetic activity as well as Chl-a concentration as biomarkers of effect. Effective photosynthetic activity (Photosystem II quantum yield; Φ_{PSII}) measurements were determined using a Pulse Amplitude Modulated fluorimeter (Phyto-PAM; Heinz Walz GmbH; Germany) in quartz cuvettes, based on the average of three values per replicate and using the same methodology described in Corcoll et al. (2012b). The Φ_{PSII} provides an estimate of the maximum efficiency of PSII photochemistry. Measurements of all t₀ samples (before addition of Ni in the media) were used as a reference of photosynthetic yield. Time-response assessment of Ni chronic toxicity and effective concentration calculation were performed following the response of the Φ_{PSII} for each collection time using the control microcosms as a 100 % of efficiency at each collection time. Measurements were performed after 15 min of dark adaptation at room temperature and Φ_{PSII} was measured three times every 10 s until Φ_{PSII} values stabilized.

After measuring the Φ_{PSII} , samples were kept on ice before chlorophyll-a extraction. Samples were subsequently centrifuged at 5000 rpm for 5 min and the pellets were resuspended in 10 mL of 90 % acetone (v/v; Fisher Scientific). Pigments were extracted at 4°C during 12 h in the dark and then filtered onto GF/C filters (1.2 µM; Whatman). Pheophytin-corrected chlorophyll-a was determined spectrophotometrically (CaryEclipse; Varian) by measuring absorbance before and after acidification using 60 µL of HCl (ACS grade; Fisher Scientific; Steinman et al., 2006). Chlorophyll-a values were estimated by regression using the Phyto-PAM values ($R^2 = 0.92$, p-value < 0.001). Using the conversion factor between the surface of each tile (23 cm²) and suspension volume used for the different descriptors, measured chlorophyll-a (Chl-a) values such as dry-weight biomass (DW) are expressed by the scraped surface (cm⁻²). We also used the chlorophyll-a concentrations and dry-weight biomass to calculate the autotrophic Index (AI) following the formula: $AI = DW \text{ (mg/cm}^2\text{)}/Chl\text{-a (mg/cm}^2\text{)}$ (Steinman et al., 2006). This index provides information on the trophic status or relative viability of the biofilm community. If the index increases, it suggests that the autotrophic community is decreasing compared to the heterotrophic community.

5.3.4 Exposure medium analysis and Ni speciation

At each collection time and for each channel, two replicates of exposure medium samples were collected to measure the concentration of cations and model Ni speciation. To that end, a polypropylene syringe (20 mL; Fisher Scientific) was carefully rinsed three times with ambient media and used to filter exposure medium using polysulfonate filters (0.45 µm; VWR International). Samples were acidified to 10 % (v/v) HNO₃ (trace metal grade; Fisher Scientific) in a polyethylene tube (15 mL; Fisher Scientific) and stored at 4°C before subsequent analyses.

The constituent elements of the Fraquil medium such as cations (Ca, Mg, K, Na, P, Si) and metals (Cu, Co, Fe, Mn, Mo, Ni, Zn) were measured by ICP-AES. The Ni detection limit was 0.01 µM. Nickel speciation in Fraquil medium was calculated using MINEQL+ software at each sampling time. The software's default thermodynamic database was updated using the National Institute of Standards and Technology's Critically Selected Stability Constants of Metal Complexes database (v8.0). Chemical equilibrium modelling showed that Ni strongly bound to EDTA present (5 µM) in the Fraquil medium. As such, for a total Ni concentration lower than 5 µM, Ni was predominantly complexed by EDTA, whereas above 5 µM of total Ni, its main form was its free form with Ni²⁺ concentration, which could be approximated as follows: [Ni²⁺] = [Ni]_T - 5 µM. A figure showing the major chemical forms of Ni in the Fraquil medium as a function the total concentration in the medium is presented in the Appendix II (see Figure 12-1).

5.3.5 Data and statistical analyses

Data were log-transformed before statistical analyses in order to satisfy the assumption of normality and homogeneity of variances. A p-value of 0.05 or less was considered significant. We used a two-way repeated ANOVA (*rstatix* package; v 0.7.0) in order to test if there was a statistical difference between the two photoperiods and the two temperatures during time exposure. More specifically, we also tested the difference using a single one-way ANOVA within a same time and a same Ni concentration treatment. This ANOVA was followed by a Tukey post-hoc test to compare between conditions (p-value adjusted with *Bonferroni* method). To model dose-response curves and extract effective concentrations (*drc* package; v 3.0.1), the Φ_{PSII} values measured at specific times were plotted against calculated free Ni concentrations. Dose-response curves were fitted to the data using the four-parameter log-logistic model. A linear discriminant analysis (LDA) was applied with every descriptor (*ade4* package; v 1.7.16) to individualize data into similarly

composed groups. All statistical analyses were performed with the R software (v4.0; <https://cran.r-project.org>).

5.4 Results

5.4.1 Effects of temperature and light conditions on control biofilms

Table 5-1 shows the means and standard deviations of bioaccumulated Ni and biological parameters ($n = 6$) in the control biofilms. Dissolved Ni concentrations remained below the detection limit (*i.e.* 0.01 μM of dissolved Ni) throughout the experiments in control microcosms (*i.e.* without Ni addition). However, background Ni accumulation by control biofilms was detected with values ranging from 0.24 to 0.94 $\mu\text{mol/g}$ dry weight. The highest values were measured in biofilms exposed to the T14P12 conditions at day 4 (Table 5-1). However, except for that value, no statistical differences were found between exposure time within each condition. The internalized concentrations therefore remained stable with time.

The biofilm dry weights varied amongst a single condition and increase with exposure time in particular in the T20P16 condition. For this last condition, the biofilm biomass at the first sampling date (*i.e.* t0) was already higher than at the end of the two other conditions and increases by a factor of 2.7 over time highlighting the effect of temperature. Indeed, without distinction of sampling dates, the biomass means were $0.52 \pm 0.09 \text{ mg/cm}^2$, $0.47 \pm 0.18 \text{ mg/cm}^2$ and $1.32 \pm 0.55 \text{ mg/cm}^2$ respectively for T14P16, T14P12 and T20P16. The biomass in the condition T20P16 was thus 2.6 and 2.8 times higher than those of T14P16 and T14P12, respectively. For a given condition, statistical differences between sampling dates were found, but not necessarily in comparison with day 0.

Table 5-1 : Means \pm standard deviations ($n = 6$) of dry biomass, chlorophyll-a concentrations, internalized Ni concentrations, photosynthetic yield and autotrophic index in control biofilm. In the case of condition T1P1 at time 7, Chl-a concentrations were estimated by regression using values obtained by Phyto-PAM and not by spectrophotometry. See materials and methods for more details. "*" indicates significant differences between times within conditions ($p < 0.05$). A figure presenting the data as regressions is also provided in the Appendix II (see Figure 12-2).

Conditions	Exposure time (day)	Biomass (mg dry weight/cm ²)			[Chl-a] (µg/cm ²)			[Ni] _{Bio} (µmol/g dry weight)		Photosynthesis yield		Autotrophic index				
		0	1	4	7	0	1	4	7	0	1	4	7	0		
T1P1: 14°C 16/8	0	0.41	\pm	0.06	28	\pm	12	0.30	\pm	0.15	0.45	\pm	0.02	16.3	\pm	7.2
	1	0.52	\pm	0.09	26	\pm	3	0.39	\pm	0.18	0.46	\pm	0.02	20.3	\pm	8.0
	4	0.50	\pm	0.04	44	\pm	4	0.36	\pm	0.09	0.46	\pm	0.01	11.8	\pm	3.5
	7	0.63	\pm	0.05	66	\pm	21	0.33	\pm	0.14	0.46	\pm	0.02	10.4	\pm	4.1
T1P2: 14°C 12/12	0	0.58	\pm	0.05	37	\pm	6	0.56	\pm	0.03	0.41	\pm	0.01	15.8	\pm	2.8
	1	0.31*	\pm	0.04	32	\pm	7	0.62	\pm	0.30	0.46*	\pm	0.02	9.7	\pm	2.5
	4	0.32*	\pm	0.08	41	\pm	5	0.94*	\pm	0.54	0.43	\pm	0.01	8.4	\pm	6.2
	7	0.66	\pm	0.14	65*	\pm	5	0.45	\pm	0.10	0.44	\pm	0.02	10.3	\pm	5.2
T2P1: 20°C 16/8	0	0.77*	\pm	0.23	110	\pm	18	0.28	\pm	0.05	0.42	\pm	0.02	6.5	\pm	3.7
	1	1.08	\pm	0.13	128	\pm	13	0.31	\pm	0.05	0.46*	\pm	0.03	8.3	\pm	1.8
	4	1.35	\pm	0.11	145*	\pm	8	0.28	\pm	0.07	0.44	\pm	0.02	9.3	\pm	1.9
	7	2.07	\pm	0.32	116	\pm	15	0.24	\pm	0.04	0.41	\pm	0.02	18.3*	\pm	7.7

In comparison to biomass, Chl-a concentrations also show similar values in the case of T14P16 and T14P12 conditions, but 2.5 to 3.8-fold higher in the case of T20P16. Average values were $40.5 \pm 8.3 \mu\text{g}/\text{cm}^2$, $49 \pm 14 \mu\text{g}/\text{cm}^2$ and $157 \pm 16 \mu\text{g}/\text{cm}^2$ for T14P16, T14P12 and T20P16, respectively. However, if Chl-a concentrations only varied slightly over the seven days of experiment in the T20P16 conditions, the two other conditions showed an increasing trend by a factor of 2. Consequently, the calculated autotrophic index follows a increase over time in T20P16 indicating a potential shift in the community (increase of heterotrophy at the detriment of autotrophy) conversely to the conditions T14P16 and T14P12 where the autotrophix index slightly decreases. On the other hand, the environmental factors had no effect on the photosynthetic efficiency during the 7 days of exposure. The average values were 0.46 ± 0.01 for T14P16, 0.44 ± 0.02 for T14P12 and 0.43 ± 0.02 for T20P16 (relative units) with no apparent trends.

As mentioned in the materials and methods section, the biofilm was collected from the Cap-Rouge River and was then inoculated and cultured for one month in a culture channel. The different experiments were then carried out successively, leaving a two-week period between each experiment in order to modify the environmental conditions and acclimate the biofilm. The biofilm used in condition T20P16 was thus grown for a longer period of time than the biofilms studied in the conditions T14P16 and T14P12 (approximately 45 days and 21 days longer, respectively). To summarize, the biofilm used in condition T20P16 had much higher Chl-a concentrations and dry weight biomass than those used in T14P16 and T14P12. This difference suggests that biofilm colonization and growth are likely to be dependent on environmental parameters such as temperature. Thus, in conclusion, abiotic conditions affect the community structure and different community structures can also show different sensitivity to Ni. Note that a difference of 4 hours in the photoperiod (T14P16 vs T14P12) did not have a significant effect on the same biomarkers in control biofilms.

To summarize, the different descriptors showed similar trends over time in control biofilms. However, the biofilm used in condition T2P1 had much higher Chl-a concentrations and dry weight biomass than those used in T1P1 and T1P2. This difference suggests that biofilm colonization and growth are likely to be dependent on environmental parameters such as temperature. Note that a difference of 4 hours in the photoperiod (T1P1 vs T1P2) did not have a significant effect on the same biomarkers in control biofilms.

5.4.2 Effects of temperature and light conditions on Ni-exposed biofilms

In Ni-exposed microcosms, the mean calculated free Ni ion concentrations were 0.97 ± 0.51 ; 5.57 ± 0.71 ; 23.2 ± 2.4 ; 56.1 ± 0.3 ; $116 \pm 6 \mu\text{M}$ (all sampling dates combined; $n = 12$). A table showing the evolution of total and free Ni during exposure at different times is presented in Table 12-3 (Appendix II). Statistical differences in free Ni concentrations were found between times and conditions for a same Ni concentration of exposure (ANOVA; p -value < 0.05). However, as suggested by the standard deviation, the calculated concentrations remained close to the desired concentrations.

Figure 5-2 presents the time-course of Chl-a concentrations and dry weight biomass as a function of the free Ni concentrations. Throughout the experiment and for each tested condition, the biomass in Ni-exposed microcosms remained stable or slightly increased during the 7 days of exposure with a more pronounced effect in the condition T20P16. Furthermore, despite no clear statistical differences, Chl-a concentrations appeared to decrease over time in Ni-exposed microcosms. This decrease was more pronounced in the T14P12 condition. Given the increase in biomass and decrease in Chl-a concentrations, the autotrophic index increased over time as for the controls. However, the greater the exposure concentration was, the greater the increase in the autotrophic index was with a clear difference after 7 days of exposure. This increasing trend appeared only in conditions T14P16 and T14P12, the autotrophic index remaining relatively stable in condition T20P16.

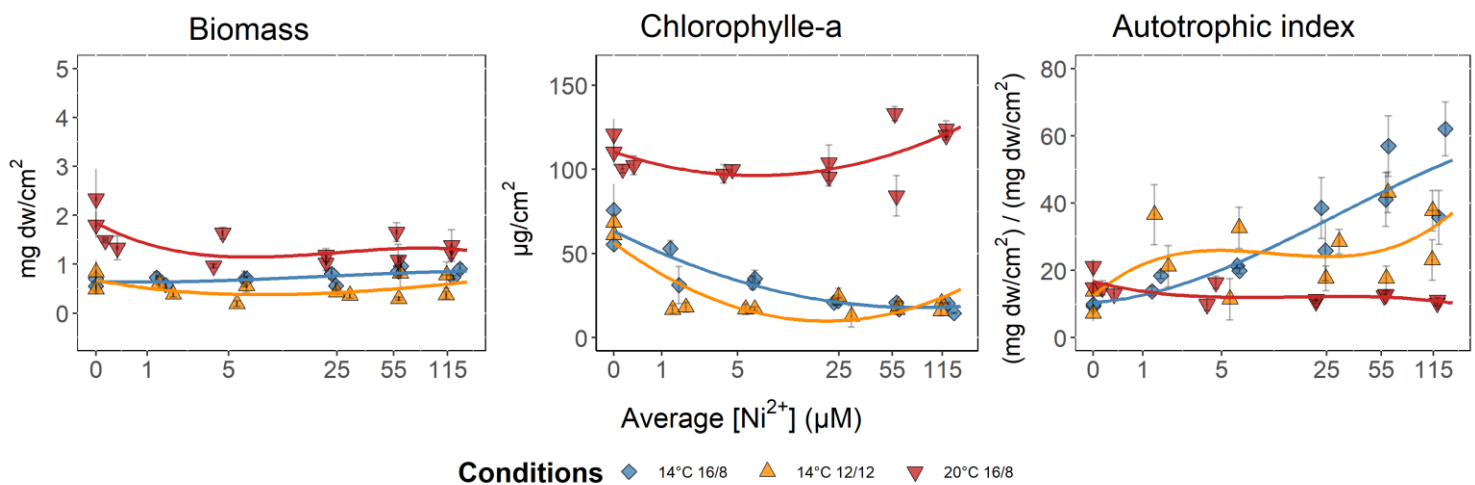


Figure 5-2 : Dose responses of the biomass, the concentration of chlorophyll-a and the autotrophic index ($n = 3$) as a function of the free Ni concentration for each condition of temperature and photoperiod (T14P16 = 14°C in 16/8; T14P12 = 14°C in 12/12; and T20P16 = 20°C in 16/8). The curves plotted correspond to second degree polynomial regressions. A version of this figure presenting all the sampling times is provided in the Appendix II (see Figure 12-3).

5.4.3 Influence of photoperiod and temperature on Ni bioaccumulation

Ni accumulation by biofilms as a function of the free calculated Ni for the three environmental conditions is illustrated in Figure 5-3. A one-way ANOVA was first used to determine possible statistical differences among experiments conducted with different environmental conditions. At day 0 (*i.e.* before addition of Ni in any microcosm), the accumulated Ni concentrations remained within the same order of magnitude as those of the controls (values ranging from 0.3 to 1.6 μmol/g dw). Indeed, for each conditions tested, and except for one sample found as an outlier using the interquartile range approach (condition T14P12 for microcosms defined as $[Ni^{2+}] = 115 \mu M$ at day 0; $[Ni]_{Bio} = 3.9 \mu mol/g dw$), no statistical differences were found between the accumulated Ni concentrations between each channel on day 0.

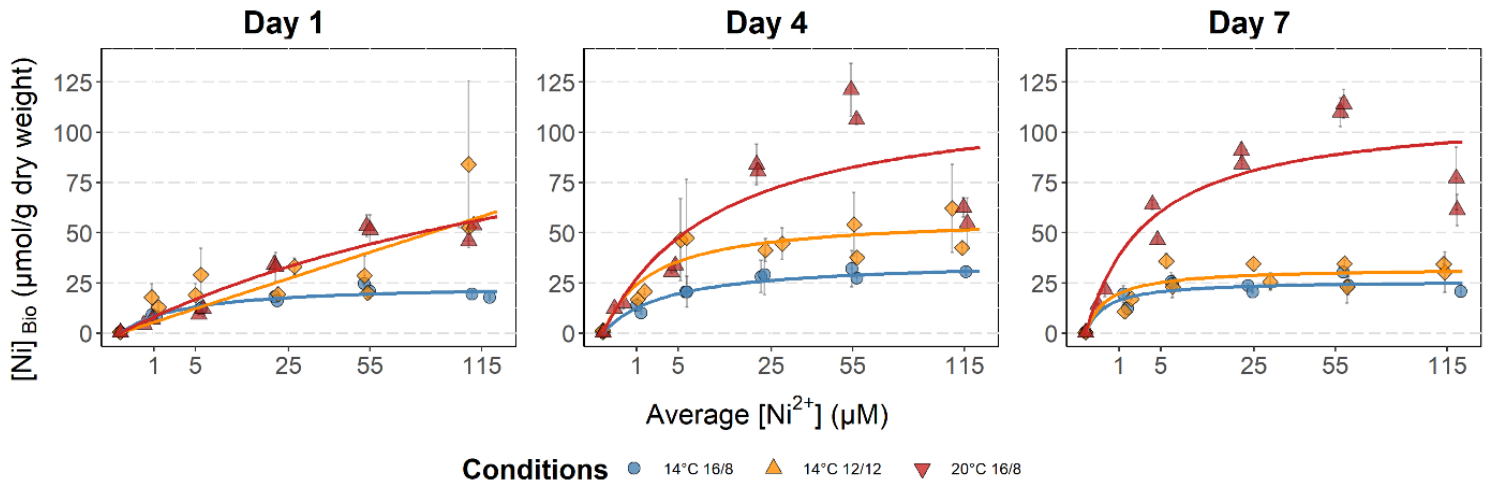


Figure 5-3 : Internalized Ni concentrations by biofilms ($n = 3$ for different the different conditions (14°C and $16/8$ light/dark cycle in blue; 14°C and $12/12$ light/dark cycle in yellow; $20^{\circ}\text{C} 16/8$ light/dark cycle in red) as a function of the calculated free Ni concentrations. Each panel represents an exposure time. The regressions correspond to Michaelis-Menten models. The Ni accumulation of control samples were ranging from 0.03 to $0.6 \mu\text{M}$ of Ni^{2+} whatever the sampling times (non exposed channels).

If we first compare the two photoperiods, Ni accumulation in biofilms increased up to $25 \mu\text{M}$ of Ni^{2+} for the three Ni-exposure sampling times (day 1, 4 and 7). At higher Ni concentrations (55 and $115 \mu\text{M}$), the accumulated Ni contents remained similar with average values below $30 \mu\text{mol/g dw}$. This trend was observed at each sampling time (Figure 5-3). Accumulation peaked after the first day of exposure, regardless of the exposure concentrations, with little to no increase at days 4 and 7. Only the $115 \mu\text{M}$ of Ni^{2+} treatment was significantly different over the three sampling times (*i.e.* day 1, 4 or 7). The other exposure concentrations did not show a significant difference over the different sampling dates. Nevertheless, biofilms exposed with a $12/12$ photoperiod tend to globally have higher average internalized Ni concentrations than biofilms exposed with a $16/8$ photoperiod. The Table 5-2 shows the results of a two-way ANOVA with free Ni^{2+} concentrations, photoperiod and time as influencing parameters on the Ni content in biofilms. Despite the significant two-way interactions found between the time and the photoperiod as well as with Ni^{2+} concentration, no 2-way interaction effect was found between the Ni^{2+} concentration and the photoperiod resulting in a non-significant interaction. These results suggest that a difference of 4 hours in lighting (*i.e.* a difference that may occur within a season of temperate regions) does not have a marked effect on Ni internalization by biofilms. Nevertheless, even though the differences

are not sufficient to have a significant 2-way interaction, some treatments (*i.e.* 115 µM Ni²⁺; Figure 5-3) could induce significant differences throughout the exposure.

Table 5-2 : Results of the three-way ANOVA with time as a repeated measure applied on accumulated Ni by biofilms between conditions T1P1 and T1P2. These two experiments differ by the photoperiod used: 16/8 against 12/12. DFn: degrees of freedom in the numerator. DFd: degrees of freedom in the denominator. F: F-statistic value. p: p-value of the F-statistic. ges: generalized effect size (amount of variability due to the within-subjects factor).

Effect	DFn	DFd	F	p	P < 0.05	ges
[Average Ni ²⁺]	5.0	52.0	216.1	1.62E-33	*	0.8
Photoperiod	1.0	52.0	95.4	2.32E-13	*	0.3
Time	2.1	110.3	401.3	1.79E-52	*	0.9
[Average Ni ²⁺] : Photoperiod	5.0	52.0	1.3	2.98E-01		0.03
[Average Ni ²⁺] : Time	10.6	110.3	13.5	1.10E-15	*	0.5
Photoperiod : Time	2.1	110.3	14.3	1.79E-06	*	0.2
[Average Ni ²⁺] : Photoperiod : Time	10.6	110.3	0.5	8.79E-01		0.04

If we now compare the two temperatures tested, similar accumulation patterns were found for the condition T20P16. Regardless of the Ni concentrations, the biofilm exposed at a temperature of 20°C showed an increasing internalized concentration between days 1 and 4, and a plateau reached beyond day 4. Biofilms grown at 20°C and exposed to Ni systematically showed a significantly higher Ni accumulation for exposure concentrations greater than 1 µM. When all sampling times are pooled together, the average internalized Ni at 20°C were higher by a factor ranging from 1.6 to 4.2. Table 5-3 shows the results of a two-way ANOVA with time as a repeated measure between conditions T14P16 and T20P16 to assess interactive effects of temperature. Significant interaction was found between Ni²⁺ concentration, time and temperature. This difference highlights the effect of temperature on Ni accumulation by biofilms.

Table 5-3 : Results of the three-way ANOVA with time as a repeated measure applied on accumulated Ni concentrations by biofilms between conditions T1P1 and T2P1. These two experiments differ by the photoperiod used: a light/dark cycle of 16/8 against 12/12. DFn: degrees of freedom in the numerator. DFd: degrees of freedom in the denominator. F: F-statistic value. p: p-value of the F-statistic. ges: generalized effect size (amount of variability due to the within-subjects factor).

Effect	DFn	DFd	F	p	P < 0.05	ges
[Average Ni ²⁺]	5	55	398.515	7.05E-42	*	0.898
Temperature	1	55	88.914	4.38E-13	*	0.283
Time	1.56	85.64	1102.19	8.24E-58	*	0.938
[Average Ni ²⁺] : Temperature	5	55	5.324	4.63E-04	*	0.106
[Average Ni ²⁺] : Temps	7.79	85.64	33.813	3.90E-23	*	0.699
Temperature : Time	1.56	85.64	3.872	3.40E-02	*	0.051
[Average Ni ²⁺] : Temperature : Time	7.79	85.64	5.164	3.36E-05	*	0.262

5.4.4 Influence of temperature and light on Ni toxicity

Dose-response curves were fitted using the PSII efficiency as a function of the free Ni²⁺ concentrations. Their respective EC₁₀, EC₂₀ and EC₅₀ were estimated with 95% confidence intervals for each environmental condition (Figure 5-4). The photosynthetic yield was found to be affected by the concentration of Ni²⁺ and the effect increased with exposure time. Regardless of the sampling time considered, the curves show a decreasing trend starting from a concentration of 5 µM. However, the maximum percentages of inhibition (compared to the control) were between 16 – 25 %, 36 – 51 % and 53 – 65 % for days 1, 4 and 7, respectively. These results demonstrate the chronic toxicity of Ni over time on the photosynthetic efficiency of biofilms. For condition T20P16, the curves at 4 and 7 days are very close to those obtained for T14P16 and T14P12 where the toxic effect over time is more gradual.

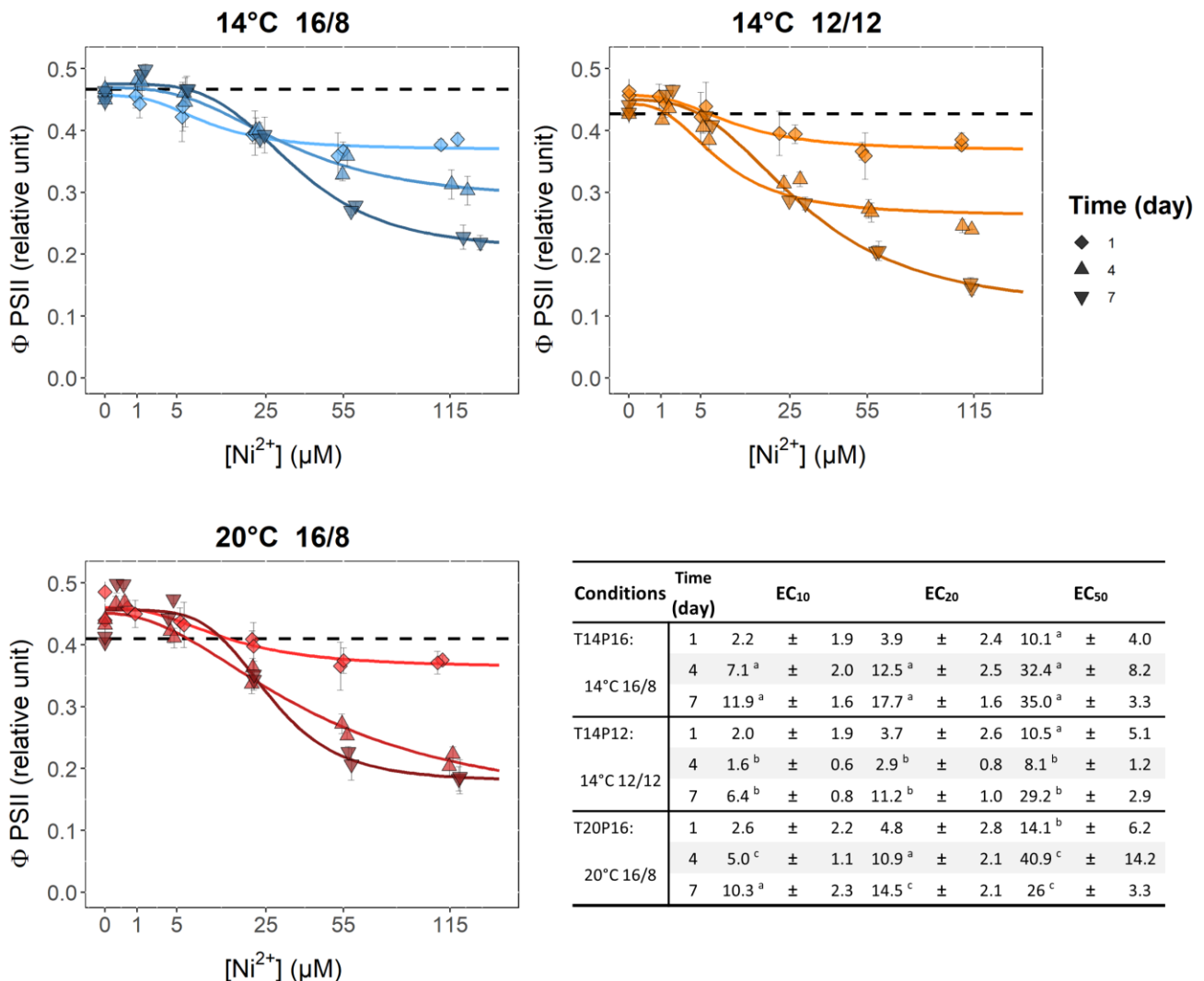


Figure 5-4 : Photosynthesis efficiency as function of Ni exposure for three environmental conditions tested.

Scatterplots present time-response curves based on the decrease in Φ_{PSII} after Ni addition (mean \pm SD; $n = 3$) for each exposure duration. Measurements of all t_0 samples (before addition of Ni in the media) were used as a reference to model relative dose-response curves. The dotted line shows the median value of the control samples. Values of control samples (non exposed channels) were ranging from 0.39 to 0.50 whatever the sampling times. A summary of the effective concentrations calculated from each time curve is provided in the table for each condition (estimate \pm standard error). The letters indicate significant differences between conditions within a same sampling time ($p < 0.05$).

However, the PSII efficiency was negatively correlated with the bioaccumulated Ni ($R^2 = 0.33$, p-value < 0.001). Correlation coefficients calculated for each condition separately increased as follows: T14P12 ($R^2 = 0.22$, p-value < 0.001) < T14P16 ($R^2 = 0.32$, p-value < 0.001) < T20P16 ($R^2 = 0.51$, p-value < 0.001). The stronger correlation observed in condition T20P16 could be attributed to the greater bioaccumulation described above. Based on the final sampling time (day 7), calculated EC_{50s} were statistically different between conditions T14P16, T14P12 or T20P16 (t test; p < 0.05). Calculated EC₅₀ values were ranged by conditions as follows: T20P16 < T14P12 < T14P16. Thus, phototrophic biofilm exposed at 20°C showed a lower tolerance to Ni in comparison to those exposed at 14°C.

5.4.5 Interaction between environmental factors and biofilm parameters

A LDA was carried out with all the measured biological parameters and Ni²⁺ concentrations for the day 7, and condition T20P16 was well discriminated (data not shown). This finding is consistent with the results described above, as the different descriptors have shown similar responses for conditions T14P16 and T14P12. However, Figure 5-5 presents an LDA performed with the data obtained after 7 days of exposure normalized by the respective starting conditions (i.e. day 7 / day 0) in order to consider the observed differences of the communities from the first sampling time (i.e. day 0). Following this normalization, the three environmental conditions are not clearly discriminated. These results suggest that environmental conditions affected the community during the acclimation phase (and thus before the Ni exposure) and that this effect led, at least partially, to a difference in Ni responses of biofilms.

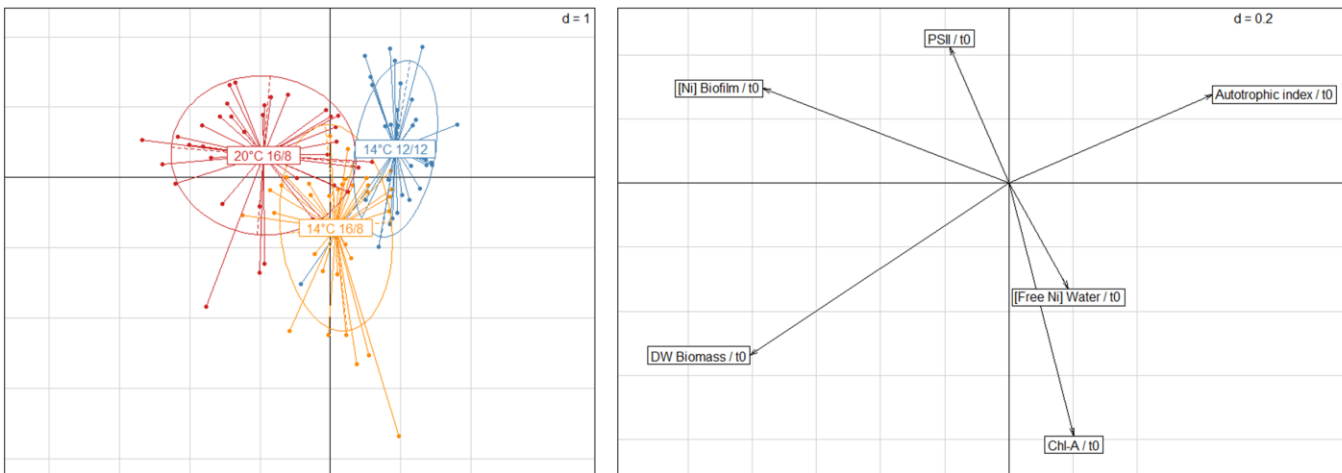


Figure 5-5 : Linear discriminant analysis (LDA) of the different conditions after the 7 days of exposure (left panel) based on the different studied biomarkers (right panel) for all Ni treatments. All the parameters were normalized by their start values (i.e. by their respective t_0) in order to discriminate the influence of environmental factors on response to Ni.

5.5 Discussion

5.5.1 Ni effect on biofilm

Despite the fact that Chl-a concentrations and dry weight biomass were much lower at 14°C in comparison to those at 20°C, similar trends were found between both parameters in Ni-exposed biofilms (Figure 5-2). Although not significant, biomass and Chl-a concentrations were observed to slightly increase and decrease, respectively, over time. The toxic effects of Ni observed in this study are in accordance with those found in the literature on biofilms and other microorganisms, and with other metals in general. Ni has been shown to cause the disappearance of cyanobacterial populations and reduced photosynthetic biomass in a periphytic biofilm (Lawrence et al., 2004). Fechner et al. (2011), who exposed biofilms to low (0.09 μM) and high (0.85 μM) dissolved Ni treatments, showed low variations of both dry weight biomass and Chl-a, however important changes in both bacterial and eukaryotic communities were also observed. In addition, the new metabarcoding approach has allowed for the observation of significant changes in eukaryote and prokaryote community compositions along a coastal sediment Ni concentration gradient (Gillmore et al., 2021). More precisely, these community changes were mainly correlated

with the dilute-acid extractable concentration of Ni in the sediments, which explained 26, 23, and 19% of the variation for eukaryotes, diatoms, and prokaryotes, respectively. However, to our knowledge, no similar study has been done specifically for Ni on natural freshwater biofilms.

At 14°C, the autotrophic index increased with exposure time in Ni-exposed biofilms. This suggests a shift from autotrophic to heterotrophic biofilms. Biofilm exposed to Ni at 20°C also showed an increasing trend, but values remained relatively stable despite higher biomass and Chl-a values. These results suggest that Ni exposure led to a modification of the assemblage in favour of heterotrophic organisms. Ancion et al. (2010) exposed biofilms to different urban runoff treatments containing metal mixtures of Zn, Cd and Cu during short (5 days) and long term (21 days) experiments. The authors found significant differences in bacterial community structure occurring after only 3 days of treatment confirming the rapid and sensitive reactivity of microbial populations to metal exposure. Additionally, it has also been shown that chronic exposures to Cu resulted in effects upon bacterial community structure (Tlili et al., 2011; Lambert et al., 2012). Our results are in agreement as the autotrophic index slightly increased after 7 days and above the first exposure concentration (1 µM of Ni²⁺; Figure 5-2).

In addition, a concentration of 25 µM of Ni²⁺ was found to have a significant inhibitory effect on photosynthetic processes, consequently impeding CO₂ fixation, as has been previously observed with other metals such as Cu and Zn (Figure 5-4; Corcoll et al., 2011; Lambert et al., 2017). Indeed, above this threshold concentration, Ni toxicity affected photosynthetic efficiency, and its resultant impact increased over time, demonstrating long-term effects (Figure 5-4). Conversely, for lower concentrations, the absence of significant effect resulting from Ni exposure on photosynthetic efficiency suggests that Ni did not drastically affect the algal physiologic state. Interestingly, the amount of internalized Ni increased with exposure to free Ni²⁺ concentrations up to a threshold concentration of 25 µM, at which point accumulation reached a plateau. At higher concentrations (e.g. 55 and 115 µM of Ni²⁺; Figure 5-3), internalization was no longer dependent on exposure concentration, likely due to the Ni-induced toxicity on the phototrophic compartment. If a saturation of Ni transporter mechanisms could be advanced considering the results of T14P16 and T14P12, the data obtained in T20P16 indicate an abrupt decrease at the highest tested Ni concentration (e.g. 115 µM of Ni²⁺) which is more consistent with a toxic effect than a saturation effect. In other words, these results suggest that Ni-induced toxicity explains the plateau observed for internalized concentrations for exposures greater than 25 µM of Ni²⁺ and this, from the first time of exposure. Similar conclusions were reached in biofilms exposed for 28 days to different Ni concentrations (dissolved concentrations ranging from 5.5 µM to 105 µM) at 15 and 21°C

(Fadhlaoui et al., 2020). Accumulated Ni increased with Ni exposure concentration, with the highest internal values observed at 25 µM Ni²⁺, followed by a marked decrease above this exposure concentration. In fact, nickel toxicity may induce direct and indirect effects, with the observed phototrophic cellular death possibly explaining the observed plateau in metal bioaccumulation, which could subsequently increase available organic matter as nutrient for the heterotrophic compartments (Massieux et al., 2004; Boivin et al., 2005). If metals were to interfere with the functioning of heterotrophs (Fechner et al., 2011; Pesce et al., 2018), changes in the structure and diversity of the community towards more tolerant species could also rapidly occur (Ancion et al., 2010; Tlili et al., 2011; Morin et al., 2017). This would provide explanation as to why biomass increased over time while Chl-a concentrations decreased. Furthermore, responses to Ni were quantifiable after 24 h of exposure, thus confirming the rapid, along with the high reactivity, of biofilms to metal exposure in terms of accumulation, information of particular importance for future impact assessments.

5.5.2 Influence of temperature and light variations on metabolism

Intra-daily or seasonal variation of conditions in natural environments can occur and are likely to influence the sensitivity of microbial communities to contaminants. For instance, Villeneuve et al. (2010) observed that light intensity or hydrodynamic conditions affect the structure and diversity of river biofilms. Variations in environmental factors are well-known phenomena that make difficult the establishment of relationships between metal exposure and the observed biological effects (Bonet et al., 2013; Faburé et al., 2015; Lambert et al., 2017). In our study, while photoperiod had no significant effect on the growth of biofilms unexposed to Ni, biofilm formation was more productive at high temperature (see Table 5-1 and Figure 5-2). An increase in temperature is known to favour the metabolism of organisms such as bacteria and algae (Lürling et al., 2013). Additionally, several microcosm studies found that an increasing temperature influenced global phototrophic community structure, both in terms of algal biomass and in terms of the distribution of main algal classes. For instance, the structural parameters of periphytic microalgal communities (e.g. cell densities such as Chl-a content per cm²) were affected by temperature, especially above 21°C among the four tested temperatures (18, 21, 24 and 28°C; Larras et al., 2013). In this study, the authors observed a decrease in diatom diversity in periphyton communities between different temperature treatments highlighting the dependence of biofilm communities on seasonal and environmental characteristics. Similar conclusions were

reached by Lambert et al. (2016) and Morin et al. (2017). Both studies demonstrated that an increase of temperature led to a shift in diatom assemblage composition with a strong decrease in diversity leading to a modification of the community tolerance towards Cu. Furthermore, the lack of significant effect of temperature on the photosynthetic efficiency of control phototrophic communities suggests that the experimental warming did not drastically affect the physiologic state of phototrophic organisms within the biofilm studied. If photosynthetic activity is directly related to metabolism, which is dependent upon temperature, a difference of 6°C did not seem to be sufficient to observe a significant difference. These results are in agreement with several studies which found no effect on the maximum PSII quantum yields (Larras et al., 2013; Pesce et al., 2018; Chaumet et al., 2020). However, some discrepancy was found, for example in a study examining the effect of a 10°C temperature rise (18°C and 28°C) on the tolerance to Cu for phototrophic biofilm (Lambert et al., 2017). Indeed, a significant decrease was observed in PSII values for control biofilms at 28°C (in comparison to 18°C), which revealed an inhibitory effect of temperature on photosynthesis. These results highlighted the importance of the initial taxonomic composition and/or the difference in the temperature gradients tested. Concerning heterotrophic organisms, temperature is known to benefit bacterial growth and exopolysaccharide (EPS) production (Boivin et al., 2005; More et al., 2014), which has been demonstrated in the field (Faburé et al., 2015). A warming stress was observed to have a significant influence on extracellular enzymatic activity such as the β -glucosidase, an enzyme involved in carbon degradation, suggesting that the metabolism of organisms such as bacteria and fungi were enhanced (Pesce et al., 2018; Chaumet et al., 2020). Our findings are therefore in agreement with an increase of the autotrophic index at 20°C in control biofilms. Although the LDA was not able to discriminate the influence of the two temperatures when parameters were normalize by their respective conditions at day 0, the two conditions seems to dissociate along the x-axis which was related to the amplitude of variation in the autotrophic index (Figure 5-5).

Among the light components and as mentioned by Cheloni & Slaveykova (2018), most of the studies dealing with light effects focused on ultra violet radiation (within the spectrum of UVA or UVB), while the understanding of the role of the photosynthetically active radiation (PAR) and solar light in trace metal effects was overlooked. Based on our data, we found no evidence that photoperiod is as critical as temperature. Chaumet et al. (2020), who exposed biofilms in microcosms to two photoperiods (16/8 and 10/14 light/dark cycle) and two temperatures (10 and 26°C), found an interaction between the influence of both parameters. The study highlights the influence of temperature but also photoperiod on biofilm metabolism and, in particular, the parameters related to heterotrophic organisms (*i.e.* polysaccharide and protein content, and β -

glucosidase activity). This agrees with our results as the LDA discriminates the two photoperiods tested along the y-axis which was related to the Chl-a and the autotrophic index (Figure 5-5). This suggests that a light/dark cycle of 12/12 was beneficial for heterotrophic organisms in comparison to 16/8. This result is important if Ni toxicity is dependent upon either autotrophic or heterotrophic organisms, should one be more affected than the other, there is the potential for additive/synergistic effects caused by Ni exposure and photoperiod. As biofilms are composed of highly interconnected microorganisms (Battin et al., 2016), a strong effect on one compartment could generate an indirect effect on the other, thus leading to structural and functional changes. On the other hand, in terms of photosynthetic yield, Chaumet et al. (2020) found no marked effects of photoperiod, regardless of exposure time. It thus appears that photoperiod is not more influential as an external stress when compared to temperature. However, Corcoll et al. (2012) evaluated in a microcosm the relationship between short-term light intensity changes on the toxicity of Zn to fluvial biofilms with different photo-acclimation. Depending on the treatment, biofilms were characterized by different structural (Chl-a, dry-weight biomass, EPS, algal groups/taxonomy) and physiological attributes (photosynthetic pigments). The sensitivity of biofilms exposed to a multi-stress situation (*i.e.* sudden change in light intensity and Zn exposure) varied according to photo-acclimation pre-treatments. Furthermore, light intensity has been shown to be one of the environmental factors which determined the seasonality of biofilm responses in the field (Bonet et al., 2013). Therefore, it would appear that light intensity and spectral composition are more important than the photoperiod in regards to the capacity of biofilm to tolerate metal exposure.

5.5.3 Interactions between environmental factors and nickel toxicity and accumulation

The effects of environmental factors on Ni toxicity were significant in the case of temperature. The 2-way ANOVA analyses conducted in this study confirmed an interaction between Ni bioaccumulation and temperature (Table 5-2), but not with the photoperiod (Table 5-3). Interestingly, these results suggest that metal accumulation in natural systems may vary with temperature. In addition, temperature modulated the functional effects of Ni, as shown by the measured photosynthetic efficiency values in Ni-exposed biofilms. Calculated EC_{50s} using the Φ_{PSII} after 7 days showed statistical differences between the three conditions with a decreasing trend in toxicity as follows: T14P16 < T14P12 < T20P16 (Figure 5-4). Biofilms exposed to 20°C

accumulated higher levels of Ni (*i.e.* 1.6 to 4.2-fold higher at 20°C; Figure 5-3), which is in accordance with the lower EC₅₀ in that condition (Figure 5-4). Overall, biofilm appeared to be more impacted and more productive at 20°C than at 14°C. However, using all descriptors, the LDA was not able to clearly discriminate the temperature condition from the others (see Figure 5-5). Nevertheless, these results highlight the influence of temperature on the metabolism of the phototrophic component of the biofilm and illustrate the previous conclusions that this factor influenced Ni accumulation and thus, the Ni sensitivity of biofilms. However, because temperature affected the community structure during the acclimatization phase resulting in observable differences from day 0, temperature might have directly or indirectly modified Ni sensitivity of the two biofilms exposed at 14 or 20 °C. This is in agreement with studies that found an influence of temperature on the vulnerability of phototrophic and heterotrophic microbial communities to metal toxicity (Lambert et al., 2016; Lambert et al., 2017; Pesce et al., 2018). All these studies showed that a temperature increase modulates the response of biofilm to chronic Cu exposure depending on the function considered (*i.e.* phototrophic or heterotrophic organisms).

To our knowledge, in any previous efforts made to understand the link between tolerance acquisition and taxonomic composition of the community to metal exposure, few studies have closely investigated bioaccumulation. For instance, Friesen et al. (2017) utilized microcosms to expose natural biofilm of the same inoculum to Se for 21 days under different light and nutrient conditions. The authors found that the different environmental conditions tested resulted in different taxonomic composition within biofilms, but also significant differences in internalized Se concentrations. Their findings suggest that factors other than total dissolved Se concentration in the water influence Se accumulation in the biofilm, including taxonomic composition and physicochemical characteristics of the water. Lambert et al. (2016) and Pesce et al. (2018) exposed biofilms to Cu using similar methods to the current study and found that internalized Cu tended to decrease with increasing temperature, albeit statistically non-significant. However, Cu speciation is known to be highly sensitive to pH and organic ligands (*e.g.* dissolved organic matter, algal exudates) and only a small proportion of Cu is usually present as the free ion (Mueller et al., 2012; Macoustra et al., 2020). If authors emphasized that this reduction of Cu bioaccumulation was not due to a limitation of dissolved Cu concentrations, they also mentioned the possibility of a difference in exposure due to Cu bioavailability. If dissolved organic matter is also known to play a role in Ni speciation (Macoustra et al., 2021), using free metal concentrations, as in this study, ensures that the approach can be generalized to various water chemistry conditions, thus allowing a better lab-to-field extrapolation. To our knowledge, only Fadhloui et al. (2020) exposed biofilms to Ni in microcosms at different temperatures. These authors found no apparent differences in

accumulated Ni between the two temperatures tested (15 and 21°C), contrasting with our results. However, the range in accumulated metal was similar to that found in our study with conditions T14P16 and T14P12 (around 40 µmol/g dw after 28 days of exposure). Using confocal laser scanning microscopy (CLSM) and scanning transmission X-ray microscopy (STXM), Lawrence et al. (2019) investigated Ni bioaccumulation and its precise location within river biofilms. The authors showed that Ni was strongly associated with EPS and that 4-fold more nickel was concentrated in specific microcolonies than in overall biofilms. As a comparison Se was shown to be associated with protein and polysaccharide biofilm components (Yang et al., 2016). Findings also suggest an important role for specific community members in the sorption and concentration of Ni (and more generally metals such as Se) in aquatic biofilm communities. It could be hypothesized that the structure of the biofilm, such as the taxonomic composition, may explain the differences of accumulation found in this study based on the idea that specific temperatures are more favourable for some organisms. This hypothesis could explain the higher bioaccumulation of biofilms exposed at 20°C compared to those exposed at 14°C. From this perspective, using community-based approaches, such as metabarcoding, while investigating bioaccumulation as a function of the free metal ion concentration would provide important information about how internalized metal concentrations are being affected by taxonomic community composition or specific organisms (Gillmore et al., 2021).

Our results are coherent with those published in a previous field study (Laderriere et al., 2021). Differences were found in the observed relationships between free metal ions and biofilm metal concentrations between two regions distanced 1700 km apart (northern and southern eastern Canada). The two regions were different in terms of climate, ecosystems and thus environmental conditions (*i.e.* temperature and photoperiod). The southern biofilm showed higher internalized concentrations of metals studied (Cu, Ni and Cd) for the same concentration of free metal ions in ambient water as compared to the northern biofilms. Our results suggest that temperature plays an important role in the bioaccumulation of metals by the biofilm and that this factor should be taken into account in the use of biofilm as a bio-indicator over large geographical scales.

5.6 Conclusions

Variability in environmental factors make it difficult to establish a causal link between metal exposure and observed biological effects. Furthermore, environmental conditions, which include high background metal concentrations could favour benthic microbial communities tolerant to

metals. In this context, microcosm approaches are interesting because they allow us to study the influence of specific parameters while remaining at the community scale. In this study, the influence of interactions between environmental factors such as temperature and photoperiod, and Ni exposure on Ni bioaccumulation and toxicity were investigated. Nickel exposure caused a chronic effect on the efficiency of PSII, the percentage of inhibition increasing with the duration of exposure. On the other hand, Chl-a concentration values decreased when biomass increased over time for the different exposure concentrations. This suggests that the heterotrophic compartment was less impacted than the phototrophic one. Furthermore, our results suggest that temperature has a stronger effect on Ni accumulation than photoperiod. Indeed, biofilms exposed at a temperature of 20°C bioaccumulated more Ni than those exposed at 14°C for a given exposure concentration and were characterized by a lower EC₅₀ value. This suggests that temperature influenced directly (e.g. by influencing cell metabolism) or indirectly (e.g. by modifying biofilm structure/composition) the Ni vulnerability of biofilms. In a context where freshwater biofilms may be used as indicators of metal exposure, these results imply that seasonal variations in the bioaccumulation response of metals is likely to occur.

Further studies should focus on the different functional compartments (e.g. phototrophic and heterotrophic) of biofilms by using descriptors to assess interactive effects of multiple stressors at the community level. Indeed, it would be interesting to explore Ni toxicity in the heterotrophic compartment of biofilms to examine if the vulnerability of microbial communities to subsequent Ni exposure depends on the studied function. In order to allow extrapolation of laboratory data to the natural environment, it appears crucial to understand the links between bioaccumulation, changes in environmental conditions and the taxonomic community composition of freshwater biofilms.

5.7 Acknowledgments

This research was funded by the Fonds de recherche du Québec–Nature et technologies, grant number 2014-MI-183237 and by the Canada Research Chair Program, grant number 950-231107. Séverine Le Faucher is supported by the Research Partnership Chair E2S-UPPA-Total-Rio Tinto (ANR-16-IDEX-0002). The authors would like to thank Anissa Bensadoune and Jean-François Dutil for providing help with chemical analyses. We also thank the EcotoQ network for its financial support to V.L. We also thank Betty Chaumet for her assistance with statistics and Scott Hepditch for his language assistance.

6 BIBLIOGRAPHIE 2^E ARTICLE

- Ancion, P.Y., Lear, G., Lewis, G.D., 2010. Three common metal contaminants of urban runoff (Zn, Cu & Pb) accumulate in freshwater biofilm and modify embedded bacterial communities. *Environ. Pollut.* 158, 2738–2745. <https://doi.org/10.1016/j.envpol.2010.04.013>
- Battin, T.J., Besemer, K., Bengtsson, M.M., Romani, A.M., Packmann, A.I., 2016. The ecology and biogeochemistry of stream biofilms. *Nat. Rev. Microbiol.* 14, 251–263. <https://doi.org/10.1038/nrmicro.2016.15>
- Boivin, Y., Massieux, B., Breure, A.M., Ende, F.P. Van Den, Greve, G.D., Rutgers, M., Admiraal, W., 2005. Effects of copper and temperature on aquatic bacterial communities. *Aquat. Toxicol.* 71, 345–356. <https://doi.org/10.1016/j.aquatox.2004.12.004>
- Bonet, B., Corcoll, N., Acuña, V., Sigg, L., Behra, R., Guasch, H., 2013. Seasonal changes in antioxidant enzyme activities of freshwater biofilms in a metal polluted Mediterranean stream. *Sci. Total Environ.* 444, 60–72. <https://doi.org/10.1016/j.scitotenv.2012.11.036>
- Bonnineau, C., Artigas, J., Chaumet, B., Dabrin, A., Faburé, J., Ferrari, B.J.D., Lebrun, J.D., Margoum, C., Mazzella, N., Miège, C., Morin, S., Uher, E., Babut, M., Pesce, S., 2020. Role of biofilms in contaminant bioaccumulation and trophic transfer in aquatic ecosystems: current state of knowledge and future challenges. *Rev. Environ. Contam. Toxicol.* 253, 115–153. https://doi.org/10.1007/398_2019_39
- Chaumet, B., Mazzella, N., Neury-Ormanni, J., Morin, S., 2020. Light and temperature influence on diuron bioaccumulation and toxicity in biofilms. *Ecotoxicology* 29, 185–195. <https://doi.org/10.1007/s10646-020-02166-8>
- Cheloni, G., Slaveykova, V.I., 2018. Combined effects of trace metals and light on photosynthetic microorganisms in aquatic environment. *Environments* 5, 1–19. <https://doi.org/10.3390/environments5070081>
- Corcoll, N., Bonet, B., Leira, M., Guasch, H., 2011. Chl-a fluorescence parameters as biomarkers of metal toxicity in fluvial biofilms: An experimental study. *Hydrobiologia* 673, 119–136. <https://doi.org/10.1007/s10750-011-0763-8>
- Corcoll, N., Bonet, B., Leira, M., Montuelle, B., Tlili, A., Guasch, H., 2012a. Light history influences the response of fluvial biofilms to Zn exposure. *J. Phycol.* 48, 1411–1423. <https://doi.org/10.1111/j.1529-8817.2012.01223.x>

- Corcoll, N., Bonet, B., Morin, S., Tlili, A., Leira, M., Guasch, H., 2012b. The effect of metals on photosynthesis processes and diatom metrics of biofilm from a metal-contaminated river: A translocation experiment. *Ecol. Indic.* 18, 620–631. <https://doi.org/10.1016/j.ecolind.2012.01.026>
- Faburé, J., Dufour, M., Autret, A., Uher, E., Fechner, L.C., 2015. Impact of an urban multi-metal contamination gradient: Metal bioaccumulation and tolerance of river biofilms collected in different seasons. *Aquat. Toxicol.* 159, 276–289. <https://doi.org/10.1016/j.aquatox.2014.12.014>
- Fadhloui, M., Laderriere, V., Lavoie, I., Fortin, C., 2020. Influence of temperature and nickel on algal biofilm fatty acid composition. *Environ. Toxicol. Chem.* 39, 1566–1577. <https://doi.org/10.1002/etc.4741>
- Fechner, L.C., Gourlay-Francé, C., Tusseau-Vuillemin, M.H., 2011. Low exposure levels of urban metals induce heterotrophic community tolerance: A microcosm validation. *Ecotoxicology* 20, 793–802. <https://doi.org/10.1007/s10646-011-0630-4>
- Flemming, H.C., Wingender, J., 2010. The biofilm matrix. *Nat. Rev. Microbiol.* 8, 623–633. <https://doi.org/10.1038/nrmicro2415>
- Friesen, V., Doig, L.E., Markwart, B.E., Haakensen, M., Tissier, E., Liber, K., 2017. Genetic characterization of periphyton communities associated with selenium bioconcentration and trophic transfer in a simple food chain. *Environ. Sci. Technol.* 51, 7532–7541. <https://doi.org/10.1021/acs.est.7b01001>
- Gillmore, M.L., Golding, L.A., Chariton, A.A., Stauber, J.L., Stephenson, S., Gissi, F., Greenfield, P., Juillot, F., Jolley, D.F., 2021. Metabarcoding reveals changes in benthic eukaryote and prokaryote community composition along a tropical marine sediment nickel gradient. *Environ. Toxicol. Chem.* 40, 1892–1805. <https://doi.org/10.1002/etc.5039>
- Guasch, H., Artigas, J., Bonet, B., Bonnneau, C., Canals, O., Corcoll, N., 2016. The use of biofilms to assess the effects of chemicals on freshwater ecosystems, in: Romaní, A.M., Guasch, H., Balaguer, M.D. (Eds.), In *Aquatic Biofilms: Ecology, Water Quality and Wastewater Treatment*. Caister Academic Press, Spain, pp. 125–144. <https://doi.org/10.21775/9781910190173.06>
- Harasim, P., Filipek, T., 2015. Nickel in the environment. *J. Elem.* 20, 525–534. <https://doi.org/10.5601/jelem.2014.19.3.651>
- Hassler, C.S., Slaveykova, V.I., Wilkinson, K.J., 2004. Discrimination between intra- and extracellular metals using chemical extractions. *Limnol. Oceanogr. Methods* 2, 237–247. <https://doi.org/10.4319/lom.2004.2.237>

Hobbs, W.O., Collyard, S.A., Larson, C., Carey, A.J., O'Neill, S.M., 2019. Toxic burdens of freshwater biofilms and use as a source tracking tool in rivers and streams. Environ. Sci. Technol. 53, 11102–11111. <https://doi.org/10.1021/acs.est.9b02865>

Laderriere, V., Faucheur, S. Le, Fortin, C., 2021. Exploring the role of water chemistry on metal accumulation in biofilms from streams in mining areas. Sci. Total Environ. 784, 146986. <https://doi.org/10.1016/j.scitotenv.2021.146986>

Laderriere, V., Paris, L.E., Fortin, C., 2020. Proton competition and free ion activities drive cadmium, copper, and nickel accumulation in river biofilms in a nordic ecosystem. Environments 7, 1–13. <https://doi.org/10.3390/environments7120112>

Lambert, A., Morin, S., Artigas, J., Volat, B., Coquery, M., Neyra, M., Pesce, S., 2012. Structural and functional recovery of microbial biofilms after a decrease in copper exposure : Influence of the presence of pristine communities. Aquat. Toxicol. 109, 118–126. <https://doi.org/10.1016/j.aquatox.2011.12.006>

Lambert, A.S., Dabrin, A., Foulquier, A., Morin, S., Rosy, C., Coquery, M., Pesce, S., 2017. Influence of temperature in pollution-induced community tolerance approaches used to assess effects of copper on freshwater phototrophic periphyton. Sci. Total Environ. 607–608, 1018–1025. <https://doi.org/10.1016/j.scitotenv.2017.07.035>

Lambert, A.S., Dabrin, A., Morin, S., Gahou, J., Foulquier, A., Coquery, M., Pesce, S., 2016. Temperature modulates phototrophic periphyton response to chronic copper exposure. Environ. Pollut. 208, 821–829. <https://doi.org/10.1016/j.envpol.2015.11.004>

Larras, F., Lambert, A.S., Pesce, S., Rimet, F., Bouchez, A., Montuelle, B., 2013. The effect of temperature and a herbicide mixture on freshwater periphytic algae. Ecotoxicol. Environ. Saf. 98, 162–170. <https://doi.org/10.1016/j.ecoenv.2013.09.007>

Lavoie, I., Lavoie, M., Fortin, C., 2012. A mine of information: Benthic algal communities as biomonitoring of metal contamination from abandoned tailings. Sci. Total Environ. 425, 231–241. <https://doi.org/10.1016/j.scitotenv.2012.02.057>

Lavoie, I., Morin, S., Laderriere, V., Fortin, C., 2018. Freshwater diatoms as indicators of Combined long-term mining and urban stressors in Junction Creek (Ontario, Canada). Environments 5, 30. <https://doi.org/10.3390/environments5020030>

Lawrence, J.R., Chenier, M.R., Roy, R., Beaumier, D., Fortin, N., Swerhone, G.D.W., Neu, T.R., Greer, C.W., 2004. Microscale and molecular assessment of impacts of nickel, nutrients, and

oxygen level on structure and function of river biofilm communities. *Appl. Environ. Microbiol.* 70, 4326–4339. <https://doi.org/10.1128/AEM.70.7.4326>

Lawrence, J.R., Swerhone, G.D.W., Neu, T.R., 2019. Visualization of the sorption of nickel within exopolymer microdomains of bacterial microcolonies using confocal and scanning electron microscopy. *Microbes Environ.* 34, 76–82. <https://doi.org/10.1264/jsme2.ME18134>

Leguay, S., Lavoie, I., Levy, J.L., Fortin, C., 2016. Using biofilms for monitoring metal contamination in lotic ecosystems: The protective effects of hardness and pH on metal bioaccumulation. *Environ. Toxicol. Chem.* 35, 1489–1501. <https://doi.org/10.1002/etc.3292>

Lürling, M., Eshetu, F., Faassen, E.J., Kosten, S., Huszar, V.L.M., 2013. Comparison of cyanobacterial and green algal growth rates at different temperatures. *Freshw. Biol.* 58, 552–559. <https://doi.org/10.1111/j.1365-2427.2012.02866.x>

Macoustra, G.K., Jolley, D.F., Stauber, J.L., Koppel, D.J., Holland, A., 2021. Speciation of nickel and its toxicity to Chlorella sp. in the presence of three distinct dissolved organic matter (DOM). *Chemosphere* 273, 128454. <https://doi.org/10.1016/j.chemosphere.2020.128454>

Macoustra, G.K., Jolley, D.F., Stauber, J.L., Koppel, D.J., Holland, A., 2020. Amelioration of copper toxicity to a tropical freshwater microalga: Effect of natural DOM source and season. *Environ. Pollut.* 115–141. <https://doi.org/10.1016/j.envpol.2020.115141>

Massieux, B., Boivin, M.E.Y., Van Den Ende, F.P., Langenskiöld, J., Marvan, P., Barranguet, C., Admiraal, W., Laanbroek, H.J., Zwart, G., 2004. Analysis of structural and physiological profiles to assess the effects of Cu on biofilm microbial communities. *Appl. Environ. Microbiol.* 70, 4512–4521. <https://doi.org/10.1128/AEM.70.8.4512-4521.2004>

Moe, S.J., De Schamphelaere, K., Clements, W.H., Sorensen, M.T., Van den Brink, P.J., Liess, M., 2013. Combined and interactive effects of global climate change and toxicants on populations and communities. *Environ. Toxicol. Chem.* 32, 49–61. <https://doi.org/10.1002/etc.2045>

More, T.T., Yadav, J.S.S., Yan, S., Tyagi, R.D., Surampalli, R.Y., 2014. Extracellular polymeric substances of bacteria and their potential environmental applications. *J. Environ. Manage.* 144, 1–25. <https://doi.org/10.1016/j.jenvman.2014.05.010>

Morin, S., Lambert, A.S., Rodriguez, E.P., Dabrin, A., Coquery, M., Pesce, S., 2017. Changes in copper toxicity towards diatom communities with experimental warming. *J. Hazard. Mater.* 334, 223–232. <https://doi.org/10.1016/j.jhazmat.2017.04.016>

Mueller, K.K., Loftis, S., Fortin, C., Campbell, P.G.C., 2012. Trace metal speciation predictions in natural aquatic systems: Incorporation of dissolved organic matter (DOM) spectroscopic quality. Environ. Chem. 9, 356–368. <https://doi.org/10.1071/EN11156>

Namba, H., Iwasaki, Y., Heino, J., Matsuda, H., 2020. What to survey? A systematic review of the choice of biological groups in assessing ecological impacts of metals in running waters. Environ. Toxicol. Chem. 39, 1964–1972. <https://doi.org/10.1002/etc.4810>

Pesce, S., Lambert, A.-S., Morin, S., Foulquier, A., Coquery, M., Dabrin, A., 2018. Experimental warming differentially influences the vulnerability of phototrophic and heterotrophic periphytic communities to copper toxicity. Front. Microbiol. 9, 1424. <https://doi.org/10.3389/fmicb.2018.01424>

Serra, A., Guasch, H., Admiraal, W., Van Der Geest, H.G., Van Beusekom, S.A.M., 2010. Influence of phosphorus on copper sensitivity of fluvial periphyton: The role of chemical, physiological and community-related factors. Ecotoxicology 19, 770–780. <https://doi.org/10.1007/s10646-009-0454-7>

Steinman, A.D., Lamberti, G.A., Leavitt, P.R., 2006. Biomass and Pigments of Benthic Algae, in: Elsevier (Ed.), In: Methods in Stream Ecology. pp. 357–379. <https://doi.org/10.1016/b978-012332908-0.50024-3>

Stewart, T.J., Behra, R., Sigg, L., 2015. Impact of chronic lead exposure on metal distribution and biological effects to periphyton. Environ. Sci. Technol. 49, 5044–5051. <https://doi.org/10.1021/es505289b>

Tercier-Waeber, M.-L., Stoll, S., Slaveykova, V.I., 2012. Trace metal behavior in surface waters: Emphasis on dynamic speciation, sorption processes and bioavailability. Arch. des Sci. 65, 119–142.

Tlili, A., Corcoll, N., Arrhenius, Å., Backhaus, T., Hollender, J., Creusot, N., Wagner, B., Behra, R., 2020. Tolerance patterns in stream biofilms link complex chemical pollution to ecological impacts. Environ. Sci. Technol. 54, 10745–10753. <https://doi.org/10.1021/acs.est.0c02975>

Tlili, A., Maréchal, M., Bérard, A., Volat, B., Montuelle, B., 2011. Enhanced co-tolerance and co-sensitivity from long-term metal exposures of heterotrophic and autotrophic components of fluvial biofilms. Sci. Total Environ. 409, 4335–4343. <https://doi.org/10.1016/j.scitotenv.2011.07.026>

Villeneuve, A., Montuelle, B., Bouchez, A., 2010. Influence of slight differences in environmental conditions (light, hydrodynamics) on the structure and function of periphyton. *Aquat. Sci.* 72, 33–44. <https://doi.org/10.1007/s00027-009-0108-0>

Yang, S.I., George, G.N., Lawrence, J.R., Susan, G., Kaminskyj, W., Dynes, J.J., Lai, B., Pickering, I.J., 2016. Multispecies biofilms transform selenium oxyanions into elemental selenium particles: studies using combined synchrotron X-ray fluorescence imaging and scanning transmission X-ray microscopy. *Environ. Sci. Technol.* 50, 10343–10350. <https://doi.org/10.1021/acs.est.5b04529>

7 ROLE OF SEASONALITY IN THE RESPONSE AND TOLERANCE OF PERIPHERYTIC BIOFILM TO NICKEL

RÔLE DE LA SAISON DANS LA RÉPONSE ET LA TOLÉRANCE D'UN BIOFILM PÉRIPHERYTIQUE EXPOSÉ AU NICKEL

Auteurs : Vincent Laderriere^{1,2}, Soizic Morin^{2,3}, Mélissa Eon², Claude Fortin^{1,2}

Affiliations :

¹ Institut national de la recherche scientifique, Centre Eau Terre Environnement, 490 rue de la Couronne, Québec, Canada

² EcotoQ, 490 rue de la Couronne, Québec, Canada

³ Institut national de recherche pour l'agriculture, l'alimentation et l'environnement, EABX, 50 avenue de Verdun, Cestas, France

Titre de la revue ou de l'ouvrage :

Prêt à soumettre

Contribution des auteurs :

Vincent Laderriere: methodology, software, formal analysis, investigation, data curation, writing – original draft, visualization.

Soizic Morin: conceptualization, methodology, writing – review & editing, supervision.

Mélissa Eon: methodology, formal analysis.

Claude Fortin: conceptualization, methodology, writing – review& editing, supervision, project administration, funding acquisition.

7.1 Abstract

Whereas low concentrations of some metals can occur naturally in freshwater ecosystems, anthropogenic activities like mining operations represent a long-standing concern of discharge. Subsequently released into aquatic environments, metals are likely to come in contact with microbial communities such as periphytic biofilm, which plays a key role as a primary producer in stream ecosystems. The present study assessed the effects of four increasing nickel (Ni) concentrations (0 to 6 µM) on two different natural biofilm communities collected in different seasons. Using two 28-day microcosm studies, biofilms collected during summer were exposed to Ni with a 16/8 light/dark cycle while those collected during the winter were exposed with a photoperiod of 8/16. The two biofilms were characterized by different structural (dry weight biomass, Chl-a content, proteins and polysaccharides) and functional (photosynthetic yield, activity of two extracellular enzymes) characteristics as well as Ni bioaccumulation. In parallel, their tolerance acquisition were monitored over time using short-term toxicity tests. The results demonstrated that the two communities were characterized by different structural profiles (e.g. autotrophic index, proteins and polysaccharides). Communities showed significant differences in Ni accumulated content for each treatment with systematically lower values in the case of the biofilm exposed to the winter photoperiod. The β -glucosidase and β -glucosaminidase showed no marked effects of Ni exposure and were globally similar between the two communities. Furthermore, biofilms previously exposed to the highest long-term Ni concentration ($[Ni^{2+}] = 6 \mu M$) revealed no acute effects in subsequent short-term toxicity tests based on the PSII yield, suggesting a tolerance acquisition by the phototrophic community. Taken together, the results suggest that the biofilm response to Ni exposure was mainly conditioned by their initial characteristics and that the responses to Ni can thus be seasonally dependent.

Keywords: Biomonitoring, Photosynthesis, Accumulation, Photoperiod, Metals, PICT

7.2 Introduction

Freshwater ecosystems provide numerous services in addition to harboring a significant portion of the biodiversity on which humans depend. Nowadays it is well known that anthropogenic pressures could have severe and persistent repercussions on aquatic ecosystem health, thus reaffirming the need to develop tools to evaluate the ecological integrity of these environments (Reid *et al.*, 2019). While low concentrations of metals can occur naturally in freshwater ecosystems, anthropogenic activities like mining operations represent a long-standing concern of discharge (Ancion *et al.*, 2013). In fact, mines can release metals that may lead to concentrations in surface waters several times higher than natural background levels, even after closure if they are not adequately rehabilitated (Lavoie *et al.*, 2012; Leguay *et al.*, 2016; Vendrell-Puigmitja *et al.*, 2020). It is well recognized that such contamination leads to a loss of biodiversity, from bacteria to fish (Weber *et al.*, 2008; Morin *et al.*, 2012; Mebane *et al.*, 2020). Among all studied metals in ecotoxicology, Ni has received less attention than other metals while presenting an important ecotoxicological risk in regions where it is extracted: e.g. Philippines and Indonesia (Gissi *et al.*, 2016), New Caledonia (Gillmore *et al.*, 2021), Canada (Laderriere *et al.*, 2021), among others (U.S. Geological Survey, 2021).

In order to better understand the dynamic behaviour and the consequences of contaminant exposure in the environment and their potential ecological effects on natural ecosystems, biomonitoring approaches have been shown to have a high potential. For instance, freshwater biofilms are known to integrate and react quickly to anthropic contamination making it a useful bioindicator (Stewart *et al.*, 2015; Faburé *et al.*, 2015; Bonnneau *et al.* 2020). Biofilms are composed of many ecological groups including microalgae, fungi, bacteria and protozoa embedded in a self-produced exopolysaccharide matrix. They cover almost every surfaces in freshwater environments (Flemming & Wingender 2010; Battin *et al.* 2016). In addition to being at the base of the trophic chain and to constantly grow to regenerate biomass, they are sessile, involved in ecosystem processes and contribute substantially to global biogeochemical fluxes (Guasch *et al.*, 2016; Battin *et al.*, 2016). These characteristics provide biofilms potential to be an effective tool for integrating spatial and temporal variations in contaminant sources as well as possible ecological effects on higher trophic levels (Hobbs *et al.*, 2019). Metals are known to impact both phototrophic and heterotrophic communities of biofilms and various biomarkers have been developed in the last decades. For instance, chlorophyll-a (Chl-a) content (Corcoll *et al.*, 2011), photosynthetic activity (Lambert *et al.*, 2016), antioxidant enzyme activities (Bonet *et al.*,

2012), extracellular enzymes activities (Pesce *et al.*, 2018), microbial respiration (Tlili *et al.*, 2011) may be altered allowing to measure the response of living organisms to metals. Moreover, bioaccumulation by biofilms has shown a great potential as a biomonitoring tool for both metallic (Lavoie *et al.*, 2012; Leguay *et al.*, 2016; Laderriere *et al.*, 2021) and organic contaminants (Fernandes *et al.* 2020; Bonnneau *et al.* 2020). In addition, because of the fast accumulation and the slow release of metals by biofilms, they constitute an integrative indicator of metal exposure occurring over a period of hours or days (Ancion *et al.*, 2010; Faburé *et al.*, 2015; Dranguet *et al.*, 2017).

Discriminating toxicant-induced effects from those induced by biotic or abiotic factors on biological communities is challenging. In this context, the pollution-induced community tolerance (PICT) has been introduced first by Blanck *et al.*, (1988) and allows for a better characterization of the effects of contaminants on the structural and functional changes of biological communities (Tlili *et al.* 2016). In the case of biofilms, an increase in community tolerance from chronic exposure to contaminants might be the result of the disappearance of sensitive species and dominance of tolerant ones. Metal contamination is known to lead to structural and functional changes in phototrophic (Morin *et al.*, 2012; Vendrell-Puigmitja *et al.*, 2020) and heterotrophic communities (Ancion *et al.*, 2010; Ancion *et al.*, 2013). In this context, a community that has been exposed chronically to contaminants can become more tolerant than the unexposed reference community (Tlili *et al.* 2016). Based on a short-term toxicity test using a physiological endpoint, the acquisition of tolerance can be measured by a dose-response approach and ultimately provide Effective Concentrations (EC). However, contaminants may have an impact on different functions, highlighting the necessity to use a large set of functional and structural descriptors covering more than one microbial component (*i.e.* phototroph or heterotroph; Tlili *et al.*, 2011; Pesce *et al.*, 2018). Additionally, environmental factors such as temperature (Morin *et al.*, 2017; Pesce *et al.*, 2018), nutrients (Serra *et al.*, 2010; Tlili *et al.*, 2010) and light (Navarro *et al.*, 2008; Corcoll *et al.*, 2012; Cheloni & Slaveykova, 2018) are known to influence the sensitivity of phototrophic and heterotrophic periphytic communities to metal. About light, the majority of the studies focused on light intensity and spectral composition (*e.g.* ultraviolet radiation) and to our knowledge, few studies have focused on the photoperiod. These studies are often based on unicellular green algae and few studies have worked on their effects on non-model organisms such as biofilms (Cheloni & Slaveykova, 2018). Moreover, species-species interactions are known to influence metals toxicity dissimilarly depending on the exposure duration and light conditions (Cheloni *et al.*, 2019). Thus, in the context of PICT using periphytic biofilms, there is still a lack of knowledge about the links between changes in exposure biomarkers (*i.e.* increase or decrease in the

response), such as bioaccumulation and the combined effects of metal exposure and environmental factors.

In previous studies, bioaccumulation of metals by freshwater biofilms has been proved to have a universal potential as a proxy for metal bioavailability, despite large geographical scales in lotic ecosystems (Laderriere *et al.*, 2021). Furthermore, bioaccumulation of Ni by biofilms and their sensitivity were shown to be modified by temperature suggesting that seasonal variations in the bioaccumulation of metals are likely to occur (submitted data; see section 5). The aim of this experimental microcosm study was to assess the impact of environmentally relevant Ni concentrations on natural microbial communities collected in two different seasons. The qualification of August (summer) or December (winter) biofilms will therefore be used in the text. Considering that the two communities originated from two different seasons, the overall objective was to study the effects of chronic Ni exposure on their sensitivity and tolerance in relation to their structural and functional characteristics. Thus, two biofilms, grown for one month in a natural pond in two different seasons, were chronically exposed to different concentrations of Ni according to a summer (light dark/cycle of 16/8) and a winter (8/16) photoperiod. At each sampling time, biofilms were collected to be structurally (dry weight biomass, Chl-a content, proteins and polysaccharides) and functionally (functions associated with autotrophs: photosynthetic yield, and heterotrophs: β -glucosidase and β -glucosaminidase activities) characterized and to determine the Ni content. In addition, short-term toxicity tests were conducted on both communities to measure their capacity to tolerate subsequent Ni exposure over time. We postulated that both the photoperiod (in relation to the initial characteristics of the two communities) and the chronic Ni exposure would modify microbial community structure leading to changes in the capacity of phototrophic and heterotrophic communities to tolerate subsequent acute exposure to Ni.

7.3 Materials & methods

7.3.1 Experimental set-up

For biofilm colonization, glass slides (L: 26.5 cm; W: 6 cm; surface: 159 cm²) were submerged (between 10 and 20 cm beneath the water surface) for one month in August and in December 2018 in the Gazinet-Cestas pond (44°46'30.1"N, 0°41'44.3"W). The physico-chemical characteristics of the pond are presented in Appendix III (see Table 13-1). After a month, colonized glass slides were collected and were randomly placed in artificial channel systems.

Slides were placed horizontally under a water column height of about 5 cm. Biofilms were exposed under controlled light conditions ($40 \mu\text{mol}\cdot\text{photons}/\text{m}^2/\text{s}$ measured at the level of the glass slides; LICOR LI-250 light meter) and the water temperature was $14.7 \pm 0.5^\circ\text{C}$. This temperature has been chosen as an intermediate between the two seasons and this temperature was kept stable during the two experiments to avoid an influence of this parameter. Two experiments were carried with two different photoperiods: 16/8 (diurnal cycle mimicking the summer season) and 8/16 (cycle of the winter season). Prior to the start of the exposure with the addition of Ni, a period of two weeks was allowed for the biofilm to acclimatize to the artificial channel systems.

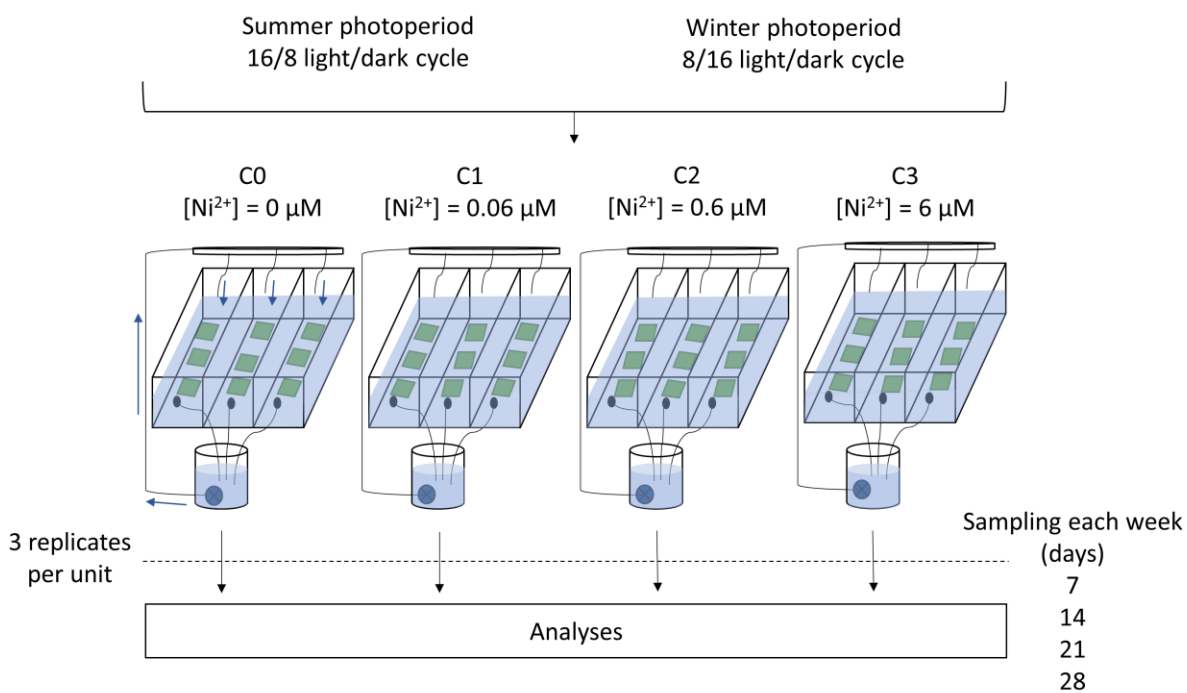


Figure 7-1: Graphical representation of the experimental design. Each square represents a glass tile colonized by biofilms.

The experimental set-up was composed of four exposure units, each supplied with recirculating filtered pond water (successive filtration up to $250 \mu\text{m}$; see Figure 7-1). Each unit was divided in three dependent artificial streams (L: 50 cm; W: 9.2 cm; H: 5 cm) sharing the same 10 L refill reservoir. A submersible pump was used to maintain oxygenation, flow ($9 \times 10^{-5} \text{ m}^3/\text{s}$) and to simulate a river environment. Four dissolved Ni concentrations were tested and precisely

determined (mean \pm SD; n = 6): a control (*i.e.* no added Ni: C0), a low contaminated (C1: [Ni]_T = 0.5 μ M; [Ni²⁺] = 0.06 μ M), a moderately contaminated (C2: [Ni]_T = 3.5 μ M; [Ni²⁺] = 0.6 μ M) and a highly contaminated (C3: [Ni]_T = 20 μ M; [Ni²⁺] = 6 μ M) one. At each sampling time, half of the exposure medium volume was renewed with freshly filtered water of the pond. Nickel concentrations were adjusted according to the treatments before renewal to maintain the concentration in the exposure units using a Ni stock solution (ICP standard solution of 10 g/L of Ni in 4% HNO₃ (v/v); SCP Science). The two experiments were carried out for 28 days and biofilm was sampled each week (7, 14, 21 and 28 days).

7.3.2 Water analyses and Ni speciation

Temperature, pH and conductivity were measured every week before and after exposure medium partial renewal using an *in-situ* probe (WTW, Germany). Water samples were also taken before and after the renewal to follow physico-chemical parameters over time. The results are presented in Appendix III (see Table 13-3 and 13-4). For each unit, 1 L of water was collected from the reservoir, filtered (polysulfonate; Ø = 0.45 μ m; VWR International) and stored at 4°C until analysis. Dissolved nutrients were measured by ion chromatography (COMPACT 881 IC Pro, Metrohm, Switzerland) coupled with a conductivity detector (Metrohm 850 IC, Switzerland) and total organic carbon (TOC) was analyzed using an organic carbon analyzer (TOC-VW, Shimadzu, France). Aliquots of 15 mL were collected at the same time as biofilm sampling (one sample per channel; n = 3) for elemental quantification (Ca, Co, Cu, Fe, K, Mg, Mn, Mo, Ni, Na, P, Pb, Si, Zn) by inductively coupled plasma atomic emission spectroscopy (ICP-AES; Varian Vista AX CCD). Polysulfonate filters were also used to filter the water samples that were subsequently acidified at 0.2% (v/v) HNO₃ (trace metal grade; Fisher). All samples were kept stored in a cold room (4 °C) until analysis. Nickel speciation was calculated using WHAM7 software for each sampling date based on measured concentrations both before and after the renewal. Input parameters were pH, total dissolved metal concentrations (Cu, Fe, Mn, Pb, Zn, and Ni), total anions (NO₃⁻, SO₄²⁻, and Cl⁻) and major cations (Ca, Mg, Na and K). The concentrations of fulvic (FA) and humic (HA) acids were also required for modelling purposes, which were estimated from the concentrations of dissolved organic carbon (DOC). The proportion of FA to HA was assumed to be at a 3:1 ratio and metal binding DOC to represent 60 % of the dissolved organic matter, which is made of 50% C (Perdue & Ritchie, 2003).

7.3.3 Biofilm characterization and tolerance assessment

For each condition and sampling date, three replicates of samples were collected per unit (one per channel). Biofilms were scrapped off using a razor blade and resuspended in 40 mL of Dauta medium (see Table 13-2 in Appendix III for composition details). We used an artificial medium in order to minimize differences in exposure for acute Ni toxicity tests and to be able to compare between experiments. At room temperature, the biofilm solution was then homogenized using a magnetic stirrer for 30 min at 150 rpm (Variomag multi-station agitator; Thermo-Scientific) before being subdivided for the different parameter analyses: 10 mL for PICT assessment, 10 mL for Ni bioaccumulation determination, 10 mL for Chl-a extraction, 500 µL for protein content, 500 µL for polysaccharide, 150 µL for β-glucosidase and 150 µL for β-glucosaminidase quantification. Measured values were normalized for the scraped surface (79.5 cm²) and subsequent dilutions. The details of each procedure are explained below.

7.3.3.1 Short-term bioassays and tolerance assessment

The tolerance assessment was based on short-term Ni toxicity tests by measuring the effective photosystem II quantum yield (Φ_{PSII}) using a Pulse Amplitude Modulated Fluorimeter (Phyto-PAM; Heinz Walz GmbH, Germany). The tolerance level of phototrophic biofilm to Ni was assessed every week (7, 14, 21 and 28 days) in order to follow a potential tolerance acquisition over exposure time. From 10 mL of biofilm suspension, 1 mL was resuspended in 2 mL of Ni contaminated Dauta medium to obtain a semi-logarithmic series of 8 toxicant dilutions with final test concentrations ranging from 0 to 170 µM of total Ni (*i.e.* 0 to 3 mg/L). During the 6 hours of short exposure, biofilm suspensions were kept on an agitator plate (40 rpm) under constant light ($19.5 \pm 1.5 \mu\text{mol}\cdot\text{photons}/\text{m}^2/\text{s}$; $n = 5$) and Ni toxicity was determined by measuring Φ_{PSII} after 6 h. Using MINEQL+ software, Ni was calculated to be at 94.4% under its free form (Ni^{2+}) in the Dauta medium. ECs can therefore be converted in µM of Ni^{2+} using this percentage.

7.3.3.2 Bioaccumulation

In order to measure Ni bioaccumulation, each biofilm suspension was centrifuged (6000 rpm; 5 min). A volume of 10 mL of EDTA (10 mM; pH 7) was added to the pellet to dissociate surface adsorbed Ni from intracellular content. The mixture was vortexed, and cells were recovered after

another 5 min centrifugation step. The supernatant was removed and the pellets were then lyophilized during 48 h (ALPHA1-2 Dplus CHRIST, Germany). After this step, 800 µL of concentrated nitric acid (trace metal grade; Fisher) were added to the pellets for a digestion step of 48 h. Then, 200 µL of hydrogen peroxide (trace metal grade; Fisher) were added for another 48 h. A volume of 800 µL of this digestate was then diluted in 7.2 mL of ultrapure water to reach a final HNO₃ concentration of 10% (v/v). The intracellular Ni content was determined by ICP-AES (Varian Vista AX CCD). Blank samples and the certified reference material IAEA-450 (algae) were also digested and analyzed to verify the methodology and the efficiency of the digestion method (mean Ni recovery of 81.5 ± 0.5%; n = 3).

7.3.3.3 Chlorophyll-a extraction

A volume of 10 mL of biofilm samples was centrifuged at 5000 rpm during 5 min and the pellets were resuspended in 10 mL of acetone 90 % (v/v; Fisher Scientific). In the dark, pigments were extracted in tubes placed in an ultrasonic bath during 30 min and samples were then filtered onto GF/C filters (1.2 µm; Whatman). Pheophytin-corrected Chl-a was determined spectrophotometrically (Synergy™ HT, Bioteck, USA) by measuring absorbance before and after acidification using 60 µL of HCl (ACS grade; Fisher Scientific).

7.3.3.4 Protein content

A protocol adapted to low concentrations of proteins was developed based on the methodology presented by Bradford, (1976). To determine the protein content, 4.5 mL of methanol were added to 500 µL of biofilm suspension. The samples were placed in a beaker filled with water, and placed in the ultrasonic bath for 20 min. The samples were then evaporated (SpeedVac; Thermo Fisher Scientific) and resuspended in 500 µL of ultrapure water. A volume of 2.5 mL of Bradford reagent was then added. The absorbance was measured with a microplate reader (595 nm; Synergy™ HT, Bioteck, USA). Absorbance was expressed as a protein concentration as µg Eq BSA (Bovine Serum Albumine). Based on the chemical formula of BSA (C₃₀₇₂H₄₈₂₈N₈₁₆O₉₂₈S₄₀), the results were reported in µg of C relative to the percentage of C in the molecule (53%).

7.3.3.5 Polysaccharide content

Polysaccharide content was analyzed according to Dubois *et al.* (1956). A volume of 1.25 mL of concentrated sulphuric acid and 12.5 μ L of phenol were added to 500 μ L of resuspended biofilm. The samples were left to react during 10 min at room temperature before being vortexed and incubated for 20 min at 30°C. The absorbance was then measured using a microplate reader (485 nm; Synergy™ HT, Biotek, USA). Polysaccharide concentrations were then expressed as μ g Eq glucose (D(+)-glucose anhydrous). Based on the chemical formula of glucose ($C_6H_{12}O_6$), the results were then reported in μ g of C relative to the percentage of C in the molecule (40%).

7.3.3.6 Extracellular enzymatic activities

According to the methodology outlined in Romaní *et al.* (2008), Two extracellular enzymatic activities were measured in this study: the β -glucosidase (β -glu) and the β -glucosaminidase (glsm). Two substrates were therefore used with their respective fluorescent-linked substrate: 4-methylumbelliferyl N-acetyl- β -D-glucosaminide and 4-methylumbelliferyl- β -D-glucopyranoside. The two enzymatic activity assays were done at a saturating concentration of substrate (0.3 mM). A volume of 150 μ L was added to the 150 μ L of biofilm resuspension before the solution was agitated at 80 rpm in the dark. After one hour of incubation, the reaction was stopped by addition of glycine buffer (pH = 10.4). The fluorescence of samples was then measured using a microplate reader (Synergy™ HT, Biotek, USA) at excitation-emission wavelengths of 365 and 455 nm respectively. Fluorescence values were expressed as μ g Eq MUF (7-hydroxy-4-methylcoumarin).

7.3.4 Statistical analyses

All statistical analyses were performed with the R software (v4.0; <https://cran.r-project.org/>). Data were log-transformed before statistical analyses to satisfy the assumption of normality and homogeneity of variances. A two-way repeated measures ANOVA ("rstatix" package) followed by a post-hoc Tukey test (with a Bonferroni adjusted p-value) was used to examine statistical differences in variations in water and periphyton characteristics between Ni exposure concentrations or the two photoperiod experiments (R Development Core Team, 2012). The tolerance assessment results were analyzed using the "drc" package. The four-parameter logistic model was used in order to fit dose-response curves to data and to calculate subsequent

effective concentrations (EC). These EC were then tested using a two-way repeated measures ANOVA followed by a *post-hoc* Tukey test with a Bonferroni adjusted p-value. Significance for all statistical tests was set at $p < 0.05$.

7.4 Results

7.4.1 Physico-chemical data

The mean values of the main physico-chemical parameters of the water are presented in Table 7-1. During the two experiments, water physicochemical characteristics remained similar between treatments within each photoperiod exposure, except for Ni concentrations. The complete table with all parameters (including nitrate, nitrogen, sulfate, silica, etc) is presented in Table 13-1 (Appendix III). Conductivity and pH were stable over exposure time but were significantly different between the two photoperiods tested. The dissolved organic carbon (DOC) concentrations were occasionally fluctuating over time for the two experiments leading to variations (statistically significant) in the calculated free nickel concentrations nevertheless the concentration of free Ni^{2+} remained relatively close to the nominal concentrations (see Table 7-1). The average calculated free Ni^{2+} concentrations were 0.04 ± 0.02 ; 0.60 ± 0.23 ; $5.4 \pm 2.1 \mu\text{M}$ for the 16/8 photoperiod and 0.07 ± 0.01 ; 0.66 ± 0.19 ; $7.0 \pm 1.6 \mu\text{M}$ of Ni^{2+} for the 8/16 photoperiod. In the control units (*i.e.* without added Ni), dissolved Ni concentrations remained below the limit of detection ($0.007 \mu\text{M}$) throughout the two experiments.

Table 7-1 : Physico-chemical characteristics of exposure media of the four channel systems. The values are presented as means \pm standard deviations ($n = 24$). b/DL = below detection (0.007 μM). N/A = not available. The letters a and b respectively refer to the results of Tukey tests performed between (a) the different conditions in comparison to the control (C0) within a given photoperiod, and (b) the two photoperiods tested within a given condition. The column heads refer to the long-term exposure conditions: C0 = control (i.e. no Ni); C1 = $[\text{Ni}^{2+}] = 0.06 \mu\text{M}$; C2 = $[\text{Ni}^{2+}] = 0.6 \mu\text{M}$; C3 = $[\text{Ni}^{2+}] = 6 \mu\text{M}$.

	Photoperiod 16/8								Photoperiod 8/16							
	C0		C1		C2		C3		C0		C1		C2		C3	
	pH	7.9 ^b ± 0.1	7.9 ^b ± 0.1	7.9 ^b ± 0.1	7.8 ^b ± 0.1	7.8 ^b ± 0.1	7.6 ^b ± 0.1	7.5 ^{ab} ± 0.1	7.6 ^b ± 0.1	7.5 ^{ab} ± 0.1						
Conductivity ($\mu\text{S}/\text{cm}$)	241 ^b ± 17	234 ^b ± 14	230 ^{ab} ± 14	232 ^{ab} ± 12	210 ^b ± 13	195 ^{ab} ± 9	185 ^{ab} ± 8	188 ^{ab} ± 8								
[DOC] (mg C/L)	45 ± 28	43 ^b ± 15	34 ^{ab} ± 14	35 ± 20	35 ± 5	34 ^b ± 5	42 ^b ± 20	31 ± 7								
[Ca] _{Tot} (mM)	0.60 ^b ± 0.15	0.58 ^b ± 0.15	0.55 ^b ± 0.16	0.48 ^a ± 0.19	0.53 ^b ± 0.06	0.47 ^{ab} ± 0.04	0.44 ^{ab} ± 0.04	0.44 ^a ± 0.02								
[Ca ²⁺] (mM)	0.37 ± 0.04	0.37 ^b ± 0.02	0.39 ^{ab} ± 0.03	0.38 ^b ± 0.03	0.34 ± 0.02	0.33 ^b ± 0.02	0.30 ^{ab} ± 0.03	0.32 _{ab} ± 0.01								
[Mg] _{Tot} (mM)	0.12 ^b ± 0.03	0.12 ^b ± 0.03	0.12 ^b ± 0.04	0.10 ^{ab} ± 0.04	0.11 ^b ± 0.01	0.10 ^{ab} ± 0.01	0.09 ^{ab} ± 0.01	0.11 ^a ± 0.05								
[Mg ²⁺] (mM)	0.090 ± 0.008	0.090 ^b ± 0.005	0.092 ^b ± 0.007	0.088 _b ± 0.007	0.081 ± 0.006	0.075 ^{ab} ± 0.005	0.069 ^{ab} ± 0.005	0.070 _{ab} ± 0.003								
[Ni] _{Tot} (μM)	b/DL	0.47 ^a ± 0.08	3.4 ^a ± 0.1	20 ^a ± 2	b/DL	0.51 ^a ± 0.06	3.6 ^a ± 0.5	20 ^a ± 3								
[Ni ²⁺] (μM)	N/A	0.044 ^{ab} ± 0.018	0.60 ^a ± 0.23	5.4 ^{ab} ± 2.1	N/A	0.072 ^{ab} ± 0.011	0.66 ^a ± 0.19	7.0 ^{ab} ± 1.6								

7.4.2 Structural and functional characteristics of biofilms

A series of endpoints targeting the whole community, or specific to autotrophs and heterotrophs, were used to assess the effects of chronic Ni exposure to biofilms. The main structural characteristics of biofilms are presented in Table 7-2. Effects of photoperiod on each descriptor were measured by comparing controls and Ni-exposed biofilms at the four sampling times. We used the autotrophic index, which is the ratio between biomass ($\mu\text{g}/\text{cm}^2$) to Chl-a content ($\mu\text{g}/\text{cm}^2$), to give a general overview of the composition of the two biofilms (*i.e.* autotrophic vs heterotrophic components).

Overall, as suggested by the autotrophic index values, the biofilms exposed to the two photoperiods present different structural characteristics. Indeed, dry-weight biomasses and Chl-a content per unit surface were respectively lower and higher in the case of the summer photoperiod compared to the winter one. This leads to opposite tendencies in the autotrophic index values between the two photoperiods suggesting a more heterotrophic biofilm in the case of the winter photoperiod. In relation to time, the dry weight biomass varied from one sample to another but slightly increased over time except for the control condition in the case of the summer photoperiod. For the same photoperiod, the Chl-a contents gradually increased during the 28 days except for the control (C0; $[\text{Ni}^{2+}] = 0 \mu\text{M}$) and for the highest exposure condition (C3; $[\text{Ni}^{2+}] = 6 \mu\text{M}$). For the winter photoperiod, Chl-a contents slightly increased with time for the C0 and C1 conditions, but remained stable in the case of the C2 and C3 conditions. Finally, the C3 condition showed lower Chl-a values in comparison to the other Ni treatments for the two photoperiods.

Table 7-2 : Main descriptors (mean ± standard deviation) of biofilms under control and Ni-exposure conditions at 0, 0.06, 0.6 and 6 µM of Ni²⁺ (named respectively C0, C1, C2 and C3). The letters ^a and ^b refer to the results of Tukey tests performed between (a) the different conditions in comparison to the control (C0) within a given sampling time and photoperiod, and (b) the two photoperiods tested within a given condition and time, respectively.

Time (days)	Treatment	Photoperiod 16/8						Photoperiod 8/16					
		Dry-weight biomass (mg/cm ²)		Chlorophyll-a (µg/cm ²)		Autotrophic index (x 10 ³)		Dry-weight biomass (mg/cm ²)		Chlorophyll-a (µg/cm ²)		Autotrophic index (x 10 ³)	
7	C0	0.11	± 0.08	0.09	± 0.01	1.5	± 1.3	0.42	± 0.02	0.11	± 0.03	6.6	± 1.2
	C1	0.067 ^b	± 0.043	0.09	± 0.03	1.1	± 0.8	0.35 ^b	± 0.01	0.13	± 0.05	5.1	± 1.9
	C2	0.13 ^b	± 0.07	0.070	± 0.030	3.9	± 3.5	0.36 ^{ab}	± 0.08	0.12	± 0.03	5.1	± 1.2
	C3	0.074 ^b	± 0.019	0.040	± 0.010	5.1	± 3.4	0.32 ^{ab}	± 0.07	0.06	± 0.03	13	± 11
14	C0	0.12 ^b	± 0.03	0.10	± 0.02	2.2	± 0.8	0.33 ^b	± 0.08	0.17	± 0.06	3.8	± 1.7
	C1	0.26	± 0.31	0.28	± 0.15	2.6	± 3.0	0.34	± 0.04	0.14	± 0.07	4.2	± 1.6
	C2	0.28	± 0.16	0.23 ^b	± 0.06	3.3	± 2.4	0.28	± 0.04	0.12 ^b	± 0.03	3.3	± 1.5
	C3	0.11 ^b	± 0.07	0.060	± 0.040	1.8 ^b	± 1.0	0.33 ^b	± 0.07	0.07	± 0.01	5.7 ^b	± 0.6
21	C0	0.071 ^b	± 0.036	0.09	± 0.03	0.97 ^b	± 0.60	0.52 ^b	± 0.03	0.14	± 0.06	5.9 ^b	± 2.4
	C1	0.14	± 0.13	0.39	± 0.25	0.73 ^b	± 0.34	0.46	± 0.10	0.13	± 0.03	5.4 ^b	± 1.0
	C2	0.26	± 0.12	0.30 ^b	± 0.06	2.5	± 1.6	0.35	± 0.15	0.10 ^b	± 0.05	5.1	± 3.4
	C3	0.077 ^b	± 0.067	0.070	± 0.030	1.0 ^b	± 0.7	0.48 ^b	± 0.05	0.10	± 0.04	7.4 ^b	± 2.3
28	C0	0.090 ^b	± 0.030	0.11	± 0.06	1.0 ^b	± 0.3	0.58 ^b	± 0.03	0.21	± 0.04	5.9 ^b	± 1.2
	C1	0.22	± 0.22	0.35	± 0.31	1.4 ^b	± 0.7	0.57	± 0.08	0.24	± 0.10	4.5 ^b	± 1.6
	C2	0.37	± 0.20	0.52 ^b	± 0.19	2.5	± 1.1	0.35 ^a	± 0.02	0.09 ^b	± 0.03	5.6	± 2.5
	C3	3.2 ^b	± 1.0	0.060	± 0.020	3.8	± 3.5	0.44 ^{ab}	± 0.04	0.08	± 0.02	7.6	± 2.0

Figure 7-2 presents the proteins and polysaccharides dosages as well as the β -glucosidase and β -glucosaminidase activity measurements. The data show significant differences in the protein and polysaccharide concentrations between the two photoperiods (see Figure 7-2A and 7-2B).

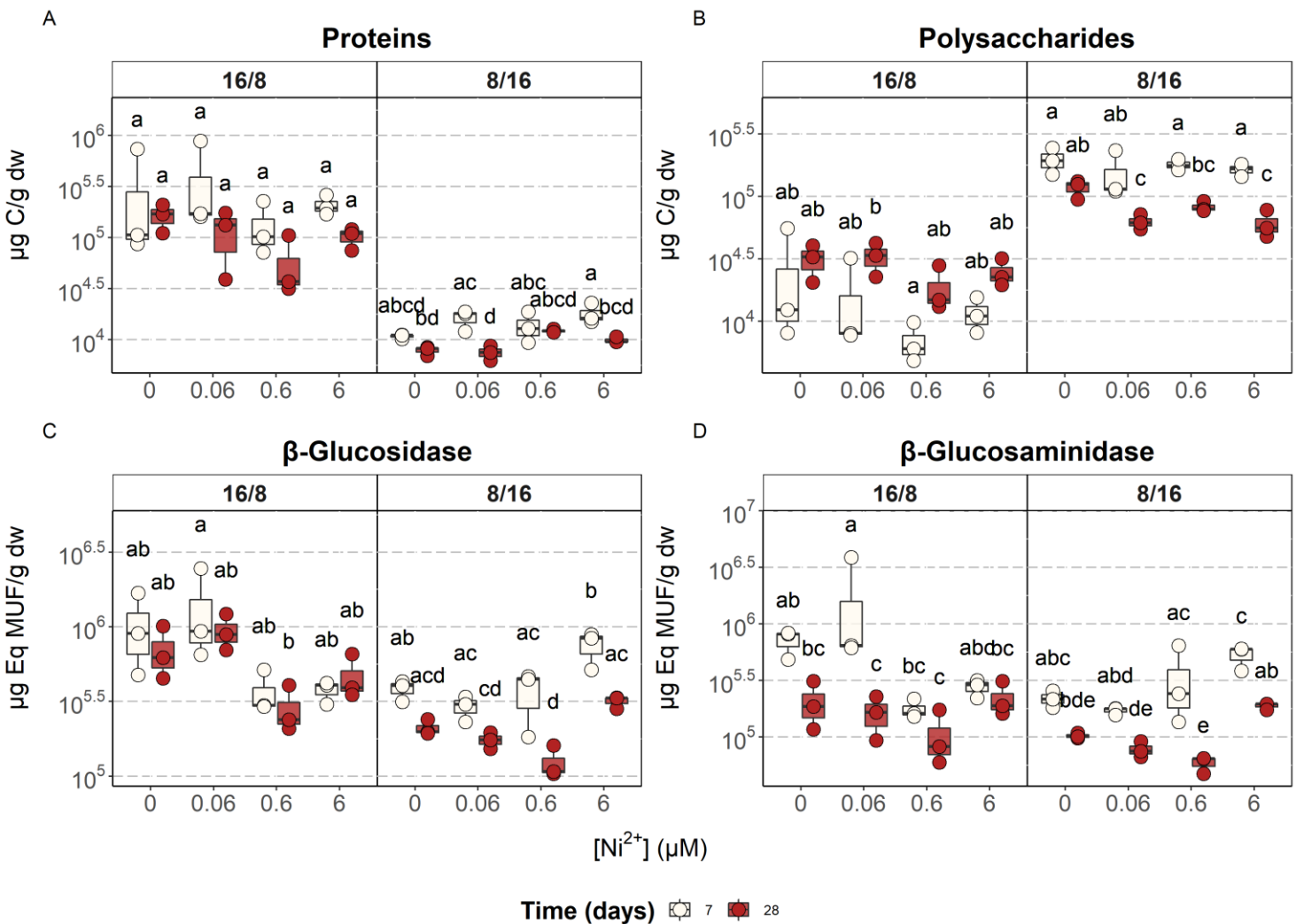


Figure 7-2 : Boxplots of proteins (A), polysaccharides (B), β -glucosidase (C) and β -glucosaminidase (D) measured in biofilms as a function of the average free Ni^{2+} exposure concentration (μM) for the two photoperiods tested (i.e. 16/8 and 8/16 of light/dark cycle) and for the first and last sampling times (days 7 (in white) and 28 (in red); $n = 3$). The letters correspond to the significant differences defined by a post hoc Tukey test ($p < 0.05$) within a given photoperiod. All sampling times are presented in Appendix III (see Figure 13-3).

Indeed, at a given Ni concentration or time the summer biofilm contained around 10 times higher and lower proteins and polysaccharides in comparison to the winter biofilm, respectively. Within a given photoperiod and sampling time, these two descriptors showed no marked effects of Ni exposure in comparison to the control. Only the polysaccharides in the case of the winter photoperiod at day 28 showed differences between the control (C0) and the C1 and C3 conditions. Nevertheless, if clear differences were observed between controls and Ni-exposed biofilms for either photoperiod, polysaccharides tend to increase over time with the summer photoperiod while a decreasing trend is observed in the case of the winter photoperiod.

The extracellular enzymatic activity of β -Glu and Glsm provide information about the effect of chronic Ni exposure on the degradation of organic matter into assimilable nutrients. Indeed, these two enzymes play a role in carbohydrate degradation and in the degradation of peptidoglycans (a component of the bacterial wall) or chitin (a polysaccharide derived from fungal walls), respectively. As shown in Figures 7-2C and 7-2D, none of the enzymatic activities were significantly affected by chronic exposure to Ni in comparison to control. In addition, by comparing the two photoperiods, these two activities did not significantly differ between the control and exposed biofilm in either community. Nevertheless, a decreasing trend over time was observed for the two enzymes, especially in the case of the winter photoperiod. Indeed, significant differences were found between days 7 and 28 notably for biofilms exposed to the highest Ni concentrations (C2 and C3). Interestingly, no differences were observed in the case of the summer photoperiod (except for Glsm in the C1 condition).

7.4.3 Nickel bioaccumulation by biofilms

Significant differences in bioaccumulated Ni were observed between the different sampling times only in the case of the C3 condition ($6 \mu\text{M}$ of Ni^{2+}) for the 8/16 photoperiod (difference between day 7 and other sampling times). Biofilm Ni content is presented in Figure 7-3 without discrimination of the sampling times. Indeed, Ni accumulation was stable over time from the first to the last sampling date in all other cases (see Figure 13-2 in Appendix III for a version presenting the different times).

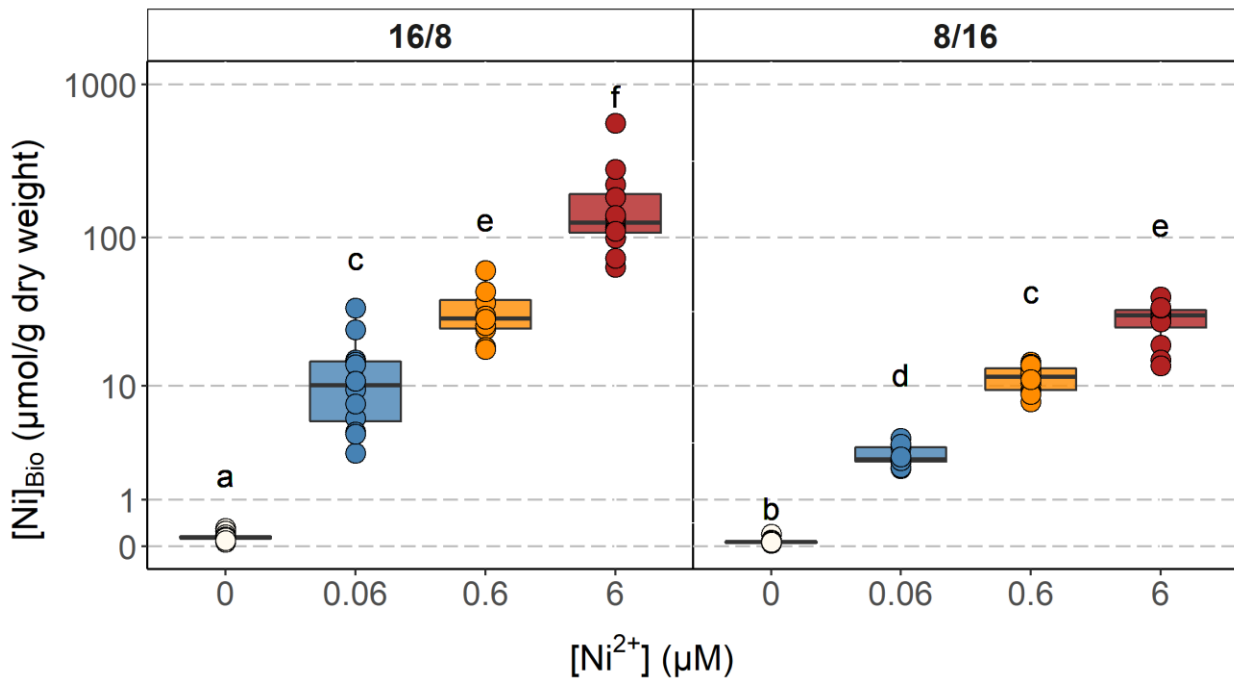


Figure 7-3: Boxplots of Ni accumulation by biofilms ($\mu\text{mol/g dw}$) as a function of the average free Ni^{2+} concentrations of exposure (μM) for the two photoperiods tested (i.e. 16/8 and 8/16 of light/dark cycle) and for all sampling times pooled together (days 7, 14, 21 and 28; $n = 12$). The letters correspond to the significative groups defined by a post hoc Tukey test ($p < 0.05$). See the Figure 13-2 presented in Appendix III for a presentation as a function of the different sampling times (day 7, 14, 21 and 28).

For the two photoperiods, Ni content in the control samples were quantifiable in both studied biofilms but remained low with 0.19 ± 0.09 and $0.09 \pm 0.05 \mu\text{mol/g dw}$ for the summer and winter photoperiod, respectively. In Ni exposed biofilms, bioaccumulation increased with increasing exposure concentrations. Nevertheless, for a given Ni treatment, bioaccumulated Ni in summer biofilms was systematically higher than to the winter biofilms exposed to a photoperiod of 8/16. For instance, at the highest Ni treatment and after 28 days of exposure, Ni accumulation reached average values of 122 ± 16 against $32.2 \pm 3.9 \mu\text{mol/g dw}$ for the summer and winter biofilms, respectively.

7.4.4 Short-term bioassays and tolerance assessment

The results obtained for the tolerance assessment of autotrophic communities using the PSII yield are presented in Figure 7-4 and Table 7-3. First, for the C3 condition, short-term toxicity tests revealed no acute effect of Ni whatever the exposure time and photoperiod considered (see Figure 7-4). This suggests that the autotrophic community developed a tolerance to Ni compared to control communities (C0) and other exposure conditions (*i.e.* C1 and C2). Accordingly, no effect concentration (EC) values were determined. Always considering the C3 condition, PSII values of the sample exposed to $[Ni]_{Tot} = 0 \mu M$ in short-term toxicity tests remained low and statistically different to the control communities (*i.e.* for the condition C0 and $[Ni]_{Tot} = 0 \mu M$ in short-term toxicity tests) whatever the sampling time and photoperiod (see Table 7-3). For instance, after 28 days of exposure, PSII values were 0.38 ± 0.01 and 0.42 ± 0.03 for C0 and 0.20 ± 0.10 and 0.28 ± 0.01 for C3 for the summer and winter biofilms, respectively. Additionally, for the C3 condition, the PSII values of the sample exposed to $[Ni]_{Tot} = 0 \mu M$ in short-term toxicity tests decreased over time in the case of the summer biofilm (PSII values of 0.32 ± 0.01 , 0.27 ± 0.03 , 0.23 ± 0.02 and 0.20 ± 0.10 at days 7, 14, 21, 28) suggesting a chronic effect of Ni as opposed to the results for the winter photoperiod (PSII values of 0.27 ± 0.01 , 0.29 ± 0.01 , 0.31 ± 0.01 and 0.28 ± 0.01 at days 7, 14, 21 and 28 respectively).

Analysis of the dose-response curves of the control condition (C0) showed no clear influence of biofilm characteristics on the sensitivity to acute Ni exposure of control autotrophic communities after 7 days of experiment (Figure 7-4). A difference in Ni sensitivity appears with increasing experiment time (*i.e.* day 7 compare to day 28) in the case of the summer biofilms but not necessarily for the winter one. Indeed, calculated EC_{20s} were statistically different (see Table 7-3) as well as the maximum percentages of inhibition between the two biofilms with $81 \pm 7\%$ and $60 \pm 1\%$ respectively for the summer and winter photoperiod (corresponding to PSII values ranging from 0.39 to 0.32 and 0.43 to 0.25). These percentages of inhibition increased with experiment time for the summer biofilms but not necessarily for the winter biofilms (see Figure 7-4). Indeed, the maximum percentage measured for the winter photoperiod were 60 ± 1 , 63 ± 3 , 53 ± 3 , $58 \pm 3\%$ at 7, 14, 21 and 28 days, respectively. Chronologically and for the summer photoperiod, the maximum percentages follow a decreasing trend over time with 81 ± 7 , 68 ± 9 , 56 ± 3 and $38 \pm 5\%$. Additionally, the dose-response curves obtained for each photoperiod after 28 days differed with statistically lower calculated EC_{20} in the case of the summer biofilms in comparison the winter one (see Table 7-3). These results highlight that seasonal variations influence biofilm response to Ni.

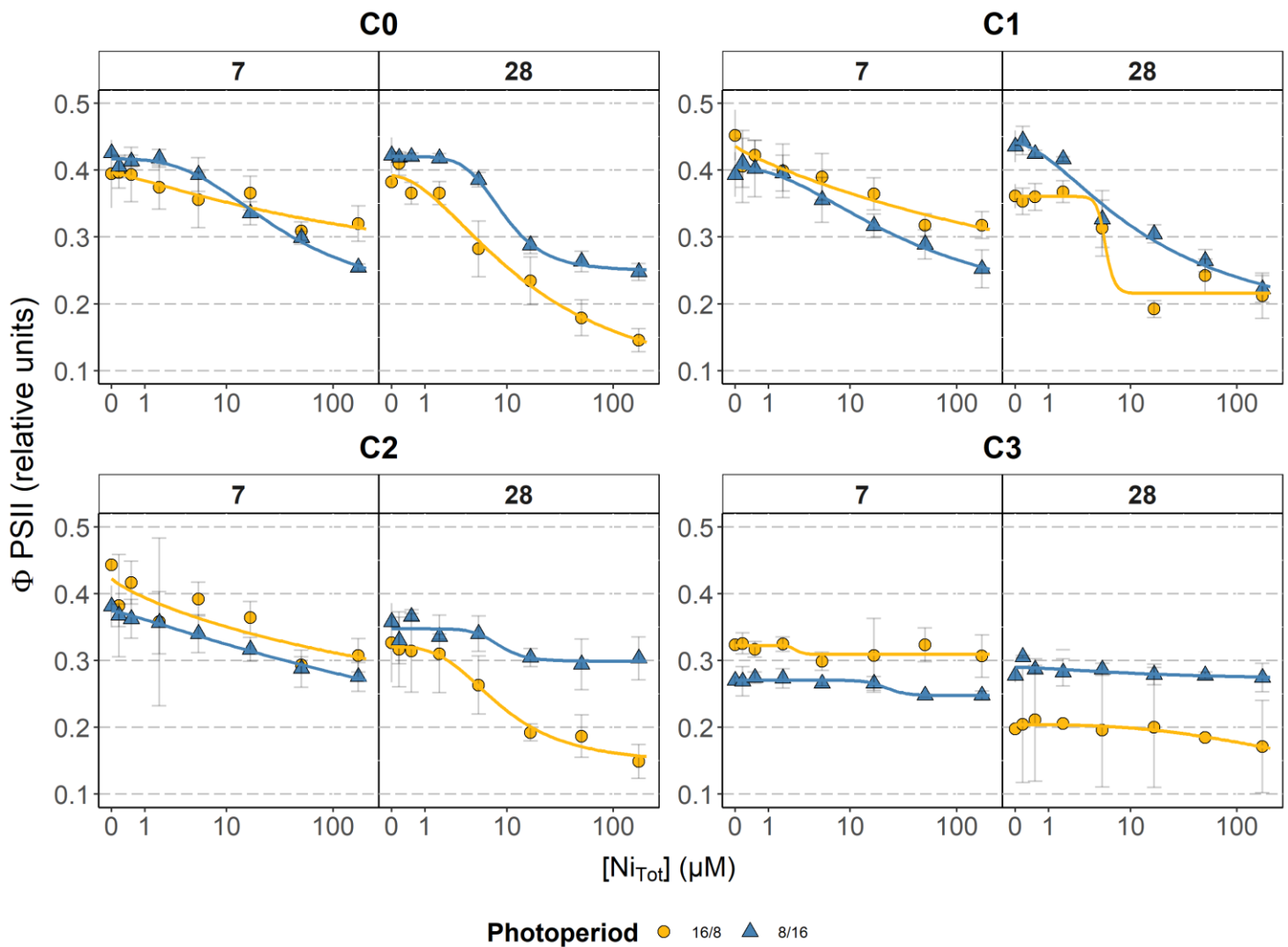


Figure 7-4 : Dose-response curves of the PSII yields in relative units (Φ_{PSII} ; mean \pm SD; n = 3) as a function of the total Ni concentrations (μM) used for the short-term toxicity test after 6 hours of exposure. The figure presents the data after 7 and 14 days of chronic exposure. A version with the four sampling dates is presented in Appendix III (see Figure 13-4). The colors and shapes refer to the photoperiod tested. The titles refer to the long-term exposure conditions: C0 = control (i.e. no Ni); C1 = $[\text{Ni}^{2+}] = 0.06 \mu\text{M}$; C2 = $[\text{Ni}^{2+}] = 0.6 \mu\text{M}$; C3 = $[\text{Ni}^{2+}] = 6 \mu\text{M}$.

Analysis of the dose-response curves of the control condition (C0) showed no clear influence of biofilm characteristics on the sensitivity to acute Ni exposure of control autotrophic communities after 7 days of experiment (Figure 7-4). A difference in Ni sensitivity appears with increasing experiment time (*i.e.* day 7 compare to day 28) in the case of the summer biofilms but not necessarily for the winter one. Indeed, calculated EC_{20s} were statistically different (see Table 7-3) as well as the maximum percentages of inhibition between the two biofilms with 81 ± 7 % and 60 ± 1 % respectively for the summer and winter photoperiod (corresponding to PSII values ranging from 0.39 to 0.32 and 0.43 to 0.25). These percentages of inhibition increased with experiment time for the summer biofilms but not necessarily for the winter biofilms (see Figure 7-4). Indeed, the maximum percentage measured for the winter photoperiod were 60 ± 1, 63 ± 3, 53 ± 3, 58 ± 3 % at 7, 14, 21 and 28 days, respectively. Chronologically and for the summer photoperiod, the maximum percentages follow a decreasing trend over time with 81 ± 7, 68 ± 9, 56 ± 3 and 38 ± 5 %. Additionally, the dose-response curves obtained for each photoperiod after 28 days differed with statistically lower calculated EC₂₀ in the case of the summer biofilms in comparison the winter one (see Table 7-3). These results highlight that seasonal variations influence biofilm response to Ni.

In comparison to control, conditions C1 and C2 show similar results. Indeed, the two photoperiod curves were similar after 7 days of exposure. Nevertheless, the curves obtained after 28 days of exposure differed with an induced short-term toxicity that was systematically more marked in the case of the summer biofilms compared to control biofilms (Figure 7-4). Overall, the results did not always provide significant ECs and the calculated EC_{20s} do not show a clear difference in Ni tolerance acquisition over time. Except for condition C3 which does not show an acute toxicity of Ni, the samples for which a significant EC could be calculated systematically show a lower value in the case of summer biofilm in comparison to the winter one. These results also argue that the two communities from two different seasons showed different responses to a chronic exposure to Ni.

Table 7-3 : Table showing mean PSII yield values ($n = 3$) and calculated EC_{20s} from dose-response curves for each treatment, sampling time and photoperiod. The EC values are expressed as μM of total dissolved Ni. However, Ni was calculated to be present at 94.4% under its free form (Ni^{2+}) in the Dauta medium. The letters a and b respectively refer to the results of Tukey tests performed between (a) the different conditions in comparison to the control (C0) within the same sampling time and photoperiod, and (b) the two photoperiods tested within the same condition and exposure time. N/S = non-significant calculated effective concentrations. N/A = not available due to the absence of any acute effects in the short-term toxicity tests.

Pre-exposure period (in days)	Treatment	Photoperiod 16/8				Photoperiod 8/16			
		Φ_{PSII} (C0)	EC ₂₀ (μM)	Φ_{PSII} (C0)	EC ₂₀ (μM)				
7	C0	0.39 \pm 0.05	N/S	0.43 \pm 0.01	6.6 \pm 1.6				
	C1	0.45 \pm 0.04	N/S	0.39 \pm 0.03	N/S				
	C2	0.44 ^b \pm 0.01	N/S	0.38 ^b \pm 0.03	N/S				
	C3	0.32 ^{ab} \pm 0.01	N/A	0.27 ^{ab} \pm 0.01	N/A				
14	C0	0.37 ^b \pm 0.01	N/S	0.41 ^b \pm 0.03	8.1 \pm 1.7				
	C1	0.40 \pm 0.03	10.3 ^b \pm 3.5	0.41 \pm 0.01	3.6 ^b \pm 1.1				
	C2	0.43 ^{ab} \pm 0.01	2.7 \pm 0.9	0.36 ^{ab} \pm 0.05	N/S				
	C3	0.27 ^{ab} \pm 0.03	N/A	0.29 ^{ab} \pm 0.01	N/A				
21	C0	0.35 \pm 0.03	7.2 ^b \pm 2.7	0.42 \pm 0.002	4.3 ^b \pm 0.9				
	C1	0.39 \pm 0.03	4.6 \pm 1.8	0.40 \pm 0.03	N/S				
	C2	0.43 ^b \pm 0.02	3.2 \pm 0.6	0.31 ^{ab} \pm 0.03	N/S				
	C3	0.23 ^{ab} \pm 0.02	N/A	0.31 ^{ab} \pm 0.01	N/A				
28	C0	0.38 ^b \pm 0.01	2.1 ^b \pm 0.7	0.42 ^b \pm 0.03	4.9 ^b \pm 0.7				
	C1	0.36 ^b \pm 0.02	3.7 \pm 1.5	0.44 ^b \pm 0.02	N/S				
	C2	0.33 ^b \pm 0.06	N/S	0.36 ^b \pm 0.01	N/S				
	C3	0.20 ^{ab} \pm 0.10	N/A	0.28 ^{ab} \pm 0.01	N/A				

7.5 Discussion

7.5.1 Community descriptors under Ni exposure

In this study, biofilms were grown on glass slides in a natural pond and transferred to the laboratory. The biofilms were then placed in the exposure units and left for acclimation for two weeks before the start of the experiments. Several studies have highlighted that the biofilm responses are strongly dependent on the ecosystem characteristics (physical, chemical and biological) of origin which may be highly seasonally dependent (Pesce *et al.*, 2009; Villeneuve *et al.*, 2010; Chaumet *et al.*, 2019). Biomass is known as a robust indicator of the long-term effects on contaminants but it does not allow for the detection of subtle variations (Sabater *et al.*, 2007).

Despite higher biomass values reported for the winter biofilms (in comparison to the summer one), biomass values show no clear trends between Ni treatments. These observations are in agreement with those published by Fechner *et al.* (2011), who exposed biofilms to low (0.09 µM) and high (0.85 µM) dissolved Ni concentrations. The authors showed low variations of both dry weight biomass and Chl-a despite changes in both bacterial and eukaryotic communities. However, our results show that the lowest Chl-a values were obtained at the highest tested Ni concentration ($[Ni^{2+}] = 6 \mu M$) with average values not exceeding 0.1 µg/cm² for both photoperiod (see Table 7-2). Furthermore, the PSII yield follow the same trend with values always statistically lower than the control, indicating a stress. A similar decrease in Chl-a has been previously observed in biofilms exposed to ultraviolet radiation (Navarro *et al.*, 2008) or Cu (Pesce *et al.*, 2018) suggesting a functional cost of tolerance acquisition. Regarding the other exposure conditions (C0, C1 and C2), the Chl-a values increase over time and are globally higher in the summer biofilm than the winter biofilm due to a longer period of light accessibility. Similarly, the maximum percentage of inhibition of the PSII yield increase with exposure time for the summer photoperiod but not necessarily for the winter photoperiod. This could suggest a monoculture effect due to the artificial conditions used for the chronic exposure that may explain the increase in toxicity. Indeed, the acclimatization and exposure of a natural collected biofilm to laboratory conditions are likely to provoke structural/morphological changes and lead to a decrease in species richness. As anticipated, the autotrophic index values are much lower in this photoperiod suggesting a more autotrophic biofilm as opposed to the biofilm exposed with the winter photoperiod which is more heterotrophic.

The results for protein and polysaccharide contents also suggest that the two biofilm communities were structurally and functionally different. Indeed, these two descriptors follow opposing trends between the two photoperiods tested (see Figures 7-2A and 7-2B). Nonetheless, if these descriptors show changes over time, no clear differences were observed over the tested Ni exposure concentrations. Biofilms are typically embedded within a matrix that contains extracellular polymeric substances (EPS), including various compounds including polysaccharides, that have been shown to increase as a response to Cu and Zn exposures (Serra & Guasch, 2009; Corcoll *et al.*, 2012; Loustau *et al.*, 2019). In this work, polysaccharides did not increase with exposure to Ni. These EPS also contain extracellular enzymes, which play a key role in nutrient cycling by degrading organic matter into more assimilable molecules. For instance, β-Glu has been shown to be exclusively located in the EPS fraction (Gil-Allué *et al.*, 2015). Many studies have already highlighted that long-term exposure to metals inhibited the β-Glu activity (Tlili *et al.*, 2010; Lambert *et al.*, 2012; Faburé *et al.*, 2015). We observed no significant differences

between treatments and control in β -Glu activity. Our results are in agreement with another study that indicated that Ni did not have a strong effect on β -Glu activity in comparison to other metals (Fechner *et al.*, 2011).

7.5.2 Bioaccumulation in relation to the studied descriptors

Biofilm Ni content follows the gradient of exposure and less Ni was accumulated in the winter biofilms in comparison to the summer one. Although significant differences in the average exposure concentrations of free Ni (Table 7-1) were observed, it is not sufficient to explain the differences in bioaccumulation obtained between the two photoperiods (Figure 7-3). The accumulation of metals by biofilms is known to be modulated by major cations and protons, in agreement with the Biotic Ligand Model (BLM) principles (Buffle *et al.*, 2009). For instance, H^+ and Mg^{2+} are shown to compete for surface binding sites with Ni with affinity constants that are of the same order of magnitude in *Chlamydomonas reinhardtii* (Worms & Wilkinson, 2007). In addition, similar patterns of competitive effects were found in a field study on the accumulation of Ni or other metals (Cd, Cu, Pb or Zn) in freshwater biofilms (Leguay *et al.*, 2016; Laderriere *et al.*, 2020). Nevertheless, an ionic competition effect cannot explain the differences in bioaccumulation observed in the present study. Indeed, the winter photoperiod had statistically lower Ca and Mg concentrations (free and dissolved) than the summer one (see Table 7-1). If competition had been present, it should have been greater in the case of the summer photoperiod and thus, a lower accumulation would have been observed.

The EPS are known to have negatively charged functional groups that can bind metals (Flemming & Wingender, 2010). Indeed, based on confocal laser scanning microscopy (CLSM) and scanning transmission X-ray microscopy (STXM), several studies have observed that the binding sites for metal contaminants inside the matrix corresponded to the cell surface, capsular material around individual cells, and a layer encompassing the entire community (Hitchcock *et al.*, 2009; Lawrence *et al.*, 2019). Nutrients as well as contaminants must thus diffuse through the matrix before reaching an organism inside biofilm. Because EPS are known to represent up to 90 % of the total dry weight mass (Flemming & Wingender, 2010), these molecules are likely to affect metal diffusion. However, under conditions where equilibrium is quickly established with binding sites, the EPS likely only influence the rate of diffusion to cell surfaces (Torre *et al.*, 2000). Indeed, the rate constants for complex formation with binding sites in the biofilm are generally much larger than biological internalization rate constants (Buffle *et al.*, 2009). In our study, a steady-state in metal uptake was already reached after the first sampling days (*i.e.* after 7 days) and no significant

differences were found with the next sampling dates accordingly to other studies (Xie *et al.*, 2010; Ancion *et al.*, 2010; Lambert *et al.*, 2012). For instance, Ancion *et al.* (2010) exposed biofilms to Zn, Cu and Zn for up to 21 days and obtained similar results. Indeed, the authors showed that a steady-state between metals in water and in biofilm was reached between 7 and 14 days of exposure suggesting a longer process for uptake than simple adsorption which is expected to occur on a very short time scale (<< 1 day; Buffle *et al.*, 2009). Interestingly, the study also showed that the differences in the community composition was correlated to the differences observed in metal content highlighting a link between composition and accumulation of these metals (Ancion *et al.*, 2010; Ancion *et al.*, 2013).

The effect of taxonomic composition on metal accumulation is complex and still relatively little understood. Indeed, whereas some studies report an increase in bioaccumulation (Ancion *et al.*, 2013; Faburé *et al.*, 2015; Dranguet *et al.*, 2017), some report no differences (Xie *et al.*, 2010; Stewart *et al.*, 2015). The levels of uptake and accumulation in algal, bacterial and fungal cells can differ greatly (Malik, 2004). As a consequence, different accumulation levels could be explained by differences in taxonomic composition. Using combined synchrotron X-ray fluorescence imaging (XFI) and scanning transmission X-ray microscopy (STXM), Ni has been shown to be sorbed only on the sheaths of filamentous bacteria, which was also the location where high levels of Mn, Si, Ca and Fe were found (Hitchcock *et al.*, 2009; Hao *et al.*, 2016). This suggests that some species in biofilms could accumulate larger quantities of Ni compared to others. This is supported by Lawrence *et al.* (2019) who found a 4-fold higher accumulation in specific morphologically microcolony than in general biofilms. In other terms, the community composition is likely to influence Ni (or other metals) accumulation because of the presence/absence of specific organisms in biofilm communities. Similar conclusions were reached by Friesen *et al.* (2017) for Se. Starting with the same inoculum, the authors obtained different assemblages of biofilms communities and showed that uptake by the different periphytic biofilms differed significantly. In our study, the calculated autotrophic index clearly shows opposite trends suggesting two different community structures (*i.e.* autotroph during the summer photoperiod and heterotroph for the winter one) and thus, different taxonomic composition. This suggests that the metals accumulated in biofilms vary according to the composition of the biofilm.

7.5.3 Community tolerance acquisition under Ni exposure

The modifications of the dry weight biomass, Chl-a concentrations or autotrophic index globally reflect the effects of metal exposure, they do not provide information about biofilm

tolerance acquisition. PICT analysis was performed on autotrophic communities using the PSII yield. It is now well known that environmental factors such as temperature have an effect on microbial communities (e.g. shift in assemblage composition; Villeneuve *et al.*, 2011) and that these changes could modify the basal tolerance of phototrophic biofilm communities exposed to acute metal exposure (Serra *et al.*, 2010; Lambert *et al.*, 2017; Morin *et al.*, 2017). For instance, Faburé *et al.* (2015) suggest that seasonal variability of physicochemical and biological parameters (dependent on seasonal successions) can strongly influence tolerance measurements. Indeed, sharp variations in temperature could lead to the replacement of species that are less temperature-sensitive but with relatively similar metal sensitivity (Pesce *et al.*, 2018). In other terms, the basal tolerance of phototrophic biofilm communities to metals could be conditioned by the initial intrinsic characteristics of the community.

Although autotrophic and heterotrophic organisms were not identified in this study, the different descriptors measured (*i.e.* Chl-a, autotrophic index, PSII yield, β -Glu and Glsm) provided some information on the activity of the autotrophic and heterotrophic component of the biofilm. Based on these results, we can assume that the two communities were different. This could explain the lower toxicity observed in the short-term toxicity test with the winter photoperiod. Indeed, although the calculated EC_{20s} are not lower in the case of this photoperiod, the slope of the dose-response curves suggests less inhibition with increasing Ni concentrations compared to the control. While the resuspension of biofilms in the acute toxicity tests may have led to the presence of cell exudates, these are not expected to change the speciation of Ni. Indeed, Ni concentrations are relatively high and the biomass was resuspended in fresh Dauta medium. Nevertheless, another interesting point is that the biofilm exposed using the winter photoperiod also accumulated less for the same Ni exposure level in comparison to the summer one. A high intracellular metal content increases the probability that the cells antioxidant defences will be surpassed due to a high production of reactive oxygen species. Regarding the PSII yield, high intracellular concentrations could inhibit the photosynthesis reaction by blocking electron transfer, and consequently stop oxygen release and CO₂ fixation (Serra *et al.*, 2009). For instance, Bonet *et al.* (2012) have shown that Zn exposure concentrations and Zn content in biofilms were positively correlated to antioxidant enzymatic activities such as catalase (CAT), an enzyme implied in the transformation of reactive into non-reactive species.

Based on these results, only the communities exposed to the highest Ni concentration appeared to be more Ni-tolerant than those exposed to lower concentrations. Nevertheless, the low Chl-a and PSII yield observed for that high exposure condition are probably to be linked to a

functional cost of acclimation. Moreover, despite the fact that the summer community of the intermediate C2 condition did not appear to be more tolerant than the control, the winter community showed only slight inhibition even after 28 days. This suggests that the exposure concentration used for this condition ($[Ni^{2+}] \approx 0.6 \mu M$) has led to an acquisition of tolerance for this community. This is in agreement with studies that highlighted that seasons and taxonomic composition of biofilms play a role in the basal tolerance of autotrophic organisms to acute exposure to metals, thus decreasing their vulnerability toward this toxic stress (Faburé *et al.*, 2015; Morin *et al.*, 2017). Although Ni was toxic to autotrophs in the present study, this metal is not redox active and did not specifically impair photosynthesis compared to Cu, which is a well-known inhibitor of the PSII-photosystem (Serra *et al.*, 2009; Lambert *et al.*, 2017). Thus, one could argue that it might be more difficult to detect tolerance acquisition to a metal like Ni using photosynthesis as an endpoint in toxicity tests. Heterotrophic organisms have been shown to be impacted by Ni as indicated by the β -Glu activity (Fechner *et al.*, 2011). Based on this enzyme, the authors showed an increase in calculated EC₅₀ (and thus a better tolerance) after 3 weeks of exposure to 0.85 μM of dissolved Ni (but not for the low treatment of 0.09 μM). However, among the metals studied (Cd, Ni and Zn), Ni was shown to have the lowest reported toxicity with maximal inhibition levels of 68, 62 and 63 % respectively for the control, the low and the high exposure concentrations. The relative inhibition thus remained similar among the different Ni exposure conditions.

Metal sensitivity of phototrophic as well as heterotrophic microbial communities can vary greatly and may be poorly or effectively captured by the selected endpoint (Tlili *et al.*, 2010; Pesce *et al.*, 2018). Thus, using an approach considering different biological endpoints (*i.e.* photosynthesis, enzymatic activities, peptide synthesis, etc) related to the different functional compartments of biofilms (*i.e.* phototrophic and heterotrophic) is recommended.

7.6 Conclusion

In summary, this study is consistent with previous reports that have already shown that life history of freshwater biofilms in natural environments affects the response to metals. Taken together, our results suggests that the biofilm response following four Ni treatments was mainly conditioned by the initial properties of the algal compartment and also probably community composition. Indeed, based on the different descriptors used in this study, the two communities were different and showed different toxicity and accumulation responses for a same Ni concentration. More specifically, the winter biofilm was characterized by less Ni effects than the

summer one suggesting that responses of natural microbial communities to Ni exposure (and probably to other metals) can be seasonally dependent. In other terms metal accumulation by biofilms is influenced by a variety of parameters, such as the metal and its speciation, physico-chemical characteristic of the medium and biofilm composition. Taxonomic and/or genetic analysis could be useful to better understand the relation between metal accumulation capacities of periphytic biofilms and their effects. Furthermore, our results show that a concentration of 6 µM of Ni²⁺ (equivalent to 20 µM of dissolved Ni in our medium) is sufficient to induce tolerance acquisition (based on PSII yield) of the two communities studied. In order to allow extrapolation of laboratory data to the complex environment, an approach considering taxonomic composition, different physiological functions (such as photosynthesis and β-Glu activity) as well as the metal speciation in the medium may allow to better assess and predict the risks of metals (and not only Ni) for aquatic ecosystems.

7.7 Acknowledgments

We acknowledge the valuable assistance of Gwilherm Jan and Brigitte Delest for the help during the processing of the experiments and for the chemical analyses of water and biofilm samples. We also thank Séverine Le Faucher for logistical assistance and editing. This work was supported by the Natural Sciences and Engineering Research Council (NSERC) Discovery Grant RGPIN-2019-06823 and the Canada Research Chair program 950-231107.

8 BIBLIOGRAPHIE 3^E ARTICLE

- Ancion, P.Y., Lear, G., Dopheide, A., Lewis, G.D., 2013. Metal concentrations in stream biofilm and sediments and their potential to explain biofilm microbial community structure. *Environ. Pollut.* 173, 117–124. <https://doi.org/10.1016/j.envpol.2012.10.012>
- Ancion, P.Y., Lear, G., Lewis, G.D., 2010. Three common metal contaminants of urban runoff (Zn, Cu & Pb) accumulate in freshwater biofilm and modify embedded bacterial communities. *Environ. Pollut.* 158, 2738–2745. <https://doi.org/10.1016/j.envpol.2010.04.013>
- Battin, T.J., Besemer, K., Bengtsson, M.M., Romani, A.M., Packmann, A.I., 2016. The ecology and biogeochemistry of stream biofilms. *Nat. Rev. Microbiol.* 14, 251–263. <https://doi.org/10.1038/nrmicro.2016.15>
- Blanck, H., Wängberg, S., Molander, S., 1988. Pollution-Induced Community Tolerance — A new ecotoxicological tool, eds J. Cai. ed, *Functional Testing of Aquatic Biota for Estimating Hazards of Chemicals*. <https://doi.org/10.1520/STP26265S>
- Bonet, B., Corcoll, N., Guasch, H., 2012. Antioxidant enzyme activities as biomarkers of Zn pollution in fluvial biofilms. *Ecotoxicol. Environ. Saf.* 80, 172–178. <https://doi.org/10.1016/j.ecoenv.2012.02.024>
- Bonnineau, C., Artigas, J., Chaumet, B., Dabrin, A., Faburé, J., Ferrari, B.J.D., Lebrun, J.D., Margoum, C., Mazzella, N., Miège, C., Morin, S., Uher, E., Babut, M., Pesce, S., 2020. Role of biofilms in contaminant bioaccumulation and trophic transfer in aquatic ecosystems: current state of knowledge and future challenges. *Rev. Environ. Contam. Toxicol.* 253, 115–153. https://doi.org/10.1007/398_2019_39
- Bradford, M.M., 1976. A rapid and sensitive method for the quantitation of microgram quantities of protein utilizing the principle of protein-dye binding. *Anal. Biochem.* 72, 248–254. <https://doi.org/10.1016/j.cj.2017.04.003>
- Buffel, J., Wilkinson, K.J., Van Leeuwen, H.P., 2009. Chemodynamics and bioavailability in natural waters. *Environ. Sci. Technol.* 43, 7170–7174. <https://doi.org/10.1021/es9013695>
- Chaumet, B., Morin, S., Hourtané, O., Artigas, J., Delest, B., Eon, M., Mazzella, N., 2019. Flow conditions influence diuron toxicokinetics and toxicodynamics in freshwater biofilms. *Sci. Total Environ.* 652, 1242–1251. <https://doi.org/10.1016/j.scitotenv.2018.10.265>
- Cheloni, G., Gagnaux, V., Slaveykova, V.I., 2019. Species-species interactions modulate copper

- toxicity under different visible light conditions. *Ecotoxicol. Environ. Saf.* 170, 771–777. <https://doi.org/10.1016/j.ecoenv.2018.12.039>
- Cheloni, G., Slaveykova, V.I., 2018. Combined effects of trace metals and light on photosynthetic microorganisms in aquatic environment. *Environments* 5, 1–19. <https://doi.org/10.3390/environments5070081>
- Corcoll, N., Bonet, B., Leira, M., Guasch, H., 2011. Chl-a fluorescence parameters as biomarkers of metal toxicity in fluvial biofilms: An experimental study. *Hydrobiologia* 673, 119–136. <https://doi.org/10.1007/s10750-011-0763-8>
- Corcoll, N., Bonet, B., Leira, M., Montuelle, B., Tlili, A., Guasch, H., 2012. Light history influences the response of fluvial biofilms to Zn exposure. *J. Phycol.* 48, 1411–1423. <https://doi.org/10.1111/j.1529-8817.2012.01223.x>
- Dranguet, P., Slaveykova, V.I., Le Faucheur, S., 2017. Kinetics of mercury accumulation by freshwater biofilms. *Environ. Chem.* 14, 458–467. <https://doi.org/10.1071/EN17073>
- Dubois, M., Gilles, K.A., Hamilton, J.K., Rebers, P.A., Smith, F., 1956. Colorimetric method for determination of sugars and related substances. *Anal. Chem.* 28, 350–356. <https://doi.org/10.1021/ac60111a017>
- Faburé, J., Dufour, M., Autret, A., Uher, E., Fechner, L.C., 2015. Impact of an urban multi-metal contamination gradient: Metal bioaccumulation and tolerance of river biofilms collected in different seasons. *Aquat. Toxicol.* 159, 276–289. <https://doi.org/10.1016/j.aquatox.2014.12.014>
- Fechner, L.C., Gourlay-Francé, C., Tusseau-Vuillemin, M.H., 2011. Low exposure levels of urban metals induce heterotrophic community tolerance: A microcosm validation. *Ecotoxicology* 20, 793–802. <https://doi.org/10.1007/s10646-011-0630-4>
- Fernandes, G., Bastos, M.C., de Vargas, J.P.R., Le Guet, T., Clasen, B., dos Santos, D.R., 2020. The use of epilithic biofilms as bioaccumulators of pesticides and pharmaceuticals in aquatic environments. *Ecotoxicology* 29, 1293–1305. <https://doi.org/10.1007/s10646-020-02259-4>
- Flemming, H.C., Wingender, J., 2010. The biofilm matrix. *Nat. Rev. Microbiol.* 8, 623–633. <https://doi.org/10.1038/nrmicro2415>
- Friesen, V., Doig, L.E., Markwart, B.E., Haakensen, M., Tissier, E., Liber, K., 2017. Genetic characterization of periphyton communities associated with selenium bioconcentration and trophic transfer in a simple food chain. *Environ. Sci. Technol.* 51, 7532–7541.

<https://doi.org/10.1021/acs.est.7b01001>

Gil-Allué, C., Schirmer, K., Tlili, A., Gessner, M.O., Behra, R., 2015. Silver nanoparticle effects on stream periphyton during short-term exposures. *Environ. Sci. Technol.* 49, 1165–1172. <https://doi.org/10.1021/es5050166>

Gillmore, M.L., Golding, L.A., Chariton, A.A., Stauber, J.L., Stephenson, S., Gissi, F., Greenfield, P., Juillet, F., Jolley, D.F., 2021. Metabarcoding reveals changes in benthic eukaryote and prokaryote community composition along a tropical marine sediment nickel gradient. *Environ. Toxicol. Chem.* 40, 1892–1805. <https://doi.org/10.1002/etc.5039>

Gissi, F., Stauber, J.L., Binet, M.T., Golding, L.A., Adams, M.S., Schlekat, C.E., Garman, E.R., Jolley, D.F., 2016. A review of nickel toxicity to marine and estuarine tropical biota with particular reference to the South East Asian and Melanesian region. *Environ. Pollut.* 218, 1308–1323. <https://doi.org/10.1016/j.envpol.2016.08.089>

Guasch, H., Artigas, J., Bonet, B., Bonnneau, C., Canals, O., Corcoll, N., 2016. The use of biofilms to assess the effects of chemicals on freshwater ecosystems, in: Romaní, A.M., Guasch, H., Balaguer, M.D. (Eds.), In *Aquatic Biofilms: Ecology, Water Quality and Wastewater Treatment*. Caister Academic Press, Spain, pp. 125–144. <https://doi.org/10.21775/9781910190173.06>

Guasch, H., Ginebreda, A., Geiszinger, A., 2012. Emerging and priority pollutants in river, In Handboo. ed, The Handbook of Environmental Chemistry. Springer. [https://doi.org/10.1016/0143-1471\(82\)90111-8](https://doi.org/10.1016/0143-1471(82)90111-8)

Hao, L., Guo, Y., Byrne, J.M., Zeitvogel, F., Schmid, G., Ingino, P., Li, J., Neu, T.R., Swanner, E.D., Kappler, A., Obst, M., 2016. Binding of heavy metal ions in aggregates of microbial cells, EPS and biogenic iron minerals measured in-situ using metal- and glycoconjugates-specific fluorophores. *Geochim. Cosmochim. Acta* 180, 66–96. <https://doi.org/10.1016/j.gca.2016.02.016>

Hitchcock, A.P., Dynes, J.J., Lawrence, J.R., Obst, M., Swerhone, G.D.W., 2009. Soft X-ray spectromicroscopy of nickel sorption in a natural river biofilm. *Geobiology* 7, 432–453. <https://doi.org/10.1111/j.1472-4669.2009.00211.x>

Hobbs, W.O., Collyard, S.A., Larson, C., Carey, A.J., O'Neill, S.M., 2019. Toxic burdens of freshwater biofilms and use as a source tracking tool in rivers and streams. *Environ. Sci. Technol.* 53, 11102–11111. <https://doi.org/10.1021/acs.est.9b02865>

- Laderriere, V., Le Faucheur, S., Fortin, C., 2021. Exploring the role of water chemistry on metal accumulation in biofilms from streams in mining areas. *Sci. Total Environ.* 784, 146986. <https://doi.org/10.1016/j.scitotenv.2021.146986>
- Laderriere, V., Paris, L.E., Fortin, C., 2020. Proton competition and free ion activities drive cadmium, copper, and nickel accumulation in river biofilms in a nordic ecosystem. *Environments* 7, 1–13. <https://doi.org/10.3390/environments7120112>
- Lambert, A., Morin, S., Artigas, J., Volat, B., Coquery, M., Neyra, M., Pesce, S., 2012. Structural and functional recovery of microbial biofilms after a decrease in copper exposure : Influence of the presence of pristine communities. *Aquat. Toxicol.* 109, 118–126. <https://doi.org/10.1016/j.aquatox.2011.12.006>
- Lambert, A.S., Dabrin, A., Foulquier, A., Morin, S., Rosy, C., Coquery, M., Pesce, S., 2017. Influence of temperature in pollution-induced community tolerance approaches used to assess effects of copper on freshwater phototrophic periphyton. *Sci. Total Environ.* 607–608, 1018–1025. <https://doi.org/10.1016/j.scitotenv.2017.07.035>
- Lambert, A.S., Dabrin, A., Morin, S., Gahou, J., Foulquier, A., Coquery, M., Pesce, S., 2016. Temperature modulates phototrophic periphyton response to chronic copper exposure. *Environ. Pollut.* 208, 821–829. <https://doi.org/10.1016/j.envpol.2015.11.004>
- Lavoie, I., Lavoie, M., Fortin, C., 2012. A mine of information: Benthic algal communities as biomonitoring of metal contamination from abandoned tailings. *Sci. Total Environ.* 425, 231–241. <https://doi.org/10.1016/j.scitotenv.2012.02.057>
- Lawrence, J.R., Swerhone, G.D.W., Neu, T.R., 2019. Visualization of the sorption of nickel within exopolymer microdomains of bacterial microcolonies using confocal and scanning electron microscopy. *Microbes Environ.* 34, 76–82. <https://doi.org/10.1264/jsme2.ME18134>
- Leguay, S., Lavoie, I., Levy, J.L., Fortin, C., 2016. Using biofilms for monitoring metal contamination in lotic ecosystems: The protective effects of hardness and pH on metal bioaccumulation. *Environ. Toxicol. Chem.* 35, 1489–1501. <https://doi.org/10.1002/etc.3292>
- Loustau, E., Ferriol, J., Koteiche, S., Gerlin, L., Leflaive, J., Moulin, F., 2019. Physiological responses of three mono-species phototrophic biofilms exposed to copper and zinc. *Environ. Sci. Pollut. Res.* 26, 35107–35120. <https://doi.org/10.1007/s11356-019-06560-6>
- Malik, A., 2004. Metal bioremediation through growing cells. *Environ. Int.* 30, 261–278. <https://doi.org/10.1016/j.envint.2003.08.001>

- Mebane, C.A., Schmidt, T.S., Miller, J.L., Balistrieri, L.S., 2020. Bioaccumulation and toxicity of cadmium, copper, nickel, and zinc and their mixtures to aquatic insect communities. Environ. Toxicol. Chem. 39, 812–833. <https://doi.org/10.1002/etc.4663>
- Morin, S., Cordonier, A., Lavoie, I., Arini, A., Blanco, S., Duong, T.T., Tornés, E., Bonet, B., Corcoll, N., Faggiano, L., Laviale, M., Pérès, F., Becares, E., Coste, M., Feurter-Mazel, A., Fortin, C., Guasch, H., Sabater, S., 2012. Consistency in diatom response to metal-contaminated environments, in: Guasch, H, Ginebreda, A., Geiszinger, A. (Eds.), Emerging and Priority Pollutants in Rivers. Springer-Verlag Berlin Heidelberg, pp. 117–146. https://doi.org/10.1007/978-3-642-25722-3_5
- Morin, S., Lambert, A.S., Rodriguez, E.P., Dabrin, A., Coquery, M., Pesce, S., 2017. Changes in copper toxicity towards diatom communities with experimental warming. J. Hazard. Mater. 334, 223–232. <https://doi.org/10.1016/j.jhazmat.2017.04.016>
- Navarro, E., Robinson, C.T., Behra, R., 2008. Increased tolerance to ultraviolet radiation (UVR) and cotolerance to cadmium in UVR-acclimatized freshwater periphyton. Limnol. Oceanogr. 53, 1149–1158. <https://doi.org/10.4319/lo.2008.53.3.1149>
- Perdue, E.M., Ritchie, J.D., 2003. Dissolved organic matter in freshwaters, in: Heinrich D.H., Turekian, K.K. (Eds.), Treatise on Geochemistry. Elsevier, pp. 273–318. <https://doi.org/10.1016/B0-08-043751-6/05080-5>
- Pesce, S., Batisson, I., Bardot, C., Portelli, C., Montuelle, B., Bohatier, J., 2009. Response of spring and summer riverine microbial communities following glyphosate exposure. Ecotoxicol. Environ. Saf. 72, 1905–1912. <https://doi.org/10.1016/j.ecoenv.2009.07.004>
- Pesce, S., Lambert, A.-S., Morin, S., Foulquier, A., Coquery, M., Dabrin, A., 2018. Experimental warming differentially influences the vulnerability of phototrophic and heterotrophic periphytic communities to copper toxicity. Front. Microbiol. 9, 1424. <https://doi.org/10.3389/fmicb.2018.01424>
- Reid, A.J., Carlson, A.K., Creed, I.F., Eliason, E.J., Gell, P.A., Johnson, P.T.J., Kidd, K.A., MacCormack, T.J., Olden, J.D., Ormerod, S.J., Smol, J.P., Taylor, W.W., Tockner, K., Vermaire, J.C., Dudgeon, D., Cooke, S.J., 2019. Emerging threats and persistent conservation challenges for freshwater biodiversity. Biol. Rev. 94, 849–873. <https://doi.org/10.1111/brv.12480>
- Romaní, A.M., Fund, K., Artigas, J., Schwartz, T., Sabater, S., Obst, U., 2008. Relevance of

- polymeric matrix enzymes during biofilm formation. *Microb. Ecol.* 56, 427–436. <https://doi.org/10.1007/s00248-007-9361-8>
- Sabater, S., Guasch, H., Ricart, M., Romaní, A., Vidal, G., Klünder, C., Schmitt-Jansen, M., 2007. Monitoring the effect of chemicals on biological communities. The biofilm as an interface. *Anal. Bioanal. Chem.* 387, 1425–1434. <https://doi.org/10.1007/s00216-006-1051-8>
- Serra, A., Corcoll, N., Guasch, H., 2009. Copper accumulation and toxicity in fluvial periphyton: The influence of exposure history. *Chemosphere* 74, 633–641. <https://doi.org/10.1016/j.chemosphere.2008.10.036>
- Serra, A., Guasch, H., 2009. Effects of chronic copper exposure on fluvial systems: Linking structural and physiological changes of fluvial biofilms with the in-stream copper retention. *Sci. Total Environ.* 407, 5274–5282. <https://doi.org/10.1016/j.scitotenv.2009.06.008>
- Serra, A., Guasch, H., Admiraal, W., Van Der Geest, H.G., Van Beusekom, S.A.M., 2010. Influence of phosphorus on copper sensitivity of fluvial periphyton: The role of chemical, physiological and community-related factors. *Ecotoxicology* 19, 770–780. <https://doi.org/10.1007/s10646-009-0454-7>
- Stewart, T.J., Behra, R., Sigg, L., 2015. Impact of chronic lead exposure on metal distribution and biological effects to periphyton. *Environ. Sci. Technol.* 49, 5044–5051. <https://doi.org/10.1021/es505289b>
- Tlili, A., Berard, A., Blanck, H., Bouchez, A., Cássio, F., Eriksson, K.M., Morin, S., Montuelle, B., Navarro, E., Pascoal, C., Pesce, S., Schmitt-Jansen, M., Behra, R., 2016. Pollution-induced community tolerance (PICT): towards an ecologically relevant risk assessment of chemicals in aquatic systems. *Freshw. Biol.* 61, 2141–2151. <https://doi.org/10.1111/fwb.12558>
- Tlili, A., Bérard, A., Roulier, J.L., Volat, B., Montuelle, B., 2010. PO43- dependence of the tolerance of autotrophic and heterotrophic biofilm communities to copper and diuron. *Aquat. Toxicol.* 98, 165–177. <https://doi.org/10.1016/j.aquatox.2010.02.008>
- Tlili, A., Maréchal, M., Bérard, A., Volat, B., Montuelle, B., 2011. Enhanced co-tolerance and co-sensitivity from long-term metal exposures of heterotrophic and autotrophic components of fluvial biofilms. *Sci. Total Environ.* 409, 4335–4343. <https://doi.org/10.1016/j.scitotenv.2011.07.026>
- Torre, M.C.A., Beaulieu, P., Tessier, A., 2000. In situ measurement of trace metals in lakewater using the dialysis and DGT techniques. *Anal. Chim. Acta* 418, 53–68.

[https://doi.org/10.1016/S0003-2670\(00\)00946-6](https://doi.org/10.1016/S0003-2670(00)00946-6)

U.S. Geological Survey, 2021. Mineral commodity summaries 2021: U.S. Geological Survey. Reston, VA. <https://doi.org/10.3133/mcs2021>

Vendrell-Puigmitja, L., Abril, M., Proia, L., Espinosa Angona, C., Ricart, M., Oatley-Radcliffe, D.L., Williams, P.M., Zanain, M., Llenas, L., 2020. Assessing the effects of metal mining effluents on freshwater ecosystems using biofilm as an ecological indicator: Comparison between nanofiltration and nanofiltration with electrocoagulation treatment technologies. *Ecol. Indic.* 113. <https://doi.org/10.1016/j.ecolind.2020.106213>

Villeneuve, A., Bouchez, A., Montuelle, B., 2011. In situ interactions between the effects of season, current velocity and pollution on a river biofilm. *Freshw. Biol.* 56, 2245–2259. <https://doi.org/10.1111/j.1365-2427.2011.02649.x>

Villeneuve, A., Montuelle, B., Bouchez, A., 2010. Influence of slight differences in environmental conditions (light, hydrodynamics) on the structure and function of periphyton. *Aquat. Sci.* 72, 33–44. <https://doi.org/10.1007/s00027-009-0108-0>

Weber, L.P., Dubé, M.G., Rickwood, C.J., Driedger, K., Portt, C., Brereton, C., Janz, D.M., 2008. Effects of multiple effluents on resident fish from Junction Creek, Sudbury, Ontario. *Ecotoxicol. Environ. Saf.* 70, 433–445. <https://doi.org/10.1016/j.ecoenv.2007.08.001>

Worms, I.A.M., Wilkinson, K.J., 2007. Ni uptake by a green alga. 2. Validation of equilibrium models for competition effects. *Environ. Sci. Technol.* 41, 4264–4270. <https://doi.org/10.1021/es0630341>

Xie, L., Funk, D.H., Buchwalter, D.B., 2010. Trophic transfer of Cd from natural periphyton to the grazing mayfly *Centroptilum triangulifer* in a life cycle test. *Environ. Pollut.* 158, 272–277. <https://doi.org/10.1016/j.envpol.2009.07.010>

9 DISCUSSION GÉNÉRALE ET CONCLUSION

L'ensemble de ces travaux de thèse a permis de mieux caractériser les liens existants entre conditions environnementales (température et photopériode), exposition aux métaux et accumulation par les biofilms périphytiques d'eau douce. Les différents chapitres ont participé à l'acquisition de nouvelles connaissances en vue de l'utilisation des biofilms dans une perspective de biosuivi.

La thèse s'est articulée autour de trois axes principaux :

- Identifier, selon les hypothèses du modèle du ligand biotique, les paramètres physico-chimiques clés (pH, alcalinité, concentrations en métaux) qui régissent la bioaccumulation des métaux par les biofilms d'eau douce.
- Investiguer l'effet de variables environnementales (température et photopériode) sur la bioaccumulation du Ni par les biofilms d'eau douce selon un gradient de concentrations d'exposition.
- Raisonner à l'échelle de la communauté : mettre en lien l'accumulation du Ni, l'acquisition de tolérance et la composition du biofilm (c.à.d. autotrophe vs hétérotrophe).

9.1 Approche de terrain

Ce premier chapitre fait suite aux travaux de Lavoie *et al.* (2012) ainsi que de Leguay *et al.* (2016) dans les régions de l'Estrie, de la Mauricie et de l'Abitibi au Québec. En effet, ces études ont démontré une forte corrélation entre les quantités de métaux accumulés dans le biofilm et les concentrations en ions libres métalliques dans les eaux de surface (modélisées avec le logiciel *WHAM7*). Le premier chapitre de cette thèse s'intéressait donc à tester cette relation à une plus large échelle géographique et plus précisément, dans deux écosystèmes différents présentant des activités minières importantes : la ville de Sudbury dans le sud de l'Ontario et le nord du Nunavik (le site minier étudié se situe à environ 90 km à l'ouest du village inuit de Kangiqsuuaq). À ce jour, l'article découlant de ce premier chapitre est l'une des premières études démontrant des tendances similaires dans l'accumulation des métaux dans le biofilm à si large échelle géographique (distance d'environ 1700 km entre les sites). De plus, cette étude est l'une des premières s'opérant dans une région nordique. Une deuxième partie de ce chapitre a examiné l'influence des paramètres physico-chimiques clés jouant un rôle dans l'internalisation des métaux par le biofilm. L'idée sous-jacente était d'appliquer le modèle du ligand biotique (BLM)

aux biofilms naturels au moyen d'un jeu de données conséquent. De plus, cette thèse s'est particulièrement intéressée au Ni, un métal moins souvent étudié que d'autres métaux divalents tels que le Cu, le Pb, le Zn ou le Cd.

Les résultats ont indiqué que plus la concentration en métaux dissous (Ni, Cu et Cd) dans l'eau augmente (totale ou libre) et plus la concentration en métaux internalisés par le biofilm augmente, et ce, quel que soit le site ou le moment de prélèvement. Dans ce chapitre, l'attention s'est portée sur la proportion de métal libre plutôt que totale, en se basant sur les hypothèses du modèle du ligand biotique (BLM) qui stipulent que la forme ionique libre est représentative de la biodisponibilité des métaux (Campbell, 1995). Les résultats acquis sont venus conforter ceux préalablement obtenus et ont permis de mettre en évidence l'importance de certaines variables physico-chimiques inhérentes à chaque site d'étude sur cette corrélation (Leguay *et al.* 2016; Laderriere *et al.* 2020). En effet, une relation linéaire entre métaux libres dans l'eau et métaux accumulés dans le biofilm ainsi qu'une bonne concordance entre les différentes études ont été mises en évidence (Figure 9-1). De plus, les valeurs de bioaccumulation sont comparables entre les biofilms issus de rivières aux caractéristiques différentes et sont concordantes dans le temps pour les sites échantillonnés plusieurs fois. Les quantités internalisées par le biofilm sont cohérentes avec les concentrations en métal libre en solution, et ce, pour tous les sites étudiés (contaminés ou non).

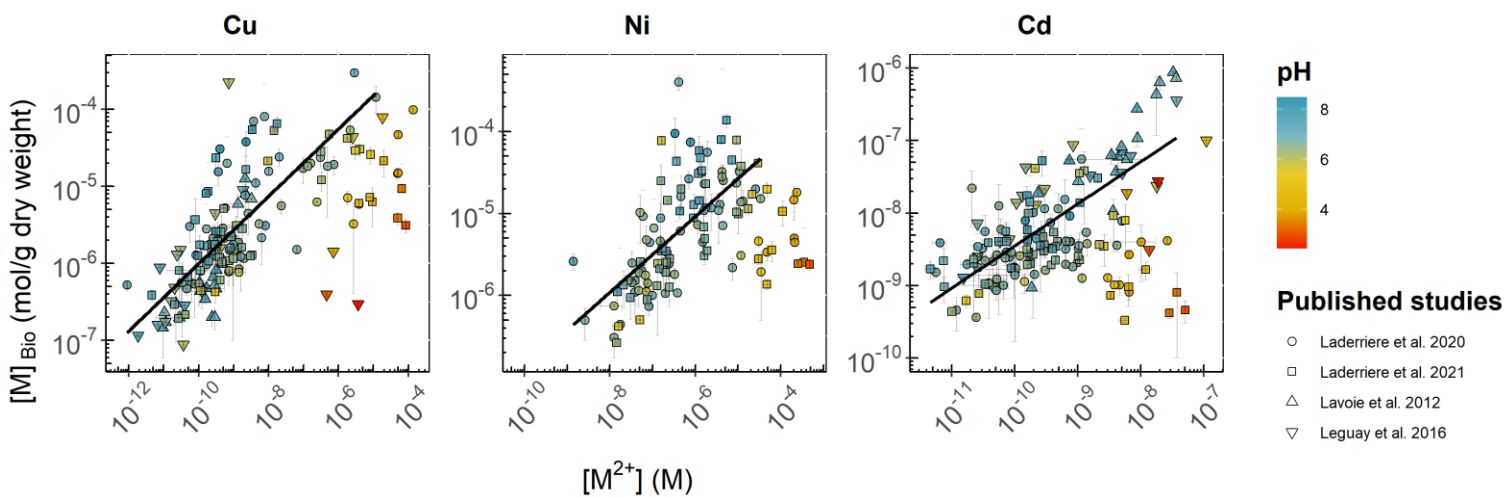


Figure 9-1 : Quantités de métaux bioaccumulés par le biofilm (Cu, Ni et Cd) en fonction des concentrations en ions métalliques libres (Cu^{2+} , Ni^{2+} , Cd^{2+}). Le gradient de couleur représente les valeurs de pH relevées pour chaque site d'échantillonnage. La forme des points fait référence à l'étude dont sont originaires les données. Les droites représentent les régressions tracées avec l'ensemble des données présentant un pH supérieur ou égal à 6.

Cependant, si une relation linéaire se dessine sur l'ensemble des données, l'exclusion des sites présentant un pH acide ($\text{pH} < 6$) améliore considérablement la robustesse des régressions. En effet, les quantités bioaccumulées retrouvées aux sites présentant un pH faible ne suivent pas la tendance des données issues de sites où le pH est autour de la neutralité ($\text{pH} > 6$), les quantités de métaux accumulés étant inférieures à celles prédictes par régression (Figure 9-1). Ceci suggère que l'accumulation de métaux par les biofilms est sensible à l'effet des protons (comme pour de nombreux organismes vivants aquatiques). Dans l'idée de prédire la bioaccumulation du biofilm pour les sites présentant un pH acide, ceux-ci nécessiteraient leur propre modèle. Cependant, il est à souligner que cette situation reste rare et se produit pour des cours d'eau fortement anthropisés où le pH constitue un problème en tant que tel. Cette thèse a donc apporté des informations complémentaires quant au rôle clé que joue le pH et du seuil à partir duquel il devient important.

Notons que les quantités de métaux bioaccumulés varient sur deux ordres de grandeur à l'intérieur de certaines fourchettes de concentrations en ions métalliques libres (par exemple en $[\text{Ni}]_{\text{Bio}}$ pour $[\text{Ni}^{2+}]$ comprises entre 10^{-6} et 10^{-5} M) (Figure 9-1). De plus, lorsque les jeux de données de ces quatre publications (Lavoie *et al.* 2012; Leguay *et al.* 2016; Laderriere *et al.* 2020; Laderriere *et al.* 2021) sont séparés en sous-jeu par région, les pentes des régressions sont différentes (Figure 9-2). Par exemple, le biofilm issu de Sudbury (rouge sur la Figure 9-2) bioaccumule plus de Cu, Ni et Cd que celui du Nunavik (bleu sur la Figure 9-2) pour une même concentration d'exposition en ions libres. Ce constat pose la question des variables, autres que la concentration en ions métalliques, qui influent sur la bioaccumulation des métaux par le biofilm. En effet, ces différences ne peuvent pas seulement s'expliquer par l'effet seul du pH. Selon les hypothèses du BLM, un effet de compétition ionique peut s'opérer pour l'internalisation des métaux au travers des membranes biologiques (Lavoie *et al.* 2012). En effet, ces mécanismes de transport ne sont pas nécessairement spécifiques (Blaby-Haas & Merchant, 2012). Ces travaux ont aussi porté sur les effets de compétition ionique observés sur le terrain comme hypothèse d'explication de ces différences de bioaccumulation. Les résultats suggèrent que l'accumulation de métaux par les biofilms est sensible à un effet compétiteur du Mg et des autres métaux. Des résultats similaires ont été trouvés par Leguay *et al.* (2016) où l'effet compétiteur du Mg semblait plus important que celui du Ca dans le cas de l'accumulation du Cu ou du Pb. Dans notre étude, l'effet du Ca comme ion compétiteur sur la bioaccumulation des trois métaux d'étude n'a pas été mis en évidence, celui-ci étant corrélé au pH. Concernant la compétition avec les autres métaux, les résultats ont montré une bonne concordance avec des études en laboratoire déjà publiées (notamment les études utilisant des algues unicellulaires en exposition à des métaux seuls ou en

mélange; Flouty & Khalaf, 2015). Cependant, l'autocorrélation des données a rendu difficile l'analyse des relations entre les éléments de la colonne d'eau et leur internalisation par le biofilm. Cette autocorrélation vient du contexte minier du projet et du plan d'échantillonnage faisant intervenir plusieurs prélèvements le long d'une même rivière (selon un gradient de dilution amont vers aval) ainsi que de la relative homogénéité géologique des sites. De par les activités minières, de hautes concentrations dissoutes de plusieurs métaux sont retrouvées dans les eaux de surface. Ces concentrations se retrouvent ainsi corrélées entre elles rendant difficile la visualisation d'effets clairs de compétition. Afin de ne pas exclure ces sites tout en limitant l'autocorrélation du jeu de données au complet, une possibilité serait de sélectionner un site par rivière (et donc éviter les échantillonnages considérant un gradient de dilution après chaque intrant du cours d'eau étudié). À ce titre, la région de Sudbury semble plus appropriée que la région du Nunavik, car elle incorpore une plus grande hétérogénéité de sites (Laderriere *et al.*, 2021).

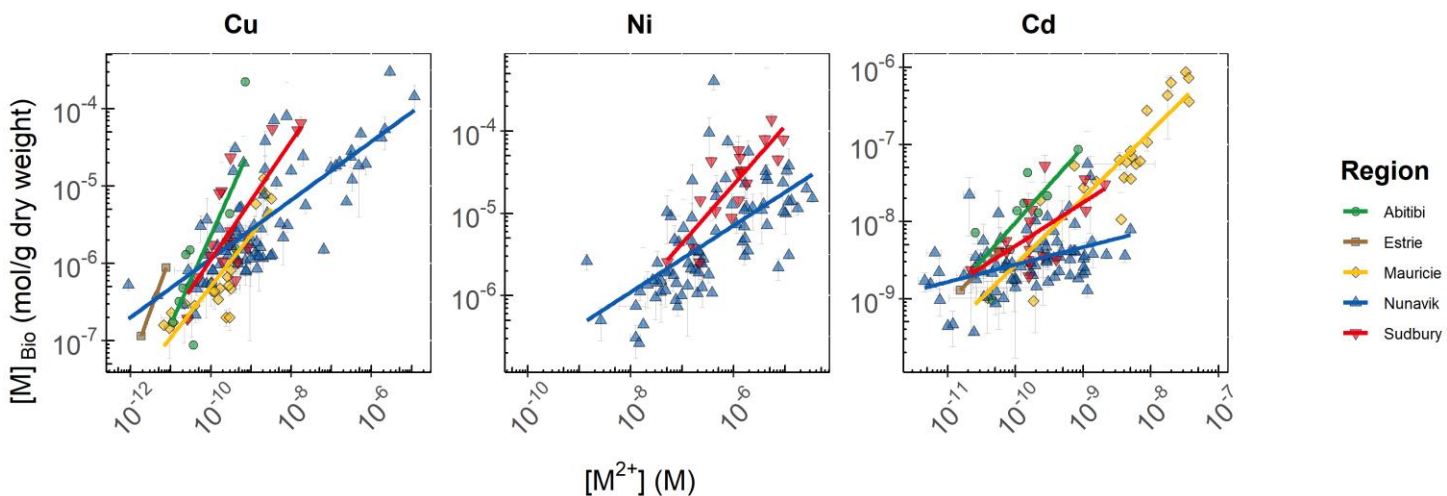


Figure 9-2 : Régressions des teneurs en métaux bioaccumulés par le biofilm (Cu, Ni et Cd) en fonction des concentrations en ions métalliques (Cu^{2+} , Ni^{2+} , Cd^{2+}) pour les sites à $\text{pH} > 6$. Les couleurs et les formes représentent les points et les régressions issues des différentes régions représentées : Abitibi (rond vert ; Leguay *et al.* 2016), Estrie (carré marron ; Leguay *et al.* 2016), Mauricie (losange jaune ; Lavoie *et al.* 2012; Leguay *et al.* 2016), Nunavik (triangle bleu ; Laderriere *et al.* 2020; Laderriere *et al.* 2021) et Sudbury (triangle inversé rouge ; Laderriere *et al.* 2021).

Dans l'ensemble, les résultats étaient très cohérents d'une étude à une autre, et ce, malgré la distance de près de 2000 km qui les sépare (Lavoie *et al.* 2012; Leguay *et al.* 2016; Laderriere *et al.* 2020; Laderriere *et al.* 2021). De plus, les résultats de ce chapitre ont permis de confirmer

le potentiel universel de la bioaccumulation en métaux du biofilm comme un proxy de la biodisponibilité des métaux malgré les différences de climat, d'écosystèmes et de pressions anthropiques. Une des perspectives à donner à ce chapitre serait donc d'incorporer un jeu de données provenant de sites ayant une plus grande variété de caractéristiques physicochimiques et de degrés de pression anthropique afin de mieux discriminer les effets de compétition ionique entre métaux et cations majeurs. Ceci permettrait une approche statistique (exemple de la régression des moindres carrés) afin de discriminer clairement quels prédicteurs sont associés à la variable réponse qu'est la bioaccumulation du biofilm.

Selon les hypothèses du BLM, le rapport de la concentration du métal internalisé sur celle de l'ion libre s'écrit (voir équation (6) section 3.4.6) :

$$\frac{[M_{Bio}]}{[M^{2+}]} = \frac{k \times K_{M^{2+}} \times [X_{Bio} \equiv]_{Tot}}{1 + K_{H^+}[H^+] + \sum_i(K_{Cat^{2+}}[Cat_i^{2+}])}$$

Considérant le cas du Cu, cette équation peut être résolue par la méthode des moindres carrées. Implémentée dans le logiciel R, cette équation peut s'écrire sous la forme suivante :

$$[Cu_{Bio}] = \frac{a[Cu^{2+}]}{1 + b[H^+] + c[Mg^{2+}] + d[Ca^{2+}] + e[Mn^{2+}] + f[Ni^{2+}] + g[Cu^{2+}] + h[Zn^{2+}] + i[Cd^{2+}] + j[Pb^{2+}]}$$

Où les lettres (*a* à *j*) sont les coefficients associés aux différents éléments pris en compte dans l'équation. Afin d'éviter un rapport, et donc une possible infinité de solutions, l'équation peut être transformée tel que:

$$[Cu_{Bio}] (1 + b[H^+] + c[Mg^{2+}] + d[Ca^{2+}] + e[Mn^{2+}] + f[Ni^{2+}] + g[Cu^{2+}] + h[Zn^{2+}] + i[Cd^{2+}] + j[Pb^{2+}]) = a[Cu^{2+}]$$

$$[Cu_{Bio}] = a[Cu^{2+}] - (b[H^+].[Cu_{Bio}] + c[Mg^{2+}].[Cu_{Bio}] + d[Ca^{2+}].[Cu_{Bio}] + e[Mn^{2+}].[Cu_{Bio}] + f[Ni^{2+}].[Cu_{Bio}] + g[Cu^{2+}].[Cu_{Bio}] + h[Zn^{2+}].[Cu_{Bio}] + i[Cd^{2+}].[Cu_{Bio}] + j[Pb^{2+}].[Cu_{Bio}])$$

Sous forme matricielle, cette équation peut s'écrire :

$$Y = X.\beta + \varepsilon$$

$$\begin{pmatrix} [Cu_{Bio}]_1 \\ \vdots \\ [Cu_{Bio}]_n \end{pmatrix} = \begin{pmatrix} [Cu^{2+}]_1 & \cdots & -[Pb^{2+}]_1, [Cu_{Bio}]_1 \\ \vdots & \ddots & \vdots \\ [Cu^{2+}]_n & \cdots & -[Pb^{2+}]_n, [Cu_{Bio}]_n \end{pmatrix} \cdot \begin{pmatrix} a \\ \vdots \\ j \end{pmatrix} + \begin{pmatrix} \epsilon_1 \\ \vdots \\ \epsilon_n \end{pmatrix}$$

$$\hat{\beta} = (X^t X)^{-1} X^t Y \quad \text{Estimation des coefficients associés à chaque variable}$$

$$\hat{Y} = X \hat{\beta} \quad \text{Calcul de la bioaccumulation prédictive par régression des moindres carrés}$$

Cependant, la régression classique prévoit que les erreurs soient indépendantes et suivent une loi normale. Or, ce n'est pas le cas ici. En effet, le plan expérimental inclut des mesures répétées. Les modèles mixtes (aussi appelés modèles à effets aléatoires) sont des outils intéressants, car ils permettent de considérer ce type d'information (ex. échantillonner une même rivière selon un gradient de dilution ou échantillonner le même site plusieurs fois dans le temps) et de généraliser l'approche afin d'estimer des paramètres d'un modèle de régression classique. Incorporer un plus ample jeu de données permettrait probablement de contourner l'autocorrélation des données et donc d'établir un modèle prédictif de la bioaccumulation des métaux par le biofilm en fonction de la chimie de l'eau.

Le développement de ces nouveaux outils améliore la capacité des exploitations minières (ou autres acteurs publics ou privés) à tenir compte de la sensibilité des écosystèmes face aux contaminants et du degré de stress exercé sur les milieux aquatiques naturels. Ce premier chapitre a donc permis d'améliorer nos connaissances sur l'évaluation du risque écologique que posent les métaux envers les organismes aquatiques dans le cadre du développement minier canadien. Néanmoins, un plus ample jeu de données est nécessaire pour aboutir à un modèle prédictif.

9.2 Approche en microcosmes

La complexité des écosystèmes naturels rend difficile l'établissement d'un lien de causalité entre l'exposition aux métaux et les effets biologiques observés. À ce titre, les études en microcosmes représentent une approche intéressante permettant de répondre à ces questions. En effet, elles permettent d'étudier les effets des contaminants au niveau de la population et de la communauté (y compris les effets indirects) dans des conditions contrôlées.

9.2.1 Effet de la température et de la photopériode sur la bioaccumulation du Ni par le biofilm

Dans la Figure 9-2, nous avons observé des différences de pente dans les régressions tracées (pour les sites à pH proche de la neutralité) entre les teneurs en métaux bioaccumulées par le biofilm (Cu, Ni et Cd) et les concentrations d'exposition en ions libres métalliques (Cu^{2+} , Ni^{2+} , Cd^{2+}). Si le chapitre 1 de cette thèse explorait le rôle de la chimie de l'eau pour expliquer ces différences, le chapitre 2 explore les effets de variables environnementales comme la température et la photopériode. Par exemple, la région du Nunavik correspond à un écosystème subarctique tandis que la ville de Sudbury, située environ 1700 km au sud, possède des caractéristiques d'un écosystème plus tempéré (notamment un important couvert forestier et des différences marquées en termes d'heures d'ensoleillement). Ces deux régions se caractérisent donc par des climats différents susceptibles d'expliquer, au moins en partie, les différences de pente observées. Pour répondre à cette question, un biofilm naturel provenant de la rivière Cap-Rouge (Québec, Canada) a été cultivé en laboratoire et exposé à différentes concentrations en Ni et ce, dans différentes conditions de température et de photopériode. L'objectif de ce volet était de venir compléter le jeu de données obtenu sur le terrain en investiguant l'influence de paramètres physiques comme la température et la photopériode sur la réponse de bioaccumulation du Ni par le biofilm.

Les résultats de ce chapitre ont permis de mesurer la bioaccumulation du Ni ainsi que la toxicité chronique induite chez un biofilm exposé à différentes concentrations en Ni dans plusieurs configurations de température et de photopériode. Les données obtenues se sont montrées en accord avec ceux qui ont déjà été publiés dans la littérature à l'exemple du Cu (Morin *et al.* 2017; Pesce *et al.* 2018) ou d'autres métaux comme le Pb (Ancion *et al.*, 2010; Stewart *et al.*, 2015) ou le Zn (Corcoll *et al.*, 2012; Lavoie *et al.*, 2012). Lors des expositions, les valeurs de concentration en chlorophylle-a ont diminué tandis que la biomasse a augmenté avec le temps pour les différentes concentrations d'exposition suggérant un impact moins fort sur le compartiment hétérotrophe. De plus, les résultats ont permis de montrer que la température (différence de 6°C), contrairement à la photopériode (différence de 4 h), a eu un effet sur la structure du biofilm entraînant une différence dans les quantités de Ni internalisées par le biofilm (voir figure 9-3). En effet, les biofilms exposés à une température de 20°C ont bioaccumulé plus de Ni que ceux exposés à 14°C pour une concentration d'exposition donnée tout en présentant une valeur CE_{50} plus faible. Au moyen d'une analyse en composantes principales (ACP ; Figure 9-3), les résultats ont permis de discriminer les biofilms selon la température. Ainsi la température a été démontrée comme modifiant la sensibilité et la réponse des biofilms au Ni. Ces résultats vont dans le sens

de ceux obtenus sur le terrain avec les différences de pente de régression obtenues entre la région de Sudbury et du Nunavik (Figure 9-2). Dans un contexte où les biofilms d'eau douce peuvent être utilisés comme outil de biosuivi, ces résultats impliquent que des variations saisonnières, en particulier liées à la température, dans la réponse de bioaccumulation des métaux sont susceptibles de se produire.

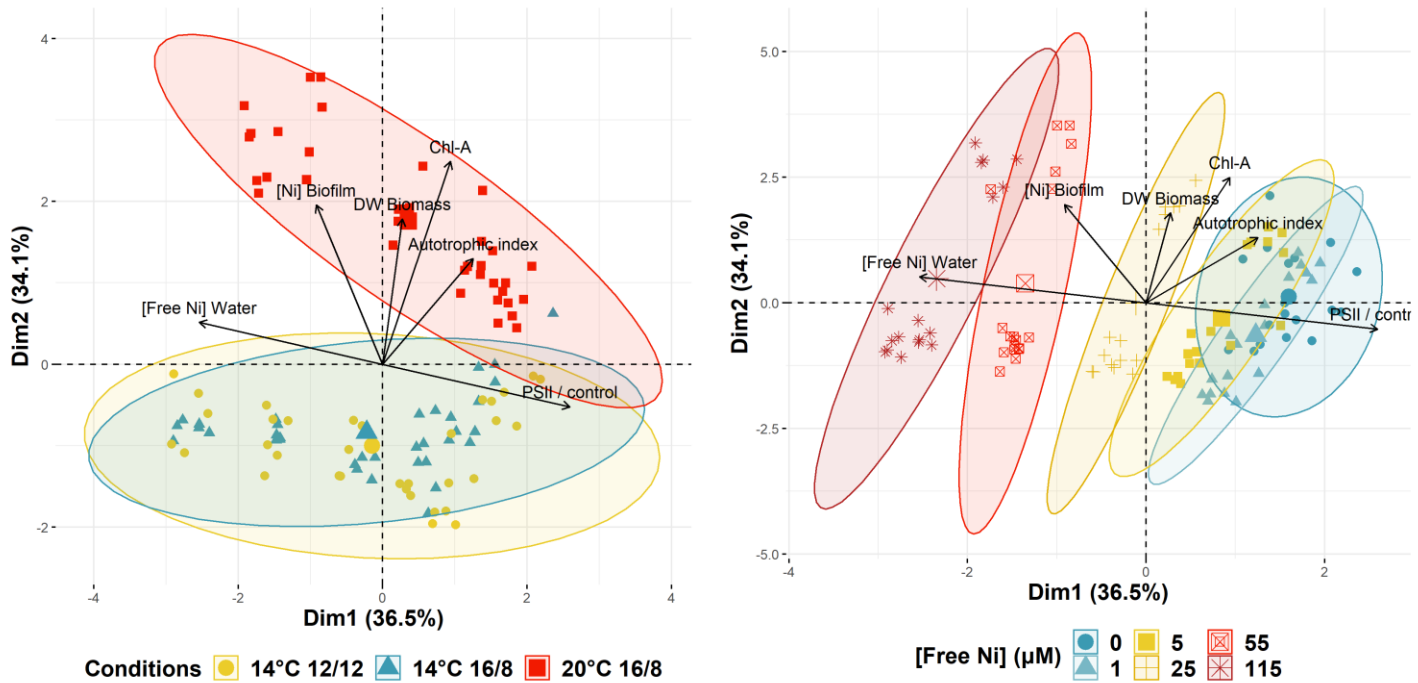


Figure 9-3 : Analyse en composantes principales (ACP) effectuée sur l'ensemble des descripteurs utilisés pour analyser la réponse du biofilm après 7 jours d'exposition à différentes concentrations en Ni sous trois conditions environnementales de photopériode et de température. L'ACP de gauche discrimine selon la condition environnementale tandis que l'ACP de droite discrimine selon la concentration d'exposition en ions Ni^{2+} . Les symboles de tailles supérieures spécifiques à chaque condition (figure de gauche) ou concentrations d'exposition en nickel libre (figure de droite) font référence au barycentre des données.

De plus, les résultats issus du terrain n'avaient pas montré d'effet de compétition des ions Ca^{2+} contrairement à ce qui est généralement trouvé dans la littérature. Seuls les ions Mg^{2+} semblaient aboutir à un effet de compétition. Afin de compléter les données obtenues sur le terrain, des expériences en canaux ont donc été entreprises en exposant un biofilm à une concentration en Ni et différentes combinaisons de concentrations en Ca et en Mg (facteur de

concentration allant de 1 à 16 par rapport aux concentrations initiales du *Fraquil Medium*). La Figure 9-4 montre une partie des résultats qui n'ont pas fait l'objet d'une publication. De manière générale, les résultats suggèrent un effet limité de ces ions, du moins lorsque $[Ni^{2+}]$ est élevée, ce qui semble confirmer les observations de terrain que ces éléments jouent un rôle limité sur la bioaccumulation du Ni. Néanmoins, il est important de noter que la concentration en Ni^{2+} utilisée ($[Ni^{2+}] = 20 \mu M$) est élevée. Un effet compétiteur des ions Ca^{2+} et/ou Mg^{2+} pourrait être plus important pour des concentrations en Ni^{2+} plus faibles.

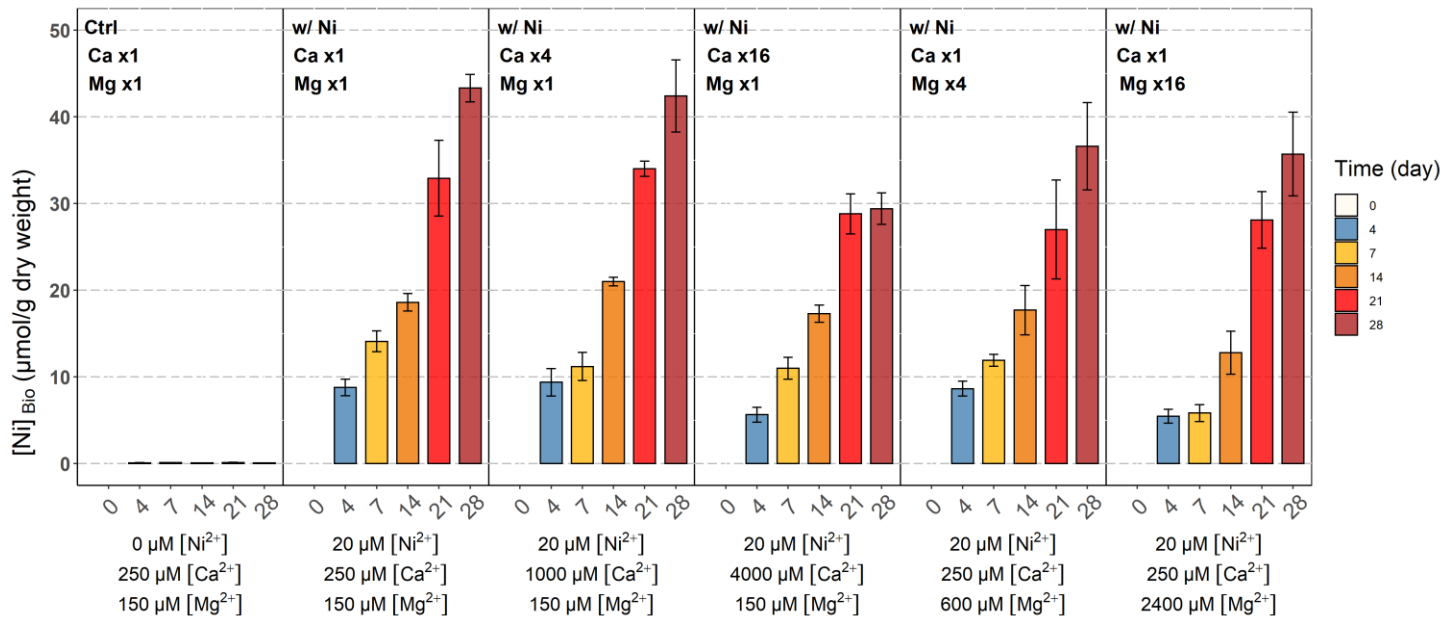


Figure 9-4 : Teneurs de Ni accumulé dans le biofilm (n = 3) en fonction du temps (en jours) selon différents traitements en Ni, Ca et Mg. Les couleurs font référence au temps d'échantillonnage du biofilm. La température était maintenue à 14°C sous une illumination d'environ 80 $\mu mol\text{-photons}/cm^2/s$ et un cycle diurne/nocturne de 16/8 (h/h).

Cependant, afin de permettre l'extrapolation des données de laboratoire à l'environnement naturel, il semble crucial de comprendre les liens entre la bioaccumulation, les changements des conditions environnementales et la composition générale des biofilms d'eau douce. C'est dans cette perspective que s'est inscrit le troisième chapitre de cette thèse.

9.2.2 Mise en lien de la bioaccumulation avec la structure, la sensibilité et la tolérance d'un biofilm exposé au Ni

Une approche multiparamétrique qui inclurait les caractéristiques inhérentes du biofilm (structure, communauté, tolérance) serait donc utile pour prédire le degré de stress causé par l'exposition aux métaux ainsi que par les effets des facteurs environnementaux. En effet, les chapitres 1 et 2 de cette thèse ont considéré le biofilm comme un « échantillonneur passif » dont le métal bioaccumulé se retrouve à l'équilibre avec les concentrations dans la colonne d'eau. De plus, les résultats du chapitre 2 (et plus particulièrement de la biomasse et de la chlorophylle-a) semblent indiquer que l'exposition au Ni du biofilm entraînait un début de changement de l'autotrophie vers l'hétérotrophie des biofilms. Le troisième chapitre vise à mieux comprendre le lien entre la structure de la communauté du biofilm (notamment la différenciation du compartiment autotrophe et hétérotrophe) et une exposition au Ni. Ces effets ont été mesurés selon différents biomarqueurs. Ainsi, ce chapitre se concentre sur les différents compartiments fonctionnels des biofilms en utilisant des descripteurs spécifiques afin d'évaluer les effets d'une exposition chronique au Ni au niveau de la communauté.

Pour ce faire, avant d'être exposées au Ni sur un temps long (28 jours), deux communautés de biofilms ont été cultivées et récoltées lors de deux saisons différentes (fin d'été et début d'hiver). Les deux communautés présentaient des caractéristiques différentes comme représentées par les analyses linéaires discriminantes effectuées sur les descripteurs structuraux et fonctionnels étudiés (Figure 9-5). Les successions saisonnières sont en effet des processus cycliques qui engendrent des fluctuations environnementales (exemple de la température du milieu) à l'origine de la variabilité de la composition taxonomique des biofilms et notamment des diatomées (Soininen and Eloranta 2004; Villeneuve *et al.* 2010; Morin *et al.* 2017). La structure et la diversité de la communauté diffèrent donc en fonction de la période d'échantillonnage. De plus, les résultats ont permis de montrer qu'une concentration d'exposition de 6 µM en ions Ni²⁺ était suffisante pour induire une acquisition de tolérance des communautés autotrophes, et ce, pour les deux communautés. En effet, les tests de toxicité court-terme (utilisant le Φ_{PSII} comme paramètre fonctionnel) n'ont pas montré d'effet dose réponse, rendant alors impossible le calcul d'une CE et ce dès le premier temps d'échantillonnage (après 7 jours). Néanmoins, les biofilms exposés à cette concentration montraient de faibles concentrations en chlorophylle-a suggérant un fort coût d'adaptation fonctionnelle. De plus, la condition C2 ([Ni²⁺] = 0,6 µM), a permis de montrer une dissociation des courbes dose réponse des deux communautés au fur et à mesure de l'exposition chronique. Ces résultats suggèrent donc que les saisons et la composition

taxonomique des biofilms jouent un rôle dans la capacité des organismes autotrophes à tolérer une exposition au Ni, diminuant ainsi leur vulnérabilité face à cette pression.

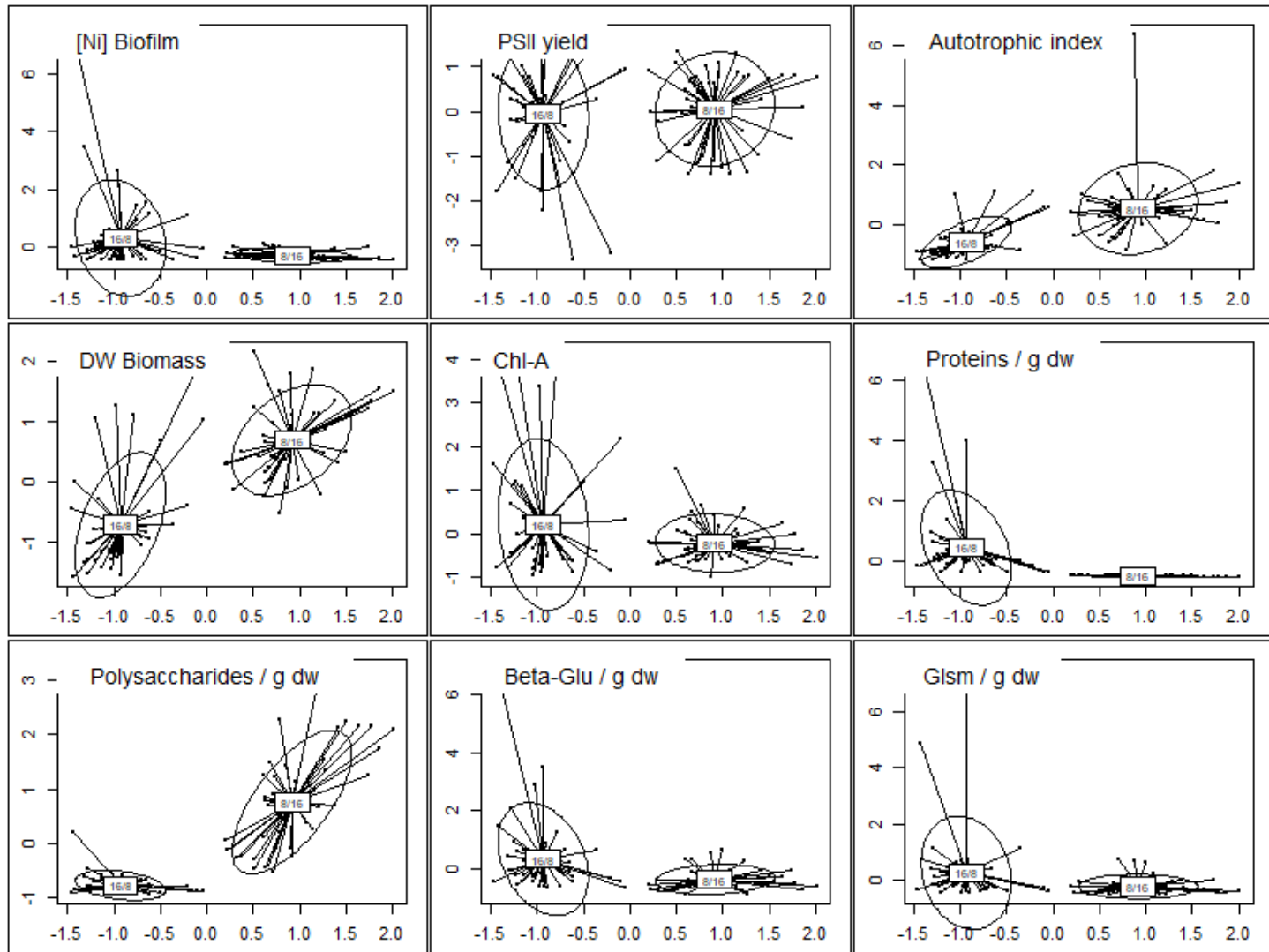


Figure 9-5 : Analyses linéaires discriminantes (LDA) effectuées pour chaque descripteur étudié avec la photopériode comme variable discriminante (16/8 à gauche et 8/16 à droite) et tous les traitements en Ni confondus.

Si aucun test de toxicité court-terme ciblant le compartiment hétérotrophe n'a été effectué, les activités enzymatiques extracellulaires (β -glucosidase et β -glucosaminidase) étaient suivies à chaque temps d'échantillonnage. Celles-ci n'ont pas montré de différence significative avec l'augmentation des concentrations d'exposition au Ni. Ces résultats sont en accord avec les

tendances observées dans le chapitre 2, où les indices autotrophiques augmentaient avec les concentrations d'exposition suggérant une plus faible toxicité induite du Ni sur les organismes hétérotrophes en comparaison des autotrophes à l'instar des résultats trouvés par Fechner *et al.* (2011). Les auteurs avaient en effet montré une plus faible toxicité du Ni sur l'activité de la β -Glu en comparaison d'autres métaux (Cd et Zn). Ceci met en évidence la variabilité de la toxicité selon la fonction considérée et donc l'importance d'utiliser une approche multifonctionnelle comme déjà suggérée par plusieurs études (Tlili *et al.* 2010; Pesce *et al.* 2018). Point intéressant, les biofilms d'hiver exposés selon une photopériode de 8/16 présentaient des quantités de Ni bioaccumulées plus faibles que celui d'été pour une même concentration d'exposition en Ni²⁺. Parallèlement, le biofilm d'hiver présentait une tolérance plus élevée lors des tests de toxicité court-terme (effectués sur le Φ_{PSII}). La bioaccumulation, tout comme l'acquisition de tolérance, est ainsi au moins en partie dépendante de la composition taxonomique des biofilms.

Les résultats suggèrent donc que la réponse des biofilms face à une exposition chronique au Ni est conditionnée par leurs propriétés initiales (structurelles et fonctionnelles), et donc fonction de la composition de la communauté. Autrement dit, l'histoire des biofilms d'eau douce dans les environnements naturels affecte leurs réponses aux métaux et serait donc susceptible d'expliquer la variabilité interrégionale relevée dans le chapitre 1 (voir Figure 9-2). Des analyses taxonomiques et/ou génétiques ou l'utilisation de technique de microscopie électronique (exemple de la microscopie électronique à balayage et à transmission (STXM) pourraient être utiles pour mieux comprendre la relation entre les capacités d'accumulation de métaux des biofilms d'eau douce et leurs effets.

9.3 Concordance des données de laboratoire au milieu naturel

Comme mentionné par Cheloni & Slaveykova (2018), une meilleure compréhension des mécanismes à l'origine des effets des métaux traces dans les environnements naturels réduira les incertitudes associées à l'extrapolation des données de toxicité du laboratoire vers le terrain. Ce projet de thèse a autant utilisé une approche de terrain qu'une approche de laboratoire au moyen de microcosmes. Les données des deux approches peuvent ainsi être comparées afin de vérifier si une extrapolation est possible au vu des éléments nouveaux apportés par les différents chapitres de cette thèse (voir Figure 9-6).

La Figure 9-6 nous permet de constater que les données de bioaccumulation en Ni par les biofilms exposés en microcosmes se superposent sur les régressions calculées à partir des

données de terrain. Cette superposition confirme que les expériences en microcosmes sont représentatives de ce qui se déroule dans les environnements naturels en termes de bioaccumulation, et ce, quel que soit le site considéré, le temps de prélèvement ou la composition taxonomique inhérente au lieu ou à la saison. De manière intéressante, les données issues de certaines conditions d'exposition se superposent mieux sur l'une ou l'autre des régressions modélisées à partir des données de terrain.

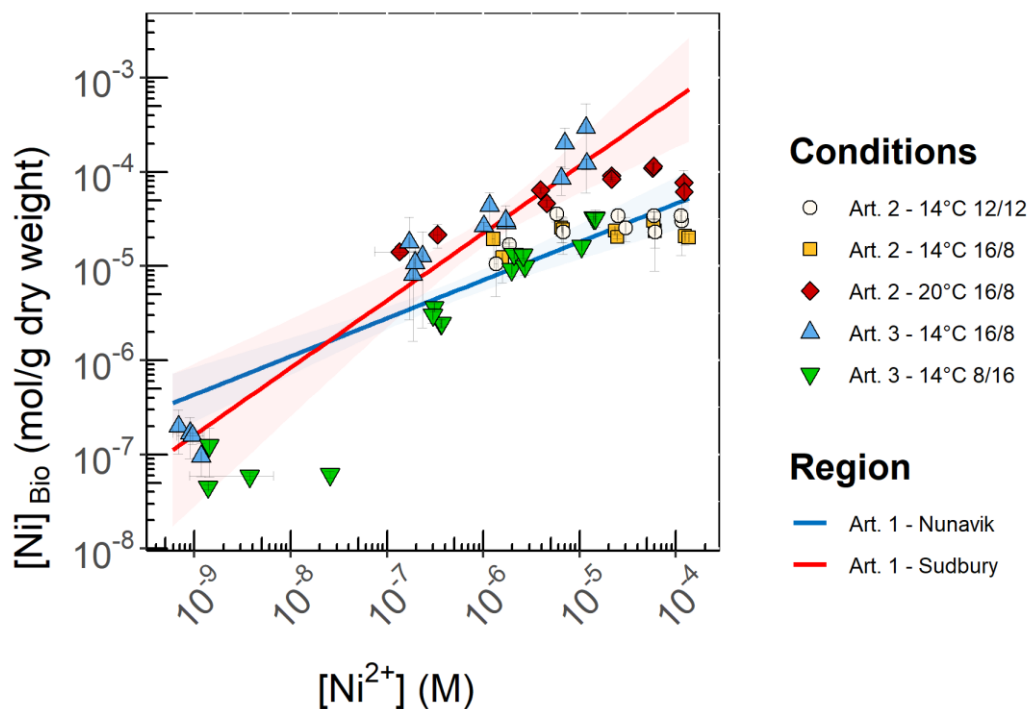


Figure 9-6 : Teneurs en Ni bioaccumulés par le biofilm en fonction de la concentration en ions Ni^{2+} . Les droites correspondent aux régressions modélisées (avec intervalles de confiance à 95%) via les données de terrain des deux régions étudiées (Nunavik en bleu et de Sudbury en rouge). Les couleurs et les formes des points différencient les conditions (ainsi que les articles référents) utilisées dans les expositions en microcosmes. À noter que les données représentées sur la présente figure sont seulement celles pour lesquelles un équilibre entre concentrations dans l'eau et dans le biofilm était atteint (c.à.d après 7 jours d'exposition dans le cas des deux chapitres).

En effet, les données issues des conditions 14°C 12/12 et 14°C 16/8 (article 2) ainsi que de 14°C 8/16 (article 3) semblent se superposer sur la régression des données du Nunavik. À l'inverse, les conditions 20°C 16/8 (article 2) et 14°C 16/8 (article 3) semblent mieux se superposer sur la régression issue de la région de Sudbury. En effet, la température est connue comme une des fluctuations environnementales majeures influant sur la composition taxonomique des biofilms (Soininen and Eloranta 2004; Villeneuve *et al.* 2010; Morin *et al.* 2017).

À ce titre, la saison estivale (en comparaison de la saison hivernale) comme la région de Sudbury (située environ 1700 km au sud du site étudié au Nunavik) se caractérisent naturellement par des conditions météorologiques plus chaudes. À l'inverse, les conditions d'exposition se positionnent le long de la régression issue des données du Nunavik regroupent un biofilm naturel prélevé en hiver ou un biofilm cultivé en laboratoire, mais exposé à des températures plus froides. Les résultats de terrain et de laboratoire vont donc dans le même sens et suggèrent que des variations de la composition taxonomique, à mettre en relation avec les conditions environnementales (en particulier la température) sont à l'origine des différences de pente observées dans le chapitre 1 et sur la Figure 9-2.

9.4 Conclusion

Le but de ces travaux de thèse était d'améliorer nos connaissances en examinant les liens entre la biodisponibilité des contaminants et l'exposition des biofilms périphytiques d'eau douce afin d'établir les bases d'un nouvel outil écotoxicologique d'évaluation du risque écotoxicologique. Cette thèse s'est donc déroulée en conditions naturelles comme en conditions contrôlées (*via* l'utilisation de microcosmes) afin de fournir les bases nécessaires pour mieux extrapoler les données du laboratoire aux milieux naturels.

Ces travaux ont tout d'abord permis d'affirmer le potentiel universel des biofilms périphytiques d'eau douce comme outil de biosuivi des expositions métalliques dans les cours d'eau de régions minières. Les régressions obtenues entre la teneur en métaux internalisés et la forme libre du métal dans les eaux de surface étaient cohérentes malgré des différences de climat, d'écosystème et de conditions physico-chimiques. Plus de données sont nécessaires (avec une plus grande hétérogénéité de sites) afin de calculer avec confiance les constantes d'affinité de chaque élément avec le biofilm pour le fonctionnement du modèle. Les régressions obtenues par région ont toutefois permis de montrer des différences de pente laissant penser que des variables autres que la chimie de l'eau influe sur la relation entre l'accumulation des métaux et leurs concentrations en ions libres dans l'eau. L'étude des interactions entre expositions au Ni et conditions environnementales (température et photopériode) sur la bioaccumulation du Ni et son impact toxique sur les biofilms a permis de montrer l'effet prépondérant de la température. En effet, si une modification de 4 h de photopériode n'a pas montré de différences, un écart de 6°C a suffisamment influencé le biofilm pour que celui-ci montre des différences significatives des teneurs en Ni accumulées. Cette différence de température pouvant se produire au cours d'une

même saison (exemple de la saison estivale) voire d'une même journée (différence diurne/nocturne) et ce, en particulier dans les cours d'eau à faible hauteur de colonne d'eau, implique que des variations de bioaccumulation sont également susceptibles de se produire.

Néanmoins, la température est connue comme étant l'un des principaux facteurs environnementaux pouvant jouer un rôle sur la succession des communautés périphytiques. Les résultats ont également montré que des communautés prélevées en deux saisons différentes (été et hiver) se caractérisaient par des quantités accumulées différentes malgré une même température d'exposition. Ceci suggère que la composition taxonomique des biofilms joue un rôle prépondérant dans les différences de pente des régressions modélisées pour chaque région d'étude et que la température pourrait avoir un effet indirect sur les quantités accumulées par le biofilm. En d'autres termes, l'accumulation de métaux par les biofilms est principalement influencée par le métal considéré et sa spéciation, les caractéristiques physico-chimiques du milieu et la composition du biofilm. Parallèlement, les résultats suggèrent que l'histoire et donc les caractéristiques intrinsèques des biofilms jouent un rôle dans la capacité des communautés à tolérer une exposition aux Ni. Bien que le Ni ait été peu étudié dans la littérature, ces résultats sont en accord avec des études portant sur d'autres métaux divalents (exemple du Zn, Cu ou Pb).

Ce projet de thèse a contribué à l'acquisition de nouvelles connaissances permettant de mieux définir les liens de causalité entre l'exposition aux métaux et les effets biologiques observés. Dans une perspective de biosurveillance et d'évaluation du risque écotoxicologique, ces travaux démontrent le potentiel universel des quantités de métaux bioaccumulées comme indicateur de la biodisponibilité des contaminants métalliques. Finalement, la composition taxonomique du biofilm semble être l'un des principaux facteurs à l'origine des différences de concentrations intracellulaires retrouvées observées en milieux naturels.

10 BIBLIOGRAPHIE DISCUSSION

- Ancion, P.Y., Lear, G., Lewis, G.D., 2010. Three common metal contaminants of urban runoff (Zn, Cu & Pb) accumulate in freshwater biofilm and modify embedded bacterial communities. Environ. Pollut. 158, 2738–2745. <https://doi.org/10.1016/j.envpol.2010.04.013>
- Blaby-Haas, C.E., Merchant, S.S., 2012. The ins and outs of algal metal transport. Biochim. Biophys. Acta 1823, 1531–1552. <https://doi.org/10.1016/j.bbamcr.2012.04.010>
- Campbell, P.G.C., 1995. Interactions between trace metals and aquatic organisms: A critique of the free-ion activity mode, in: Tessier, A., Turner, D.R. (Eds.), Metal Speciation and Bioavailability in Aquatic Systems. New York, NY, États-Unis, pp. 45–102.
- Cheloni, G., Slaveykova, V.I., 2018. Combined effects of trace metals and light on photosynthetic microorganisms in aquatic environment. Environments 5, 1–19. <https://doi.org/10.3390/environments5070081>
- Corcoll, N., Bonet, B., Leira, M., Montuelle, B., Tlili, A., Guasch, H., 2012. Light history influences the response of fluvial biofilms to Zn exposure. J. Phycol. 48, 1411–1423. <https://doi.org/10.1111/j.1529-8817.2012.01223.x>
- Fechner, L.C., Gourlay-Francé, C., Tusseau-Vuillemin, M.H., 2011. Low exposure levels of urban metals induce heterotrophic community tolerance: A microcosm validation. Ecotoxicology 20, 793–802. <https://doi.org/10.1007/s10646-011-0630-4>
- Flouty, R., Khalaf, G., 2015. Role of Cu and Pb on Ni bioaccumulation by *Chlamydomonas reinhardtii*: validation of the biotic ligand model in binary metal mixtures. Ecotoxicol. Environ. Saf. 113, 79–86. <https://doi.org/10.1016/j.ecoenv.2014.11.022>
- Laderriere, V., Faucheur, S. Le, Fortin, C., 2021. Exploring the role of water chemistry on metal accumulation in biofilms from streams in mining areas. Sci. Total Environ. 784, 146986. <https://doi.org/10.1016/j.scitotenv.2021.146986>
- Laderriere, V., Paris, L.E., Fortin, C., 2020. Proton competition and free ion activities drive cadmium, copper, and nickel accumulation in river biofilms in a nordic ecosystem. Environments 7, 1–13. <https://doi.org/10.3390/environments7120112>
- Lavoie, I., Lavoie, M., Fortin, C., 2012. A mine of information: Benthic algal communities as biomonitor of metal contamination from abandoned tailings. Sci. Total Environ. 425, 231–

241. <https://doi.org/10.1016/j.scitotenv.2012.02.057>

Lavoie, M., Fortin, C., Campbell, P.G.C., 2012. Influence of essential elements on cadmium uptake and toxicity in a unicellular green alga: the protective effect of trace zinc and cobalt concentrations. *Environ. Toxicol. Chem.* 31, 1445–1452. <https://doi.org/10.1002/etc.1855>

Leguay, S., Lavoie, I., Levy, J.L., Fortin, C., 2016. Using biofilms for monitoring metal contamination in lotic ecosystems: The protective effects of hardness and pH on metal bioaccumulation. *Environ. Toxicol. Chem.* 35, 1489–1501. <https://doi.org/10.1002/etc.3292>

Morin, S., Lambert, A.S., Rodriguez, E.P., Dabrin, A., Coquery, M., Pesce, S., 2017. Changes in copper toxicity towards diatom communities with experimental warming. *J. Hazard. Mater.* 334, 223–232. <https://doi.org/10.1016/j.jhazmat.2017.04.016>

Pesce, S., Lambert, A.-S., Morin, S., Foulquier, A., Coquery, M., Dabrin, A., 2018. Experimental warming differentially influences the vulnerability of phototrophic and heterotrophic periphytic communities to copper toxicity. *Front. Microbiol.* 9, 1424. <https://doi.org/10.3389/fmicb.2018.01424>

Soininen, J., Eloranta, P., 2004. Seasonal persistence and stability of diatom communities in rivers: Are there habitat specific differences? *Eur. J. Phycol.* 39, 153–160. <https://doi.org/10.1080/0967026042000201858>

Stewart, T.J., Behra, R., Sigg, L., 2015. Impact of chronic lead exposure on metal distribution and biological effects to periphyton. *Environ. Sci. Technol.* 49, 5044–5051. <https://doi.org/10.1021/es505289b>

Tlili, A., Bérard, A., Roulier, J.L., Volat, B., Montuelle, B., 2010. PO₄³⁻ dependence of the tolerance of autotrophic and heterotrophic biofilm communities to copper and diuron. *Aquat. Toxicol.* 98, 165–177. <https://doi.org/10.1016/j.aquatox.2010.02.008>

Villeneuve, A., Montuelle, B., Bouchez, A., 2010. Influence of slight differences in environmental conditions (light, hydrodynamics) on the structure and function of periphyton. *Aquat. Sci.* 72, 33–44. <https://doi.org/10.1007/s00027-009-0108-0>

11 ANNEXE I

Because the data set is significant, the additional data tables related to the first article of this thesis are not presented here but are publicly available via the following doi: <https://doi.org/10.5683/SP2/RBIM04>.

This dataset includes temperature, pH and means \pm standard deviations ($n = 3$) of dissolved ions at sampling sites, calculated free metal ion concentrations and measured metal biofilm content in streams of Nunavik (QC, Canada) and Sudbury (ON, Canada) in 2016.

Table 11-1 : Values and standard deviations ($n = 3$) of the physicochemical parameters of the surface water sampled in july and august 2016 for Nunavik data and in september 2016 in the case of Sudbury data.

Table 11-2 : Mean (\pm standard deviation, $n = 3$) of the free ion calculated concentrations sampled in july and august 2016 for Nunavik data and in september 2016 in the case of Sudbury data.

Table 11-3 : Mean (\pm standard deviation, $n = 3$) of the metal concentrations in biofilms sampled in july and august 2016 for Nunavik data and in september 2016 in the case of Sudbury data.

12 ANNEXE II

Table 12-1 : Recipes for the Fraquil medium used for the culture of biofilm and the experiments of Ni exposure (Morel et al. 1975).

Fraquil Medium (Morel et al. 1975)				
	Stock solution (g/L)	Quantity (mL/L)	Final concentration (mg/L)	Final concentration (mM)
CaCl ₂ . 2 H ₂ O	36.8	1	36.8	0.250
MgSO ₄ . 7H ₂ O	37.0	1	37.0	0.150
NaHCO ₃	12.6	1	12.6	0.150
Na ₂ SiO ₃ . 9H ₂ O	3.55	1	3.55	0.013
NaNO ₃	8.50	1	8.50	0.100
K ₂ HPO ₄	1.74	1	1.74	0.010
Trace Metals Solution	X	1	X	X

Trace Metal Solution				
	Stock solution (g/L)	Quantity (mL/L)	Final concentration (g/L)	Final concentration (nM)
CuSO ₄ . 5H ₂ O	0.249	1	0.249	1.00
(NH ₄) ₆ Mo ₇ O ₂₄ . 4H ₂ O	0.265	1	0.265	0.214
CoCl ₂ . 6H ₂ O	0.595	1	0.595	2.50
MnCl ₂ . 4 H ₂ O	4.55	1	4.55	23.0
ZnSO ₄ . 7H ₂ O	1.15	1	1.15	4.00
Na ₂ EDTA . 2H ₂ O	X	1.86 g	X	5000
FeCl ₃ . 6H ₂ O	X	0.122 g	X	451

Morel, F. M. M., Westall, J. C., Reuter, J. G., and Chaplick, J. P. 1975. Description of the algal growth media "Aquil" and "Fraquil." Technical Report 16. Water Quality Laboratory, Ralph Parsons Laboratory for Water Resources and Hydrodynamics, Massachusetts Institute of Technology, Cambridge, 33 pp.

Table 12-2 : Values and standard deviations (n = 5) of the physicochemical parameters of the Cap-Rouge River at the time of biofilm sampling.

n = 5	COD (mg C/L)	Br (mg/L)	Cl (mg/L)	F (mg/L)	NO ₂ (mg/L)	NO ₃ (mg/L)	SO ₄ (mg/L)	PO ₄ (mg/L)	TP (µg/L)
Mean	3.13	< 0.006	112	0.119	< 0.004	1.89	34.6	< 0.008	15.7
SD	0.06	N/A	2	0.011	N/A	0.01	0.7	N/A	0.1
LD		0.003	0.006	0.002	0.002	0.01	0.01	0.004	2

n = 5	Ca (mg/L)	Co (µg/L)	Cu (µg/L)	Fe (mg/L)	K (mg/L)	Mg (mg/L)	Mn (mg/L)	Mo (µg/L)	Na (mg/L)	Ni (µg/L)	Si (mg/L)	Zn (µg/L)
Mean	59.6	0.940	0.601	0.0912	3.49	6.55	0.104	1.67	74.2	0.675	3.14	5.29
SD	0.6	0.585	0.153	0.0150	0.03	0.05	0.001	0.68	0.9	0.300	0.03	1.47
LD	0.0006	0.6	0.4	0.001	0.002	0.0002	0.0001	1.2	0.0004	0.08	0.001	0.1

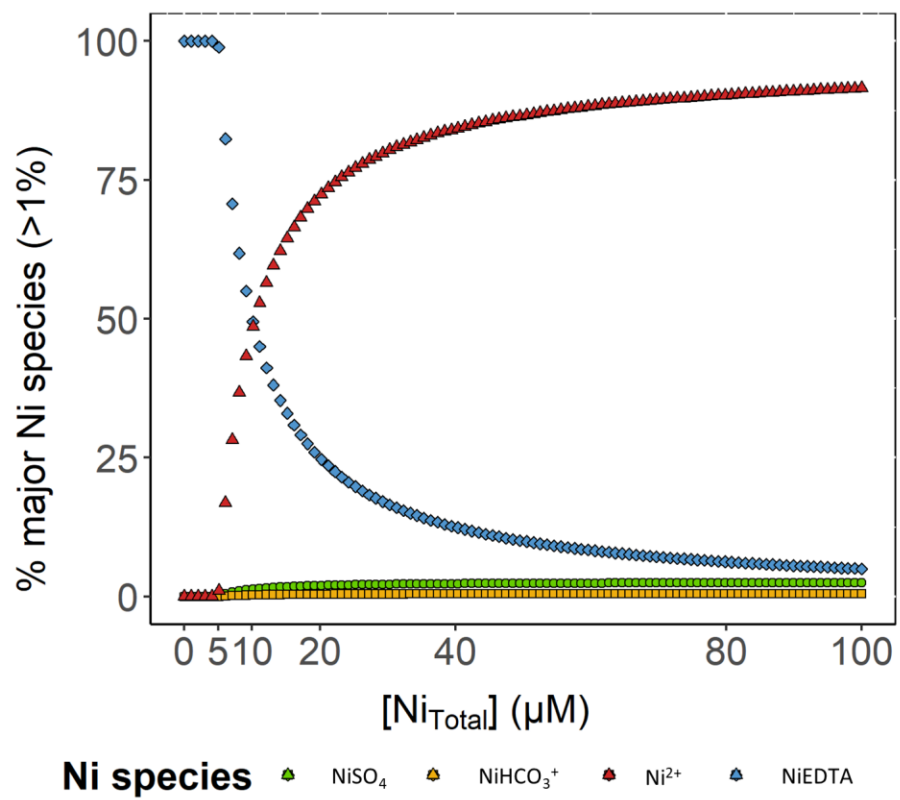


Figure 12-1: Major chemical forms of Ni in the Fraquil medium (expressed in percentage) as a function the total concentration in the medium. Only predominant chemical forms (above 1%) are represented.

Table 12-3 : Time course of total and free Ni concentrations during exposure for the three environmental conditions tested. b/DL = below detection limit. N/A = non available. Limit of detection = 0.01 µM.

Time (day)	[Ni] _{Nominal} (µM)	14°C 16/8				14°C 12/12				20°C 16/8			
		[Ni] _{Total} (µM)		[Ni ²⁺] (µM)		[Ni] _{Total} (µM)		[Ni ²⁺] (µM)		[Ni] _{Total} (µM)		[Ni ²⁺] (µM)	
0	0	b/DL		N/A		b/DL		N/A		b/DL		N/A	
	1	b/DL		N/A		b/DL		N/A		b/DL		N/A	
	5	0.02 ± 0.01				0.04 ± 0.00				0.02 ± 0.01			
	25	0.04 ± 0.02				0.08 ± 0.01				0.04 ± 0.01			
	55	0.09 ± 0.01		< 1 pM		0.15 ± 0.03				0.05 ± 0.01			< 1 pM
1	115	0.27 ± 0.14				0.44 ± 0.28				0.19 ± 0.13			
	0	b/DL		N/A		b/DL		N/A		b/DL		N/A	
	1	6.1 ± 0.1	1.0 ± 0.1	6.1 ± 0.2	1.1 ± 0.2	5.7 ± 0.2	0.7 ± 0.2	5.7 ± 0.2	0.7 ± 0.2	6 ± 0	0.7 ± 0	6 ± 0	
	5	11 ± 0	6 ± 0	11 ± 0	5 ± 0	11 ± 0	6 ± 0	11 ± 0	6 ± 0	21 ± 0	21 ± 0	21 ± 0	
	25	27 ± 0	21 ± 0	30 ± 3	24 ± 3	27 ± 3	27 ± 3	27 ± 3	27 ± 3	54 ± 1	54 ± 1	54 ± 1	
	55	60 ± 1	54 ± 1	60 ± 1	53 ± 1	61 ± 1	54 ± 1	61 ± 1	54 ± 1	117 ± 5	108 ± 4	108 ± 4	
4	115	123 ± 6	115 ± 6	115 ± 8	107 ± 7	117 ± 7	108 ± 5	117 ± 5	108 ± 4				
	0	b/DL		N/A		b/DL		N/A		b/DL		N/A	
	1	6.2 ± 0.2	1.2 ± 0.1	6.4 ± 0.3	1.3 ± 0.3	5.3 ± 0.2	0.2 ± 0.2	5.3 ± 0.2	0.2 ± 0.2	4 ± 0	4 ± 0	4 ± 0	
	5	11 ± 0	6 ± 0	11 ± 1	6 ± 0	10 ± 0	0 ± 0	10 ± 0	0 ± 0	21 ± 0	21 ± 0	21 ± 0	
	25	28 ± 1	22 ± 1	32 ± 3	26 ± 3	27 ± 3	27 ± 0	27 ± 0	27 ± 0	55 ± 1	55 ± 1	55 ± 1	
	55	63 ± 1	56 ± 1	63 ± 1	56 ± 1	63 ± 1	55 ± 1	63 ± 1	55 ± 1	116 ± 2	116 ± 2	116 ± 2	
7	115	130 ± 6	121 ± 6	119 ± 3	111 ± 3	124 ± 2	116 ± 2	124 ± 2	116 ± 2				
	0	b/DL		N/A		b/DL		N/A		b/DL		N/A	
	1	6.5 ± 0.2	1.4 ± 0.2	6.7 ± 0.3	1.6 ± 0.3	5.2 ± 0.1	0.2 ± 0.1	5.2 ± 0.1	0.2 ± 0.1	4 ± 0	4 ± 0	4 ± 0	
	5	12 ± 0	7 ± 0	11 ± 1	6 ± 1	9 ± 0	0 ± 0	9 ± 0	0 ± 0	21 ± 0	21 ± 0	21 ± 0	
	25	30 ± 1	24 ± 1	33 ± 3	27 ± 3	27 ± 0	27 ± 0	27 ± 0	27 ± 0	58 ± 1	58 ± 1	58 ± 1	
	55	67 ± 1	60 ± 1	67 ± 1	60 ± 1	65 ± 1	58 ± 1	65 ± 1	58 ± 1	121 ± 1	121 ± 1	121 ± 1	
	115	139 ± 7	130 ± 7	122 ± 8	113 ± 7	130 ± 2	121 ± 1	130 ± 2	121 ± 1				

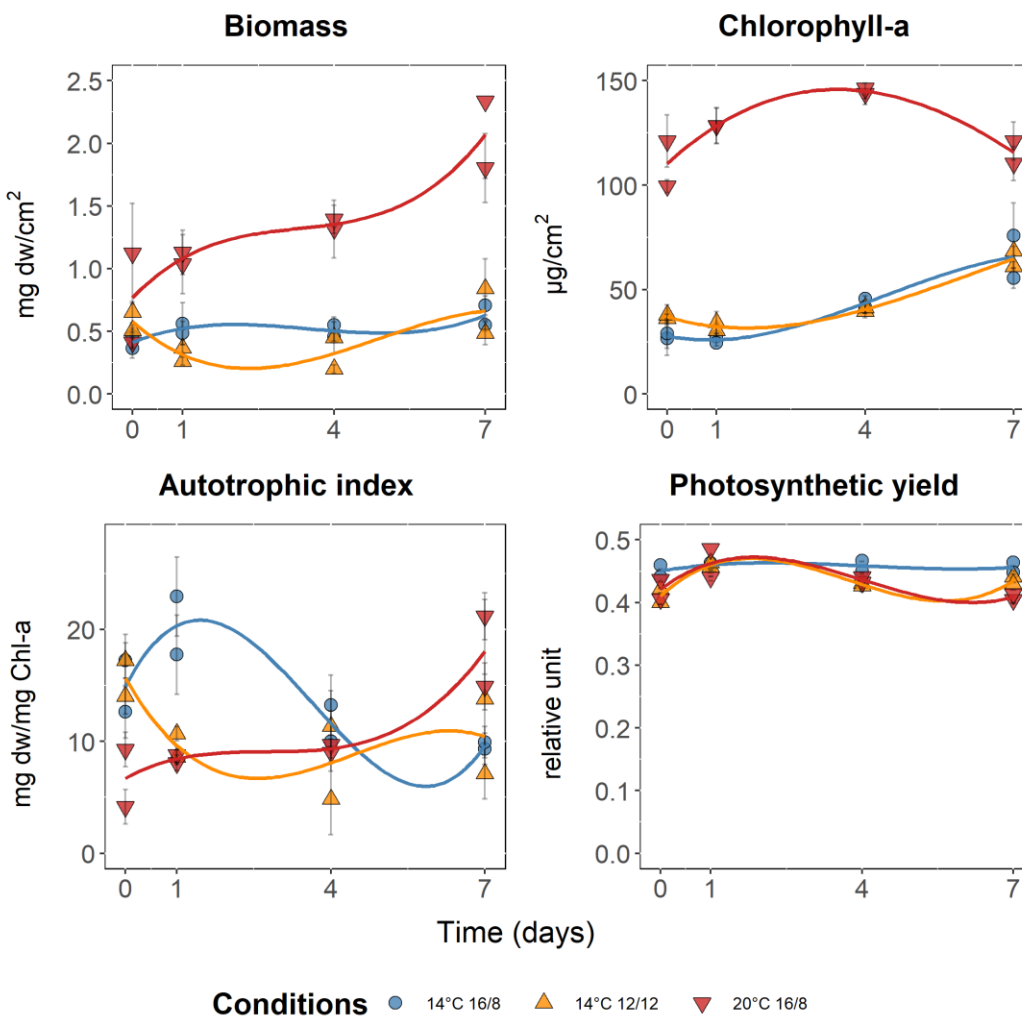


Figure 12-2 : Time course of control samples with the biomass, the concentration of chlorophyll-a, the autotrophic index and the photosynthetic yield ($n = 3$) as a function of time for each condition of temperature and photoperiod (T14P16 = 14°C in 16/8 in blue; T14P12 = 14°C in 12/12 in yellow; and T20P16 = 20°C in 16/8 in red). The curves plotted correspond to second degree polynomial regressions.

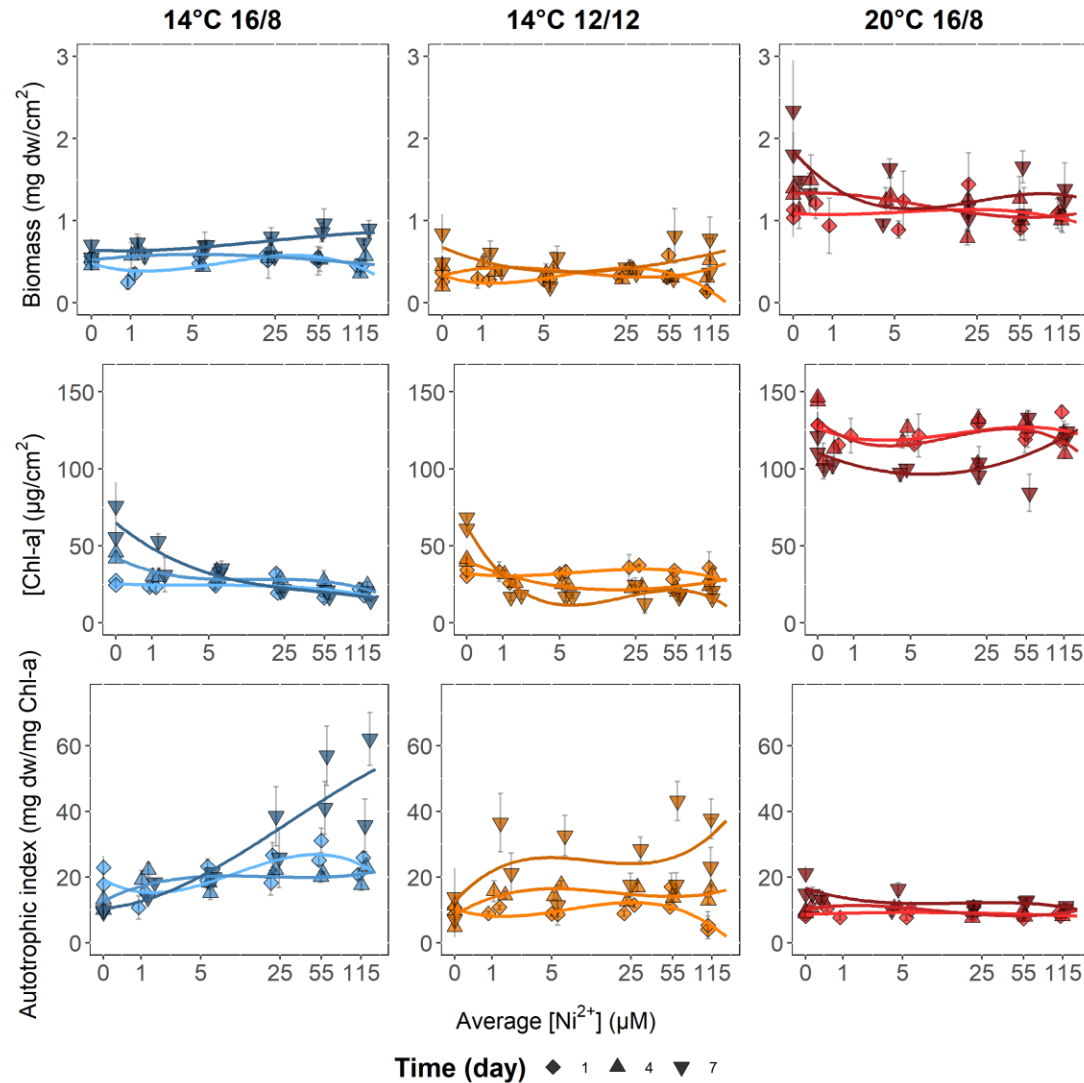


Figure 12-3 : Dose responses of the biomass, the concentration of chlorophyll-a and the autotrophic index ($n = 3$) as a function of the free Ni concentration for each environmental condition of temperature and photoperiod (14°C with 16/8 in blue; 14°C with 12/12 in yellow; and 20°C with 16/8 in red) and the different sampling times. The curves plotted correspond to second degree polynomial regressions.

13 ANNEXE III

Table 13-1 : Physico-chemical characteristics of exposure media of the four channel systems. The values are presented as means ± standard deviations (n = 24). b/DL = below detection (0.007 µM). N/A = not available. The letters a and b respectively refer to the results of Tukey tests performed between (a) the different conditions in comparison to the control (C0) within a given photoperiod, and (b) the two photoperiods tested within a given condition.

	Photoperiod 16/8								Photoperiod 8/16							
	C0		C1		C2		C3		C0		C1		C2		C3	
pH	7.9	± 0.1	7.9	± 0.1	7.9	± 0.1	7.8	± 0.1	7.6	± 0.1	7.5	± 0.1	7.5	± 0.1	7.5	± 0.0
Conductivity (µS/cm)	241	± 17	234	± 14	230	± 14	232	± 12	210	± 13	195	± 9	185	± 8	188	± 8
[DOC] (mg C/L)	45	± 28	43	± 15	34	± 14	35	± 20	35	± 5	34	± 5	42	± 20	31	± 7
[Ca] _{Total} (mM)	0.60	± 0.15	0.58	± 0.15	0.55	± 0.16	0.48	± 0.19	0.53	± 0.06	0.47	± 0.04	0.44	± 0.04	0.44	± 0.02
[Ca ²⁺] (mM)	0.37	± 0.04	0.37	± 0.02	0.39	± 0.03	0.38	± 0.03	0.34	± 0.02	0.33	± 0.02	0.30	± 0.03	0.32	± 0.01
[Mg] _{Total} (mM)	0.12	± 0.03	0.12	± 0.03	0.12	± 0.04	0.10	± 0.04	0.11	± 0.01	0.10	± 0.01	0.09	± 0.01	0.11	± 0.05
[Mg ²⁺] (mM)	0.090	± 0.01	0.09	± 0.01	0.09	± 0.01	0.09	± 0.01	0.08	± 0.01	0.07	± 0.01	0.07	± 0.01	0.07	± 0.00
[Si] (mM)	0.09	± 0.02	0.06	± 0.04	0.06	± 0.04	0.10	± 0.01	0.12	± 0.01	0.10	± 0.01	0.11	± 0.01	0.18	± 0.20
[Ni] _{Total} (µM)	b/ DL		0.47	± 0.08	3.4	± 0.1	20	± 2	b/ DL		0.51	± 0.06	3.6	± 0.5	20	± 3
[Ni ²⁺] (µM)	N/A		0.044	± 0.018	0.60	± 0.23	5.4	± 2.1	N/A		0.072	± 0.011	0.66	± 0.19	7.0	± 1.6
[NO ₃] (mM)	0.02	± 0.01	0.02	± 0.02	0.02	± 0.01	0.08	± 0.03	0.05	± 0.03	0.12	± 0.05	0.08	± 0.02	0.13	± 0.04
[NH ₄] (mM)	0.03	± 0.02	0.02	± 0.02	0.03	± 0.02	0.05	± 0.03	0.06	± 0.04	0.06	± 0.04	0.07	± 0.04	0.07	± 0.04
[SO ₄] (mM)	0.09	± 0.01	0.09	± 0.01	0.08	± 0.02	0.08	± 0.03	0.14	± 0.02	0.12	± 0.01	0.11	± 0.01	0.11	± 0.04

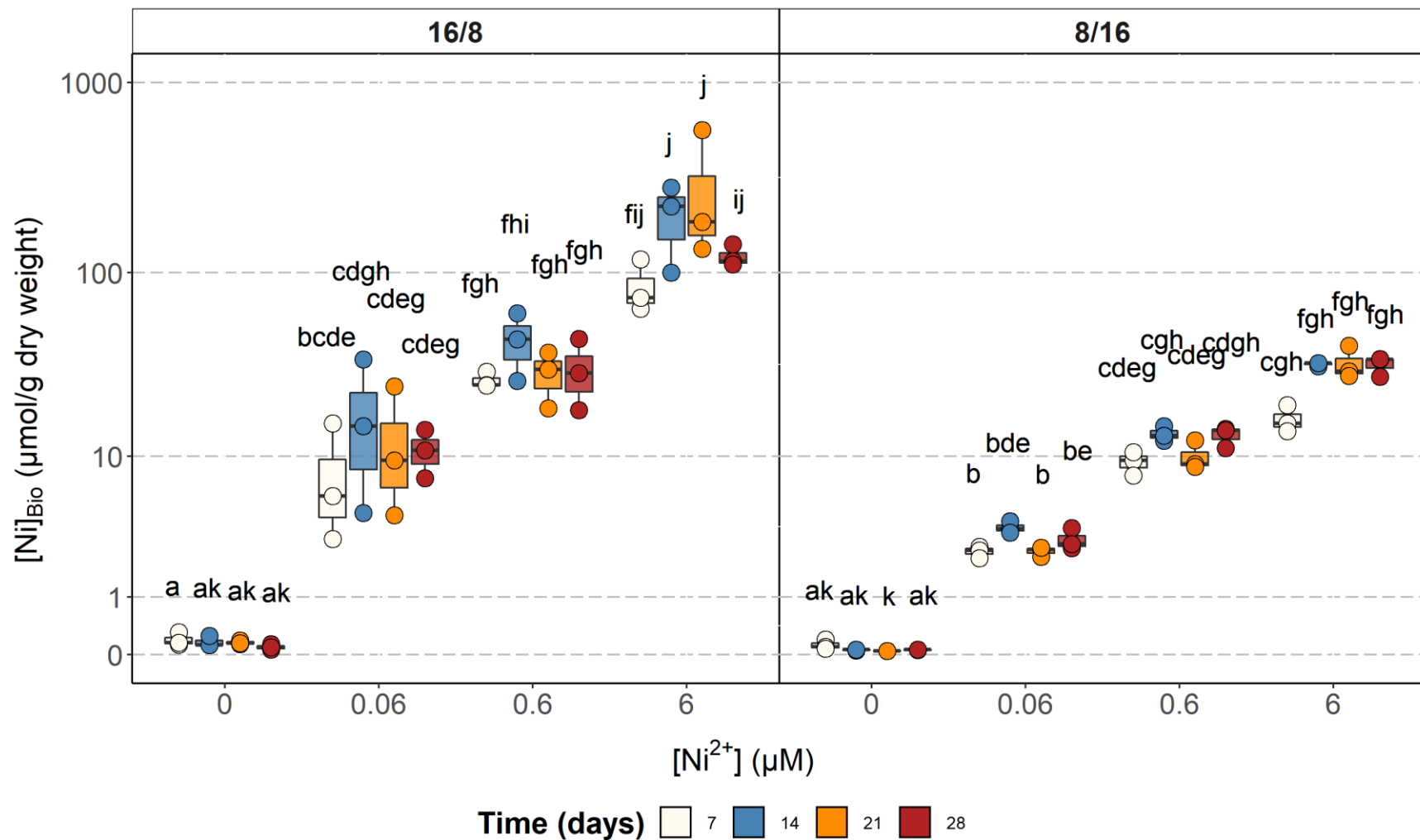


Figure 13-1 : Boxplots of the accumulated concentrations inside biofilms as a function of the average free Ni concentrations of exposure (μM) for the two photoperiods tested (i.e. 16/8 and 8/16 of light/dark cycle) and for the different sampling times ($n = 3$). The colors are representing the sampling times. The letters correspond to the significative groups defined by a post hoc Tukey test ($p < 0.05$).

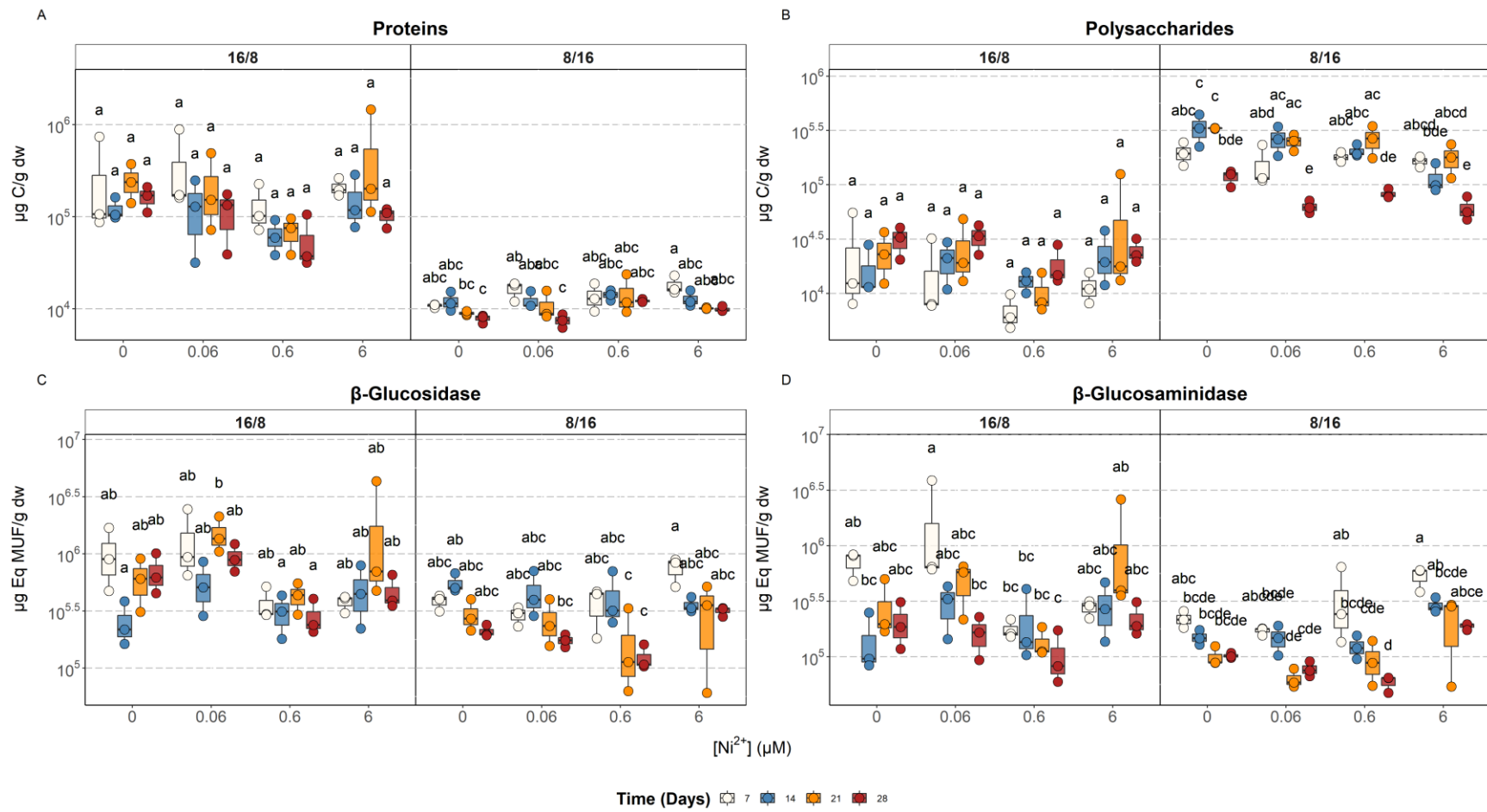


Figure 13-2 : Boxplots of proteins (A), polysaccharides (B), β -Glucosidase (C) and β -Glucosaminidase (D) measured in biofilms as a function of the average free Ni concentration of exposure (μM) for the two photoperiods tested (i.e. 16/8 and 8/16 of light/dark cycle) and for the different sampling times ($n = 3$). The colors are representing the sampling times. The letters correspond to the significative groups defined by a post hoc Tukey test ($p < 0.05$) within a same photoperiod.

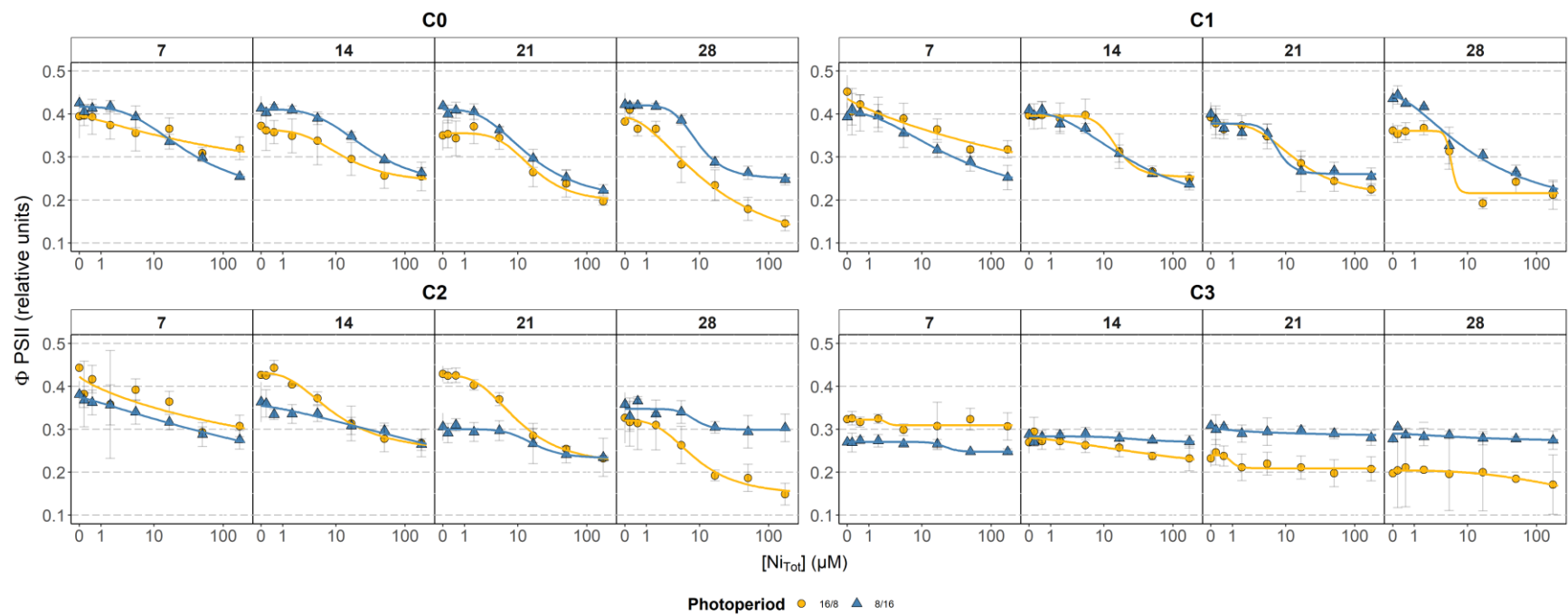


Figure 13-3 : Dose response curves of the PSII yields in relative units (Φ_{PSII} ; mean \pm SD; $n = 3$) as a function of the total Ni concentrations (μM) used for the short-term toxicity test after 6 hours of exposure. The figure presents the data for the different sampling times of each exposure units. The colors and shapes refer to the photoperiod tested.

Table 13-2 : Recipes for the Dauta medium used for the short-term toxicity test (Dauta, 1982).

Dauta medium (Dauta, 1982)				
	Stock solution (g/L)	Quantity (mL/L)	Final concentration (mg/L)	Final concentration (mM)
MgSO ₄ · 7H ₂ O	25.0	1	25.0	0.101
FeSO ₄	0.547	1	0.547	0.00360
CaCl ₂ · 2H ₂ O	25.0	1	25.0	0.170
NaHCO ₃	50.0	1	50.0	0.595
Na ₂ CO ₃	5.00	1	5.00	0.0472
KNO ₃	200	1	200	1.98
K ₂ HPO ₄	25.0	1	25.0	0.144
Na ₂ SiO ₃ · 9H ₂ O	28.4	1	28.4	0.100
Trace Metals Solution	X	1	X	X

Trace Metal Solution				
	Stock solution (g/L)	Quantity (mL/L)	Final concentration (µg/L)	Final concentration (µM)
ZnSO ₄ · 7H ₂ O	0.020	1	20	0.0696
CuCl ₂ · 2H ₂ O	0.020	1	20	0.117
MnCl ₂ · 4H ₂ O	0.400	1	400	2.02
CoCl ₂ · 6H ₂ O	0.010	1	10	0.0420
Bo ₃ H ₃	0.001	1	1	0.0162
Na ₂ MoO ₄	0.035	1	35	0.170

Dauta, A., 1982. Conditions de développement du phytoplancton. Etude comparative du comportement de huit espèces en culture. I. Détermination des paramètres de croissance en fonction de la lumière et de la température. Ann. Limnol. - Int. J. Limnol. 18, 217–262.
<https://doi.org/10.1051/limn/1982005>

Tableau 13-3 : Physico-chemical characteristics of exposure media of the four channel systems for all sampling times and for the experiment using a photoperiod of 16/8. The values are presented as means \pm standard deviations ($n = 3$). b/DL = below detection (Ca = 0.04 μM ; Mg = 0.12 μM , Ni = 0.007 μM).

Photoperiod 16/8

Conditions	Time	pH	Conductivity ($\mu\text{S}/\text{cm}$)	[DOC] (mg C/L)	[Ca] (mM)	[Mg] (mM)	[Ni] _{Total} (μM)	[Ni ²⁺] (μM)
C0	1	7.9	212	37.4	0.66 \pm 0.003	0.13 \pm 0.0007	0.0022 \pm 0.000	0.00019 \pm 0.00000
	7	8.0	257	42.4	0.75 \pm 0.002	0.15 \pm 0.0001	0.0022 \pm 0.000	0.00014 \pm 0.00000
	8	7.8	235	37.3	0.63 \pm 0.005	0.13 \pm 0.0016	0.0057 \pm 0.052	0.00054 \pm 0.00240
	14	8.0	266	91.9	0.67 \pm 0.001	0.14 \pm 0.0001	0.0028 \pm 0.009	0.00007 \pm 0.00030
	15	8.0	240	19.2	0.24 \pm 0.001	0.05 \pm 0.0003	0.0022 \pm 0.000	0.00027 \pm 0.00000
	21	7.8	253	23.4	0.65 \pm 0.001	0.13 \pm 0.0004	0.0019 \pm 0.006	0.00026 \pm 0.00030
	22	7.8	227	19.2	0.56 \pm 0.003	0.11 \pm 0.0010	0.0022 \pm 0.000	0.00032 \pm 0.00000
	28	7.8	234	88.3	0.62 \pm 0.001	0.13 \pm 0.0006	0.0022 \pm 0.000	0.00008 \pm 0.00000
C1	1	7.9	209	37.4	0.66 \pm 0.001	0.13 \pm 0.0005	0.35 \pm 0.04	0.034 \pm 0.002
	7	8.0	250	39.9	0.70 \pm 0.002	0.14 \pm 0.0005	0.61 \pm 0.05	0.051 \pm 0.002
	8	7.8	230	36.3	0.59 \pm 0.002	0.12 \pm 0.0004	0.53 \pm 0.04	0.057 \pm 0.002
	14	8.0	254	44.3	0.65 \pm 0.002	0.14 \pm 0.0008	0.52 \pm 0.05	0.039 \pm 0.002
	15	8.0	235	52.8	0.20 \pm 0.000	0.04 \pm 0.0004	0.49 \pm 0.44	0.029 \pm 0.016
	21	7.7	244	72.4	0.64 \pm 0.002	0.13 \pm 0.0003	0.44 \pm 0.10	0.024 \pm 0.005
	22	7.8	221	17.1	0.56 \pm 0.002	0.11 \pm 0.0003	0.41 \pm 0.01	0.082 \pm 0.001
	28	7.8	228	46.4	0.60 \pm 0.004	0.12 \pm 0.0007	0.41 \pm 0.06	0.033 \pm 0.003
C2	1	7.9	206	36.9	0.64 \pm 0.002	0.12 \pm 0.0000	3.5 \pm 0.5	0.55 \pm 0.03
	7	8.0	245	38.9	0.68 \pm 0.000	0.14 \pm 0.0001	3.1 \pm 0.04	0.39 \pm 0.001
	8	7.8	226	36.1	0.60 \pm 0.003	0.17 \pm 0.0004	3.4 \pm 0.1	0.57 \pm 0.01
	14	8.0	249	19.6	0.62 \pm 0.002	0.13 \pm 0.0002	3.4 \pm 0.1	0.70 \pm 0.003
	15	7.9	232	50.9	0.16 \pm 0.002	0.03 \pm 0.0004	3.5 \pm 0.1	0.37 \pm 0.004
	21	7.7	240	19.0	0.62 \pm 0.001	0.13 \pm 0.0002	3.3 \pm 0.1	0.95 \pm 0.005
	22	7.8	218	18.2	0.56 \pm 0.003	0.11 \pm 0.0003	3.4 \pm 0.2	0.92 \pm 0.01
	28	7.7	224	55.7	0.50 \pm 0.002	0.10 \pm 0.0003	3.3 \pm 0.05	0.37 \pm 0.003
C3	1	7.9	207	35.8	0.61 \pm 0.003	0.12 \pm 0.0002	15.3 \pm 1.2	3.6 \pm 0.1
	7	8.0	245	38.9	0.67 \pm 0.000	0.13 \pm 0.0004	19.1 \pm 0.5	3.6 \pm 0.02
	8	7.8	228	36.5	0.60 \pm 0.000	0.12 \pm 0.0002	19.8 \pm 1.0	5.3 \pm 0.1
	14	8.0	246	35.7	0.21 \pm 0.005	0.04 \pm 0.0016	20.6 \pm 1.1	4.2 \pm 0.04
	15	7.9	233	18.6	0.13 \pm 0.002	0.02 \pm 0.0002	20.4 \pm 1.3	6.7 \pm 0.1
	21	7.7	241	20.0	0.61 \pm 0.002	0.12 \pm 0.0001	21.1 \pm 0.2	8.1 \pm 0.01
	22	7.7	222	17.0	0.55 \pm 0.002	0.11 \pm 0.0003	21.3 \pm 0.8	8.7 \pm 0.04
	28	7.7	235	80.7	0.43 \pm 0.001	0.09 \pm 0.0002	21.7 \pm 1.0	2.9 \pm 0.1

Tableau 13-4 : Physico-chemical characteristics of exposure media of the four channel systems for all sampling times and for the experiment using a photoperiod of 8/16. The values are presented as means \pm standard deviations ($n = 3$). b/DL = below detection (Ca = 0.04 μM ; Mg = 0.12 μM , Ni = 0.007 μM).

Photoperiod 8/16

Conditions	Time	pH	Conductivity ($\mu\text{S}/\text{cm}$)	[DOC] (mg C/L)	[Ca] (mM)	[Mg] (mM)	[Ni] _{Total} (μM)	[Ni ²⁺] (μM)
C0	1	7.4	190	30.2	0.44 \pm 0.002	0.09 \pm 0.0003	0.0022 \pm 0.0000	0.00031 \pm 0.00000
	7	7.5	213	41.1	0.53 \pm 0.002	0.11 \pm 0.0003	0.0022 \pm 0.0000	0.00022 \pm 0.00000
	8	7.6	200	32.5	0.51 \pm 0.001	0.10 \pm 0.0002	0.0022 \pm 0.0000	0.00025 \pm 0.00000
	14	7.7	227	38.7	0.59 \pm 0.000	0.12 \pm 0.0003	0.0066 \pm 0.0503	0.00063 \pm 0.00285
	15	7.7	207	28.1	0.49 \pm 0.004	0.10 \pm 0.0001	0.0060 \pm 0.0656	0.00084 \pm 0.00366
	21	7.6	218	40.6	0.62 \pm 0.001	0.12 \pm 0.0002	0.0022 \pm 0.0000	0.00023 \pm 0.00000
	22	7.6	197	30.8	0.49 \pm 0.001	0.10 \pm 0.0001	0.0022 \pm 0.0000	0.00027 \pm 0.00000
	28	7.7	227	38.0	0.56 \pm 0.003	0.12 \pm 0.0002	0.0447 \pm 0.6299	0.00453 \pm 0.03595
C1	1	7.3	181	36.3	0.40 \pm 0.003	0.09 \pm 0.0004	0.63 \pm 0.04	0.097 \pm 0.003
	7	7.5	198	35.6	0.50 \pm 0.005	0.10 \pm 0.0009	0.54 \pm 0.13	0.074 \pm 0.009
	8	7.5	191	28.5	0.48 \pm 0.000	0.09 \pm 0.0001	0.48 \pm 0.03	0.076 \pm 0.002
	14	7.5	209	33.1	0.50 \pm 0.002	0.10 \pm 0.0004	0.48 \pm 0.01	0.069 \pm 0.001
	15	7.6	196	26.2	0.44 \pm 0.003	0.09 \pm 0.0001	0.44 \pm 0.01	0.072 \pm 0.001
	21	7.5	197	43.3	0.53 \pm 0.002	0.10 \pm 0.0004	0.55 \pm 0.01	0.065 \pm 0.001
	22	7.6	184	33.0	0.44 \pm 0.001	0.09 \pm 0.0001	0.49 \pm 0.02	0.067 \pm 0.001
	28	7.6	205	38.7	0.49 \pm 0.001	0.10 \pm 0.0003	0.50 \pm 0.03	0.058 \pm 0.002
C2	1	7.3	171	37.9	0.35 \pm 0.002	0.07 \pm 0.0001	3.3 \pm 0.1	0.65 \pm 0.01
	7	7.5	183	34.6	0.47 \pm 0.005	0.10 \pm 0.0007	2.9 \pm 0.1	0.57 \pm 0.01
	8	7.4	180	25.5	0.46 \pm 0.002	0.09 \pm 0.0005	3.2 \pm 0.2	0.83 \pm 0.01
	14	7.5	194	37.4	0.47 \pm 0.001	0.09 \pm 0.0003	3.2 \pm 0.2	0.58 \pm 0.01
	15	7.6	187	29.0	0.42 \pm 0.003	0.09 \pm 0.0003	3.4 \pm 0.3	0.76 \pm 0.02
	21	7.5	193	92.1	0.49 \pm 0.001	0.10 \pm 0.0001	4.1 \pm 0.2	0.26 \pm 0.01
	22	7.4	181	39.0	0.42 \pm 0.004	0.08 \pm 0.0005	4.3 \pm 0.2	0.87 \pm 0.02
	28	7.5	192	37.9	0.45 \pm 0.001	0.10 \pm 0.0003	4.1 \pm 0.5	0.80 \pm 0.03
C3	1	7.4	176	34.8	0.42 \pm 0.001	0.24 \pm 0.0003	15.6 \pm 0.4	4.9 \pm 0.03
	7	7.4	184	34.6	0.47 \pm 0.003	0.09 \pm 0.0002	15.3 \pm 0.4	4.6 \pm 0.03
	8	7.4	184	26.0	0.46 \pm 0.002	0.09 \pm 0.0004	20.6 \pm 1.6	8.2 \pm 0.1
	14	7.5	197	29.1	0.46 \pm 0.002	0.09 \pm 0.0002	20.9 \pm 1.9	7.6 \pm 0.1
	15	7.5	197	21.5	0.42 \pm 0.000	0.08 \pm 0.0002	21.2 \pm 2.0	8.6 \pm 0.1
	21	7.5	193	43.1	0.48 \pm 0.001	0.09 \pm 0.0006	22.0 \pm 1.1	6.1 \pm 0.1
	22	7.5	182	31.5	0.42 \pm 0.001	0.08 \pm 0.0001	21.9 \pm 0.3	7.6 \pm 0.02
	28	7.5	194	25.0	0.43 \pm 0.002	0.09 \pm 0.0001	22.3 \pm 1.1	8.7 \pm 0.1